INTERNATIONAL ASSOCIATION OF GEODESY

BULLETIN D'INFORMATION N. 77

IGeS BULLETIN N. 4

SPECIAL ISSUE

NEW GEOIDS IN THE WORLD

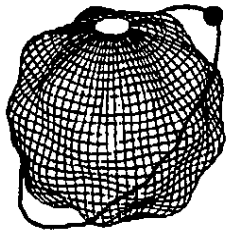

International Geoid Service
D.I.I.A.R. - Sezione Rilevamento
Politecnico di Milano
P.zza Leonardo da Vinci, 32
20133 Milano - Italy

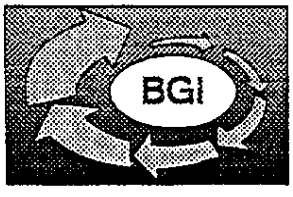

Bureau Gravimétrique International
18, Avenue Edouard Belin
31055 Toulouse Cedex - France

Table of contents

Foreword by G. Balmino, F. Sansó 2

Preparation of continental geoids

The European gravimetric quasigeoid EGG95 3
(H. Denker, D. Behrend, W. Torge)

Improvement of a high resolution geoid height model in the United States by GPS height on NAVD 88 benchmarks 13
(D. G. Milbert)

FFT geoid computations in Canada 37
(M. G. Sideris)

A preliminary gravimetric geoid for South America 53
(D. Blitzkow, J. Derek Fairhead, M. C. Lobianco)

Accuracy evaluation of the height anomaly prediction by means of gravity data in a height anomaly control network 67
(Junyong Chen)

Preparation of national geoids

Le geoide gravimetrique en Belgique: premieres résultats 77
(C. Poitevin, Z. Jiang, M. Everaert)

Geoid computations in the Nordic and Baltic area 105
(R. Forsberg)

The geoid in the Southern Alps of France 115
(H. Duquenne, Z. Jiang)

Geoid models for Great Britain and the North Sea 131
(R. Hipkin)

The new Italian quasigeoid: ITALGEO95 137
(R. Barzaghi, M.A. Brovelli, G. Sona, A. Manzino, D. Sguerso)

Gravimetric geoid for Poland area using spherical FFT 153
(A. Lyszkowics, R. Forsberg)

A new gravimetric geoid in the Iberian Peninsula 163
(M. J. Sevilla)

National investigation in Switzerland 181
(U. Marti, B. Bürki, H.-G. Kahle

Foreword

Everyone needs the geoid as a reference surface to define and properly use height systems. It is also the natural link between geodetic coordinates of high precision and satellite derived positions.

The development of regional gravimetric geoid determination is at its peak thanks to several factors: (i) an open data exchange policy which enables a given country to get data over neighbouring areas; (ii) the maturation of global gravity field models which is a slow (because difficult) process but gives better and better basis for higher resolution and precision geoid computation; (iii) the availability of better digital terrain models; (iv) the maturation of methods and software which are becoming operational; (v) the possibility to control the computed geoid by GPS/leveling points, and sometimes to use a combination strategy employing all data.

The roles of the Bureau Gravimétrique International (BGI) and of the International Geoid Service (IGeS) have been very influential if not paramount on several of these factors, as it appeared a year ago during the IAG symposium "Gravity and Geoid" held jointly in Graz, Austria, by the International Gravity Commission and the International Geoid Commission (Sept. 11-17, 1994) - of which BGI and IGeS respectively are operating arms. This is why it was decided to have a combined special issue of the Bulletins of these services on the topics of "New Geoids in the World".

An increasing number of new groups are being engaged in national or regional geoid computations and the papers published in this Bulletin describe the efforts made and results obtained, sometimes at a preliminary or intermediate stage. The race towards a centimeter-geoid was started a few years ago, the arrival line is rising on the horizon.

G. Balmino, F. Sansó

THE EUROPEAN GRAVIMETRIC QUASIGEOID EGG95

Heiner Denker, Dirk Behrend, Wolfgang Torge
Institut für Erdmessung, University of Hannover, Nienburger Straße 6
D-30167 Hannover, Federal Republic of Germany

ABSTRACT

This paper describes the current status of the European quasigeoid calculation performed at the Institut für Erdmessung (IfE). The progress made in the collection of high resolution gravity and terrain data as well as the used computation techniques are described. The calculated quasigeoid model, which was evaluated by GPS/leveling and Topex/Poseidon satellite altimeter data, shows an accuracy of $\pm 1 \ldots 5$ cm over 10 to a few 100 km distance, and of $\pm 5 \ldots 20$ cm over a few 1000 km distance, respectively. At present, long wavelength errors of the global gravity field models and the terrestrial gravity data pose the major problems.

1. INTRODUCTION

The geoid calculations performed for the whole of Europe at the beginning of the 1980s (*Torge et al.* 1982, *Brennecke et al.* 1983) were limited to an accuracy of a few decimeters with a maximum spatial resolution of some 20 km. The following decade then brought major changes through improved modeling techniques, the availability of high resolution gravity field data sets, and significant advances in the computing power, allowing now regional geoid/quasigeoid calculations with an accuracy improved up to one order of magnitude. On the other hand, also the accuracy demands in the fields of geodesy, geophysics and engineering have substantially increased. Especially the combination of ellipsoidal heights from the now fully operational Global Positioning System (GPS) with classical leveling data is one of the primary drivers for precise geoid/quasigeoid calculations, requiring cm accuracy over distances of a few km to a few 1000 km. IfE, therefore, is working on the determination of a high precision and high resolution European quasigeoid model under the auspices of the International Geoid Commission of the IAG (International Association of Geodesy). Several preliminary solutions were presented at different places since the initiation of the project in 1990 (Vienna, Prague, Wiesbaden, Beijing, Graz, Boulder). The last complete report was published in the proceedings of the Joint Symposium of the International Gravity Commission and the International Geoid Commission of the IAG held in Graz in 1994 (*Denker et al.* 1994). The intention of this paper is to give a brief overview on the status of the computations. The final results including the documentation are planned to be ready before the end of 1995.

2. COMPUTATION TECHNIQUE

In the IfE gravity field modeling effort for Europe the primary interest is in the calculation of height anomalies respectively quasigeoid undulations ζ. This has the advantage that only gravity field data observed at the Earth's surface and in its exterior enter into the calculations, while no assumptions about the gravity field in the Earth's interior are needed. If

desired, a subsequent transformation from height anomalies ζ to geoid undulations N can be performed easily by introducing a density model:

$$N = \zeta + \frac{\bar{g}-\bar{\gamma}}{\bar{\gamma}} H \,. \tag{1}$$

Here $\bar{g}$ is the mean value of gravity depending on the density model, $\bar{\gamma}$ is the mean value of normal gravity, and H is the orthometric height (for more details see e.g. *Torge* 1991).

The basic gravity field modeling strategy at IfE is based on the remove-restore technique, where a high-degree spherical harmonic model and a digital terrain model (DTM) are combined with terrestrial gravity field observations (point gravity data, etc.). In this procedure, residual observations are computed first by subtracting the effects associated with the spherical harmonic model and the DTM (or more generally the mass model). The modeling techniques are then applied to the residual data. Finally the effects of the spherical harmonic model and the DTM are added back to all predicted quantities. The remove-restore technique was used successfully in the past in connection with least squares collocation and integral formulas. Both methods give comparable results (see e.g. *Denker* 1988, *Bašić* 1989), but the utilization of integral formulas together with FFT is much more efficient. For the computation of continental-scale geoid/quasigeoid models the use of integral formulas together with FFT is the only practicable technique to date.

In our first quasigeoid computations for Europe we used the Stokes formula in planar and spherical approximation together with FFT, and we neglected the Molodensky correction terms up to now. However, the use of Stokes equation in connection with the remove-restore technique implies that the complete spectrum of the height anomalies (degree 2 to infinity) is computed from the terrestrial gravity anomalies in the integration area augmented by the global model values outside this region. In case that long wavelength discrepancies exist between the terrestrial gravity data and the global model, the application of Stokes formula will lead to an unreasonable distortion of the long wavelength gravity field components. Such effects were clearly seen in our previous quasigeoid solutions when comparing the results with satellite altimeter and GPS/leveling data. We found very long wavelength discrepancies and strong tilts between the respective surfaces (with a magnitude of several meters), which were attributed to the gravimetric quasigeoid solution.

To overcome this problem we decided to apply the least squares spectral combination technique going back to *Moritz* (1976) as well as *Sjöberg* (1981) and *Wenzel* (1982). Here the final height anomalies are obtained by

$$\zeta = \zeta_1 + \zeta_2 + \zeta_3 \tag{2}$$

with ζ_1 and ζ_2 being the components associated with the spherical harmonic model and the DTM, and ζ_3 being the contribution of the local gravity data obtained by the following equation:

$$\zeta_3 = \frac{R}{4\pi\gamma} \iint_{\sigma} (\Delta g - \Delta g_1 - \Delta g_2)\, W(\psi)\, d\sigma \tag{3}$$

with

$$W(\psi) = \sum_{l=2}^{\infty} \frac{2l+1}{l-1} w_l P_l(\cos\psi) . \quad (4)$$

In (3) and (4) $\Delta g_3 = \Delta g - \Delta g_1 - \Delta g_2$ are the residual gravity anomalies with Δg_1 and Δg_2 being the components associated with the global model resp. the DTM, $W(\psi)$ is the modified integration kernel, P_l are the Legendre polynomials of degree l, and w_l are the spectral weights. In (4) the w_l determine how much signal is taken from the terrestrial gravity data at a certain degree l, being dependent on the height anomaly error degree variances of the potential coefficients $\sigma_l^2(\varepsilon_1)$ and the gravity anomalies $\sigma_l^2(\varepsilon_{\Delta g})$:

$$w_l = \frac{\sigma_l^2(\varepsilon_1)}{\sigma_l^2(\varepsilon_1)+\sigma_l^2(\varepsilon_{\Delta g})} . \quad (5)$$

In the above equation the $\sigma_l^2(\varepsilon_{\Delta g})$ can be computed from the error covariance function of the terrestrial gravity data (see e.g. *Wenzel* 1982).

Furthermore it should be noted that the above equations assume that the "true" geocentric gravitational constant of the Earth GM is equal to the corresponding value of the reference ellipsoid GM^0, and that the gravity potential of the geoid W_0 is equal to the gravity potential of the surface of the reference ellipsoid U_0. If there exist differences in these quantities, this leads to the so-called zero order undulation

$$\zeta_0 = \frac{GM-GM^0}{r\gamma} - \frac{W_0-U_0}{\gamma} , \quad (6)$$

which has to be added in equation (2). If this basically constant term is neglected, the resulting height anomalies refer to an ideal ellipsoid with the properties $GM=GM^0$ and $W_0=U_0$, but whose dimensions (equatorial radius a) are not precisely known in terms of numerical values. This is a key problem since the ellipsoidal heights from, e.g., GPS refer to a specific reference ellipsoid (for more details see e.g. *Rapp* and *Balasubramania* 1992). Usually this problem is overcome by considering a bias term in the comparison (in many cases together with additional tilts to model long wavelength errors).

3. Data Description

This section gives an overview on the data sets currently included in the gravity field data base at IfE. The data base comprises about 2.3 million gravity data and 700 million topographical data. Figure 1 gives a graphical representation of the gravity data coverage in the computation area. From the figure it becomes clear that the coverage with gravity observations is not sufficient for some marine areas as well as for the former Soviet Union. Therefore, we decided to use altimetrically derived gravity anomalies from *Bašić* and *Rapp* (1992) for all marine areas with an insufficient data coverage. For the area of the former Soviet Union we used the 1° x 1° data set from Bureau Gravimétrique, being the only source of information available at present.

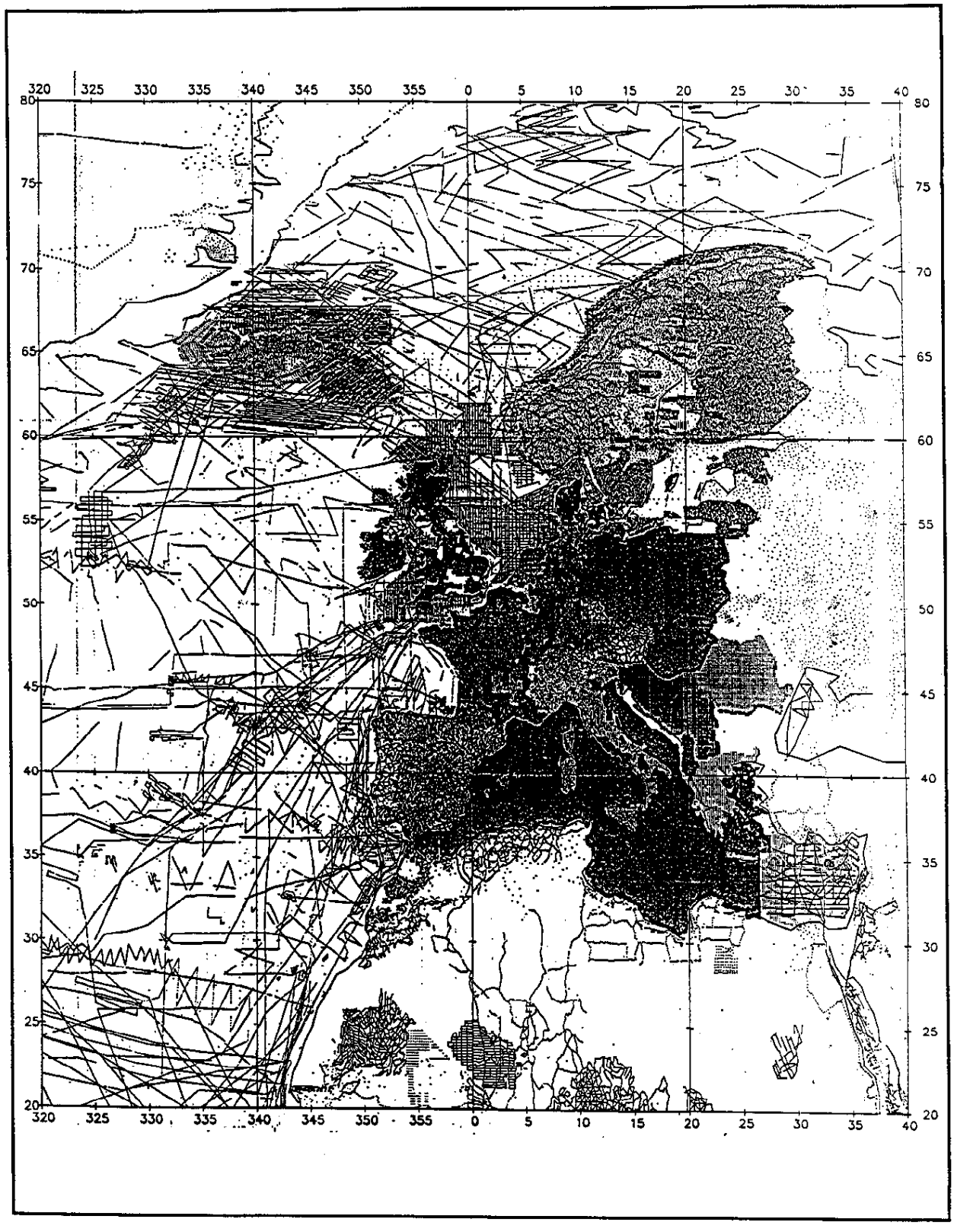

Fig. 1: Locations of point gravity data stored in the IfE data base (status Sept. 1995)

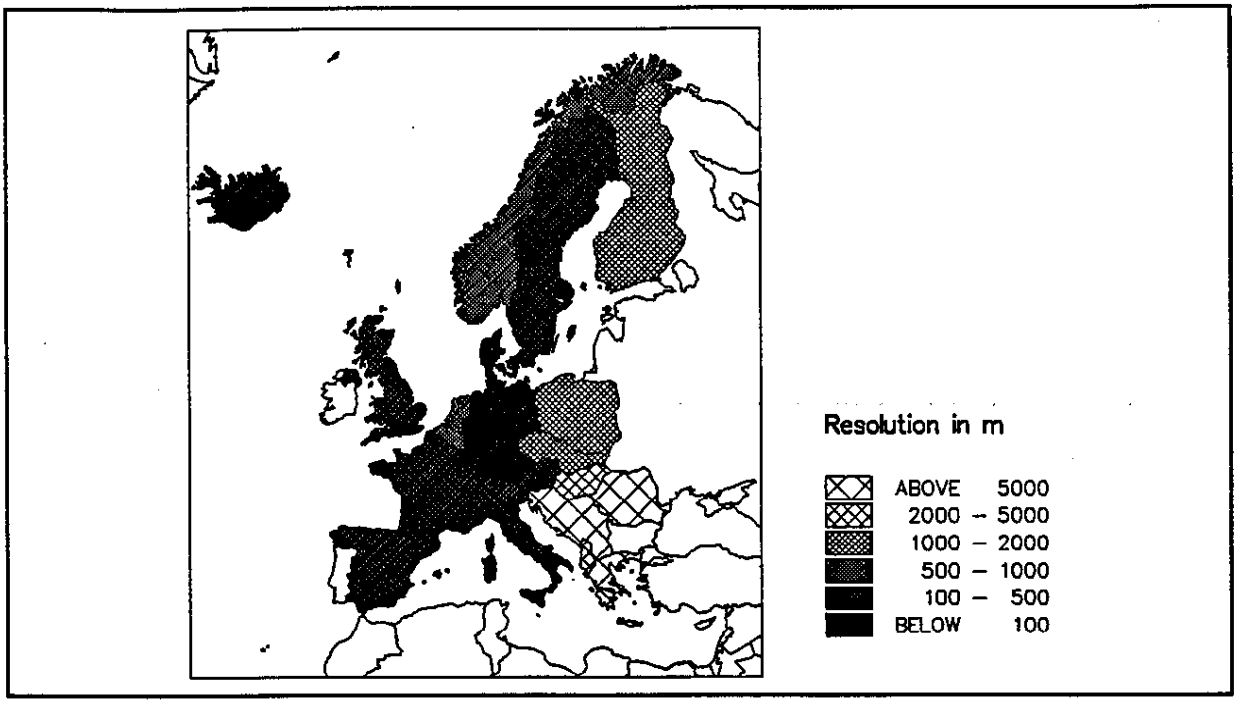

Fig. 2: Digital terrain models stored in the IfE data base (status Sept. 1995)

Prior to utilizing these data in the quasigeoid calculation, a transformation into a common reference system (IGSN 71, GRS 80 normal gravity formula) was carried out. Furtheron, all data were validated using batch and interactive procedures developed at IfE. The basic principle of this software is to compare each gravity observation with a value predicted from the adjacent stations. Unrealistic values, showing large discrepancies, were then excluded from the quasigeoid calculations.

The terrain data were subject to a similar validation process by comparing each elevation with adjacent values. Here, unlike the gravity data, unrealistic values were replaced by interpolated or apparently correct values (as is e.g. the case for intermixed numbers). Smaller gaps were filled through interpolation, larger gaps and blank areas were allocated values from ETOPO5. Finally, the digital terrain models were regridded to a common block size of $7.5'' \times 7.5''$ (or multiples of this block size) and transformed to the WGS 84 geocentric reference system. Figure 2 depicts the coverage with high resolution DTM's used for the present quasigeoid solution.

4. The 1995 Quasigeoid Solution

In 1995 a new quasigeoid solution EGG 95.01 was computed for entire Europe based on the spectral combination technique in connection with the remove-restore procedure. For the long wavelength gravity field information the spherical harmonic model OSU91A complete to degree and order 360 (*Rapp* et al. 1991) was employed. The short wavelength gravity field components were modeled using the residual terrain model (RTM) reduction technique according to *Forsberg* and *Tscherning* (1981), where the reference topography was constructed by a 15' x 15' moving average filter. The terrain reductions were all re-computed in 1995 using strict numerical integration techniques without any approximations. However, due to the large amount of computer time needed for this task, not all reductions

were finished at the time of writing this paper (about 20 % were unfinished). Therefore the existing solution is considered as preliminary, and a new solution will be carried out when all reductions are ready.

The residual gravity anomalies were gridded by a fast least squares prediction technique onto a $1.0' \times 1.5'$ grid covering the area from 25°N-77°N and 35°W-67.4°E. This yields 3,120 $\times$ 4,096 = 12,779,520 grid points. The field transformation from residual gravity to residual height anomalies was carried out using equations (2)-(4). The practical evaluation of the integral formulas was done by a 1D FFT technique suggested by *Haagmans et al.* (1993) in connection with a detailed/coarse grid approach to further speed up the computations. The major advantage of this procedure is that an exact evaluation of any integral on the sphere is possible (without periodicity effects of FFT).

For the spectral combination technique the following error covariance function for the terrestrial gravity data was used:

$$\mathrm{cov}\left(\varepsilon_{\Delta g}, \varepsilon_{\Delta g}\right) = 16\ [\mathrm{mgal}^2]\ e^{-4\psi[^\circ]}\ . \tag{7}$$

This model uses correlated noise and was suggested and applied by *Weber* (1984). The spectral weights were derived on the basis of equation (5) using the above error covariance function for the terrestrial gravity data and the error degree variances from OSU91A. It was decided to do the combination only up to degree 50, while between degrees 50 and 10000 (corresponding to the grid size used) the complete gravity field information was taken from the terrestrial gravity data (w_l=1.0). A cosine tapering window was applied between degrees 10000 and 30000. This turned out to be necessary because otherwise the integral kernel started to oscillate. The quasigeoid solution EGG 95.01 is directly comparable to the solution 94.01 as it uses the same integral kernel. For more details on this topic including a plot of the integral kernel see *Denker et al.* (1994).

The use of the spectral combination technique also permitted us to derive error estimates for the resulting height anomalies resp. differences thereof (see e.g. *Wenzel* 1982). For the spectral combination solution ($\sigma_{\Delta g} = \pm 4$ mgal) we get standard deviations for height anomaly differences of ± 15 cm over 100 km and ± 25 cm over 1000 km distance, respectively. In case of a more optimistic error estimate for the terrestrial gravity data ($\sigma_{\Delta g} = \pm 1$ mgal) we get standard deviations of ± 4 cm over 100 km and ± 12 cm over 1000 km distance, respectively. When looking at the GPS/leveling comparisons, the latter estimates appear to be more realistic (at least over shorter distances).

The major contribution to the final quasigeoid is coming from the spherical harmonic model OSU91A with values ranging from -42 m to $+68$ m and a standard deviation of ± 27 m. The standard deviations of the contributions from the DTM and the terrestrial gravity data are ± 0.03 m and ± 0.74 m respectively. However, the maximum DTM effects are about 0.8 m, while the maximum effects of the terrestrial gravity data (i.e. corrections to the OSU91A model) are exceeding 5 meters in areas where no data were used in the development of the model.

5. Evaluation of the 1995 Quasigeoid Solution and Conclusions

The quasigeoid solutions for Europe developed at IfE were evaluated by means of satellite altimeter data from the Topex/Poseidon mission and a number of GPS/leveling data sets. However, because the present solution EGG 95.01 is considered as a preliminary result due to the incomplete update of the terrain reductions (see previous section), we will report here only on some selected comparisons with GPS/leveling data. In the following we will discuss the results for the GPS/leveling campaign ISNET93 covering entire Iceland as well as for the two data sets LITH1 and LITH2 covering Lithuania (extension about 300 km). All three data sets are new, i.e. have become available since our last report in 1994 (*Denker* et al. 1994), and cover regions where also new gravity and/or terrain data were acquired. A statistics of the discrepancies between the GPS/leveling data and some selected quasigeoid solutions is given in table 1. The comparisons were always done using a bias fit as well as a bias and tilt fit in order to account for inaccuracies in the absolute positioning and for long wavelength errors of all data sets involved (GPS, leveling, quasigeoid).

First we will discuss the results for the ISNET93 data set covering entire Iceland. Here it has to be noted that the leveling data are not strictly refering to the same height datum as the connections between different network parts were only done through tide gauges. For Iceland a detailed DTM was made available just recently and, hence, was included for the

Table 1: Statistics for the comparison of selected quasigeoid solutions with different GPS/leveling data sets. Units are meters.

GPS/Leveling Data Set	Quasigeoid Solution	Bias Fit		Bias + Tilt Fit	
		RMS	Max.	RMS	Max.
ISNET93 Iceland 62 Stations	EGG1	0.335	1.058	0.320	0.907
	EAGG1	EAGG1 not available for Iceland			
	OSU91A	0.370	1.033	0.279	0.693
	EGG 94.01	0.262	0.891	0.199	0.737
	EGG 95.01	0.210	0.746	0.169	0.524
LITH1 Lithuania 38 Stations	EGG1	0.540	1.704	0.389	1.077
	EAGG1	0.514	1.627	0.374	1.033
	OSU91A	0.306	0.894	0.303	0.942
	EGG 94.01	0.255	0.785	0.252	0.832
	EGG 95.01	0.123	0.324	0.111	0.285
LITH2 Lithuania 727 Stations	EGG1	0.528	1.960	0.265	0.796
	EAGG1	0.504	1.866	0.254	0.756
	OSU91A	0.280	1.106	0.208	0.708
	EGG 94.01	0.233	0.933	0.193	0.686
	EGG 95.01	0.085	0.472	0.074	0.478

first time in the 95.01 solution. The effect of the new high resolution DTM is clearly seen in the comparison statistics. For the 95.01 solution we get an RMS difference of ± 0.21 m for the bias fit and of ± 0.17 m for the bias and tilt fit, while the corresponding values for the 94.01 solution are ± 0.26 m and ± 0.20 m, respectively. The RMS differences for the comparisons with OSU91A and the older European gravimetric solution EGG1 (*Torge* et al. 1982) are all in the order of ± 0.3 m. Furthermore in all comparisons for the ISNET93 campaign one can observe a slight improvement for the bias and tilt fit versus the bias fit, thus indicating small long wavelength discrepancies between the gravimetric quasigeoid and the GPS/leveling data in this region.

For Lithuania we have received point gravity data and a detailed DTM which was also included in our calculations for the first time in the 95.01 quasigeoid solution. Here one can see a stronger improvement of the 95.01 solution versus the older models. For the GPS/leveling data set LITH2 with 727 stations the RMS difference is ± 0.085 m for the bias fit and ± 0.074 m for the bias and tilt fit, while the correponding values for the 94.01 solution (without the new gravity and terrain data) are ± 0.233 m and ± 0.193 m, respectively, proving the importance of using reliable gravimetric and topographic data. For Lithuania (data sets LITH1 and LITH2) the older European solutions EGG1 and EAGG1 give a poorer agreement with GPS/leveling data than in Iceland for the bias fit with RMS discrepancies of about ± 0.5 m, reducing to about ± 0.25 m for the bias and tilt fit.

Further evaluations of the quasigeoid solutions developed at IfE are reported in *Denker* et al. (1994). For a local GPS/leveling data set for Lower Saxony in Germany (extension about 300 km) an RMS discrepancy of ± 0.065 m was found for the bias fit, while the corresponding value for the bias and tilt fit was only ± 0.015 m, indicating that small but significant tilts between the respective surfaces (0.7 ppm) exist in this region. For the European north-south GPS traverse with a length of about 3000 km running from Austria to northern Norway we observed also small tilts and an RMS difference for the bias and tilt fit of ± 0.16 m (compared to ± 0.22 m for the bias fit). Futhermore a preliminary comparison with EUREF (without a transformation of all leveling heights to a common reference system due to lacking information on the underlying systems) gave an RMS discrepancy of ± 0.3 m.

To conclude, significant progress was made since the initiation of the geoid project in 1990 regarding the collection of gravity and terrain data, the computation algorithm (spectral combination versus Stokes) and the evaluation of the results (use of GPS/leveling and Topex/Poseidon data). For areas with a good coverage and accuracy of the gravity and terrain data, the accuracy of the latest solution is estimated as $\pm 1 \ldots 5$ cm over 10 to a few 100 km distance, and $\pm 5 \ldots 20$ cm over a few 1000 km distance, respectively. Problems that need to be further studied in the future concern long wavelength errors of the global gravity models and the terrestrial gravity data. Moreover, some data gaps still exist.

ACKNOWLEDGMENTS

The authors would like to thank all individuals and agencies providing data for this project. A complete list of all data contributors will be given in the final report. This research was sponsored by the German Research Society (DFG), which is gratefully acknowledged.

REFERENCES

Bašić, T., R.H. Rapp (1992). Oceanwide prediction of gravity anomalies and sea surface heights using Geos-3, Seasat, and Geosat altimeter data and ETOPO5U bathymetric data. Dept. Geod. Sci. and Surv., Rep. 416, Columbus.

Bašić, T. (1989). Untersuchungen zur regionalen Geoidbestimmung mit "dm" Genauigkeit. Wiss. Arb. Univ. Hannover, Nr. 157.

Brennecke, J., D. Lelgemann, W. Torge, H.-G. Wenzel (1983). A European astro-gravimetric geoid. Deutsche Geod. Komm., Reihe B, Nr. 269, Frankfurt/Main.

Denker, H. (1988). Hochauflösende regionale Schwerefeldbestimmung mit gravimetrischen und topographischen Daten. Wiss. Arb. Univ. Hannover, Nr. 156.

Denker, H., D. Behrend, W. Torge (1994). European Gravimetric Geoid: Status report 1994. Proceed. IAG Symp. No. 113, Gravity and Geoid, Graz, Austria, Sept. 11-17, 1994, 423-433, Springer, Berlin, Heidelberg, New York.

Forsberg, R., C.C. Tscherning (1981). The use of height data in gravity field approximation. J. Geophys. Res. 86, 7843-7854.

Haagmans, R., E. de Min, M.v. Gelderen (1993). Fast evaluation of convolution integrals on the sphere using 1D FFT, and a comparison with existing methods for Stokes' integral. manuscripta geodaetica 18, 227-241.

Moritz, H. (1976). Integral formulas and collocation. manuscripta geodaetica 1, 1-40.

Rapp, R.H., Y.M. Wang, N.K. Pavlis (1991). The Ohio State 1991 geopotential and sea surface topography models. Dept. Geod. Sci. and Surv., Rep. 410, Columbus.

Rapp, R.H., N. Balasubramania (1992). A conceptual formulation of a world height system. Dept. Geod. Sci. and Surv., Rep. 421, Columbus.

Sjöberg, L. (1981). Least squares combination of satellite and terrestrial data in physical geodesy. Ann. Géophys. 37, 25-30.

Torge, W. (1991). Geodesy, 2nd edition. Walter de Gruyter, Berlin, New York.

Torge, W., G. Weber, H.-G. Wenzel (1982). Computation of a high resolution European gravimetric geoid. Proc. 2nd Int. Symp. on the Geoid in Europe and Mediterranean Area, 437-460, Rome.

Weber, G. (1984). Hochauflösende Freiluftanomalien und gravimetrische Lotabweichungen für Europa. Wiss. Arb. Univ. Hannover, Nr. 135.

Wenzel, H.-G. (1982). Geoid computation by least squares spectral combination using integral kernels. Proceed. IAG General Meet., 438-453, Tokyo.

Improvement of a High Resolution Geoid Height Model in the United States by GPS Height on NAVD 88 Benchmarks

D. G. Milbert

National Geodetic Survey, NOAA, SSMC3, 1315 East-West Hwy., Silver Spring, MD 20910

(To be submitted to Bulletin Geodesique/Journal of Geodesy)

Abstract

A geoid model, G9501, is computed on a 3' grid using over 1.5 million gravity data from the NGS database and from the Defense Mapping Agency. Computation involves a spherical approximation to perform the linearized Molodensky integration by a 2-D FFT. The integration computes a high frequency correction to an underlying OSU91A height anomaly surface. The output grid of height anomalies are then converted into the final geoid grid. A terrain correction grid at 30" resolution was computed by FFT with a spherical approximation of the classical terrain correction integral.

Intercomparison with 1889 NAD 83 (86) GPS benchmarks with NAVD 88 Helmert heights identified a 24.8 cm RMS variation about a tilted plane trend of 0.36 ppm. This tilt is almost completely described by the datum difference between the NAD 83 (86) system and the ITRF93(1995.0) reference frame. A simple, empirical covariance function with a very long characteristic length, L=500 km, was found to fit the detrended differences between the geoid model and the GPS benchmarks.

A least-squares collocation predictor lead to the development of a smooth datum corrector surface. Applying this surface to the geoid model produced a new geoid model, G9501C. This model is biased relative to a geocentric geoid, but it successfully relates the NAD 83 (86) datum to the NAVD 88 datum. Evaluation of the covariances of the differences between G9501C and the GPS benchmarks indicates an accuracy of 2.6 cm RMS with a characteristic length of L=40 km. The covariances also show a Gaussian noise source of 6.4 cm RMS. This is primarily error in GPS ellipsoid height, and is due to a variety of sources, including GPS data reduction and analysis procedures. Conversion of the datum corrector surface to a geocentric form, verifies a -72 cm bias in NAVD 88 seen by Rapp (1995).

1. Introduction

The Global Positioning System (GPS) of satellites have been instrumental in enabling us to survey at unprecedented accuracies. Baseline length repeatability of 0.1 to 0.01 parts-per-million (ppm) has become more and more common. However, many applications require the production of an orthometric height. One must then convert ellipsoidal heights obtained by GPS

into the orthometric heights typically produced by optical leveling. The conversion requires a geoid model with an accuracy, ideally, comparable to the accuracy of GPS ellipsoid heights. The combination of GPS and a geoid model provides a capability for GPS leveling of orthometric heights.

Experiences with intercomparisons of GPS ellipsoid heights on vertical benchmarks against existing high resolution (3' x 3') geoid models have shown evidence of systematic offsets and tilts (Milbert 1991a). In the conterminous United States, the offsets can approach 1 meter (m); while the tilts between the ellipsoidal, orthometric, and geoidal reference surfaces often reach 1-2 ppm. It has been found, however, that these large discrepancies can be accommodated in standard adjustment models for GPS vectors (Milbert 1991b, Zilkoski 1990). In such adjustments, GPS vectors translate and (possibly) rotate to absorb vertical datum errors between the three reference systems. The orthometric heights from these computations have been checked by subsequent vertical field work, and are found to be accurate (Satalich 1994, Soehngen et al. 1991).

The success of such an adjustment suggests that the error in high resolution geoid models is predominantly of long-wavelength. If this is the case, then the possibility exists to develop an empirical surface (corrector surface) which relates a given gravimetric geoid model to the reference system of GPS ellipsoidal heights, and to the vertical datum of one's orthometric height system. It must be understood that such a corrector surface will be a hybrid product; containing systematic errors from ellipsoidal, orthometric, and geoidal sources. Insofar as one's national ellipsoidal and orthometric height datums are free of bias, then one will develop a corresponding improvement to the geoid. Insofar as one's national ellipsoidal and orthometric height datums are biased, then the associated "improved" geoid will also be biased with respect to the Earth's true geopotential. However, such a biased geoid would have an important property: it would directly relate ellipsoidal heights in a national system to orthometric heights in a vertical datum.

Because of the increasing use of GPS in the United States for both horizontal and vertical positioning, the National Geodetic Survey (NGS) needs to support the surveying, mapping, navigational, and Geographic Information System (GIS) communities in obtaining heights in the North American Vertical Datum 1988 (NAVD 88) using GPS technology. In this paper the problem of computing an appropriate geoid corrector surface is studied. In section 2, I describe the theory and approach in computing a national, high resolution geoid model, the component data sets, and some results. In section 3, I describe the details of GPS benchmark data set used to test the geoid model. In section 4, collocation is used to compute a geoid corrector surface, and the new model is then tested against the data set. The results are discussed in section 5, and conclusions are presented in section 6.

2. The Gravimetric Geoid Model, G9501

The method for computing the gravimetric geoid model, G9501, is based on the use of the Fast Fourier Transform (FFT) to evaluate Stokes equation. As described in Schwarz et al. (1990), a bandwidth-limited signal is needed for input to the FFT convolution. This mandates the use of a remove-compute-restore procedure; where gravity anomalies from a global geopotential model are subtracted from gravity anomaly data, followed by convolution of the residual anomalies into residual geoid height, and then followed by restoration of geoid heights from that same geopotential model. Such an approach was used in the GEOID90 and GEOID93 computations for the United States (Milbert 1991a, Milbert and Schultz 1993). Recently, a greater appreciation has been made of the fact that evaluation of a set of geopotential coefficients yields a height anomaly, not a geoid height (Rapp 1992). This naturally leads the researcher to an approach where one first computes a height anomaly model by FFT, and then subsequently converts the height anomalies into geoid height. This procedure is adopted for G9501.

The FFT requires gridded data. Any gridding procedure is subject to aliasing in the presence of high-frequency signal. So, one should remove as much predictable, high-frequency content as possible. For this reason, gridding is performed on terrain corrected, Bouguer anomalies, Δg_{TB}. For anomalies on land

$$\Delta g_{TB} = g + \frac{2\gamma_a}{a}[1 + f + m + (-3f + \frac{5}{2}m)\sin^2\phi]H - 3\frac{\gamma_a}{a^2}H^2 - \gamma + A + C - 0.1119H \qquad (3.1)$$

where

$$C = \frac{1}{2}G\rho R^2 \iint_{\sigma} \frac{(H - H_P)^2}{l_0^3} d\sigma \qquad (3.2)$$

$$A = 0.8658 - 9.727 \cdot 10^{-5} H + 3.482 \cdot 10^{-9} H^2 \qquad (3.3)$$

$$l_0 = 2R \sin(\psi/2) \qquad (3.4)$$

and

g	surface gravity, tide corrected, IGSN71 system (mgals)
H	orthometric height, NAVD 88 datum (meters)
γ	normal gravity on ellipsoid, GRS80 (Somigliana's formula) (mgals)
A	atmospheric correction (Wichiencharoen 1982) (mgals)
C	terrain correction (mgals)
ϕ	geodetic latitude, NAD 83 (86) datum
a	semi-major axis, GRS80 (6378137 meters)
γ_a	normal gravity at equator, GRS80 (978032.67715 mgals)
f	ellipsoid flattening, GRS80 (0.00335281068118)
m	0.00344978600308 (GRS80)
ρ	density of topographic masses (2.67 gm/cm^3)

G gravitational constant
R mean radius of the earth
ψ spherical distance

Note the inclusion of the second order term for the normal vertical gravity gradient, derived from equation (2-124) of Heiskanen and Moritz (1967, p. 79). It has been found that failure to include this term leads to a 20 cm difference in geoid height across the United States. Details on the GRS80 system can be found in Mortiz (1992).

The gridding algorithm uses a method of continuous curvature splines in tension (Smith and Wessel 1990) with tension parameter $T_B = 0.75$. The method is one which honors the data and does not display large oscillations in areas without data coverage. The product is a 3' by 3' regular grid extending from 24°N to 53°N and 230°E to 294°E (66°W to 130°W). Thus, the grid contains 581 rows and 1281 columns. To provide edge control to the grid, synthetic gravity anomalies were computed on the geoid, and combined with the ship and terrestrial anomalies. The synthetic anomalies were obtained by evaluating the OSU91A global geopotential model (Rapp et al. 1991) in gravity void areas of the oceans In addition, all anomalies are prefiltered by computing mean value and mean location of the anomalies in 3' x 3' cells centered over the regular 3' latitude and longitude intersections. This prefiltering step is recommended by Smith and Wessel to reduce spatial aliasing effects prior to gridding.

The height anomaly, ζ, of Molodensky theory can be computed through the gradient solution (Moritz 1980, p.414)

$$\zeta = \frac{R}{4\pi\gamma}\iint_{\sigma}(\Delta g^{*} + G_1)S(\psi)\,d\sigma = \bar{S}(\Delta g^{*} + G_1) \tag{3.5}$$

where

$$G_1 = \frac{R^2}{2\pi}\iint_{\sigma}\frac{h - h_P}{l_0^3}\,\Delta g\,d\sigma \tag{3.6}$$

$$S(\psi) = \frac{1}{\sin\frac{\psi}{2}} - 4 - 6\sin\frac{\psi}{2} + 10\sin^2\frac{\psi}{2} - (3 - 6\sin^2\frac{\psi}{2})\ln(\sin\frac{\psi}{2} + \sin^2\frac{\psi}{2}) \tag{3.7}$$

and

Δg^{*} Molodensky surface anomaly
$S(\psi)$ Stokes function
$\bar{S}(.)$ Operator form of Stokes equation

Under the assumption of a linear relationship between surface anomalies and height, one may approximate $\bar{S}(G_1) \doteq \bar{S}(C)$ (Moritz, 1980, p. 418, Eq 48-30). A more exact equation is derived by Wang (1993). Tests of the linearity assumption and the higher order terms of the Molodensky series are made by Li et al. (1995). Since the extra terms found by Wang are included in the geopotential model of ζ, we may approximate the G_1-corrected, surface anomalies by terrain corrected, free air anomalies (Faye anomalies), $\Delta g_{TF} = \Delta g_F + C$. That is,

$$\Delta g_{TF} = \Delta g_{TB} + 0.1119H \doteq \Delta g^* + G_1 \,. \tag{3.8}$$

Combining (3.5) with (3.8), we will solve,

$$\zeta = \frac{R}{4\pi\gamma} \iint_{\sigma} (\Delta g_{TB} + 0.1119H) S(\psi)\, d\sigma \tag{3.9}$$

Thus, the next step is to restore the Bouguer plate term, + $0.1119H$, to the Δg_{TB} grid, using a grid of 3' x 3' mean elevations; yielding a grid of Faye anomalies.

Equation (3.9) is solved in a remove-compute-restore procedure using the FFT formulation of Strang van Hees (1990) in (3.11),

$$\Delta g_+ = \Delta g_{TF} - \Delta g_{360} \tag{3.10}$$

$$\zeta_+ = \frac{R\Delta\phi\Delta\lambda}{4\pi\gamma} F^{-1}[F(\Delta g_{+Q} \cos\phi_Q) F(S(\phi_P - \phi_Q, \lambda_P - \lambda_Q))] \tag{3.11}$$

$$\zeta = \zeta_+ + \zeta_{360} \tag{3.12}$$

where

Δg_+	high-frequency part of gravity anomalies
Δg_{360}	geopotential model gravity anomalies (OSU91A)
$\Delta\phi, \Delta\lambda$	grid spacing
F, F^{-1}	direct and inverse, two-dimensional, Fourier transforms
ζ_+	high-frequency part of height anomalies
ζ_{360}	geopotential model height anomalies (OSU91A)

and, where Stokes function, S, is evaluated with a mean latitude, ϕ_m, and the approximation,

$$\sin \tfrac{1}{2}\psi \doteq [\sin^2 \tfrac{1}{2}(\phi_P - \phi_Q) + \sin^2 \tfrac{1}{2}(\lambda_P - \lambda_Q)\, (\cos^2\phi_m - \sin^2 \tfrac{1}{2}(\phi_P - \phi_Q))\,]^{\frac{1}{2}} \tag{3.13}$$

The input grid, Δg_+, (580 rows, 1280 columns) had 50% zero padding on all four edges to eliminate the effect of cyclic convolution (Gleason 1990). No tapering of Δg_+ was performed, since the long wavelength part has already been removed. The FFT subroutine has an option

which exploits the Hermitian symmetry resulting from real valued grids. Thus, doubled computation speed and storage efficiency was obtained without resorting to Hartley transforms. Future computations of the convolution in (3.11) will likely use the one-dimensional FFT formulation of Haagmans et al. (1993). While Haagmans' formulation requires more arithmetic operations, it is a more exact representation of Stokes integral. For a comparison of different kernel formulations, consult Li and Sideris (1994).

As a final step, the height anomaly grid, ζ, is converted to the G9501 geoid height model, N, by the relation

$$N = \zeta + \frac{\Delta g_B}{\gamma} h \tag{3.14}$$

where

Δg_B simple Bouguer anomaly ($\Delta g_B = \Delta g_{TB} - C$)

Figure 1 displays a shaded relief image of the G9501 geoid height model. The geoid heights range from a low of -52.3 m in the Atlantic Ocean to a high of -7.4 m in the Rocky Mountains. As seen in earlier models (Milbert 1991a), significant short wavelength structure is evident.

From the foregoing it is evident that the G9501 gravimetric geoid model is derived from three data sources: point gravity, digital terrain, and geopotential coefficients. A few remarks concerning accuracy are appropriate. Over 1.8 million gravity points, both ship and terrestrial, went into the gridding. The data were a combination of NGS-held data and quality controlled data from the Defense Mapping Agency. Almost all of the data were not on monumented points, and due to the consequent uncertainty in elevation, the anomalies can be considered to have a nominal accuracy of about 1 milligal (mGal). The digital terrain data came primarily from the 30" point topography database, TOPO30, distributed by the National Geophysical Data Center (Row and Kozleski 1991). The 30" point data were originally derived from 1:250,000 scale maps, and are considered accurate to 30 meters (50 meters in the mountains). The 30" elevation set was used to compute both terrain corrections, and 3' x 3' mean elevations. And, as discussed earlier, the OSU91A model (Rapp et al. 1991) was used to compute the long-wavelength gravity anomaly and geoid height grids. The OSU91A model was computed using GEM-T2 coefficients as a foundation. Approximate estimates of OSU91A geoid error in the U. S. are ±26 cm in the oceans and ±38 cm over land (Rapp 1992).

I now close this section by detailing the computation of the terrain corrections, C, of Equation (3.2). The terrain corrections were computed on a regular 30" grid by means of the FFT convolution of Sideris (1985), but altered by the FFT formulation for ψ of Strang Van Hees (1991),

$$C = KF^{-1}[F(H^2)R] - (2K)H \cdot F^{-1}[F(H)R] + KH^2R(0,0) \tag{3.15}$$

where, for this equation,

K	$G\rho/2$
F,F^{-1}	direct and inverse, two-dimensional, Fourier transforms
H	grid of elevations
H^2	grid of squared elevations
R	analytic transform of l_0^{-3} represented by

$$R = \frac{2\pi}{\epsilon} e^{-2\pi\epsilon(u^2+v^2)^{1/2}} \tag{3.16}$$

and, where ϵ denotes a small distance to avoid singularity in the formulation.

The grid of input heights (24°- 53°N, 230°- 296°E; 3480 rows, 7920 columns) was edge-tapered with a bell cosine function of 1° width, and then zero padded by an additional 3° width on all four edges. A 50% pad was felt wasteful, due to the rapid decay of the l_0^{-3} kernel. The final terrain correction grid was extracted from the output of (3.15), and it spans the region 25°- 51°N, 232°- 294°E. As with the convolution of (3.11), an FFT subroutine which exploits Hermitian symmetry was used. Terrain corrections at all gravity points in the region were then computed with bilinear interpolation.

3. The GPS Benchmark Data Set

NGS is engaged in a project to establish a high accuracy Federal Base Network (FBN), and an associated Cooperative Base Network (CBN), through nationwide measurement of GPS baselines to 1 ppm accuracy or better. The FBN stations are located at a nominal 1° x 1° spacing, are surveyed to 1 ppm accuracy, and are maintained at the expense of NGS. A portion of the FBN is set at a nominal 3° x 3° spacing, and is surveyed to 0.1 ppm accuracy. NGS encourages individual states to establish additional 1 ppm stations at about 15' x 15' spacing. These additional stations are designated CBN. The FBN and CBN stations are often observed in a single cooperative GPS survey, frequently known as a High Accuracy Reference Network (HARN). These surveys are typically performed on a state-by-state basis. (Milbert and Milbert 1994, Bodnar 1990)

One of the objectives of the FBN/CBN effort is to upgrade the geodetic control within a state. This is done by occupation of existing high order control points, connected by classical, terrestrial measurements, with subsequent readjustment. It is clear that those FBN/CBN points that are on NAVD 88 benchmarks provide a powerful data set for accuracy assessment and improvement of geoid models. Figure 2 displays the locations of 1889 points that are leveled benchmarks with NAVD 88 Helmert orthometric heights, and which have GPS measured ellipsoidal heights in the NAD 83 (86) reference system as of June 1995. The irregular distribution illustrates the state-by-state approach to the surveying, and the different levels of state participation.

The FBN/CBN (HARN) survey effort began with Tennessee (1990) and is scheduled to have all 50 states surveyed by 1997. Over this period major advances have been made in GPS receivers, processing models, vector reduction software, orbit accuracy, and in the GPS constellation itself. In addition, the surveys were designed to provide accurate *horizontal* control. Data reduction and analysis procedures focused on horizontal accuracies. Typical observing procedures are static, and involve occupation of a point for about 6 hours on two different days (three days for 0.01 ppm). Orbit relaxation was used for the 0.01 ppm coordinates until 1994, when orbit accuracies obviated the need for that particular process. Meteorological data were not always taken on site. Only recently has the influence of antenna phase center variation (Schluper et al. 1994) been incorporated into processing software. For these reasons, the FBN/CBN surveys can not be considered as a homogenous set. And, one must expect a level of error in the GPS ellipsoidal heights greater than that associated with continuously operating GPS receivers.

The positioning and navigation communities require coordinates in the NAD 83 (86) datum. While being primarily a horizontal, classical network, the NAD 83 (86) was controlled by VLBI and Doppler data sets, and can be considered three-dimensional. Steve Frakes, National Geodetic Survey, has computed the seven parameter Helmert transformation from NAD 83 (86) to ITRF93(1995.0) with 8 points common to both reference systems. The results are summarized in Table 1. The RMS of fit was 8 millimeters (mm).

Table 1 -- Transformation from NAD 83 (86) to ITRF93(1995.0)			
ΔX	-0.9769	± 0.0166	m
ΔY	+1.9392	± 0.0137	m
ΔZ	+0.5461	± 0.0141	m
ω_X	-0.0264	± 0.0006	arc sec
ω_Y	-0.0101	± 0.0005	arc sec
ω_Z	-0.0103	± 0.0004	arc sec
scale	-0.0068	± 0.0017	ppm

Figure 3 portrays the datum differences between NAD 83 (86) and ITRF93(1995.0) ellipsoidal heights referred to the GRS80 ellipsoid. It is seen that the non-geocentricity of the NAD 83 (86) reference frame induces a smooth, systematic difference in ellipsoidal heights. The values range from -0.28 to -1.64 m, and have an average tilt of about 0.3 ppm. Of particular note, this tilt is considerably smaller than the 1 to 2 ppm often seen in local intercomparisons. Summarizing, the ellipsoidal heights in the data set will contain vertical random error, and will have a long wavelength systematic error component caused by datum definition.

The NAVD 88 datum is expressed in Helmert orthometric heights, and was computed in 1991. The network contains over 1 million kilometers (km) of leveling at precisions ranging from 0.7 to 3.0 mm/$\sqrt{}$km, and incorporates corrections for rod scale, temperature, level collimation, astronomic, refraction, and magnetic effects (Zilkoski et al. 1992). For geoid analysis in a local region, leveling can be considered nearly error free. Accuracy assessment of leveling at a national scale is problematic. An interesting result is that shown in Figure 8 of Zilkoski et al. (1992). Two independent leveling data sets, that of Canada and that of the United States, match at the 11 cm level or better at 14 points along the Canadian-U.S. border. While repeatability is not a measure of accuracy, the agreement is remarkable.

The NAVD 88 datum was realized by a single datum point, Father Point/Rimouski, in Quebec, Canada. The strategy and the value of the constraint were based on a number of factors. But, the foremost requirement was to minimize recompilation of national mapping products. Thus, there is no guarantee that the NAVD 88 datum coincides with the normal potential, U_0, defined by the GRS80 system. A recent study by Rapp (1995) compares ITRF90 Doppler positions and a hybrid global geopotential model against various national vertical datums. Rapp found a mean offset for the NAVD 88 datum of -72 cm with 321 Doppler points. The sense of the sign is that the zero level surface of the NAVD 88 datum is below the Earth's geoid, $W=U_0$. Also of interest is that Rapp found a different offset of -38 cm, when comparing a subset of 180 Doppler points in the eastern U.S. The source of this difference is unknown. Summarizing, the orthometric heights in the data set will contain little vertical random error, but any such error will be highly correlated. The orthometric heights will also have a systematic offset, caused by datum definition and possible long wavelength error components.

4. Collocation and Residual Analysis

Based on the forgoing results, it does seem clear that both our national ellipsoidal height datum (NAD 83 (86)) and orthometric height datum (NAVD 88) are biased with respect to an ideal geocentric, best-fit, global reference system. Therefore, the computation of an empirical surface to improve the geoid will lead to a biased geoid in the United States. But, as discussed earlier, such a geoid model will directly relate NAD 83 (86) and NAVD 88; a strong desire of our user community.

Modeling of the geoid and datum difference errors begins by forming residuals, e, in the sense of

e = G9501 geoid height - (NAD 83 (86) ellipsoid height - NAVD 88 orthometric height).

Next, since collocation requires centered quantities (Moritz 1980, p. 76), a tilted plane model was computed using the 1889 values of e. Results are shown in Table 2.

Table 2 -- Results from Tilted Plane Fit	
mean offset	-32.8 cm
tilt	0.36 ppm
azimuth	322°
RMS	24.8 cm

It is seen that the orientation and the magnitude of the tilt closely agree with values obtained from the NAD 83 (86) to ITRF93(1995.0) datum differences in Figure 3. Further, the mean offset of -32.8 cm closely matches a combination of a nominal ellipsoid height error of 100 cm and orthometric height error of -72 cm. These results suggests that, aside from an offset, no additional east-west vertical datum error is evident in the NAVD 88 system.

Figure 4 displays an empirical covariance function fit to the covariance statistics of the detrended geoid residuals. The fit is made using a simple function of the form

$$C = C_0 e^{(-d^2/L^2)} \tag{4.1}$$

where
d = the spherical distance between points (km)
L = characteristic length (km)
C_0 = function variance (m^2)

In Figure 4, the solid line indicates a function fit of $L = 500$ km and $C_0 = (0.185)^2$ m^2. The plus symbols display the covariance statistics. It is seen that the residual error is sizable and correlated over a long length scale. Thus, this error (or errors) is a smooth, slowly-varying effect; but of a magnitude which exceeds our expectations of possible systematic effects in leveling and GPS.

The detrended residual error, $\hat{s}$, is predicted on a 30' x 30' grid using least-squares collocation with noise (Moritz 1980, p.102-106). The prediction formula is

$$\hat{s} = C_{st}(C_{tt} + C_{nn})^{-1} \tag{4.2}$$

where
C_{tt} = signal covariance between observations
C_{st} = signal covariance between predicted signal and observations
C_{nn} = covariance of random measuring errors, taken as diagonal and constant: $C_{nn} = s_o^2 I$

Before the grid is computed, the prediction process is iterated to establish a value of s_0^2 consistent with the residual misfit about the predictions of (4.2). It was found the RMS of residuals from the prediction step matched the assigned noise when $s_0^2 = (6.5)^2$ cm^2 for the n=1889 points. The trend reported in Table 2 was then restored to the detrended signal grid, resulting in the final corrector surface grid (adjusted in sign to provide an additive correction).

Figure 5 portrays a correction that when added to the G9501 geoid model, will directly relate NAD 83 (86) ellipsoid heights and NAVD 88 Helmert orthometric heights. In viewing this figure it must be recalled that the GPS benchmarks used to develop this grid all lie within the U.S. borders; and that highs or lows in the oceans or in other countries are extrapolations, and are not reliable. With this in mind, it is seen that the predominant effect is a tilt in the northwest-southeast direction. The correction is smooth within the U.S. and seldom exceeds a meter.

To test the efficacy of this process, the correction was added to the G9501 geoid height model to produce a new geoid model, G9501C. Residuals were computed between the G9501C model and the geoid heights inferred at the 1889 GPS benchmarks. The RMS was 6.43 cm, with no offset or trends applied. Thus, the improvement process is seen to be successful, although the geoid model is known to be biased relative to the Earth's geoid.

Of particular interest, the covariance statistics for the G9501C model residuals were computed, and an empirical covariance function of the form (4.1) was then developed. These results are portrayed in Figure 6. Unlike Figure 4, which was plotted to a distance of 1000 km, Figure 6 is only plotted to a distance of 100 km. At this closer scale, a drop is seen in the statistics from $C = (0.064)^2$ m^2 at $d = 0$, down to $C = (0.026)^2$ m^2 at $d = 5$ km. This reduction is evidence of an uncorrelated (white-noise) process. For this reason, the empirical covariance function is fit to the remaining, correlated signal; yielding $L = 40$ km and $C_0 = (0.026)^2$ m^2.

The source of the 6.4 cm of uncorrelated error is undoubtedly error in the GPS ellipsoidal heights. Both geoid height and leveling errors are correlated, and leveling is much too precise to contribute significantly to the value. In addition, free-air gravity anomalies are too well known in the U.S. (1 to 2 milligal) to be a error source. Parks and Milbert (1995) report a relationship of 3 to 4 mm of geoid error to a milligal of gravity error when using 3' x 3' high resolution geoid models. As mentioned earlier, error in the GPS ellipsoid heights of the data set was expected. The 6.4 cm magnitude is not inconsistent with those field survey and reduction procedures.

The correlated error is difficult to interpret. It could be lower order leveling as well as geoid error. For example, standard errors of Second-Order leveling can range from 2.1 to 3.0 mm/$\sqrt{}$km, or about 1.5 to 2.1 cm over 50 km. Details on the NAVD 88 weighting system can be found in Zilkoski et al. (1992). A detailed analysis of variance of these errors against gravity, GPS, and leveled benchmark accuracy is deferred to future research.

This section is closed by computing one final grid. There is a component of the corrector surface known to come from the datum definition of NAD 83 (86), and this component is known

to the subcentimeter level. It is instructive to consider the corrector surface with the ellipsoidal datum component removed. This "geocentric corrector" will show the NAVD 88 datum error combined with geoid and regional GPS error. And, based on the statistics above, the surface should be accurate at about a 2.6 cm RMS. Figure 7 illustrates the geocentric corrector relating the G9501 geoid model and the NAVD 88 datum. An average offset of around -75 cm is seen, which agrees with the -72 cm value of Rapp (1995). However, the -38 cm value reported for the eastern United States is not evident. Further discussion of this figure is deferred to the next section.

5. Discussion

Figure 6, which shows the covariances of the differences between the GPS benchmarks and the G9501C corrected model, demonstrates the efficacy of the least-squares collocation procedure. The remarkable part is that it works so well. The detrended, correlated error was reduced from an RMS of 24.8 cm (Table 2), to an RMS of 2.6 cm, in the presence of 6.4 cm RMS Gaussian noise (Figure 6). Further, this result was obtained from a very smooth empirical covariance function of L=500 km. The error absorbed in the corrector surface (which has geoid model, NAVD 88, and GPS sources) falls into two distinct spectral domains: long-wavelength (~500 km) and short-wavelength (~40 km). This suggests at least two different sources.

Interpretation of the corrector surface of Figure 5 is difficult. But the general trend (tilted plane fit in Table 2) is clearly rooted in the height difference between the NAD83 (86) and the ITRF93(1995.0) datums. Thus, interpretation of Figure 7, the geocentric corrector, is somewhat easier, since it has this error source removed.

The first remark concerning Figure 7 is that it is only valid over land, and that few GPS benchmarks contributed to its character in the central and northeast U.S. The dominant structure is an east-west tilt in the Pacific Northwest area, which then slopes back down across Montana. While the western part of Washington State is mountainous, the eastern part contains the Columbia Basin and is fairly flat, yet it shows greater tilt. In addition, other states which have equivalent or greater relief and which are well-sampled by GPS benchmarks, such as Colorado, show less structure. The problem may be related to GEOID90 and GEOID93 model problems in southern British Columbia, which are thought to be caused by some older digital elevation data. The signal is much too large to be solely due to NAVD 88 leveling error.

Next, consider the Gulf of Mexico. Over 50 cm of upward tilt is seen along Florida. This problem was originally identified by GEOID90 and GEOID93, and it may be related to the OSU91A geopotential model. About +1 meter of residual height anomaly was applied in the restore process (3.12); yet that seems to be 50% too small. By contrast, the tilt along southern Louisiana and the Gulf coast of Texas, has the opposite sign. The sense of this sign is consistent with subsidence, and there are areas here known to subside at over 1 cm /year. This could explain a portion of the differences along the coast.

A broad, 30-50 cm feature is seen near the Great Lakes, over Minnesota and Wisconsin. However, there are relatively few GPS benchmarks in this location. The GPS survey in Wisconsin dates from 1991, and was not performed to the accuracy customary for state upgrade projects. While the mid-continent gravity high is in the region, it is a narrow, linear feature, and is at a right angle to the elongation of the broad feature. The density variation of the Great Lakes was not incorporated in the computations, but Martinec et al. (1995) show the effect to be in the vicinity of ±1 cm.

It is seen that Figure 7 is very suggestive, although its interpretation is problematic. Issues from the GPS control, the NAVD 88 leveling, the theory and processing of the G9501 model, and the OSU91A model all contribute to the figure. Work will continue on this analysis, aided by new data and theory. The upcoming global geopotential model (WHS96), jointly computed by Goddard Space Flight Center and Defense Mapping Agency (Rapp and Nerem 1994), is expected to significantly reduce commission error. The GPS control survey and upgrade program will provide additional GPS benchmarks in the void areas. Ties to continuously operating GPS receivers will add valuable checks to new and existing GPS heights. Additional analysis is needed on digital elevation data sets, and on models to support accurate GPS ellipsoidal heights. It is envisioned that as advances are made in theory, processing, and data coverage, that it will become possible to build an accurate map of NAVD 88 leveling error. Figure 7 represents an early step in that direction.

It is a natural tendency for geodesists to desire national control networks based on a geocentric reference system. This preference will mean increased importance of the ITRF system in the mapping sector of the U.S. This prominence will, in turn, highlight a desire for a more accurate orthometric height system. While issues on datum redefinition are questions for the future, the synergies in improving orthometric, ellipsoidal, and geoid height are undeniable.

The National Geodetic Survey is planning to compute and distribute two new high-resolution geoid models in 1996, after the release of WHS96. One model, G96SSS, will be a purely gravimetric model, and is intended for scientific purposes. The other model, GEOID96, will incorporate a datum corrector surface derived from GPS benchmarks. While GEOID96 will be biased with respect to the Earth's true geopotential, its bias will allow the direct conversion of ellipsoidal heights in the NAD 83 (86) reference system to orthometric heights in the NAVD 88 datum. By the release of two models, NGS will support scientific research, as well as meet our responsibilities to the surveying, mapping, navigational, and GIS communities.

6. Conclusions

A geoid model, G9501, was computed by means of a 2-D FFT convolution about the OSU91A global reference. Intercomparison with 1889 NAD 83 (86) GPS benchmarks with NAVD 88 Helmert heights identified a 24.8 cm RMS variation about a tilted plane trend of 0.36 ppm. This tilt is almost completely described by the datum difference between the NAD 83 (86)

system and the ITRF93(1995.0) reference frame. A simple, empirical covariance function with a long characteristic length, L=500 km, was found to fit the detrended differences between the geoid model and the GPS benchmarks.

The least-squares collocation predictor lead to the development of a smooth datum corrector surface. Applying this surface to the geoid model produced a new geoid model, G9501C. This model is biased from a geocentric geoid, but it successfully relates the NAD 83 (86) datum to the NAVD 88 datum. Evaluation of the covariances of the differences between G9501C and the GPS benchmarks indicates an accuracy of 2.6 cm RMS with a characteristic length of L=40 km.

Gaussian noise in the GPS ellipsoidal heights of NAD 83 (86) is 6.4 cm RMS. This is due to a variety of sources, including GPS data reduction and analysis procedures, receiver type and age of surveys, orbit error, meteorological effects, and unmodeled variation of antenna phase center. The figure is more than double the error ascribed to geoid and/or leveling, and highlights the need to improve GPS ellipsoidal height accuracies.

It is seen that geoid error falls into two distinct spectral domains. One domain is long-wavelength (~500 km), while the other is short-wavelength (~40 km). This suggests at least two different error sources. It does prove that high-resolution geoid height models are very precise, and can support local survey requirements.

Computation of a geocentric corrector surface, by application of an NAD83 (86) to ITRF93(1995.0) datum transformation, yielded a map which more clearly expresses NAVD 88 datum error (along with other error sources). The result confirmed the -72 cm bias in NAVD 88 found by Rapp. However, the -38 cm value reported for the eastern United States is not evident.

Future analysis is needed to resolve the structures seen in the geocentric corrector surface. This will involve digital elevation analysis, use of the forthcoming WHS96 global geopotential model, and the incorporation of additional, higher accuracy GPS benchmarks from statewide upgrade projects.

7. Acknowledgments

Work of this scope required the contributions of dozens of individuals. Virtually every employee of the National Geodetic Survey has assisted in this effort. The gravity data set, the NAVD 88 project, and the GPS state upgrade program were vital to this study. The Defense Mapping Agency (DMA) provided a major portion of the NGS land gravity data set, and was instrumental in creation of the various 3" and 30" elevation grids in existence. Professor Richard H. Rapp has been invaluable in his support of a national geoid and in his work on high-accuracy, global geopotential models.

8. References

Bodnar, A.N., 1990: National geodetic reference system statewide upgrade policy. *Technical Papers of ACSM-ASPRS Fall Convention*, Nov. 5-10, 1990, pp. A-71-82.

Gleason, D.M., 1990: Obtaining Earth surface and spatial deflections of the vertical from free-air gravity anomaly and elevation data without density assumptions. *J. Geophys. Res.*, 95(B5), 6779-6786.

Haagmans,R., E. de Min, and M. van Gelderen, 1993: Fast evaluation of convolution integrals on the sphere using 1D FFT, and a comparison with existing methods for Stokes' integral. *Manus. Geod.*, 18(5), 227-241.

Heiskanen, W.A. and H. Moritz, 1967: *Physical Geodesy*. W.H. Freeman, San Francisco, 364 pp.

Li, Y.C., and M.G. Sideris, 1994: Minimization and estimation of geoid undulation errors. *Bull. Geod.*, 68(4), 201-219.

Li, Y.C., M.G. Sideris, and K.P. Schwarz, 1995: A numerical investigation on height anomaly prediction in mountainous areas. *Bull. Geod.*, 69(3), 143-156.

Martinec, Z., P. Vaníček, A. Mainville, and M. Véronneau, 1995: The effect of lake water on geoidal height. *Manus. Geod.*, 20(3), 193-203.

Milbert, D.G., 1991a: GEOID90: A high-resolution geoid for the United States. *EOS*, 72(49), 545-554.

Milbert, D. G., 1991b: Computing GPS-derived orthometric heights with the GEOID90 geoid height model. *Technical Papers of the 1991 ACSM-ASPRS Fall Convention*, Atlanta, Oct. 28 to Nov. 1, 1991. American Congress on Surveying and Mapping, Washington, D.C., pp. A46-55.

Milbert, K.O. and D. G. Milbert, 1994: State Readjustments at the National Geodetic Survey. *Surv. and Land Info. Sys.*, 54(4), 219-230.

Milbert, D. G., and D. Schultz, 1993: GEOID (The National Geodetic Survey Geoid Computation Program). Geodetic Services Division, National Geodetic Survey, NOAA, Silver Spring, MD.

Moritz, H., 1992: Geodetic Reference System 1980. *Bull. Geod.*, 66(2), 187-192.

Mortiz, H., 1980: *Advanced Physical Geodesy*. Herbert Wichmann Verlag, Karlsruhe, 500 pp.

Parks, W. and D. G. Milbert, 1995: A geoid height model for San Diego County, California, to test the effect of densifying gravity measurements on accuracy of GPS-derived orthometric heights. *Surv. and Land Info. Sys.*, 55(1), 21-38.

Rapp, R.H., 1995: Separation between reference surfaces of selected vertical datums. *Bull. Geod.*, 69(1), 26-31.

Rapp, R.H., 1992: Computation and accuracy of global geoid undulation models. *Proceedings of the Sixth International Geodetic Symposium on Satellite Positioning*, Columbus, Mar. 17-20, 1992. The Ohio State University, pp. 865-872.

Rapp, R. H. and R. S. Nerem, 1994: A joint GSFC/DMA project for improving the model of the Earth's gravitational field. Presented at Joint Symposium of the International Gravity Commission and the International Geoid Commission, Graz, Austria, September, 1994.

Rapp, R.H., Y.M. Wang, and N.K. Pavlis, 1991: The Ohio State 1991 geopotential and sea surface topography harmonic coefficient models, *Report No. 410*, Department of Geodetic Science and Surveying, The Ohio State University, Columbus, OH. 94 pp.

Row III, L.W. and M.W. Kozleski, 1991: A microcomputer 30-second point topography database for the conterminous United States, *User Manual, Version 1.0*, National Geophysical Data Center, Boulder, CO, 40 pp.

Satalich, J., 1994: The Santa Clara River photogrammetric mapping project. *Proceedings of the 1994 ASPRS/ACSM Annual Conference*, Reno, NV. American Congress on Surveying and Mapping, Washington, D.C., pp. 558-569.

Schupler, B.R., R.L. Allshouse, and T.A. Clark, 1994: Signal characteristics of GPS user antennas. *Navigation*, 41(3), 277-295.

Schwarz, K.P., M.G. Sideris, and R. Forsberg, 1990: The use of FFT techniques in physical geodesy. *Geophysical Journal International*, 100, pp. 485-514.

Sideris, M.G., 1985: A fast Fourier transform method for computing terrain corrections. *Manus. Geod.*, 10(1), 66-73.

Smith, W.H.F., and P. Wessel, 1990: Gridding with continuous curvature splines in tension. *Geophysics*, 55(3), 293-305.

Soehngen, H.F., Z.A. Blackman, E. Lange, 1991: Geoid modeling and effect on computed orthometric elevations for a county wide GPS project, Nassau County, New York, *Technical Papers of the 1991 ACSM-ASPRS Fall Convention*, Atlanta, Oct. 28 to Nov. 1, 1991. American Congress on Surveying and Mapping, Washington, D.C., A261-A278.

Strang Van Hees, G., 1990: Stokes formula using fast Fourier techniques. *Manus. Geod.*, 15(4), 235-239.

Wang, Y.M., 1993: Comments on proper use of the terrain correction for the computation of height anomalies. *Manus. Geod.*, 18(1), 53-57.

Wichiencharoen, C., 1982: Fortran programs for computing geoid undulations from potential coefficients and gravity anomalies. Internal Report of the Department of Geodetic Science and Surveying, The Ohio State University, Columbus, OH.

Zilkoski, D.B., 1990: Establishing vertical control using GPS satellite surveys. *Proceedings of the 19th International Federation of Surveying Congress (FIG)*, Commission 5, pp. 281-294.

Zilkoski, D.B., J.H. Richards, and G.M. Young, 1992: Results of the general adjustment of the North American Vertical Datum of 1988. *Surv. and Land Info. Sys.*, 52(3), 133-149.

Figure Captions

Figure 1 -- Shaded Relief of G9501 Geoid Height Model.

Figure 2 -- 1889 Leveled Benchmarks with NAVD 88 Helmert Orthometric Heights and GPS Ellipsoidal Heights in the NAD 83 (86) Reference System

Figure 3 -- Datum Differences Between NAD 83 (86) and ITRF93(1995.0) Ellipsoidal Heights Referred to the GRS80 Ellipsoid, Contour Interval = 4 cm.

Figure 4 -- Empirical Covariance Function and Detrended Error Statistics.

Figure 5 -- Corrector Surface for the G9501 Geoid Height Model Relating NAD 83 (86) and NGVD 88, Contour Interval = 10 cm.

Figure 6 -- Empirical Covariance Function and Error Statistics for G9501(Corrected).

Figure 7 -- Contour Plot of Geocentric Corrector Surface Relating G9501, ITRF93(1995.0), and NGVD 88, Contour Interval = 5 cm.

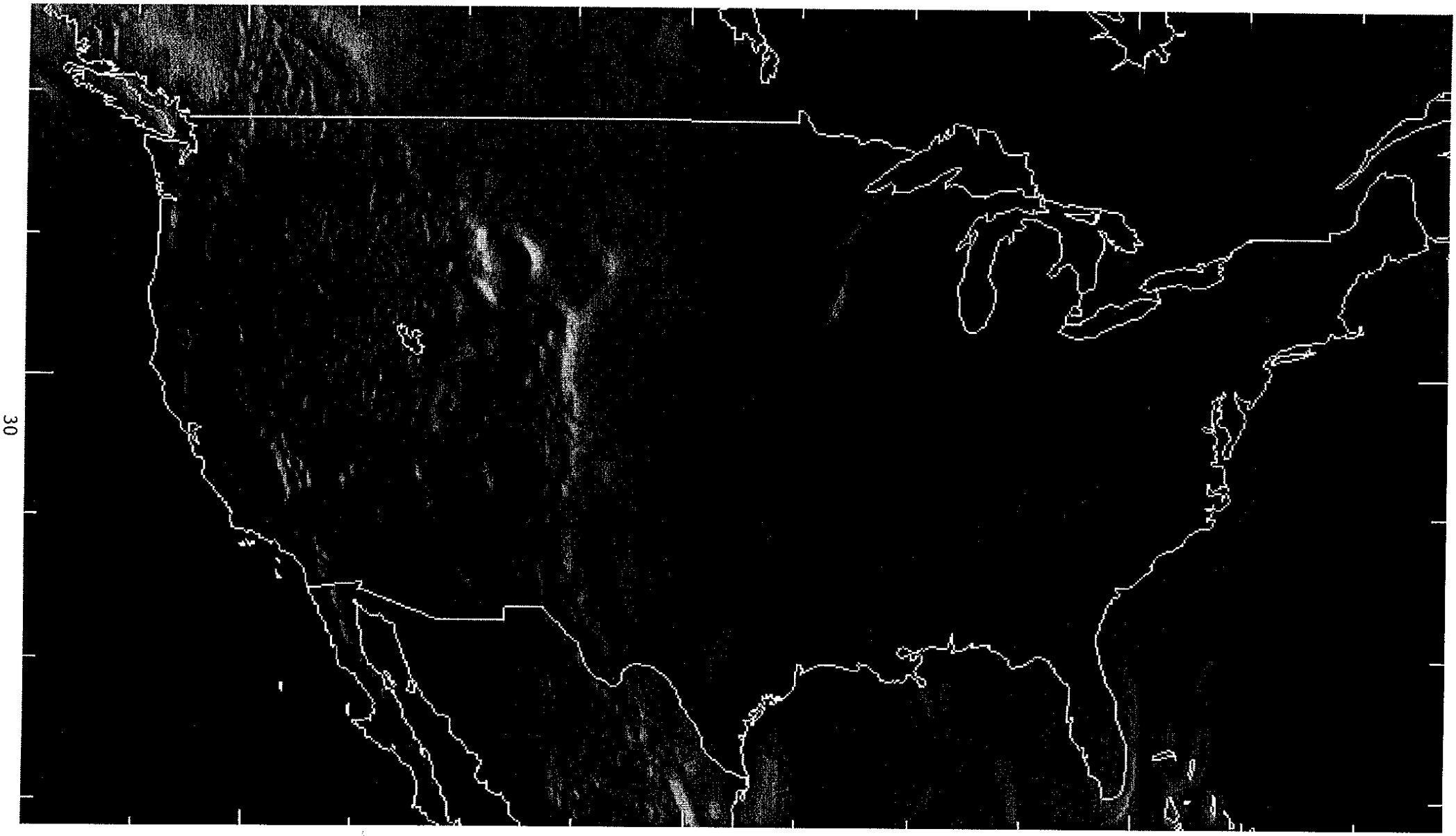

FIGURE 1 -- G9501 GEOID HEIGHT MODEL

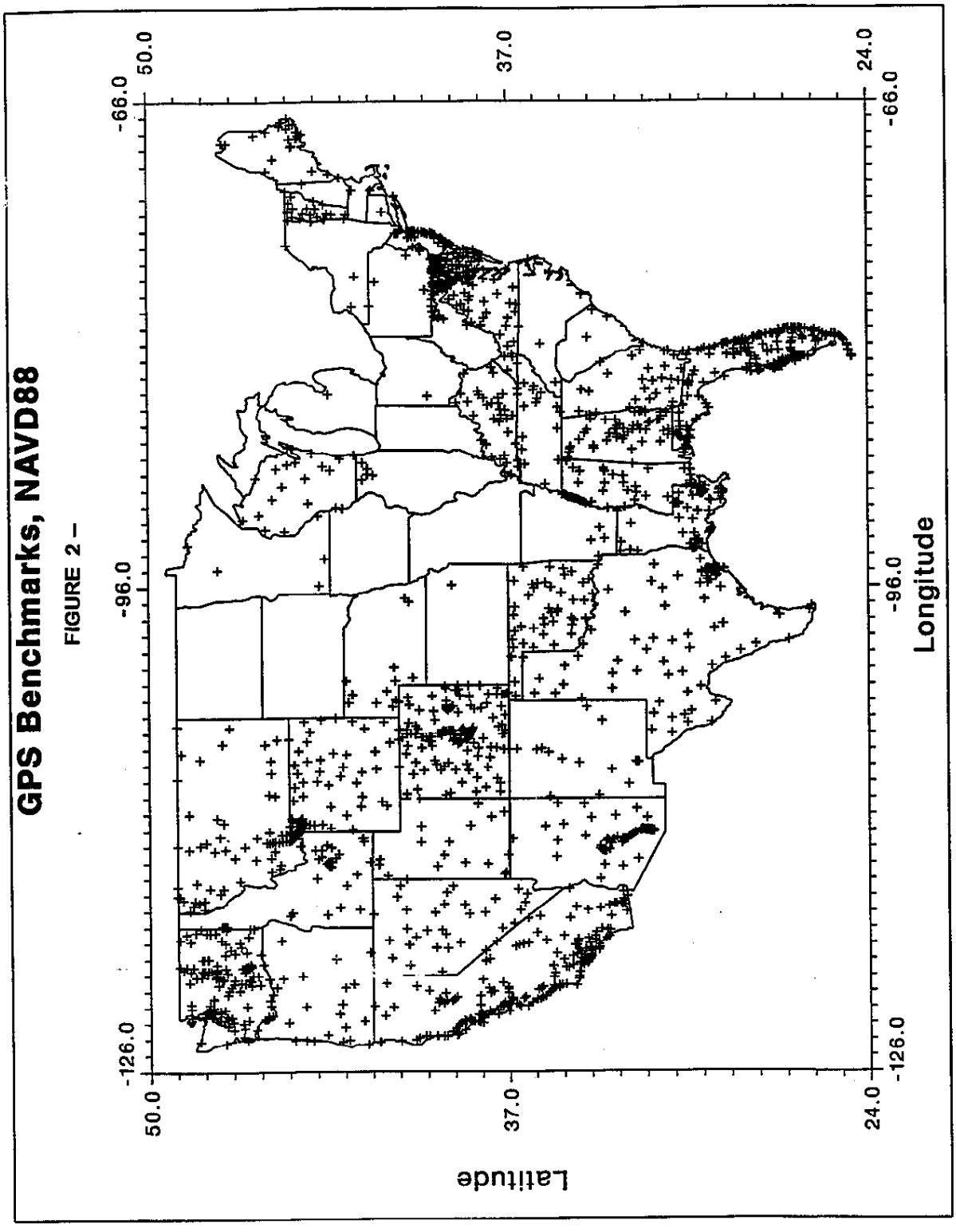
GPS Benchmarks, NAVD88
-66.0
50.0
37.0
24.0
-66.0
-96.0
-96.0
-126.0
50.0
37.0
24.0
-126.0
Latitude
Longitude

FIGURE 2 –

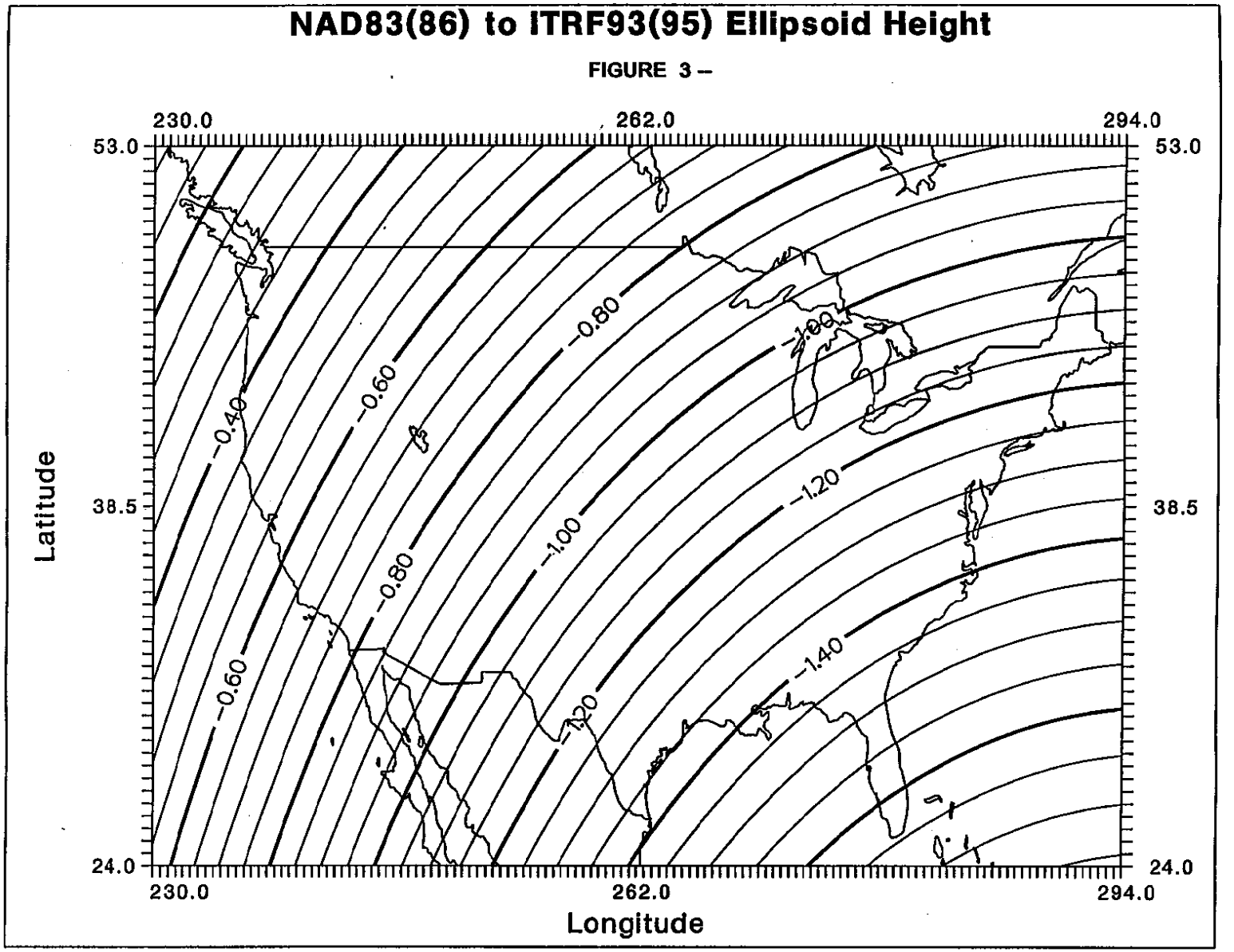
NAD83(86) to ITRF93(95) Ellipsoid Height
230.0
262.0
294.0
53.0
38.5
24.0
Latitude
Longitude
-0.40
-0.60
-0.80
-1.00
-1.20
-1.40

FIGURE 3 –

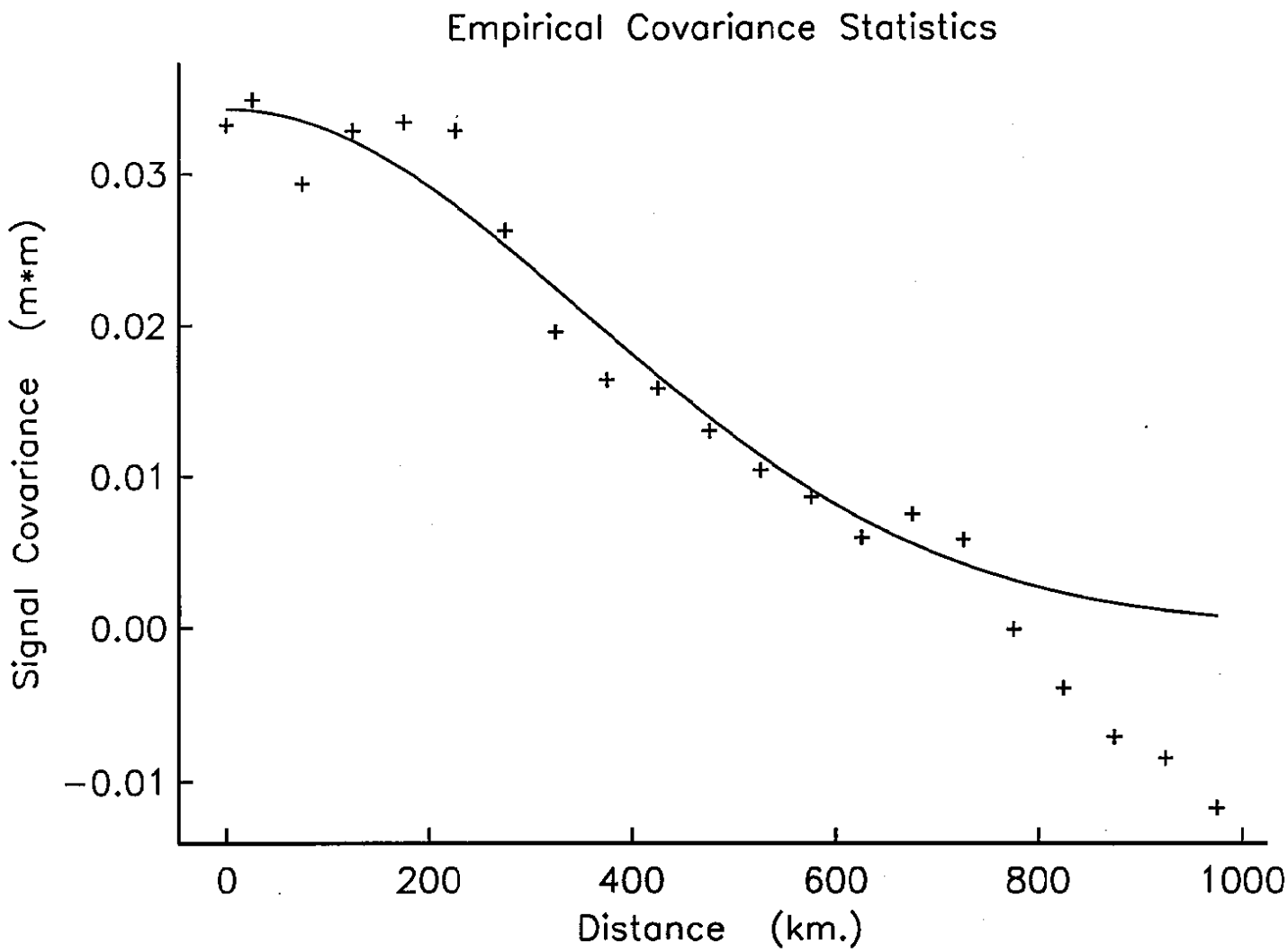
Empirical Covariance Statistics
Signal Covariance (m*m)
0.03
0.02
0.01
0.00
−0.01
0
200
400
600
800
1000
Distance (km.)

FIGURE 4 –

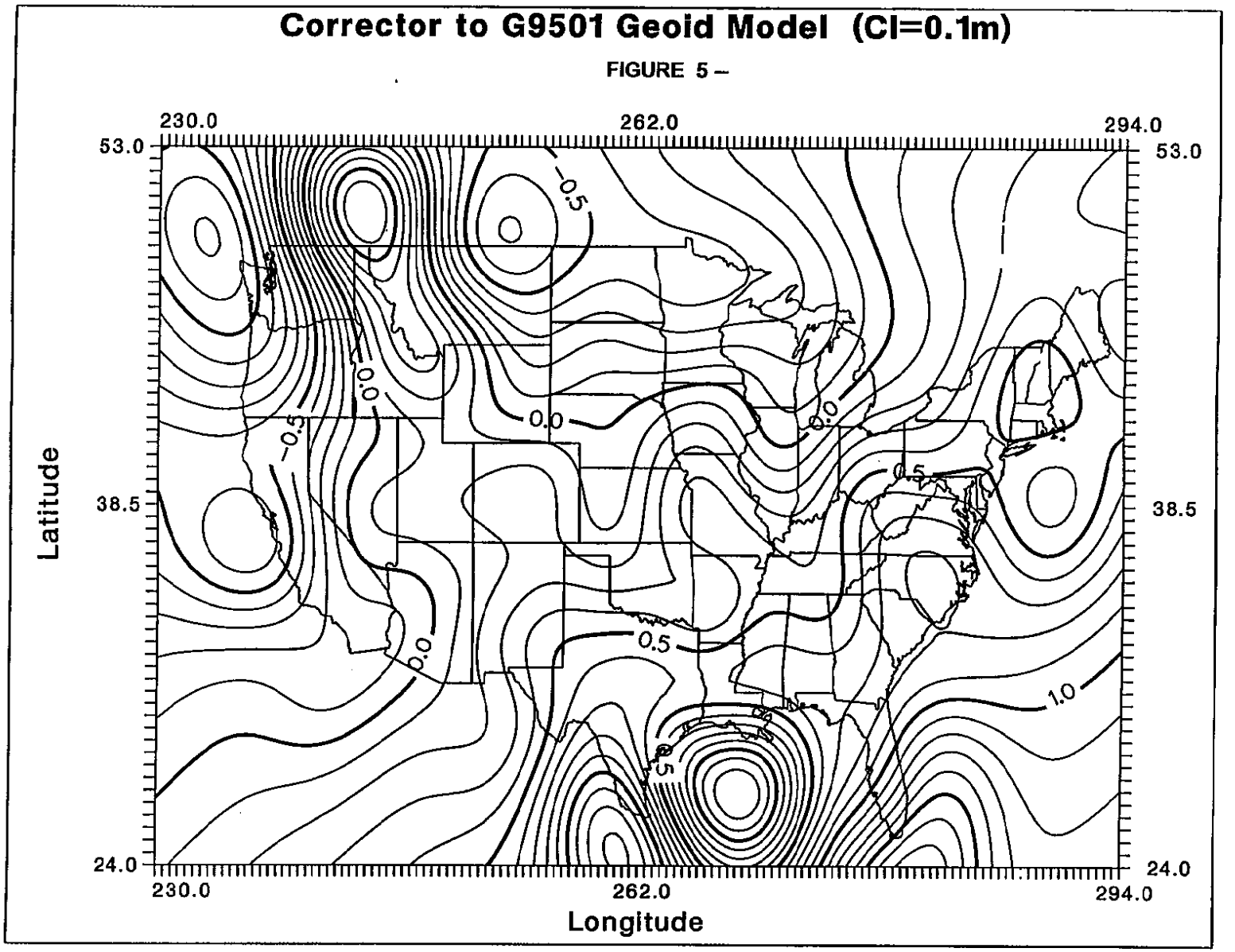
Corrector to G9501 Geoid Model (CI=0.1m)
230.0
262.0
294.0
53.0
38.5
24.0
Latitude
Longitude
-0.5
0.0
0.5
1.0

FIGURE 5 –

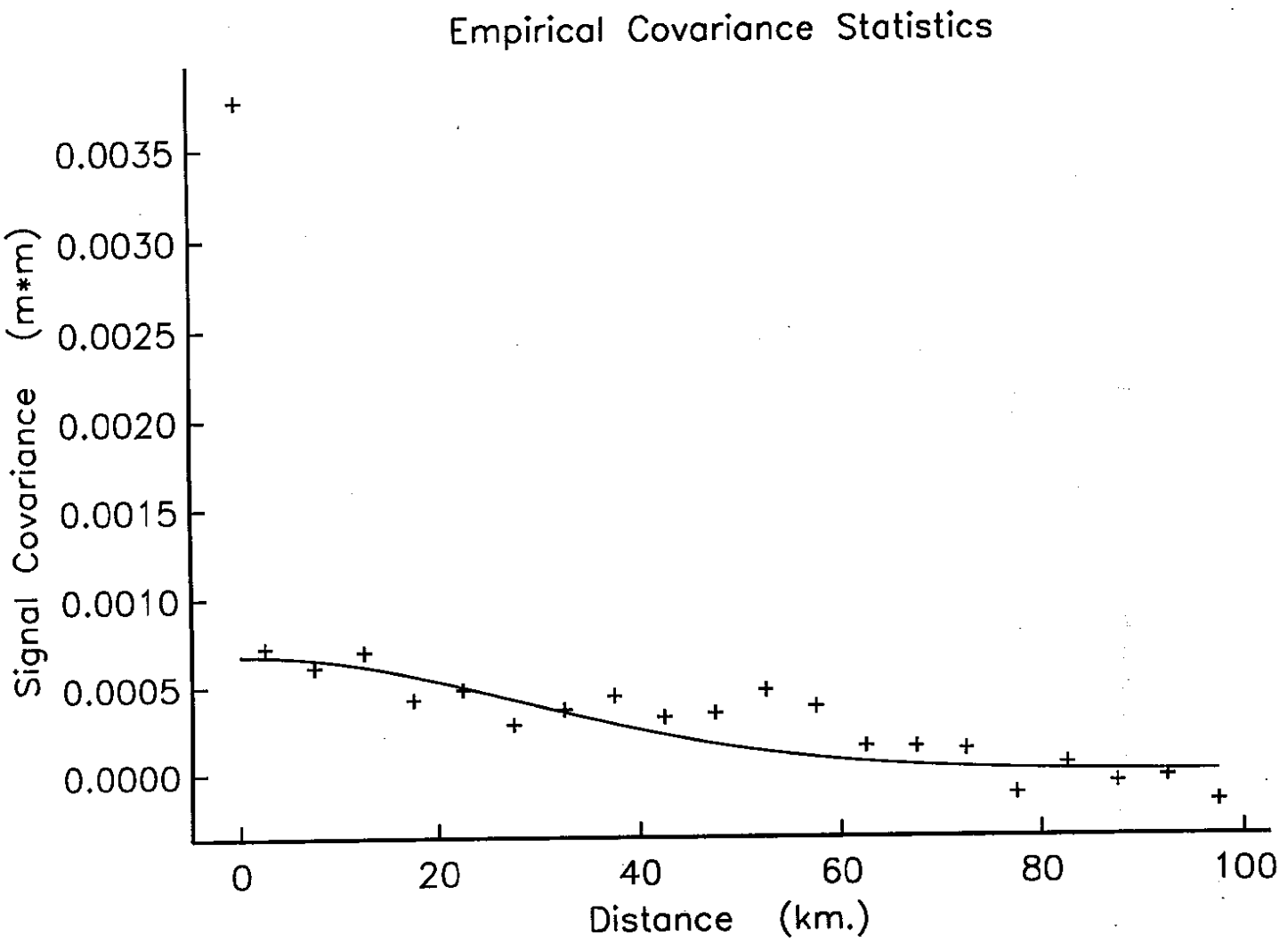
Empirical Covariance Statistics
Signal Covariance (m*m)
0.0035
0.0030
0.0025
0.0020
0.0015
0.0010
0.0005
0.0000
0
20
40
60
80
100
Distance (km.)

FIGURE 6 –

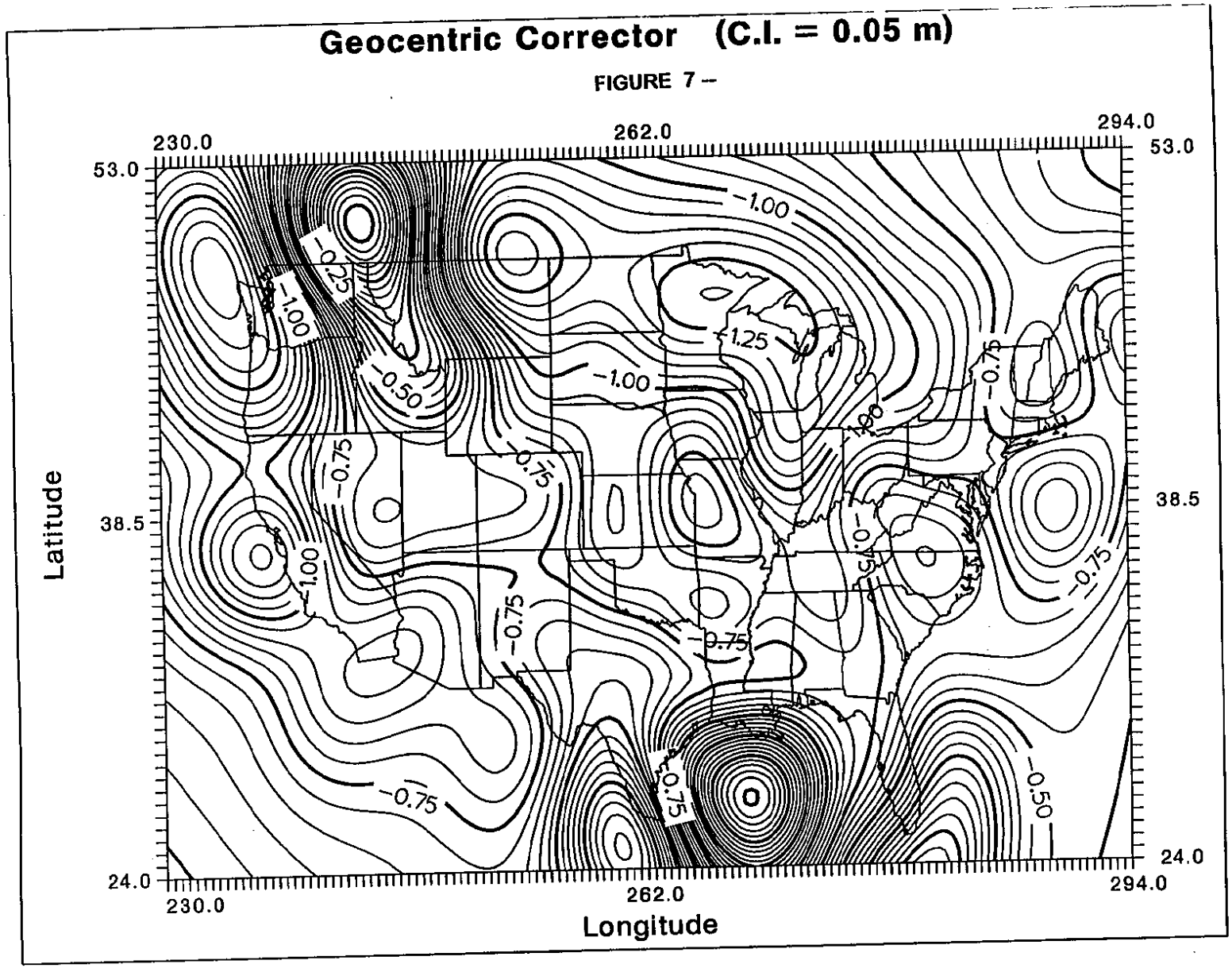
Geocentric Corrector (C.I. = 0.05 m)
230.0
262.0
294.0
53.0
38.5
24.0
Latitude
Longitude
-1.00
-0.25
-0.50
-0.75
1.25
-0.00

FIGURE 7 –

FFT GEOID COMPUTATIONS IN CANADA

Michael G. Sideris
Department of Geomatics Engineering
The University of Calgary
Calgary, Alberta, Canada

ABSTRACT

The paper outlines the currently available FFT methods of geoid computation and their application in recent geoid computations in Canada. More specifically, the various ways of evaluating the Stokes integral (e.g. using planar approximation, mean-latitude spherical approximation, analytical kernel spectrum, and rigorous one-dimensional spherical evaluation) are presented and intercompared. The applicability of these methods to the computation of the direct and indirect effect of the topography is discussed as well, and recommendations are made for improving the accuracy, memory requirements, data handling and efficiency of the techniques. Finally, recent FFT-based solutions for the Canadian geoid are compared to other geoid solutions and to results from GPS and leveling on benchmarks. Accuracy estimates are given, indicating that, with proper treatment of datum discrepancies, the absolute geoid undulation accuracy can reach a level of 4 cm while the relative accuracy can reach sub-ppm levels for baselines with length varying from tens of kilometres to more than 1000 kilometres.

1. INTRODUCTION - GEOID AND TERRAIN REDUCTIONS

Stokes' boundary value problem (BVP) is the gravimetric determination of the geoid Γ, which is the equipotential surface of the Earth's gravity field corresponding to the mean sea level. Stokes problem deals with the determination of a potential, harmonic outside the masses, from gravity anomalies Δg given everywhere on the geoidal surface. Consequently, since no masses are allowed outside Γ, the topography of the Earth must be eliminated mathematically. Assuming that Γ encloses all masses, the classical BVP is to determine the disturbing potential T, which satisfies Laplace's equation under the a boundary condition on Γ, which is given by the "fundamental equation of physical geodesy" (Heiskanen and Moritz, 1967). Dividing T by the normal gravity γ (Bruns' equation), we obtain the geoid undulation N as

$$N = \frac{T}{\gamma} = \frac{R}{4\pi\gamma} \iint_{\sigma} \Delta g S(\psi) d\sigma = \frac{1}{\gamma} S\Delta g, \tag{1}$$

where S is Stokes' operator, R is the mean radius of the Earth, and σ denotes the Earth's surface. $S(\psi)$ is Stokes' function and is given by the expression

$$S(\psi) = \frac{1}{\sin(\psi/2)} - 6\sin\frac{\psi}{2} + 1 - 5\cos\psi - 3\cos\psi \ln(\sin\frac{\psi}{2} + \sin^2\frac{\psi}{2}), \tag{2}$$

$$\sin^2\frac{\psi}{2} = \sin^2\frac{\varphi_P - \varphi}{2} + \sin^2\frac{\lambda_P - \lambda}{2}\cos\varphi_P\cos\varphi. \tag{3}$$

ψ is the spherical distance between the data point (φ, λ) and the computation point (φ_P, λ_P).

Equation (1) gives N provided that there are no masses outside the geoidal surface. One way to take care of the topographic masses of density ρ (usually assumed constant) is Helmert's condensation reduction, which is used here as a representative from a number of possible terrain reductions. It is applied as follows: (a) remove all masses above the geoid; (b) lower station from point P on the Earth's surface to point P_O on the geoid using the free-air reduction F; and (c) restore the masses condensed on a layer on the geoid with density $\sigma = \rho H$, where H is the orthometric height. This procedure gives the gravity anomaly on the geoid computed from the expression $\Delta g_o = \Delta g_P - A_P + F + A^c_{P_o} = \Delta g_P + F + \delta A = \Delta g^{FA} + \delta A$. $\Delta g^{FA} = (\Delta gP + F)$ is the free-air gravity anomaly at P, A_P is the attraction of the topography above the geoid at P, and $A^c_{P_o}$ is the attraction of the condensed topography at P_o.

Obviously, the attraction change δA is not the only change associated with this reduction. Due to the shifting of masses, the potential changes as well by an amount $\delta T = T_{P_o} - T^c_{P_o}$ called the indirect effect on the potential, where T_{P_o} is the potential of the topographic masses at P_o and $T^c_{P_o}$ is the potential of the condensed masses at P_o. Due to this potential change, the use of eq. (1) with Δg_o produces not the geoid but a surface called the co-geoid. Thus, before applying Stokes' equation, the gravity anomalies must be transformed from the geoid to the co-geoid by applying a small correction $\delta\Delta g = \partial\gamma/\partial h \delta T/\gamma$ called the indirect effect on gravity; this is usually small ($\delta\Delta g < 1$ *mGal*) and is omitted in most cases. The final expression giving N can now be written as

$$N = \frac{1}{\gamma} S(\Delta g^{FA} + \delta A + \delta\Delta g) + \frac{1}{\gamma}\delta T = N^c + \delta N, \tag{4}$$

where N^c is the co-geoidal height and δN is the indirect effect on the geoid. The attraction change is equal to the classical terrain correction c; for more discussion, see Wichiencharoen (1982), Wang and Rapp (1990) and Sideris (1990). In linear approximation, using k for Newton's gravitational constant and $l = [(x_P - x)^2 + (y_P - y)^2]^{1/2}$,

$$\delta A = c = \frac{1}{2} k\rho \iint_E \frac{H^2 - H_P^2}{l^3} dxdy - H_P k\rho \iint_E \frac{H - H_P}{l^3} dxdy, \tag{5}$$

$$\delta N = -\frac{\pi k\rho}{\gamma} H_P^2 - \frac{k\rho}{6\gamma} \iint_E \frac{H^3 - H_P^3}{l^3} dxdy. \tag{6}$$

The use of eq. (1) requires gravity anomalies all over the Earth for the computation of a single geoid undulation. Obviously, this is impractical to say the least and thus, in practice, some modifications of the technique are necessary. Firstly, we can only apply eq. (1) in a limited region. Then, the long wavelength contributions of the gravity field will not be present in the results and must be computed in another way. They are provided by a set of spherical harmonic coefficients (geopotential model). Secondly, the integral is discretized and is computed as a summation using discrete data. Due to the density of the gravity data, which on the average is no better than 5' × 5', the short wavelengths will not be present (aliased). They are computed by using topographic heights, which are usually given in the form of a 1 km × 1 km Digital Terrain Model (DTM). The computation of geoid undulations N by combining a geopotential model (GM), mean free air gravity anomalies Δg^{FA}, and heights H in a DTM is based on the following formula:

$$N = N^{GM} + N^{\Delta g} + N^{H}, \qquad \Delta g = \Delta g^{FA} - \Delta g^{GM} - \Delta g^{H}. \tag{7}$$

Although geoid undulations are more sensitive to the low to medium frequencies of the field, in rough topography all three data sets are necessary for estimating N. Note that the gravity anomalies used with Stokes' equation have the contributions of the topography and the GM removed. Thus, the remove (preprocessing) stage involves the computation and removal of the GM and terrain contributions from the free-air gravity anomalies, and the restore (postprocessing) step involves the restoration of the GM contribution and the terrain contribution to N via the indirect effect term N^H. With Helmert's condensation reduction, $\Delta g^H = -\delta A = -c$ and $N^H = \delta N = \delta T/\gamma$.

In spherical approximation, the geopotential model part of Δg and N is given by the following formulas (see, e.g., Kearsley et al., 1985):

$$\Delta g^{GM} = G\sum_{n=2}^{n_{max}}(n-1)\sum_{m=0}^{n}[C_{nm}\cos m\lambda_P + S_{nm}\sin m\lambda_P]P_{nm}(\sin\varphi_P), \tag{8}$$

$$N^{GM} = R\sum_{n=2}^{n_{max}}\sum_{m=0}^{n}[C_{nm}\cos m\lambda_P + S_{nm}\sin m\lambda_P]P_{nm}(\sin\varphi_P), \tag{9}$$

where C_{nm}, S_{nm} are the fully normalized geopotential coefficients of the anomalous potential, P_{nm} are the fully normalized Legendre functions (Heiskanen and Moritz, 1967), φ and λ are geocentric latitude and longitude, n_{max} is the maximum degree of the geopotential model, and G is the mean gravity of the Earth.

2. GEOID UNDULATIONS BY FFT

2.1. Planar Approximation Of Stokes' Integral

Point gravity anomalies as input. The geoidal height $N^{\Delta g}$ computed from Δg's given by eq. (1) in an area E can be expressed in planar approximation by a two-dimensional convolution integral (Kearsley et al., 1985). Using $M \times N$ gridded point gravity anomalies with spacing Δx and Δy, the geoid undulation at a point (x_k, y_l) can be evaluated by the following discrete convolution, denoted by $*$:

$$\begin{aligned} N^{\Delta g}(x_k, y_l) &= \frac{1}{2\pi\gamma}\sum_{i=0}^{M-1}\sum_{j=0}^{N-1}\Delta g(x_i, y_j)\, l_N(x_k - x_i, y_l - y_j)\Delta x\Delta y \\ &= \frac{\Delta x\Delta y}{2\pi\gamma}\Delta g(x_k, y_l) * l_N(x_k, y_l), \end{aligned} \tag{10}$$

$$l_N(x_k - x_i, y_l - y_j) = \begin{cases} [(x_k - x_i)^2 + (y_l - y_j)^2]^{-1/2}, & x_k \neq x_i \ \text{ or } \ y_l \neq y_j \\ 0, & x_k = x_i \ \text{ and } \ y_l = y_j \end{cases}. \tag{11}$$

To account for the singularity of l_N, the kernel is set to zero at the origin (see eq. 11) and the contribution to $N^{\Delta g}$ of the gravity anomaly at the computation point must be evaluated separately. Approximately, this contribution is (Heiskanen and Moritz, 1967; Schwarz et al., 1990)

$$dN^{\Delta g}(x_k, y_l) \approx \frac{\sqrt{\Delta x \Delta y}}{\gamma\sqrt{\pi}} \Delta g(x_k, y_l). \tag{12}$$

A slightly better approximation for $dN^{\Delta g}$ can be found in Haagmans et al. (1993). Geoid undulations can then be evaluated by the two-dimensional (2D) FFT as follows:

$$\begin{aligned} N^{\Delta g}(x_k, y_l) &= \frac{\Delta x \Delta y}{2\pi\gamma} F^{-1}\{F\{\Delta g(x_k, y_l)\}\, F\{l_N(x_k, y_l)\}\} \\ &= \frac{\Delta x \Delta y}{2\pi\gamma} F^{-1}\{\Delta G(u_m, v_n)\, L_N(u_m, v_n)\}, \end{aligned} \tag{13}$$

where F denotes the direct and F^{-1} denotes the inverse 2D discrete Fourier transform (DFT), and u and v are the frequencies corresponding to x and y, respectively. ΔG has to be computed by the DFT while L_N can be evaluated either by the DFT or by the continuous Fourier transform (CFT) which gives $L_N = (u^2 + v^2)^{-1/2} = q^{-1}$, where q is the radial frequency, and then be discretized for use in eq. (13). L_N defined as q^{-1} is called the analytically-defined spectrum of Stokes' kernel. Although the analytically-defined spectrum has some advantages compared with the discrete one, such as no DFT required for its evaluation and no effect of leakage and aliasing, it is not suitable for the computation of discrete convolution if we want the results to be the same as those from numerical integration. For more details and numerical results, Li (1993) and Sideris and Li (1993) should be consulted.

Equations (10) and (13) show clearly how FFTs can be used for the efficient evaluation of convolutions. Thus, in the sequel, we will only show how to give convolution form to the various integrals of interest without writing explicit formulas for their FFT-evaluation.

Mean gravity anomalies as input. If the input data are $M \times N$ gridded mean gravity anomalies $\overline{\Delta g}$, eqs. (10) and (13) still hold with $\overline{\Delta g}$ and $\overline{\Delta G}$ in place of Δg and ΔG, and $\overline{l_N}$ and $\overline{L_N}$ in place of $\Delta x \Delta y l_N$ and $\Delta x \Delta y L_N$, respectively, with

$$\begin{aligned} \overline{l_N}(x_k, y_l) &= \int_{x_k-\Delta x/2}^{x_k+\Delta x/2} \int_{y_l-\Delta y/2}^{y_l+\Delta y/2} \frac{1}{\sqrt{x^2+y^2}} dxdy \\ &= x\ln(y+\sqrt{x^2+y^2}) + y\ln(x+\sqrt{x^2+y^2}) \Big|_{x_k-\Delta x/2}^{x_k+\Delta x/2} \Big|_{y_l-\Delta y/2}^{y_l+\Delta y/2}. \end{aligned} \tag{14}$$

We call $\overline{L_N}$ the mean Stokes' kernel spectrum. An alternative approach can be found in Sideris and Tziavos (1988).

2.2. Spherical Form Of Stokes' Integral

The approximations introduced by the planar form of Stokes' integral can be minimized or avoided by using the spherical Stokes' integral. With gridded gravity anomalies, taking into account eq. (3), the spherical form of Stokes' integral, i.e. eq. (1), can be written explicitly as

$$N^{\Delta g}(\varphi_l, \lambda_k) = \frac{R}{4\pi\gamma} \sum_{j=0}^{N-1} \sum_{i=0}^{M-1} \Delta g(\varphi_j, \lambda_i) \cos\varphi_j \, S(\varphi_l, \lambda_k, \varphi_j, \lambda_i) \Delta\varphi\Delta\lambda. \tag{15}$$

With different approximations of Stokes' kernel function on the sphere, geoid undulations can be evaluated at all gridded points simultaneously by means of either the one-dimensional (1D) or the 2D fast Fourier transform.

Approximated spherical kernel. In order to transform eq. (15) into a convolution integral, Strang van Hees (1990) suggested to approximate $cos\varphi_P cos\varphi$ in eq. (3) by $cos^2\overline{\varphi}$, or by the slightly more accurate $cos^2\overline{\varphi}$ - $sin^2(\phi_P - \phi)/2$, where $\overline{\varphi}$ is the mean latitude of the computation area. In this case, eq. (3) becomes

$$\begin{aligned} sin^2\frac{\psi}{2} &\approx sin^2\frac{\varphi_p-\varphi}{2}+sin^2\frac{\lambda_p-\lambda}{2}cos^2\overline{\varphi} \\ &\approx sin^2\frac{\varphi_p-\varphi}{2}+sin^2\frac{\lambda_p-\lambda}{2}(cos^2\overline{\varphi}\,sin^2\frac{\varphi_p-\varphi}{2}) \end{aligned} \tag{16}$$

and eq. (15) takes the convolution form

$$\begin{aligned} N^{\Delta g}(\varphi_l,\lambda_k) &= \frac{R}{4\pi\gamma}\sum_{j=0}^{N-1}\sum_{i=0}^{M-1}\Delta g(\varphi_j,\lambda_i)cos\varphi_j S(\varphi_l-\varphi_j,\lambda_k-\lambda_i,\overline{\varphi})\Delta\varphi\Delta\lambda \\ &= \frac{R\Delta\varphi\Delta\lambda}{4\pi\gamma}[\Delta g(\varphi_l,\lambda_k)cos\varphi_l]*S(\varphi_l,\lambda_k,\overline{\varphi}). \end{aligned} \tag{17}$$

The approximation of eq. (15) by eq. (17) makes it possible to compute geoid undulations over large areas on the sphere on all grid points simultaneously by using the two-dimensional Fourier transform. Its disadvantages are that it requires considerable amounts of computer memory because 100% zeros are padded in the latitude and longitude direction, and that additional errors are introduced due to the approximation made on the kernel function. This error can be minimized by the use of the multi-band spherical FFT method proposed by Forsberg and Sideris (1993), which is briefly described below.

Approximated Spherical Kernel With Many Bands. Since the errors of the above approximation increase from the centre of the area to the north and south edges, Forsberg and Sideris (1993) proposed to subdivide the area in t narrow overlapping bands along the longitude direction. To improve the approximation in eq. (16), $cos\varphi_P cos\varphi$ can be written as $cos\varphi_P cos[\varphi_P - (\varphi_P - \varphi)]$. In each sub-area, φ_P can be considered as constant and again taken as equal to the mean latitude $\overline{\varphi}_t$. In this case, eq. (3) is approximated by

$$\begin{aligned} sin^2\frac{\psi}{2} &\approx sin^2\frac{\varphi_p-\varphi}{2}+sin^2\frac{\lambda_p-\lambda}{2}cos\overline{\varphi}_t cos[\overline{\varphi}_t-(\overline{\varphi}_t-\varphi)] \\ &\approx sin^2\frac{\varphi_p-\varphi}{2}+sin^2\frac{\lambda_p-\lambda}{2}[cos^2\overline{\varphi}_t cos(\overline{\varphi}_t-\varphi) \\ &+ cos\overline{\varphi}_t sin\overline{\varphi}_t sin(\overline{\varphi}_t-\varphi)] \end{aligned} \tag{18}$$

and again the computations are done using eq. (17) for each band (with $\overline{\varphi}_t$ in place of $\overline{\varphi}$). Note that for all points along the parallel of mean latitude, an exact solution to the spherical Stokes' integral is obtained.

Rigorous Spherical Kernel. To overcome the limitations of the previous 2D FFT method, Haagmans et al. (1993) made use of the fact that it provides the exact undulations for all the points along the parallel of mean latitude. Using this property and the addition theorem of the Fourier transform, they came up with an approach which allows for the evaluation of the true discrete spherical Stokes integral without approximation, parallel by parallel, by means of the 1D FFT. In fact, for results on a certain parallel of latitude φ_l using data along a parallel of

latitude φ_j, ψ changes only with λ_k-λ_i and Δg changes only with λ_j and thus the 2D discrete Stokes integral of eq. (15) takes the form

$$N(\varphi_l,\lambda_k)=\frac{R}{4\pi\gamma}\sum_{j=0}^{N-1}\Big[\sum_{i=0}^{M-1}\Delta g(\varphi_j,\lambda_i)\cos\varphi_j S(\varphi_l,\varphi_j,\lambda_k-\lambda_i)\Delta\lambda\Big]\Delta\varphi,\quad \varphi_l=\varphi_1,\varphi_2,\ldots,\varphi_N. \tag{19}$$

The brackets in eq. (19) contain a one-dimensional discrete convolution with respect to λ, i.e., along a parallel, and can be evaluated by the one-dimensional (1D) FFT. By employing the addition theorem of DFT, the discrete Stokes integral for the fixed parallel can be evaluated by (Haagmans et al., 1993)

$$N(\varphi_l,\lambda_k)=\frac{R\Delta\varphi\Delta\lambda}{4\pi\gamma}F_1^{-1}\Big\{\sum_{j=0}^{N-1}F_1\{\Delta g(\varphi_j,\lambda_k)\cos\varphi_j\}F_1\{S(\varphi_l,\varphi_j,\lambda_k)\}\Big\},\quad \varphi_l=\varphi_1,\varphi_2,\ldots,\varphi_N, \tag{20}$$

where F_1 and F_1^{-1} denote the 1D Fourier transform operator and its inverse. Equation (20) yields the geoidal heights for all the points on one parallel which are identical to those obtained by direct summation using eq. (15) point by point.

The major advantage of the 1D spherical FFT approach is that it gives exactly the same results as those obtained by direct numerical integration. In addition, it only needs to deal with one one-dimensional complex array each time, resulting in a considerable saving in computer memory as compared to the 2D FFT technique discussed before. Moreover, the adoption of FFT makes it far more computationally efficient than the classical direct numerical integration. Detailed comparisons of various techniques can be found in Haagmans et al. (1993) and Forsberg and Sideris (1993).

To obtain results which are identical to those from numerical integration, proper zero-padding must be applied to the data; for details, see Sideris and Li (1992 and 1993) and Li (1993). This is true for both the spherical and the planar approximations of Stokes' integral. They also hold for the terrain correction integrals that will be discussed below and, in general, for any other gravity field convolution integrals evaluated by FFT.

3. FFT-EVALUATION OF TERRAIN EFFECTS

Defining the kernel function $l_c(x,y) = (x^2 + y^2)^{-3/2}$, the terrain effects given by eqs. (5) and (6) can be written in convolution forms. The singularity of the l_c kernel function is again bypassed by setting $l_c(0,0) = 0$. This is of no practical consequence because these integrals contain not the heights but the height differences which are zero when $x = x_P$ and $y = y_P$. For a detailed discussion on the singularity of the terrain correction formula, Klose and Ilk (1993) should be consulted.

Point Heights As Input. Using $M \times N$ gridded point heights, eq. (5) can written as

$$c(x_k,y_l)=\frac{1}{2}k\rho\sum_{i=0}^{M-1}\sum_{j=0}^{N-1}\frac{H^2(x_i,y_j)-H^2(x_k,y_l)}{[(x_k-x_i)^2+(y_l-y_j)^2]^{3/2}}\Delta x\Delta y$$
$$-H(x_k,y_l)k\rho\sum_{i=0}^{M-1}\sum_{j=0}^{N-1}\frac{H(x_i,y_j)-H(x_k,y_l)}{[(x_k-x_i)^2+(y_l-y_j)^2]^{3/2}}\Delta x\Delta y$$

$$= \frac{1}{2} k\rho \Delta x \Delta y \{ H^2(x_k, y_l) * l_c(x_k, y_l) - H^2(x_k, y_l)[o(x_k, y_l) * l_c(x_k, y_l)] \qquad (21)$$
$$- 2H(x_k, y_l)[H(x_k, y_l) * l_c(x_k, y_l) - H(x_k, y_l)\{o(x_k, y_l) * l_c(x_k, y_l)\}]\},$$

where $o(x_k y_l)$ has the value of one, i.e. $o(x_k y_l) = 1$, for all grid points.

Similarly, the indirect effect on the geoid, which is given by eq. (6), can be written in the convolution form

$$\delta N(x_k, y_l) = -\frac{\pi k \rho}{\gamma} H^2(x_k, y_l) - \frac{k\rho}{6\gamma} \sum_{i=0}^{M-1} \sum_{j=0}^{N-1} \frac{H^3(x_i, y_j) - H^3(x_k, y_l)}{[(x_k - x_i)^2 + (y_l - y_j)^2]^{3/2}} \Delta x \Delta y$$
$$= -\frac{\pi k \rho}{\gamma} H^2(x_k, y_l) - \frac{k\rho}{6\gamma} \Delta x \Delta y \{ H^3(x_k, y_l) * l_c(x_k, y_l) \qquad (22)$$
$$- H^3(x_k, y_l)[o(x_k, y_l) * l_c(x_k, y_l)]\}.$$

Mean Heights As Input. If the input are $M \times N$ mean gridded heights $\overline{H}$, the above equations still hold with $\overline{H}^n$ in place of H^n, $n = 1,2,3$, and l_c in place of $\Delta x \Delta y l_c$, with

$$\bar{l}_c(x_k, y_l) = \int_{x_k - \Delta x/2}^{x_k + \Delta x/2} \int_{y_l - \Delta y/2}^{y_l + \Delta y/2} \frac{1}{(x^2 + y^2)^{3/2}} dx dy = \frac{(x^2 + y^2)^{1/2}}{xy} \Big|_{x_k - \Delta x/2}^{x_k + \Delta x/2} \Big|_{y_l - \Delta y/2}^{y_l + \Delta y/2} \qquad (23)$$

It is interesting to mention here that the above equations can also be evaluated by using an analytical kernel spectrum. Although they then require fewer Fourier transformations, this approach is not recommended for numerical evaluations. The reasons are the same as those given for Stokes' integral. Thus, to obtain by FFT identical results as those from numerical integration, the discrete kernel should be used and all convolutions should be evaluated using proper zero-padding; see more details in Li (1993), Sideris (1994b), Li and Sideris (1994a and 1994b).

Gravity terrain corrections can also be computed by the three-dimensional fast Fourier transform (3D FFT) method. A detailed description of the 3D FFT method along with numerical results can be found in Peng (1994) and Peng et al. (1995).

4. COMPARISON OF *N* OBTAINED WITH DIFFERENT KERNEL FUNCTIONS

To investigate how seriously the approximations of Stokes' kernel affect the results, geoid undulations were computed in all of Canada. The data used were 5' × 5' Faye gravity anomalies (terrain effects were computed using a 1 km × 1 km DTM) and the OSU91A geopotential model. In the computations, 100% zeros (50% to each side) were padded around the gravity anomalies in both the East-West and the North-South directions when the 2D FFT method was used, and only in the East-West direction when the 1D FFT method, i.e., eq. (20), was used. The Canadian geoid computed by the 1D FFT method is shown in Figure 1.

The statistical information of the differences between using the "rigorous spherical kernel" (RSK), i.e. eqs. (2) and (19), and the various approximate kernels is summarized in Table 1. More specifically, ASK stands for "approximated spherical kernel" (see eqs. 16, 17), APK stands for "approximated planar kernel" (see eqs. 10 and 11), and ADK stands for "analytically

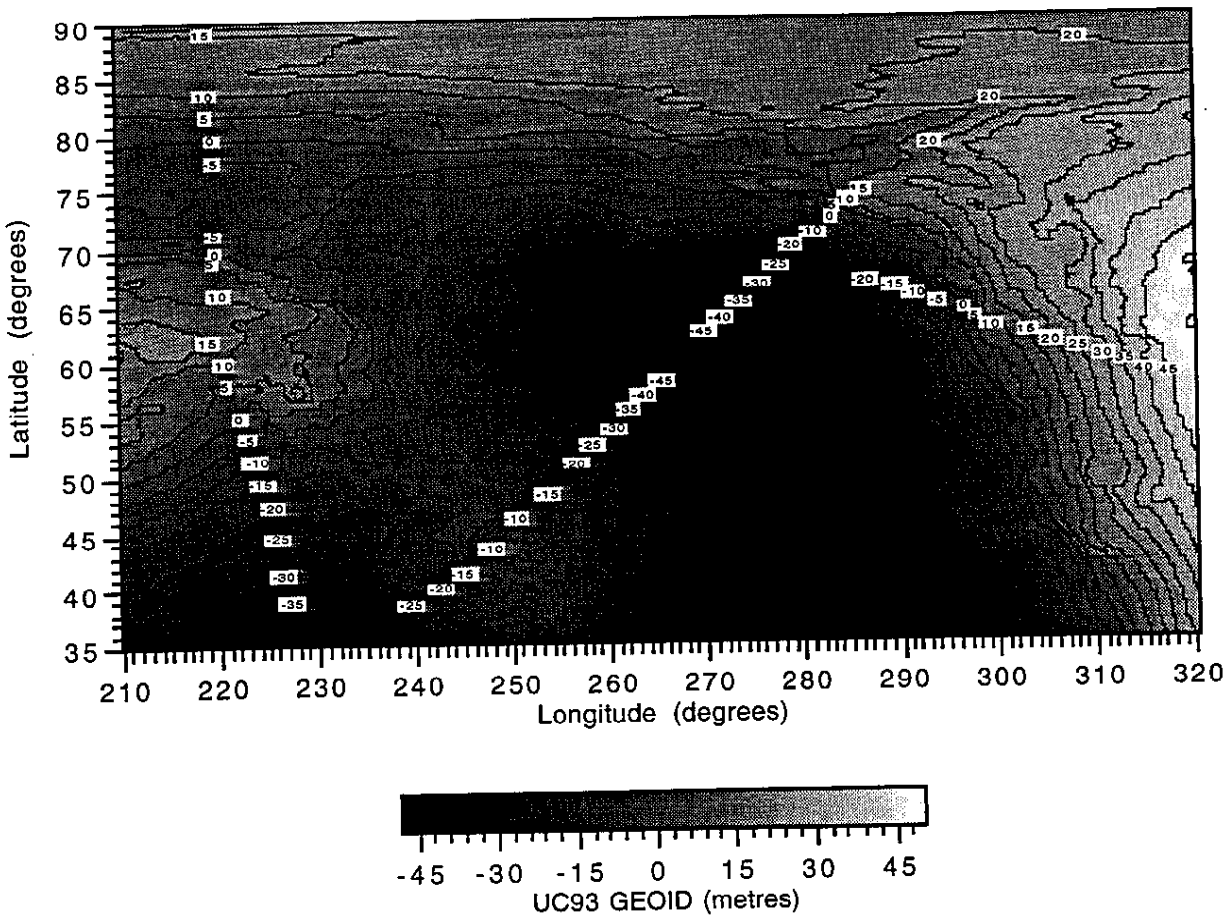

Figure 1 - Contour map of the UC93 Canadian geoid

defined kernel" spectrum, i.e., $L_N = q^{-1}$. As can be seen from Table 1, the geoid undulation errors introduced by the use of the approximated kernels are about 1 to 2 m in terms of maximum or minimum values. It is obvious that these errors are not negligible for precise geoid determination. According to Table 1, the approximated planar kernels, especially the analytically-defined kernel spectrum, introduce 50% larger geoid errors as compared with those due to the use of the approximated spherical kernel. This is because the planar kernels only use the first term in the spherical Stokes kernel, and neglect the meridian convergence. More explanations about this can be found in Sideris and Li (1993) and Li (1993).

Table 1
Comparison of geoid undulations from different kernel functions, in metres

Differences	Max	Min	Mean	RMS	σ
RSK - ASK	1.32	-0.98	-0.03	0.20	0.19
RSK - APK	0.97	-1.42	-0.11	0.31	0.29
RSK - ADK	1.47	-1.89	-0.09	0.32	0.31
APK - ADK	1.08	-1.23	0.01	0.07	0.07

It was found that the geoid errors due to the use of the approximated spherical kernel were relatively larger in the north and the south boundary areas than in the area around the centre latitude. This was the result of using $cos^2\bar{\varphi}$ instead of $cos\varphi_P cos\varphi$, while the differences

between $cos^2\bar{\varphi}$ and $cos\varphi_p cos\varphi$ were smaller in the area around the central latitude of the computation area. On the other hand, the geoid errors due to the use of the planar Stokes formula had a tendency of decrease from the north to the south area. This was expected because the neglect of the meridian convergence has a more serious effect at higher latitudes.

5. GEOID COMPARISONS AT GPS BENCHMARKS

First, comparisons were made on 280 benchmarks in the mountainous province of British Columbia (B.C.) using different kernel functions. Figure 2 shows the locations of the GPS stations on benchmarks in Western Canada. Table 2 summarizes the statistics of the differences before and after fitting out the systematic biases and tilts by using a four-parameter transformation; see Heiskanen and Moritz (1967) and Sideris (1993). Table 2 indicates that the overall agreement between the gravimetric and the GPS/leveling-derived geoid is around 30 cm

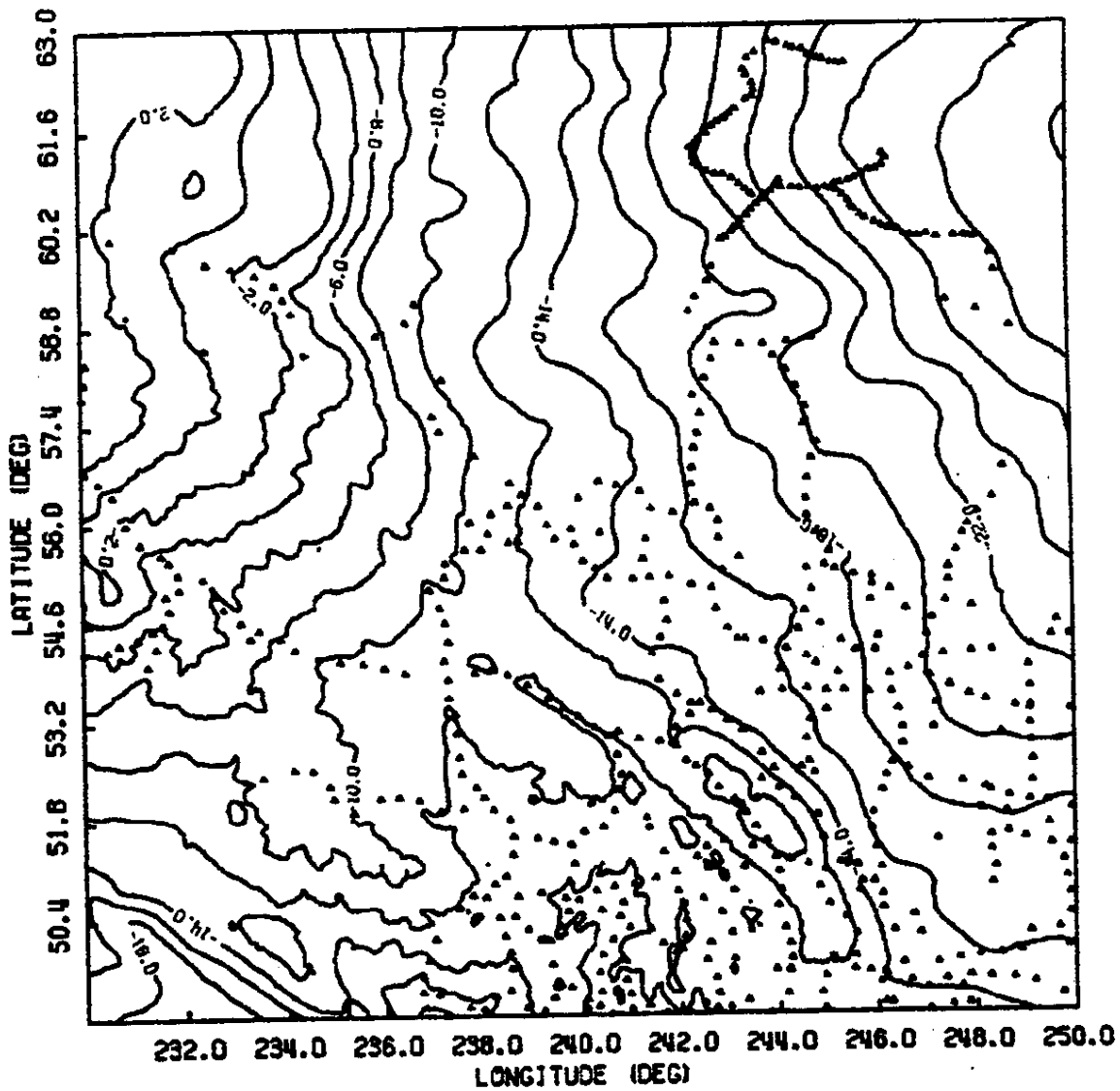

Figure 2 - Location of GPS stations in Western Canada (geoid contour interval: 2 m)

in terms of standard deviation (σ), and there exist systematic biases between the two kinds of geoid representations with a mean value of about 3 m. This systematic biases are due to the

systematic difference between the gravimetric geoid and the orthometric height datum as well as the long wavelength errors in the gravimetric geoid. After fitting out the systematic biases, it can be seen that there is a 7 cm improvement for the standard deviations of the differences. The remaining differences, mainly due to the effect of the high frequency errors in the reduced Faye gravity anomalies, the errors in leveling and in GPS-derived ellipsoidal heights, and the geopotential coefficient errors, can only be further reduced by improving the data accuracy and, probably, by using a smaller grid size for the gravity anomalies and heights.

Table 2

Comparison of the gravimetric with the GPS/leveling-derived undulations in B.C., in metres, before and after fit (in parentheses) for different kernel functions

Differences	Max	Min	Mean	RMS	σ
GPS/leveling - RSK	-1.93 (1.20)	-4.34 (-0.74)	-3.23 (0.00)	3.25 (0.24)	0.30 (0.24)
GPS/leveling - ASK	-2.10 (1.08)	-4.20 (-0.71)	-3.26 (0.00)	3.27 (0.23)	0.29 (0.23)
GPS/leveling - APK	-1.75 (1.17)	-4.12 (-0.75)	-3.05 (0.00)	3.07 (0.26)	0.33 (0.26)
GPS/leveling - ADK	-0.85 (1.68)	-4.42 (-1.04)	-2.93 (0.00)	2.95 (0.36)	0.38 (0.35)

Table 2 also shows that, for absolute geoid determination, all kernel functions, except for the analytically-defined one, have a similar performance in terms of either the root-mean-square differences or the maximum and minimum differences. This, however, does not imply that the use of the approximated kernel functions does not introduce additional errors. The similar performance indicated by Table 2 is because the GPS/leveling benchmarks used in the comparisons are located within the mean latitude area of the whole computational region, where the geoid errors due to the use of the approximated kernel functions are much smaller. The use of the analytically-defined kernel spectrum results in a 10 cm larger root-mean-square difference, and about 90 cm larger range between maximum and minimum differences.

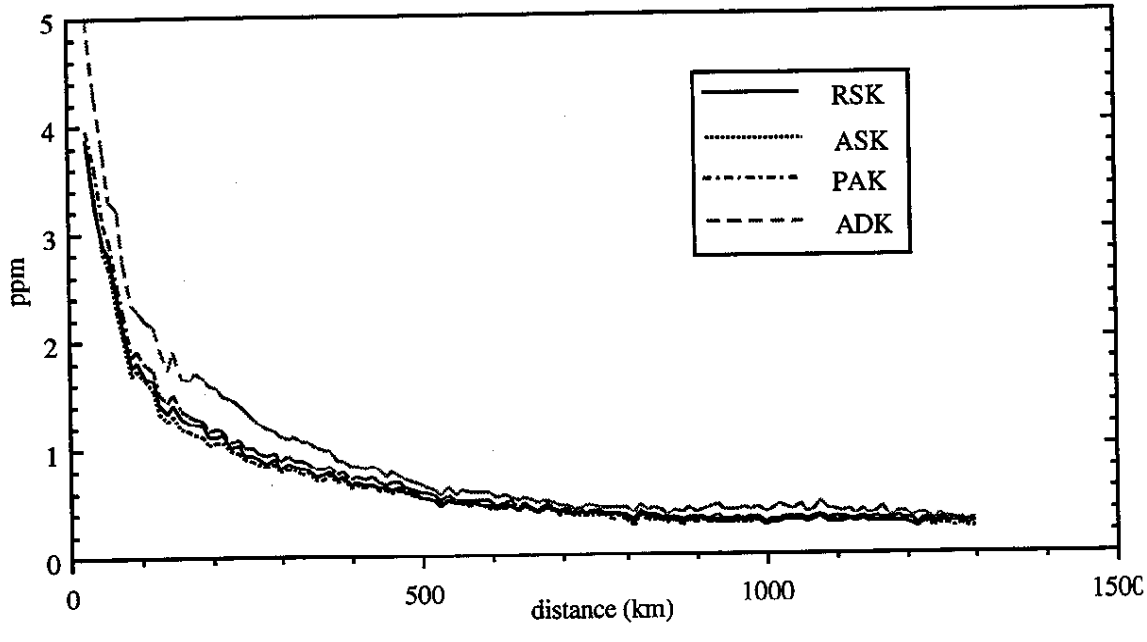

Figure 3 - Relative differences between the gravimetric and the GPS/leveling-derived geoid on 280 benchmarks in British Columbia (after fit) for different kernel functions

Figure 3 shows the relative differences between the two geoid representations in ppm. According to this figure, the use of both the spherical kernels and the approximated planar kernel provides similar relative differences: about 1 to 4 ppm for distances of 20 km to 200 km, and 0.4 to 1 ppm for distances of 200 to 800 km. The use of the analytically-defined kernel spectrum results in a little bit larger relative differences.

Comparisons were also made in the three GPS/leveling networks in the mostly flat province of Alberta. Table 3 gives the statistics of the differences, and Figure 4 shows the relative differences, in ppm, after fitting out the systematic biases, and intercompares them to those obtained in British Columbia. Table 3 shows that, in Alberta, the gravimetric geoid agrees very well with the GPS/leveling-derived geoid. After fit, the maximum difference is only about 15 cm while the standard deviation is less than 6 cm. The relative agreement between the geoids in Alberta, as shown in Figure 4, is about 0.5 to 1.4 ppm for distances between 30 and 100 km, and about 0.3 to 0.5 ppm for distances of 100 to 200 km. Similar relative agreements have also been achieved in other computation areas, such as the Great Slave Lake area in the Northwest Territories (She, 1993; Sideris, 1993). This relative agreement is of the same order as the required relative accuracy of the first-order leveling according to the Canadian specifications for vertical control networks (Schwarz et al., 1987).

Table 3
Comparison of the gravimetric with the GPS/leveling-derived undulations in Alberta, in metres

Area (# of points)	Max	Min	Mean	RMS	σ
Northern Alberta (51)	-0.37 (0.15)	-0.69 (-0.13)	-0.54 (0.00)	0.54 (0.06)	0.08 (0.06)
Central Alberta (52)	-0.95 (0.18)	-1.44 (-0.12)	-1.13 (0.00)	1.14 (0.06)	0.11 (0.06)
Southern Alberta (106)	0.05 (0.14)	-0.90 (-0.11)	-0.39 (0.00)	0.43 (0.04)	0.19 (0.04)

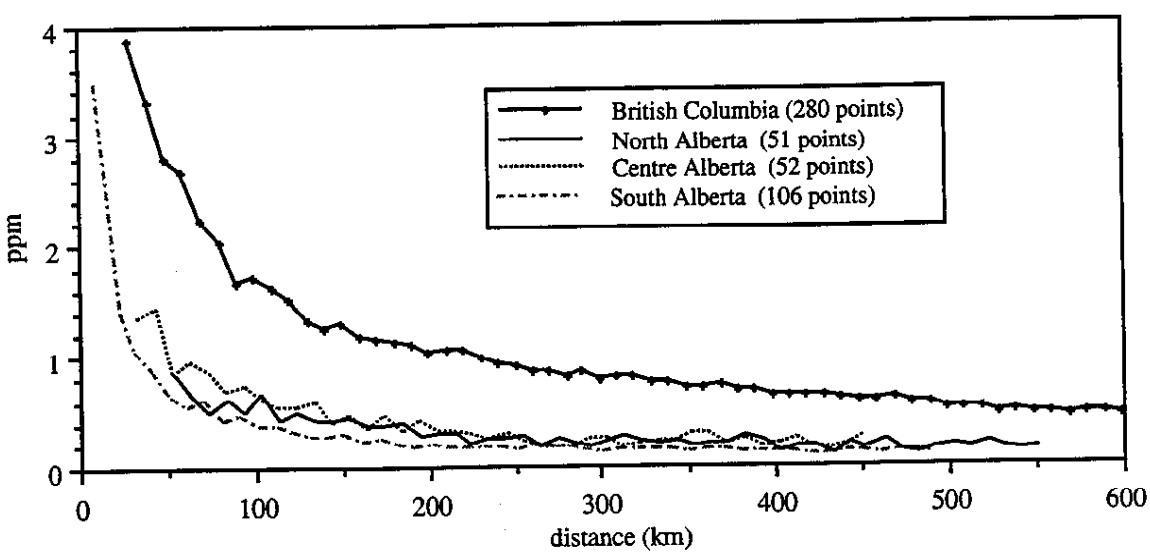

Figure 4 - Relative differences between the gravimetric and the GPS/leveling-derived geoid in Alberta and British Columbia (after fit)

There are many reasons that make the discrepancies between the gravimetric and the GPS/leveling-derived geoid much larger in British Columbia than in Alberta. For example, the accuracy of the geometric leveling may be poorer in the mountainous areas of British Columbia. The main reason, however, is probably due to the lack of gravity observations in the north-west area around the GPS/leveling network. When the comparisons were done only on 203 more reliable benchmarks in the southern part of British Columbia, after removing the systematic biases, the absolute difference (1σ) between the two geoid representations was only

10 cm, and the relative difference was 1.3 to 4.1 ppm for distances of 20 to 100 km, and 0.5 to 1.3 ppm for distances of 100 to 240 km (She, 1993; Sideris and She, 1995).
Finally, the gravimetric undulations computed by FFT were compared to other geoid solutions available in Canada. Six geoid models were used in the comparison. These models are: OSU91A, UNB90 by the University of New Brunswick, GSD91 by the Geodetic Survey Division of Canada, UC92 (planar 2D FFT) and UC93 (spherical 1D FFT) by the University of Calgary; for a detailed description, consult Sideris (1993), She (1993) and Sideris and She (1995). Both the absolute comparisons and the relative comparisons were made between the gravimetric geoid and the GPS/leveling-derived geoid.

Table 4
Differences between GPS/leveling and gravimetric geoid undulations in B.C. after a datum fit, in meters (203 stations)

GEOID MODEL	MIN	MAX	MEAN	RMS	σ
OSU91A	-2.46	2.40	0.00	0.77	0.77
UNB90	-1.47	2.19	0.00	0.71	0.71
GSD91	-0.41	0.31	0.00	0.15	0.15
UC92	-0.32	0.29	0.00	0.12	0.12
UC93	-0.19	0.18	0.00	0.10	0.10

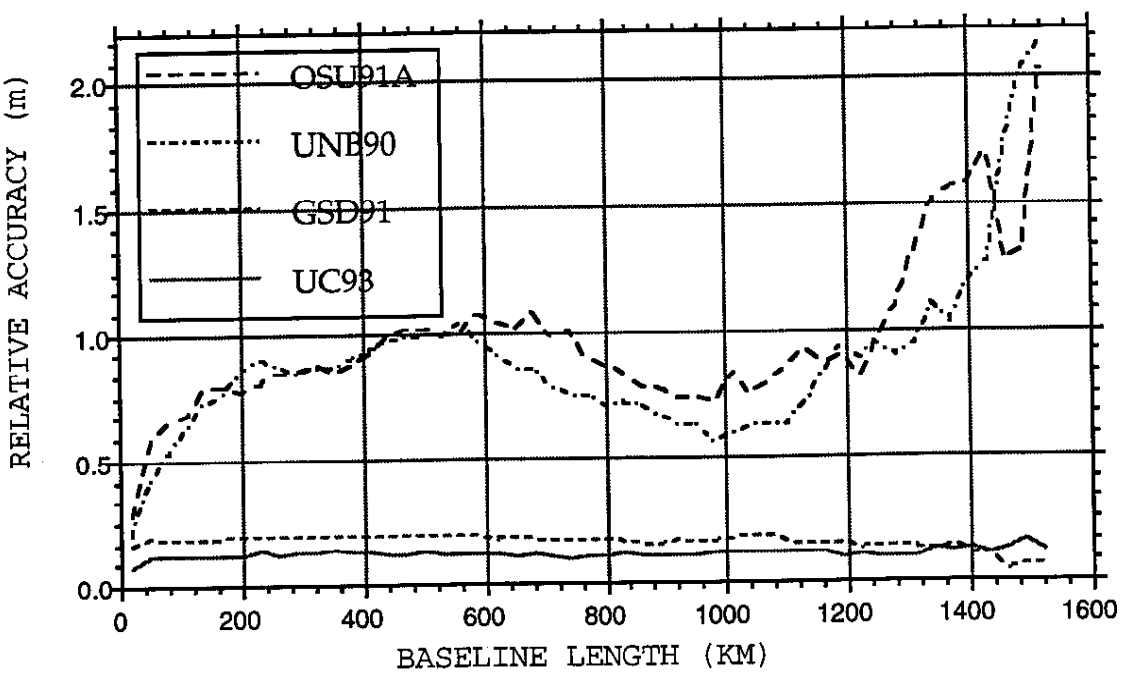

Figure 5 - Relative undulation accuracy in B.C. (203 Stations)

A comparison of different geoid models, as seen from Table 4 and Figure 5 which show the results after a datum fit at the 203 most reliable benchmarks in B.C., indicates that the UC93 geoid had the best agreement with the GPS/leveling data. It is also evident that the addition of local gravity data and height data improved the reference geoid computed from the OSU91A geopotential model significantly over distances from tens of kilometres to over 1000 km; see also Schwarz et al. (1987). The improvement was especially large over short and medium baselines (below 400 km) in rough terrain such as British Columbia. Figure 5 shows that the relative agreement improved from 14 to 2.3 ppm (OSU91A) to 4 to 0.3 ppm (UC93) for baselines of 20 km to 400 km. The relative agreement is between 10 and 15 cm for the UC93

geoid, which corresponds to about 4.1 to 1.3 ppm for short baselines of 20 to 100 km, 1.3 to 0.5 ppm for baselines of 100 to 200 km, and 0.5 to 0.1 ppm or less for baselines of 200 to over 1000 km.

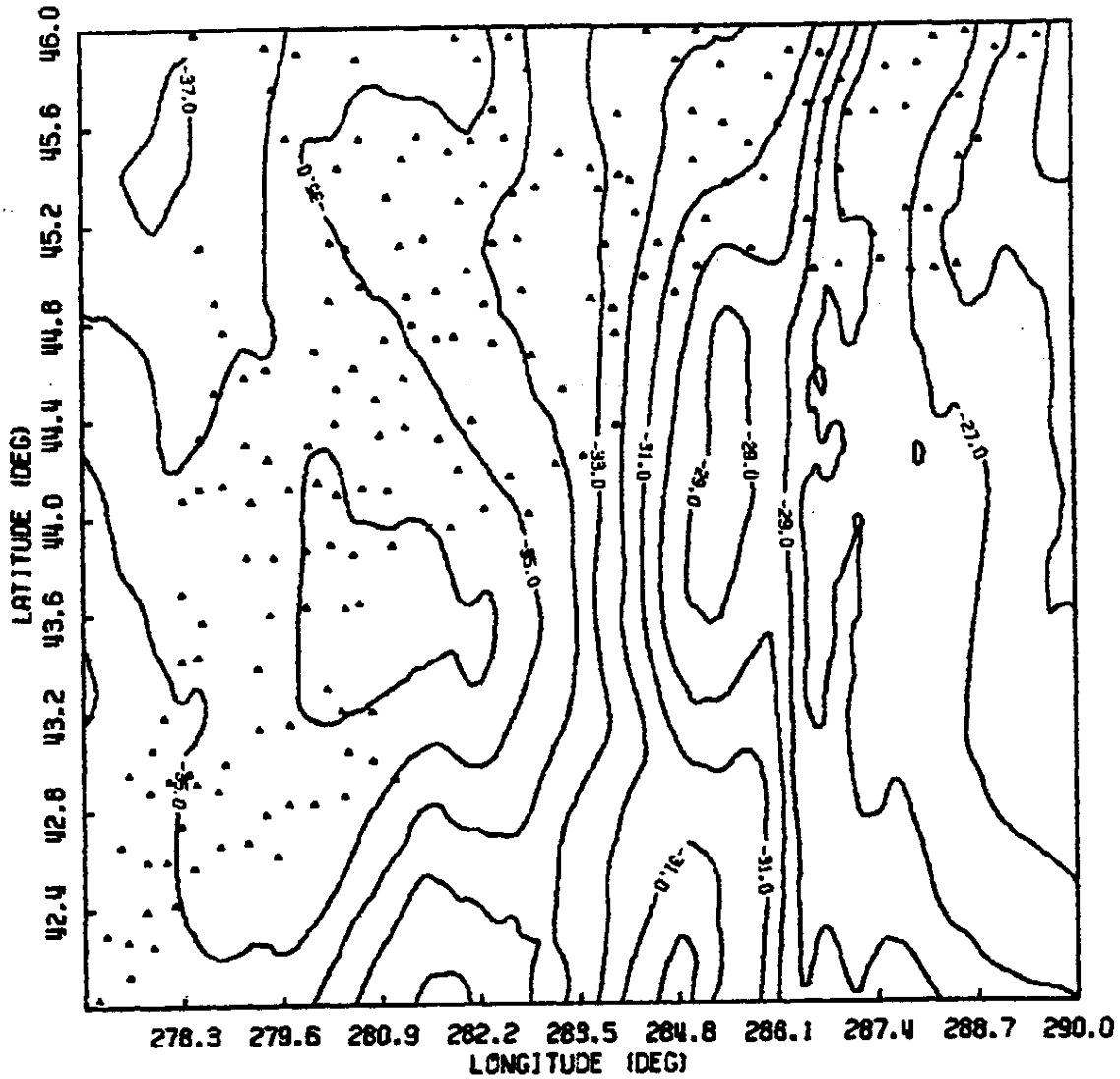

Figure 6 - Location of GPS stations in Quebec/Ontario (geoid contour interval: 1 m)

Table 5
Differences between GPS/leveling and gravimetric geoid undulations in Ontario/Quebec after a datum fit, in meters (197 stations)

GEOID MODEL	MIN	MAX	MEAN	RMS	σ
OSU91A	-0.59	0.54	0.00	0.19	0.19
UNB90	-0.31	0.36	0.00	0.12	0.12
GSD91	-0.26	0.24	0.00	0.10	0.10
UC92	-0.24	0.26	0.00	0.10	0.10
UC93	-0.22	0.25	0.00	0.10	0.10

Using the GPS points on benchmarks shown in Figure 6, comparisons were also made in the provinces of Quebec and Ontario. The comparison made on 197 yielded a difference of 10 cm

RMS for the UC93 geoid (see Table 5). Note that due to the excellent data coverage, even the OSU91A model alone performs well in this area. Figure 7 shows the results of the relative undulation accuracy. As shown in this figure, the relative agreement is between 6 and 14 cm for the UC93 geoid, which is equivalent to about 3 to 1 ppm for short baselines of 20 to 100 km, 1 to 0.7 ppm for baselines of 100 to 200 km, and 0.7 to 0.1 ppm for baselines of 200 to over 1000 km.

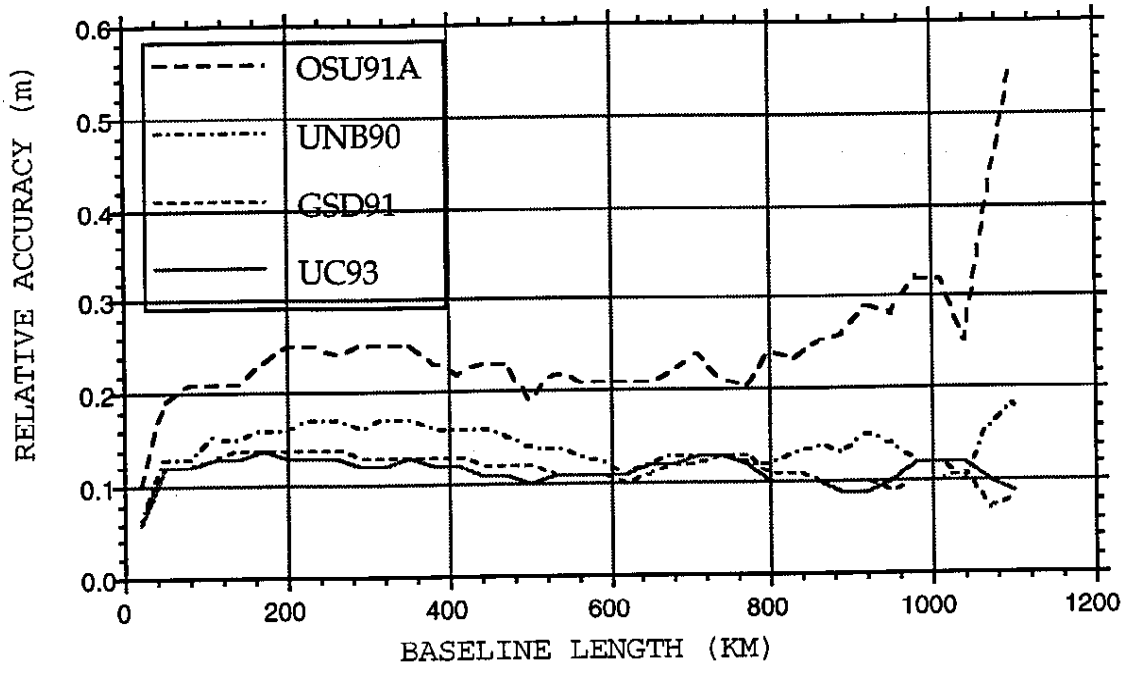

Figure 7 - Relative undulation accuracy in Ontario/Quebec (197 stations)

In relatively flat areas such as Ontario/Quebec, the GSD91 geoid which was computed by planar FFT without zero padding was almost at the same level of agreement with GPS/leveling data as the UC93 geoid which was evaluated by the discrete spherical Stokes integral. But in the mountainous areas of British Columbia, UC93 outperformed GSD91. In Ontario/Quebec, UNB90 was almost at the same level of accuracy as other geoid files. But in all the other GPS networks, UNB90 was poorer than other geoid models. In southern Alberta, the results from UNB90 were even poorer than those of OSU91A. A possible reason for the poorer performance of UNB90 might be that the geoid was obtained through integration, point by point, using data in a spherical cap of certain limited radius around each computation point while the FFT-based techniques made use of all the data on the grid simultaneously. Another one might be the improper modeling of the topography. As it can be seen from the maximum and minimum values in Tables 4 and 5, large differences exist among the various geoid models. And from Figures 5 and 7 it can be seen that long-wavelength errors are present in the OSU91A solution, illustrating the need for improvement of the low degree and order geopotential coefficients.

6. CONCLUSIONS AND RECOMMENDATIONS

The conclusions drawn from the theoretical developments and the numerical results in this research are as follows. (i) For the FFT-based methods to give results identical to those from numerical integration, zero-padding should always be used and the analytically defined kernel spectra should be avoided. (ii) For absolute geoid determination, the original rigorous spherical kernel function should be used instead of the approximated ones and the evaluation should be

done by the exact 1D-FFT method. In Canada, the use of the approximated kernel functions introduced additional geoid errors with a standard deviation of 25 cm and a maximum value of about 190 cm. (iii) It is possible to determine relative gravimetric geoid undulations in mountainous areas with an accuracy below 10 cm (1σ) with respect to GPS/leveling. After removing the systematic biases and tilts, the root-mean-square discrepancies between the two geoid representations on 280 benchmarks in British Columbia, which is a typical mountainous region, was about 23 cm, and on 209 benchmarks in Alberta, which is a typical flat and well surveyed region, was about 4 cm. The relative agreement was 1 to 2.5 ppm in British Columbia and is 0.3 to 1.4 ppm in Alberta for distances of 30 to 200 km.

For further improvements in accuracy, the following recommendations are made based on results obtained by Li (1993), Wang (1993) and Li and Sideris (1994). (i) For applications where only a GM will be used for geoid computations, this GM should be improved by tailoring it using local or regional gravity anomalies. Accuracy improvements of the order of 50% have been observed. (ii) With a given geopotential model and known variances of its coefficients, the contribution of the model can be improved by more than 10 percent when the coefficients are weighted by factors dependent on the signal-to-noise ratio. (iii) The errors of the gravity observations should be filtered out by a Wiener-type optimal filter. (iv) The predicted geoid errors should be estimated by error propagation because they can give valuable information about the weak areas in terms of insufficient data accuracy and coverage (Sideris, 1995b). (v) To achieve a gravimetric geoid in mountainous areas with a relative accuracy of 0.4 to 1.3 ppm for distances of 20 to 100 km, the high frequency information should be carefully considered. This can be achieved by significantly improving both the gravity anomalies and the digital topographic heights in terms of data coverage, density, and precision. (vi) To provide a reasonable external standard for evaluating the accuracy of gravimetric geoid undulations, it is necessary to investigate the quality (accuracy) of the geoid undulations derived by GPS/leveling. This is more important in mountainous areas, because it is usually believed that the accuracy of the orthometric heights is much poorer in these areas (Schwarz and Sideris, 1993; Sideris, 1994a).

The memory requirements, data handling and efficiency of the FFT methods can be further improve by a combination of the following factors. (i) Performing 2D Fourier transformations by applying the 1D FFT algorithm for each direction. (ii) Using the properties of the FFT that allow the use of two real functions as the real and imaginary part of a complex function. This allows for the transformations of two real functions or the convolution of two real functions with the same kernel function simultaneously. (iii) Using the fast Hartley transform instead of the FFT; the memory and time requirements are reduced by up to a factor of two (Li and Sideris, 1992 and 1995). (iv) Applying system input-output relations for handling heterogeneous, noisy data as input (Sideris, 1994b and 1995b). (v) Developing hybrid spectral methods that produce gridded undulations from irregular gravity anomalies as input (Sideris, 1995a).

ACKNOWLEDGEMENTS: Financial support for this research has been provided by a Natural Sciences and Engineering Research Council of Canada operating grant and a contract from the Geodetic Survey of Canada. The author is grateful to Bin Bin She and Ye Cai Li for performing all computations.

REFERENCES

FORSBERG, R; SIDERIS, MG: Geoid computations by the multi-band spherical FFT approach. *Manuscripta Geodaetica* 18(2): 82-90, 1993.

HAAGMANS, R; DE MIN, E; VAN GELDEREN, M: Fast evaluation of convolution integrals on the sphere using 1D FFT, and a comparison with existing methods for Stokes integral. *Manuscripta Geodaetica* 18: 227-241, 1993 .

HEISKANEN, WA; MORITZ, H: *Physical Geodesy*. W.H. Freeman and Company. San Francisco, 1967.

KEARSLEY, AHW; SIDERIS, MG; KRYNSKI, J; FORSBERG, R; SCHWARZ, KP: White Sands revisited - A comparison of techniques to predict deflections of the vertical. UCSE Report No. 30007, Department of Surveying Engineering, The University of Calgary, Calgary, Alberta, 1984 .

KLOSE, U; ILK, KH: A solution to the singularity problem occurring in the terrain correction formula. *Manuscripta Geodaetica* 18: 263-279, 1993 .

LI, YC: Optimized spectral geoid determination. UCGE Report No. 20050, Department of Geomatics Engineering, The University of Calgary, Calgary, Alberta, Canada, 1993.

LI, YC; SIDERIS, MG: The fast Hartley transform and its application in physical geodesy. *Manuscripta Geodaetica* 17(6): 381-387, 1992.

LI, YC; SIDERIS, MG: Improved gravimetric terrain corrections. *Geophysical Journal International* 119(3): 740-752, 1994a.

LI, YC; SIDERIS, MG: Minimization and estimation of geoid undulation errors. *Bulletin Geodesique* 68(4): 201-219, 1994b.

LI, YC; SIDERIS, MG: Evaluation of 2-D and 3-D geodetic convolutions by the Hartley transform. To appear in *Geomatics Research Australasia*, December issue, 1995.

PENG, M: Topographic effects on gravity and gradiometry by the 3D FFT and FHT methods. UCSE Report No. 20064. Department of Geomatics Engineering, The University of Calgary, Calgary, Alberta, 1994.

PENG, M; LI, YC; SIDERIS, MG: First results on the computation of terrain corrections by the 3D-FFT method. *Manuscripta Geodaetica* 20(6), 1995.

SCHWARZ, KP; SIDERIS, MG: Heights and GPS. *GPS World* 4(2): 50-56, 1993.

SCHWARZ, KP; SIDERIS, MG; FORSBERG, R: Orthometric heights without leveling. *Journal of Surveying Engineering* 113(1): 28-40, 1987.

SCHWARZ, KP; SIDERIS, MG; FORSBERG, R: The use of FFT techniques in physical geodesy. *Geophysical Journal International* 100: 485-514, 1990.

SHE, BB: A PC-based unified geoid for Canada. UCGE Report No. 20051. Department of Geomatics Engineering, The University of Calgary, Calgary, Alberta, 1993.

SIDERIS, MG: Rigorous gravimetric terrain modelling using Molodensky's operator. *Manuscripta Geodaetica* 15: 97-106, 1990.

SIDERIS, MG: Tests of a gravimetric geoid in GPS networks. *Surveying and Land Information Systems* 53(2): 94-102, 1993.

SIDERIS, MG: "Chapter 4: Regional Geoid Determination" of the *book Geophysical Interpretation of the Geoid* edited by P. Vanicek and N. Christou. CRC Press Inc., 1994a.

SIDERIS, MG: Geoid determination by FFT techniques. Lecture notes for the International School for the Determination and Use of the Geoid. Milan, Italy, Oct. 10-15, 1994b.

SIDERIS, MG: Fourier geoid determination with irregular data. To appear in *Manuscripta Geodaetica*, 1995a.

SIDERIS, MG: On the use of heterogeneous noisy data in spectral gravity field modeling methods. Accepted for publication in the *Journal of Geodesy*, 1995b.

SIDERIS, MG; TZIAVOS, IN: FFT-evaluation and applications of gravity field convolution integrals with mean and point data. *Bulletin Geodesique* 62: 521-540, 1988.

SIDERIS, MG; LI, Y: Improved geoid determination for leveling by GPS. *In Proc. of the Sixth International Geodetic Symposium on Satellite Positioning*, pp. 873-882, Columbus, Ohio, March 17-20, 1992.

SIDERIS, MG; LI, YC: Gravity field convolutions without windowing and edge effects. *Bulletin Geodesique* 67: 107-118, 1993.

SIDERIS, MG; SHE, BB: A new, high-resolution geoid for Canada and part of the U.S. by the 1D FFT method. *Bulletin Geodesique* 69(2): 92-108, 1995.

STRANG VAN HEES, G: Stokes' formula using fast Fourier techniques. *Manuscripta Geodaetica* 15: 235-239, 1990.

WANG, YM: On the optimal combination of potential coefficient model with terrestrial gravity data for FFT geoid computations. *Manuscripta Geodaetica* 8(6): 406-416, 1993.

WANG, YM; RAPP, RH: Terrain effects on geoid undulation computations. *Manuscripta Geodaetica* 15: 23-29, 1990.

WICHIENCHAROEN, C: The indirect effects on the computation of geoid undulations. OSU Rep. 336, Department of Geodetic Science and Surveying, The Ohio State University, Columbus, Ohio, 1982.

A PRELIMINARY GRAVIMETRIC GEOID FOR SOUTH AMERICA

Denizar Blitzkow
EPUSP-PTR - Caixa Postal 61548 - 05424-970 São Paulo - SP - Brazil

J. Derek Fairhead
GETECH-University of Leeds - Department of Earth Science - Leeds - UK LS2 9JT

Maria Cristina Lobianco
IBGE - DEGED - Av. Brasil, 15671 - 21 241 Rio de Janeiro - RJ - Brazil

ABSTRACT

South American Gravity Project (SAGP), a project undertaken and coordinated by the Geophysical Exploration Technology (GETECH) - University of Leeds, has been responsible for the collection and compilation of gravity data as well as topographic data in South and Central America. The project compiled 2,297,373 gravity points on land, marine and airborne. All gravity values have been adjusted to IGSN71 by using " Latin American Gravity Standardization Net 1977" (SILAG 77) and "Rede Gravimétrica Fundamental Brasileira" established by Observatório Nacional in Brazil. The anomalies are referred to WGS-84. The data were acquired from the International Gravity Bureau (BGI), Toulouse, France, from Defense Mapping Agency, Saint Louis, from oil companies and many national academic and non-academic organizations in different countries. Topographic and bathymetric data were used to generate a topographic model in a 3' grid and from that a terrain correction grid of 5' has also been derived. Nevertheless, several data gaps still exist and new measurements are needed to accomplish a homogeneous coverage. In Brazil a specific project called Anglo-Brazilian Gravity Project (ABGP) has been designed to infill some of these gaps in the north and west parts of the country. A new effort is now being undertaken by Escola Politécnica - University of São Paulo (EPUSP) and GETECH to estimate mean gravity anomaly values and to use them for geoid computations in South America. This paper is intended to describe the processing carried out with all the available informations from SAGP and ABGP in order to derive the best Helmert mean gravity anomaly value of 30' x 30'. A resume of the main theoretical topics related to the geoid determination will be summarized. A geoid model for South America will be presented.

1. INTRODUCTION

Geophysical Exploration Technology (GETECH) - University of Leeds has been involved in the compilation of gravity and geomagnetic data from many different parts of the world since 1986. One of its projects was the South American Gravity Project (SAGP) which collected gravity data for South and Central America and its margins delimited by the latitudes of 60° S and 25° N and longitudes 25° W and 100° W. Topographic and bathymetric data have been collected in the same area and a digital terrain model generated. Nevertheless, several data gaps still exist and new measurements are needed to accomplish a homogeneous coverage. In Brazil a specific project called Anglo-Brazilian Gravity Project (ABGP) has been designed to infill some of these gaps in the north and west parts of the country. In the first three years of the ABGP (1991-1994) several thousands of new gravity stations have already been established. ABGP has been benefited from an agreement between Fundação Instituto Brasileiro de Geografia e Estatística (IBGE - DEGED) and EPUSP, but also had collaborations from other organizations like Observatório Nacional (ON) [SOUSA, et al., 1993], [ESCOBAR, 1993] and Companhia de Pesquisas de Recursos Minerais (CPRM). Data have been delivered to the project by these organizations as well as by IAG-USP [SHUKOWSKY et al., 1991]

Taking advantage of the SAGP and ABGP gravity data base, a new effort is now being undertaken by GETECH and Escola Politécnica - University of São Paulo (EPUSP), through the EPUSP and GETECH agreement, to estimate mean gravity anomalies in block sizes of 30' x 30', from 5' initial values. The 30' mean values have been used to construct a geoid model for South America, presented in this paper. It is expected that the data be used also for local geoid model in different countries. These activities are related to the Sub-Commission for the Geoid in South America (SCGSA).

2. THE SPECTRAL COMPONENTS

The determination of geopotential models and their improvements in the last few years are responsible for the decomposition of the elements of the anomalous potential, in particular the geoidal height, in two different spectral components: one of long wavelength and another of short wavelength. The first one is derived directly from the model. The second is computed using a convenient modification of the Stokes integral. When least squares collocation is used the geopotential model is important to eliminate the systematic part which allows to consider the short wavelength component as a random variable. Recently, the facilities to obtain digital terrain models (DTM) in a grid and in this way to use interpolation procedures, can be a good reason to use FFT technique [SCHWARZ et al., 1990].

3. THE MODIFIED STOKES INTEGRAL

The geoid height expressed in terms of a series of spherical harmonic functions can be split out in the following form according to: [BLITZKOW, 1986]

$$N(\theta,\lambda) = -R\sum_{n=2}^{l}\sum_{m=0}^{n}(\bar{J}_{nm}\bar{Y}^{c}_{nm} + \bar{K}_{nm}\bar{Y}^{s}_{nm}) - R\sum_{n=l+1}^{\infty}\sum_{m=0}^{n}(\bar{J}_{nm}\bar{Y}^{c}_{nm} + \bar{K}_{nm}\bar{Y}^{s}_{nm}) \quad (1)$$

or briefly:

$$N(\theta,\lambda) = N_l(\theta,\lambda) + \delta N_l(\theta,\lambda) \quad (2)$$

which means to separate the geoidal height in two different spectral components, one of long wavelength and another of short wavelength. The first component N_l is obtained easily from a geopotential model. If gravity data is available in the region around the computation point the second component can be estimated using a convenient modification of the Stokes integral. Without details which can be found in [BLITZKOW et al., 1991] the mathematical expressions are:

$$\delta N_l(\theta,\lambda) = \frac{R}{4\pi\gamma}\int\int \delta\Delta g_l \delta S^m_l(\psi) sen\psi d\psi d\alpha \quad (3)$$

where:

$$\delta\Delta g_l = \Delta g - \sum_{n=0}^{l}\sum_{m=0}^{n}(C_{nm}Y^{c}_{nm} + D_{nm}Y^{s}_{nm}) \quad (4)$$

which means to subtract the long wavelength component from the observed gravity anomaly, and

$$\delta S^m_l(\psi) = \delta S_l(\psi) - \overline{\delta S_l}(\psi) \quad (5)$$

with

$$\delta S_l(\psi) = S(\psi) - S_l(\psi) \quad (6)$$

$$S_l(\psi) = \sum_{n=2}^{l}\frac{2n+1}{n-1}P_n(\psi) \quad (7)$$

$$\overline{\delta S_l}(\psi) = \sum_{i=0}^{l}\frac{2i+1}{2}t_i P_i(\cos\psi) \quad (8)$$

for the determination of t_i coefficients see [VANÍCEK et al., 1987] and [BLITZKOW et al., 1991].

4. GETECH DATA BASE

At the end of SAGP 2,297,373 land, marine and airborne gravity points were collected in South and Central America [GREEN & FAIRHEAD, 1991]. All gravity values have been adjusted to IGSN71 by using " Latin American Gravity Standardization Net 1977" (SILAG 77) and "Rede Gravimétrica Fundamental Brasileira" established by Observatório Nacional in Brazil [FAIRHEAD et al., 1991]. The data have been acquired from the International Gravity Bureau (BGI), Toulouse, France, from Defense Mapping

Agency, Saint Louis, USA, from oil companies and many national academic and non-academic organizations in different countries. The final gravity distribution is shown in figure 1. The analysis carried out on the gravity data to check against inconsistencies and different origins are explained in [GREEN & FAIRHEAD, 1991].

Besides the gravity stations, a 3' x 3' grid of topography and bathymetry was produced in order that terrain corrections could be applied. Four types of elevation data have been used to construct the grid:

1. Worldwide topographic grid (ETOPO5).
2. Values picked from topographic maps.
3. Heights at gravity stations.
4. Shoreline location.

A detailed description of these sources and the way they have been used can be found in [GREEN & FAIRHEAD, 1991] .

The DTM of South America is in a process of improvement at this moment with topographic maps being digitized, so that a new model will be available very soon.

In order to partially fill the gaps a special project has been designed for Brazil, the Anglo-Brazilian Gravity Project (ABGP). The activities have been undertaken through the agreement between Escola Politécnica - Universidade de São Paulo (EPUSP-PTR) and University of Leeds/GETECH. The field work activities benefited from the agrement between EPUSP and (IBGE) who accomplished the field measurements. The present gravity distribution in Brazil is shown in figure 2. A total of approximately 10 000 points have been added to SAGP coming from ABGP and from other organizations mentioned in the introduction.

5. DATA PROCESSING

5.1 SAGP PROCESSING

After the validation process was completed at the time of SAGP, terrain correction, Free Air and Bouguer anomalies were computed. The derived gravity anomalies are referred to WGS-84 through the theoretical formula:

$$\gamma_{84} = 978032.67714 \frac{(1+0.00193185138639 \sin^2 \phi}{\sqrt{1-0.00669437999013 \sin^2 \phi}} \text{ mGal} \qquad (9)$$

The Free Air correction has been applied using the following empirical equation:

$$FAC = 0.3083293357 + 0.0004397732 \cos^2 \phi)h + 7.2125x10^{-8} h^2 \qquad (10)$$

which is a function of the latitude ϕ and the orthometric height h.

The sea bottom points have been treated according to the following expression: [BGI, 1991]

$$FAC = (2k\rho_w^s - \Gamma) D_1 mGal \qquad (11)$$

where D_1 is the depth of water, ρ_w^s=1027 kg x m^{-3}, Γ = 0.3086 mGal/m, k = $2\pi G$ with G the gravitational constant. For the Bouguer correction an infinite slab expression has been used with a density of 2.67 g/cc for land stations and 1.17 g/cc for marine points. A curvature correction has also been applied. For a detailed description refer to [GREEN & FAIRHEAD, 1991].

Terrain corrections were calculated for all land and marine gravity points in South America taking into consideration only the " outer zone " (from 5 km to 166.7 km). To estimate this correction the 3' digital terrain model described before has been used. For more details about the terrain correction and informations on the range of this correction in particular in the Andes, refer again to [GREEN & FAIRHEAD, 1991].

Because the expression (9) includes the mass of the atmosphere, a correction has been applied to the observed gravity values to be consistent according to the following equation:

$$\delta g_A = 0.87 e^{-0.116 \times H^{1.07}} mGal \qquad (12)$$

where H is the elevation in kilometers.

5.2 PRESENT PROCESSING

The onshore data base available at GETECH (which includes coordinates, heights and anomalies computed according to the aforementioned description, and a source code) have been sorted in longitude by blocks of 1° x 1° and sorted in latitude in each block. The arithmetic mean has been used to estimate a mean anomaly for each block of 5' x 5' if at least two points existed in the cell. When a mean value was computed, the coordinates of the centre of the block was derived as a position for the mean. If just one point was available in one 5' block, the anomaly value with the existing coordinates were maintained. As a result the final file with mean values of 5' x 5' grid is not in a complete regular grid, but some coordinates are shifted from the centre. The SAGP data file does not include any information on the accuracy of the different values available in the record for each station. So, an estimation of accuracy of the mean gravity value has been computed using the following slightly modified version of the empirical formula presented in [KIM and RAPP, 1990]:

$$\vartheta = MAX\{2, INT(20/\sqrt{n} + 0.05 + |\Delta g| + 0.5)\} \qquad (13)$$

which is a function of the number of points 'n' and the module of the gravity anomaly Δg, between other constants.

Once the mean value was estimated the difference between the mean and individual values has been calculated and recorded in a specific file if the absolute value exceeds

200% of the mean. This procedure has been used to look for any big error still present in the original file of gravity anomalies. Despite carrying out a careful validation process in SAGP, a few new errors have been found and corrected. Cells of 1° x 1° with suspected problems has been analysed using NDVS (New Data Validation Software) developed at GETECH. It provides with facilities to look for the anomalies in a 3-D and in this way find out some inconsistencies.

After completing the estimation of mean values an interpolation process was carried out: the objective being to estimate a value for as many empty blocks of 5' as possible by taking advantage of the existing values around them. Therefore a mean value has been assigned to every empty block when at least three values were available either to the north, south, east or west of the empty cell. In this process an arithmetic mean has been used again. Figure 3 shows the final distribution of 5' mean values.

In a further step, the 3' topographic grid mentioned above has been used to estimate mean heights for blocks of 5' x 5'. As the data are in a 3' grid, for each cell a total of 2 x 2 values occur considering the borders. The fact that the values of the borders are used for two different cells creates some correlation that has not been taken into account in the mean estimation at this time. The mean heights can be used to restore the mean Free Air anomaly in the blocks of 30' x 30'.

Finally a similar processing has been carried out to estimate mean terrain correction from the 5' terrain correction grid.

6. RESULTS AND CONCLUSION

A complete file has been created with different 5' mean values: free air anomaly, Bouguer anomaly, height and terrain correction. From this file, mean values of 30' x 30' have been derived. In this case it has been derived a mean Faye anomaly in the following way: the mean free air anomaly has been restored from mean Bouguer anomaly and mean height. Due to the smoothness of the Bouguer anomaly it is very well known that the mean value of this anomaly is more representative than the two other quantities, in particular when the distribution of the point values in the cell is poor. Finally the mean terrain correction has been added. The Faye anomaly is a good approximation to the Helmert second condensation method [BLITZKOW et al., 1994]

Off-shore it has been used gravity anomalies derived from altimetry data.

In order to use these data for South America geoid calculations a validation experiment has been done in Brazil. A total of 398 Doppler and GPS points on the levelling network have been used to derive the satellite geoidal height N_S. The cartesian coordinates related to WGS-84 have been referred to ITRF90 using the following transformation parameters: [McCARTHY, 1992; p.18]

$T_1 = -0.060$ m $\qquad \alpha_1 = +0.01830$ "

$T_2 = 0.517$ m $\qquad \alpha_2 = -0.0003$ "

$T_3 = 0.223$ m $\qquad\qquad \alpha_3 = -0.0070$ "

$K = 0.011$ PPM

The idea is to have a geoid referred to a geocentric/ITRF90 oriented ellipsoid defined by:

$a = 6{,}378{,}137$ m
$e^2 = 0.00669437999$

In order that a gravimetric geoid (derived from gravity data and/or geopotential model) be referred to WGS-84 ellipsoid it is necessary to estimate a zero order undulation N_0 due to the fact that the best fit ellipsoid to the geoid is not (or may not be) the WGS-84 ellipsoid. To do that the satellite undulations have been compared in a first step with JGM2, up to n = 36. The term N_0 is computed according to: [BLITZKOW & SÁ, 1983]

$$N_o = \frac{\sum_{i=1}^{n}(N_{Si} - N_{Gi})}{n} \qquad (14)$$

The result of the comparison has been $N_0 = -1.21$m and a RMS difference of 2.30m. Using the model up = 72 the result is $N_o = -1.40$ m and the RMS difference 2.27 m.

The mean gravity anomalies, after remove the long wavelength component according to (4), have been used in the modified Stokes integral (3). As a reference field it has been used JGM2 geopotential model up to n = 36. Finally the spheroidal undulation derived from the same model has been added. This is the "remove-restore" technique. A new comparison has been done with the satellite undulations. The differences are shown in the figure 4. The new zero order undulation estimated is $N_0 = -1.49$ m. The RMS difference is 2.39 m. This compairison showed two basic systematic effects: the first in 32 GPS points in the central part of Brazil; the second in all points in central-north Amazonas basin. Further analysis are necessary to be carried out with respect to these problems.

Using both the satellite and gravity derived undulations the geoid (quasi-geoid) map (Fig. 5) for South America has been computed and presented. The satellite undulations are referred to WGS-84/ITRF90 according to the transformation parameters mentioned before. To the gravity/GEMT2 undulations the zero order term of -1.40 m has been added.

It is difficult to estimate the error of the geoidal heights now presented. It depends on many different conditions: quality and distribution of the gravity data, quality and distribution of the Doppler and GPS points, the accuracy of the leveling network, and, in particular, the consistency of the digital terrain model. In this respect, the DTM is in a major process of improvement at this time, as mentioned before. It is a expected an improvement in the restored mean free air anomaly and consequently in the geoid compilation after the new DTM be available. The RMS difference obtained from the comparison of satellite and gravimetric undulations is

certainly a good measure. Actually the relative error should be better. It is expected a relative error better than 1 cm/km.

ACKNOWLEDGEMENT

The data pre-processing for this paper has been done at GETECH by the first author in two different stays: the first one through the agreement between CNPq/Royal Society and the second supported by FAPESP (Fundação de Amparo à Pesquisa do Estado de São Paulo). All data used in this study has been approved by owners/providers. We are specially grateful to DMA and BGI for releasing gravity data.

REFERENCES

BLITZKOW D; SÁ N. C. de (1983) As alturas geoidais Doppler e a separação elipsóide-esferóide de referência. Revista Brasileira de Geofisica, 2, pp. 19-24.

BLITZKOW D. (1986) A combinação de diferentes tipos de dados na determinação das alturas geoidais. Tese de doutoramento apresentada ao Departamento de Geofísica do IAG/USP. São Paulo.

BLITZKOW D., CINTRA J.P., FORTES L.P.S. (1991) A contribution to the geoid determination. IN: Recent geodetic and gravimetric research in Latin America. Edited by W. Torge. Springer-Verlag. Berlin.

BLITZKOW D.; CINTRA J. P. & SGM (1994). A determinação das alturas geoidais no Uruguai - Resultados presentes e perspectivas futuras. To be published.

ESCOBAR I.P (1993). Gravity measurents in Rio de Janeiro. Personal communication.

FAIRHEAD J. D., CHEVALIER P.H., GREEN C. M., HUNT N. J., MANTON D. C., SPINK S. J., STUART G. W., WINDLE I. D., WATTS A. B. (1991) . The South American Gravity Project. Internal Technical Report. Leeds

GREEN C. M. & FAIRHEAD J. D. (1991). The South American Gravity Project. In: Recent Geodetic and Gravimetric Research in Latin America. Edited by W. Torge. Springer-Verlag, Berlin.

KIM J. H. & RAPP R. H. (1990). The development of the July 1989 1° x 1° and 30' x 30' terrestrial mean Free-Air anomaly data bases. Department of Geodetic Science and Surveying - OSU. Report 403, Ohio.

McCARTHY D. D. (1992). IERS Technical note 13. Observatoire de Paris. Central Bureau of IERS. Paris.

SCHWARZ K. P., SIDRIS M. G., FORSBERG R. (1990). The use of FFT techniques in physical geodesy. Geophus. Journal Int., vol. 100, pp. 485-514.

SHUKOWSKY W., VASCONCELLOS A. C. B. C. de, MANTOVANI M. S. M. (1991). Estruturação dos terrenos precambrianos da região sul do Brasil e oeste do uruguai e sua continuidade sob os sedimentos da bacia do Paraná: Um estudo por modelamento gravimétrico. Rev. Bras. de Geofisica 9(2), pp. 330-342.

SOUSA M. A. de, MOREIRA E. M., SANTOS A. A. dos (1993). The L_2 adjustment of the old LC & R 61 data set to the IGSN71/absolute datum. Special publication. National Observatory. Rio de Janeiro.

VANICEK P., KLEUSBERG A., CHANG R.G., FASHIR H., CHRISTOU N., HOFMAN M., KLING T., ARSENAULT T. (1987). The Canadian Geoid. Technical Report n° 129. Dept°. of Surveying Engineering - UNB. Fredericton.

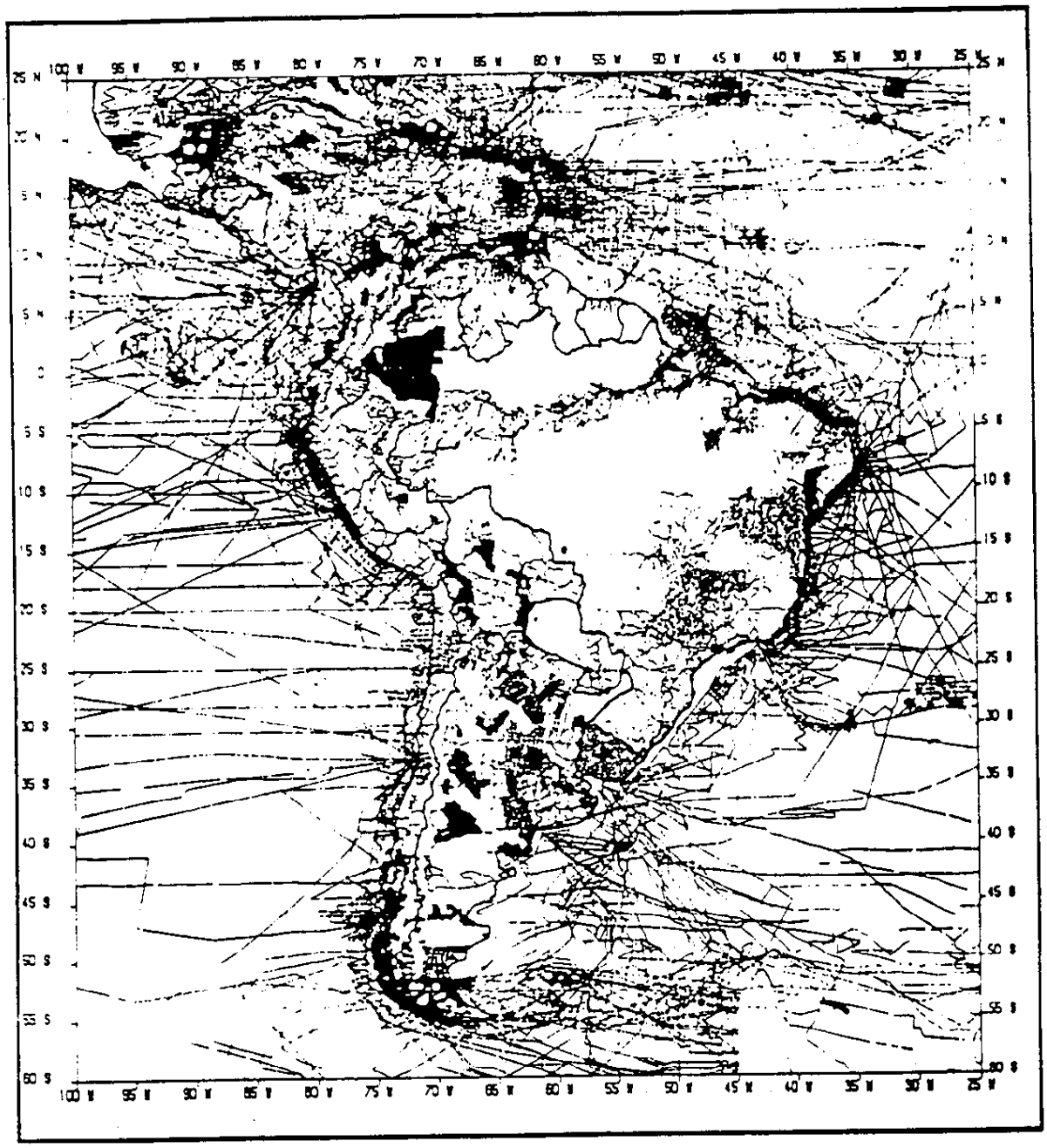

Fig.1 - Final gravity distribution of SAGP

Fig.2 - Distribution of the gravity points in Brazil

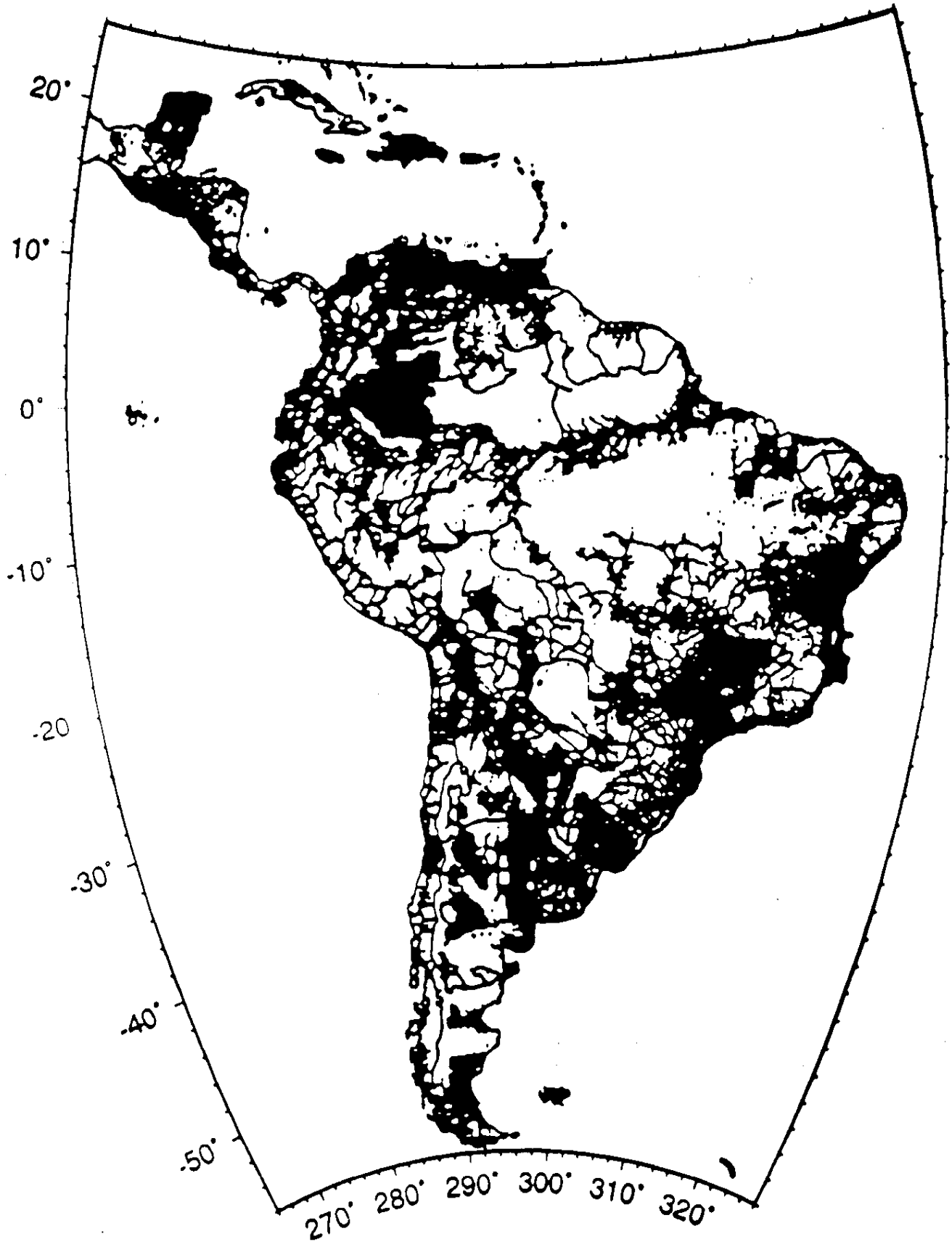

Fig.3 - Distribution of the mean 5' values

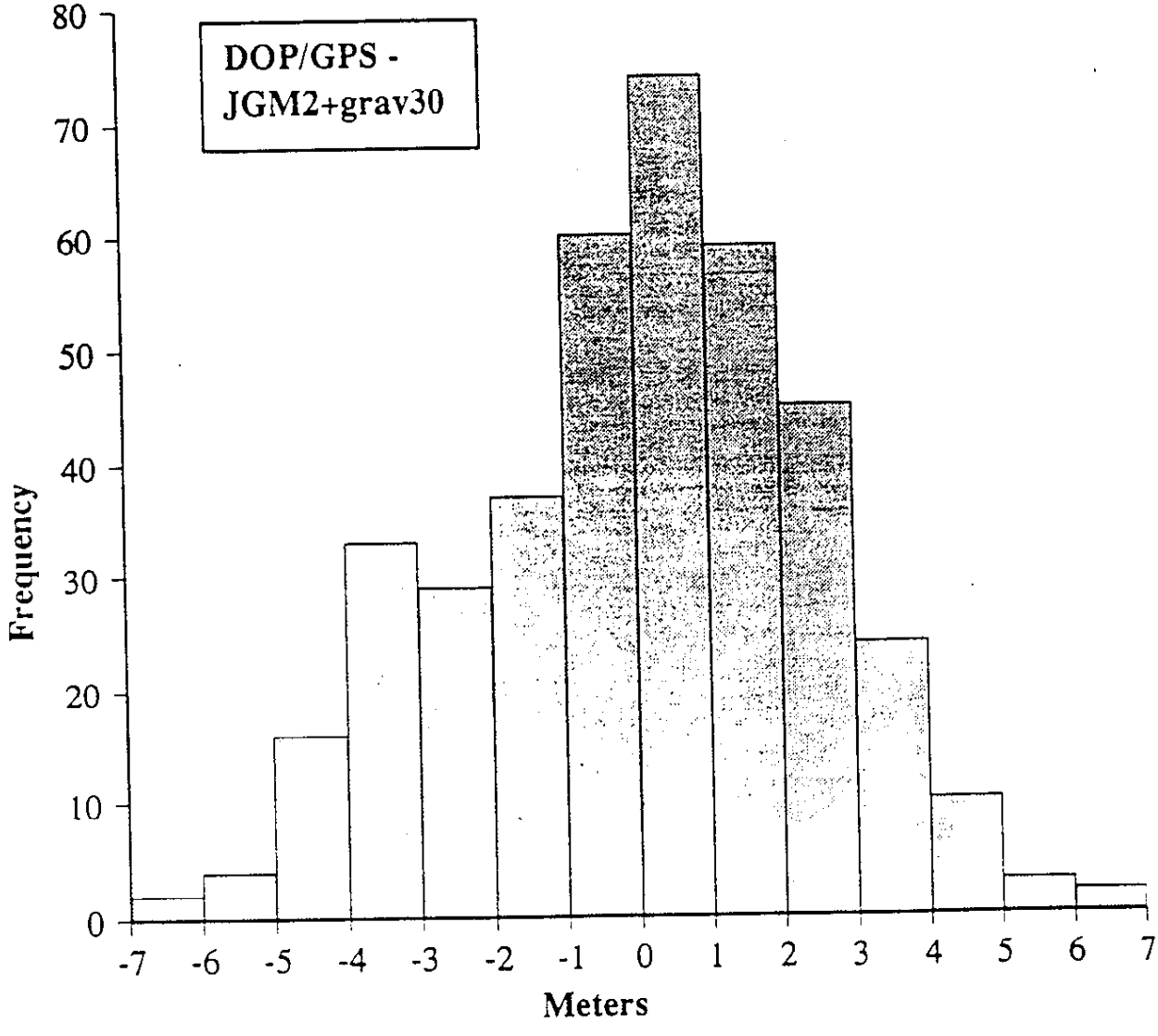

Fig.4 - Histogram of geoid differences

GEOIDAL MAP FOR SOUTH AMERICA

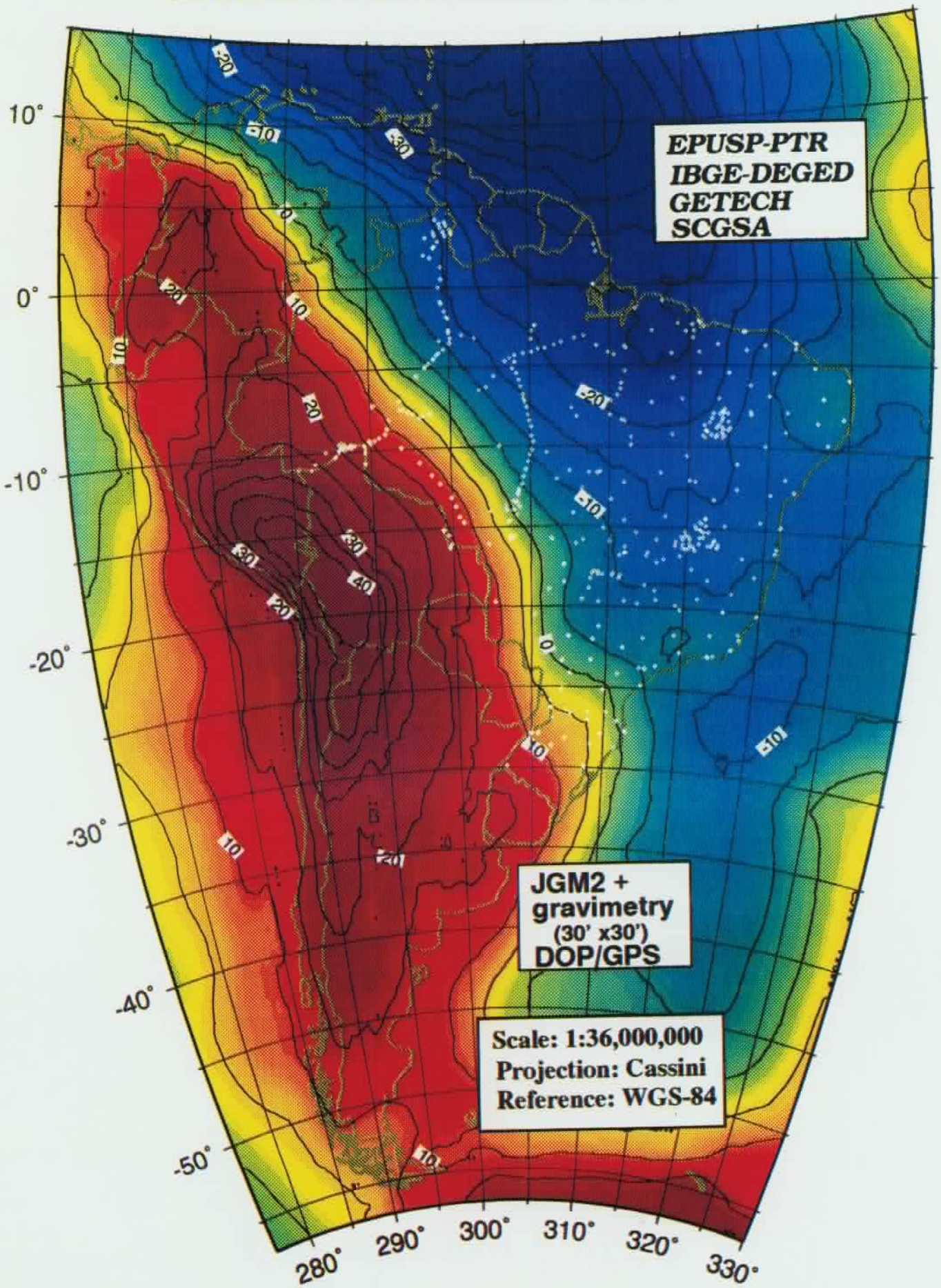

Accuracy Evaluation Of The Height Anomaly Prediction by Means of Gravity Data in a Height Anomaly Control Network

Junyong Chen
National Bureau of Surveying and Mapping
Beijing 100830,China

Abstract

In a height anomaly control network, such as astronomic (or astro-gravimetric) levelling network or GPS-levelling network, height anomalies at interpolation points are predicted usually using remove-restore technique on the basis of known height anomalies at the control points and the gravity data. This paper discusses the relationship among accuracy of the predicted height anomalies and the resolution as well as accuracy of height anomaly control network and those of gravity data. Results of a case study and its test computation in connection with practical circumstance of China are given.

I. The Height Anomaly Prediction In A Height Anomaly Control Network

The local quasi-geoid in China obtained by means of technique such as astronomic levelling, astro-gravimetric levelling and GPS-levelling (Torge et al 1989)(Tscherning C.C. 1992)(Chen J.Y.1993) is essentially a griddid control frame of height anomalies,so we can also call it as a height anomaly control network, HACN for short. It is constituted by a large number of control points of height anomalies determined by these techniques. The resolution and the accuracy of HACN therein can be defined after the completion of HACN. What we often require to know are the predicted values and its accuracy at the non-control points or so-called interpolation points in HACN. It goes without saying that these predicted values and their accuracy are closely related to the prediction techniques and the data used. Sometime in a relatively small area with less complex topography and gravity variation, it is feasible to make prediction by way of approximation based on pure mathematics without using any gravity data. However,this paper deals with problems which arise when the prediction is made by means of gravity data (including topographic data,(Sideris M.G.1985)), as it is generally applicable. Then not only do the resolution and accuracy of HACN which provides initial data and plays the major role, but also it is necessary to take into account the resolution and accuracy of the parameters of gravity field adopted in prediction.

Theoretically, in the prediction of height anomaly at interpolation points, it is not absolutely necessary to take the existing HACN into account, which can be computed directly by using gravity data with Stokes formula, Molodensky formula (Molodensky M.C.1960), Meissl formula (Meissl P.1971), and FFT (Schwarz K.P.et al 1990) technique. However,considering the problems concerning the global distribution, accuracy and resolution of measured gravity data, the ability of gravity field model in representing short wavelength, and different reference system used in different countries, the method currently widely used practically in predicting height anomalies at interpolation points in a local extent is the remove-restore technique. Generally it consists in taking known height anomalies at some control points (of

HACN) located in the vicinity of interpolation points as initial data to provide restrain for prediction, then in combination with global gravity model and surface gravity data to obtain the predicted height anomalies at interpolation points. The above computation procedure in general case is briefly described as following:

1. Within a grid of a HACN, wherein the interpolation points are located; select the known height anomaly values ς^0 at several control points around the interpolation point as initial data; compute the corresponding height anomalies ς^0_s at these control points from global gravity field model, remove ς^0_s from ς^0 ; i.e. remove the influence of long wavelength component of geoid.

2. Compute the height anomalies ς^0_g at these control points using the surface gravity data within a spherical cap of definite radius σ and with certain formula; substract values ς^0_g from (ς^0 - ς^0_s), i.e. further remove from ς^0 the influence of medium wavelength and partly short wavelength components of geoid.

3. Finally residuals ς^0_r are taken as initial values for the prediction of the height anomalies at interpolation points.

$$\varsigma^0_r = \varsigma^0 - \varsigma^0_s - \varsigma^0_g \qquad (1)$$

For the linear parts of the height anomalies at those interpolation points, their predicted values, ς_r , are obtained with certain prediction technique based on the initial values ς^0_r.

4. The height anomalies ς at interpolation points are obtained in succession by restoring, i.e. reversing the above process.

$$\varsigma = \varsigma_r + \varsigma_s + \varsigma_g \qquad (2)$$

II. Accuracy Evaluation For The Height Anomaly Prediction

There exist three main error resoures in the prediction of point height anomalies by means of remove-restore technique. The first lies in the error of initial data of prediction, it arises from the error m_0 in the height anomalies ς^0 at control points in HACN.

The second originated from error m_s which occurs in the computation of ς_s using global gravity field model. Different gravity field models used in the prediction of height anomalies bring about respectively systematic and accidental errors. A comparison of (1) and (2) shows that substraction is followed by addition in the remove-restore technique,the prediction of interpolation points is governed by control points in a gridded HACN; moreover, the control and interpolation points are not far apart; therefore,the systematic error of gravity field model is essentially compensed in the predicted results of interpolation points during the remove-restore process. The finer is the grid of HACN, i.e. the higher is the resolution of initial data, the more thoroughly is the systematic error compensated.

So far as the accidental error of gravity field model is concernd, for grids in different regions the model covers, it exhibits stochastic character; however,in a local extent of a single grid, it often demonstrates systematic character; thus it follows that in case of predicting height anomalies at interpolation points in a small extent of a grid, this accidental

error can also be weakened partly due to the reverse process in the remove-restore technique. For this reason, to evaluate m_s with degree variance or absolute error of a global gravity field model will tend to be exaggerated. Test computation shows that m_s can be expressed by an expirical value which is actually the residual error of global gravity field model in a small region surrounded with control data. Test computation also shows the value of this residual error is quite stable within the area with certain resolution and accuracy of measured surface gravity data.

The third error source is the error m_g which occurs in the computation of ς_g with surface gravity data around the interpolation points. This mainly reflects the residual influence after the compensation of the short wave-length disturbances of the local gravity fields around control and interpolation points. Hence the total error m_ς in the predicted height anomaly ς at interpolation points, in taking account of (2), can be expressed as:

$$m_\varsigma = \pm \sqrt{m_0^2 + m_s^2 + m_g^2} \qquad (3)$$

It is well-known that geoid undulation is identical to the variation in the direction of the vertical. Thus in the accuracy evaluation of the height anomalies at interpolation points, consideration can be made in such a way that in a local extent of a grid in HACN, the height anomalies at interpolation points within this grid are predicted by taking the height anomalies at control points as initial data, this is essentially to predict the differences of height anomalies between control and interpolation points, i.e. to predict the direction (relative) variation of deflection of the verticals at these two kinds of points. With regard to the height anomaly at interpolation point, m_0 is the error of initial data, this error is essentially, on an average, a fixed part in the error of the predicted height anomaly at interpolation points. This argument is fully applicable to the corresponding prediction error of deflection of the verticals.

As for m_s, as it is caused by the error of a used global gravity field model, and is partly compensated in the process of "remove" for control points and "restore" for interpolation points. In a local extent, the degree of the compensation within each grid is compatible also in an average meaning. Therefore for a given gravity field model, if long wavelength in a local extent is concerned, m_s can be regarded as a "linear interpolation error" when deflection of the vertical at interpolation point is obtained by linear approximation between the deflections of the vertical at control points, i.e. the computation of ς_s can be considered as a linear approximation of the height anomaly at interpolation points by using gravity field model; this error basically is a stable value.

While the process of applying corrections to $(\varsigma_r + \varsigma_s)$ by using the local gravity data around control and interpolation points (corresponding to computing ς_g) practically amounts to further taking into account the influence of short wavelength components of local gravity field on the deflection of the vertical. This can be considered as the nonlinear part $\delta\theta$ of the variation between deflections of the vertical at control points, or it comes to the same thing to consider ς_g as the correction term of the (local) gravity (field), its error is above mentioned m_g.

In a given HACN, or in drawing upon a plan for geoid determination, quantitative requirments should be laid on the accuracies of the height anomalies at control and interpolation points, for example, they are designated as m_0 for ς^0 and m_ς for ς respectively. Once the used gravity field model is given, the value of m_s can be obtained from the derivative of the differences between the known height anomaly at control points in HACN and the corresponding value computed from the model. Therefore, in the given plan for

geoid determination or in a HACN, once m_ζ m_0 and m_s are given, the limit value of m_g can be inferred previously according to (3).

The relations between the error m_g of the gravity correction and the resolutions of a local quasigeoid (or HACN), and also that of local gravity data is derived as following.

Assuming that the resolution of a local quasigeoid (or HACN) in the area where the interpolation points lie being d(km)×d(km), mentioned already, the error of the gravity correction applied to the height anomaly or to the deflection of the vertical at interpolation point with respect to control point being m_g and $\delta\theta$ respectively, if the interpolation point lies in the center of grid, then, without losing generality, the relationship between the two, m_g and $\delta\theta$, can be expressed as

$$\delta\theta'' = \sqrt{2}\rho'' \, m_g / 1000d \qquad (4)$$

Here the units of m_g , d and $\delta\theta$ are m, km and arc second respectively.

According to Molodensky's expirical formula(Molodensky M.C.1960) regarding error of gridded mean gravity, δg and that of deflection of the vertical $\delta\theta$, we have

$$\delta\theta'' = 0.15 \, \delta g \qquad (5)$$

Here the units of δg and $\delta\theta$ are mgal and arc second respectively. Hence, where the error of gravity correction term,m_g and the resolution of HACN are given, by introducing (5) into (4), the accuracy requirement on gravity anomaly is

$$\delta g = 1945 \, m_g / d \qquad (6)$$

Neglecting observation error, the relation between representative error of gridded mean gravity anomaly, δg and the side length L, characterizing the resolution of gridded mean gravity anomaly,is (Molodensky M.C.1960)

$$\delta g = 2c\sqrt{L} \qquad (7)$$

Here c is the coefficient of representative error; the units of L ang δg are km and mgal rspectively. By combining (6) and (7), the relation between the error of gravity correction term m_g which is applied to the predicted value of the height anomaly at interpolation point, and the resolution of local gravity data (gridded mean gravity anomaly) as well as that of geoid d is obtained.

In case of giving d and m_g, it is possible to estimate the minimum resolution L for the local gravity data should be hold, that is

$$L^\circ = 8518 \, m_g^2 / c^2 \, d^2 \qquad (8)$$

Here the unit of L° is degree and in middle area. In case of giving m_g and L°, it is possible to estimate the required resolution d of quasigeoid (or resolution of HACN), then d can be rewritten from (8) as

$$d = 92.29 \, m_g / c\sqrt{L^\circ} \qquad (9)$$

Here the symbols and units are the same as above.

Of course,We can alternately estimate the obtained possibly accuracy m_g of the gravity correction term in regions with different topography, according to the existing resolutions d and L°, the estimation formula reads

$$m_g = 0.01084\ cd\sqrt{L^\circ} \qquad (10)$$

III.The Conclusions From The Case Study

In the case study a 7°× 7° area (fig.1) with 12502 gravity points for test computation is selected. There are several kinds of topography in the area such as plain,hilly and mountain land. The resolutions of the local gravity data and DTM are 5'× 5' and 30″× 30″ respectively. The height anomalies at 26 astronomic stations in the area derived from 1st order astro-gravimetric levelling in China are taken as known values, part of these astronomic stations are taken as unknown test points during the interpolation. Height anomalies at these test points are predicted using various test computation schemes. The mean square root differences between the predicted values and corresponding known values are used to evaluate the relative merits and demerits of the various schemes. Due to numerous permutations and combinations in the comparison of various schemes as well as the huge volume of computation, the limited space of this paper defies all attempts to list the results of various test computations and their intermediate process, in what follows only a brief description of the test computations in the case study and its main conclusions are given as follows.

1. In the computation of long wavelength components ζ_s of height anomaly, two kinds of gravity field models, A and B, have been compared with each other. A are some popularly used models in geodetic comunity but without the surface gravity information of China; B is the model (Ning J.S. 1990) which does contain the detail gravity information in China. The results of computation(e.g. with Meissl formula) indicate when the radius σ of spherical cap in computing ζ_s is larger than 2.5°-3°, the final results derived from B are ananlogous to those from A, only in the area of China with dense gravity data, the obtained accuracy is slightly better. This may ascribe to the fact that in computing ζ_s using remove-restore technique, only the information of low degree (long wavelength) component of gravity field plays a major role, and the low degree coefficients of various models recently used are only slightly different.

As for the number of the degree of gravity field model adopted in the computation of ζ_s, the results obtained by extenting to 36 and 180 degrees respectively of the above mentioned two kind models have been compared, herefrom we come to the conclusion that for a same gravity field model, the results (accuracy of ζ_s) obtained by extending to high degree (e.g. 180 degree) is only slightly superior to that obtained from low degree. For example, the results obtained by extending B model to 180 is only 5-10% better than that obatained from low degree on an average. On the basis of the derivative of the differences between the known height anomaly at control points in HACN and the corresponding value computed from the model, in case of the radius of spheric cap σ=3°, using Bouguer anomaly, when B model is extended to 180 degree, the corresponding m_s can be taken as ±0.10m; accordingly, when A models is taken to 36 degree, m_s can be taken as ±0.15m.

2. In practice, ζ_s and ζ_g are computed simultaneously. Among various computation

methods, Meissl's method and FFT technique give slightly better results. However, when data processing is made by FFT technique, it requires that both the resolutions of local quasigeoid and that of local gravity field should be the same and higher. Test computation shows that in order to make the result from FFT practically valuable, the resolution should be higher than 30' × 30' at least. It is naturally possible to attain higher resolution and keep it identical for the two by way of prediction. Generally, the test result obtained from high resolution is better on an average than that from low one, whether the high one is obtained from actual measured or prediction. However in case of lacking sufficient measured gravity data in a complex topography area, and high resolution is obtained solely depending on prediction, then in such area the test computation reveals that the probability of occurrence of the error in predicted values at a few points, which are 3-4 times as large as normal error, is rather higher.

When ς_s and ς_g are computed using Meissl formula,the resolution of local quasigeoid and that of local gravity field are not necessary the same.

Besides, whether FFT technique or Meissl formula used, it is sufficient to take into account the zero order term of the formula, the gain obtained from including the first order term is rather small, only 2-3% increase in accuracy can be achieved according to the test computation, hence the need for including the first order term can be obviated.

3. Three types of gravity anomaly can be adopted in computing ς_g: Bouguer anomaly, Bouguer-topographic anomaly and Bouguer-topographic-isostatic anomaly, when the last one is used in the test computation, if the coefficients of gravity field model are extended to 36 and 180, only about 2% and 10%, on an average, amelioration in accuracy can be achieved respectively than other two types are adopted, moreover, there are lacking both in regularity and homogenerity. In view of the fact that better DTM and more computer time are needed in computing topographic and isostatic correction applied to gravity, so if high degree coefficients (e.g.180 degree) are included in computatng ς_s, it is generally sufficient to use Bouguer anomaly in deriving ς_g.

4. Various approximation methods,including collocation, can be used in predicting the short wavelength components ς_r at interpolation point, however their obtained results is analogous. When height anomaly prediction at a interpolation point is carried out in a single grid of HACN where it lies, the prediction accuracy obeys on the whole regularities (8)-(10). If simutaneous multi-points prediction is made by combing multiple grid wherein the interpolation points lie, the mean prediction accuracy tends to be decreased to a great extent according to the test computation. For example, when simultaneous multi-points prediction is made by combing 88 grids, the error of predicted results is twice as large as that of single grid prediction at least. Hence, as far as accuracy is concernd, the superiority of FFT technique relative to Meissl formula is not very outstanding.

When the prediction of ς_r is made in a single grid of HACN, its initial data are ς^0_r, which are obtained after removing the influence of long, medium and a part of short wavelength components of gravity field from the height anomalies ς^0 at control points. So ς^0_r as initial data basically bear a linear relationship with ς_r at interpolation points within a corresponding grid, then the prediction of ς_r can be made by way of simple linear interpolation with latitude,longitude and height as parameters, the effect is acceptable.

5. As for the value of c in (7)-(10), based on the practical conditions of China, extensive statistics has been made, and leading to the following values of c: 0.54 for plain; 0.81 for

hilly land; 1.08 for mountain land and 1.50 for high mountain area.

IV. Test Computation For The Accuracy Evaluation Formulas

Test computation for the accuracy evaluation formulas given in section II is briefly introduced here.

Assuming that resolutions of a HACN,d,in the east, middle and west of China are 70, 130 and 350 km respectively, and that the requirements on accuracies m_ς and m_0 at interpolation and control points in the above three areas are $\pm$1.0m, $\pm$1.5m, $\pm$2.0m and $\pm$0.9m, $\pm$1.2m, $\pm$1.5m respectively(Chen J.Y.1993). Refering to $m_s = \pm 0.15$m mentioned above, then the requirements on errors m_g of gravity correction term applied to height anomalied in the three areas are $\pm$0.39m, $\pm$0.88m and $\pm$1.3m respectively according to (3). Hence after knowing m_g and d, the requirement on resolution L° of local gravity data can be obtained by (8)(ref. *Table 1*). It should be noted here in the computationn of ς_g , the radius σ of spheric cap in which the local gravity data is taken into account should not be smaller than 3°.

If an accuracy of the 1m order for the geoid of China reference to Xian geodetic datum is required, the error m_g of gravity correction term at interpolation point should not be in general larger than $\pm$0.5m; it can be seen from *Table 2*, if a resolution of 30'×30' local gravity data holds, this requirement can only be fulfilled when the resolution of HACN approximately attains 75km on an average for whole China; while in mountain and high mountain areas, this resolution should even increase to 50km at least, however, it is very difficult to attain this resolution for a HACN in such kind areas. Otherwise, the resolution of local gravity data should be enhanced in the area, for example, achieving 5'× 5'.

An alternative solution is to pose different requirements on the accuracy of error m_g of gravity correction term in different areas, or in other words, the local geoid will be with different resolutions and different accuracies in different regions, so that the resolution of local gravity data will match with that of geoid on a practically feasible basis, and the layout of HACN for local geoid determination will conform to the need of a developing country like China and is practically feasible.

Table 1. The requirement for the resolution of local gravity data L°, when the resolution of HACN d, and the accuracy of the gravitry correction term m_g are known. (according to (8))

Region	m_g (m)	d (km)	L°			
			plain	hilly land	mountain land	mountain area
East	± 0.39	70	55'×55'	25'×25'	15'×15'	10'×10'
Middle	± 0.88	130	1°×1°	35'×35'	15'×15'	10'×10'
West	± 1.30	350	25'×25'	10'×10'	5'×5'	5'×5'

Here the last figure of L in *Table 1* has been rounding to 0 or 5.

Table 2. The requirement for the resolution of HACN d, when the accuracy of gravity correction term m_g and resolution of local gravity data L° are given. (according to (9))

m_g (m)	L°	d(km)				
		plain	hilly land	mountain land	mountain land	average
1.0	1°×1°	170	115	85	60	110
	30'×30'	240	160	120	90	150
	5'×5'	590	395	295	215	375
0.5	10×10	85	60	40	30	55
	30'×30'	120	80	60	45	75
	5'×5'	295	200	150	105	190

Here the last figure of d has been rounding to 0 or 5.

References

[1]. Chen,J.Y. (1993). On the accuracy and scheme of Chinese GPS levelling network (Chinese). Acta Geodaetica et Cartographica Sinica,Beijing.Vol.22,No.2:1-4.

[2]. Duker H.et al (1987). Local geoid determination and Comparison with GPS results. B.G.vol 161.

[3]. Meissl P. (1971). Preparations for the numerical evaluation of second order Molodensky-type formulas. Rep.163,Dep.of Geo.Sci.,Ohio State Univ.

[4]. Molodensky M.C. (1960). Thegravity field and figure of the earth. Report of the Central Researh Institute of Surveying and Mapping.

[5]. Ning J.S. et al (1990). Theory ofearth gravity field model.TU Wuhan Publ.House.

[6]. Sideris M.G. (1985). A fast Fourier trasformation method for computing terrain corrections. Manus.Geodaetica 10.

[7]. Schwarz K.P. (1990). The use of FFT techniques in physical geodesy.Geophys.J. 100.

[9]. Torge W. et al (1989). Long range geoid control through the European GPS traverse. DGK.Reihe B.No.290.

[10].Tscherning C.C. (1992). Height determination using GPS. GPS symp. Barcelona Spain.

Figure 1 The Area for Test Computation

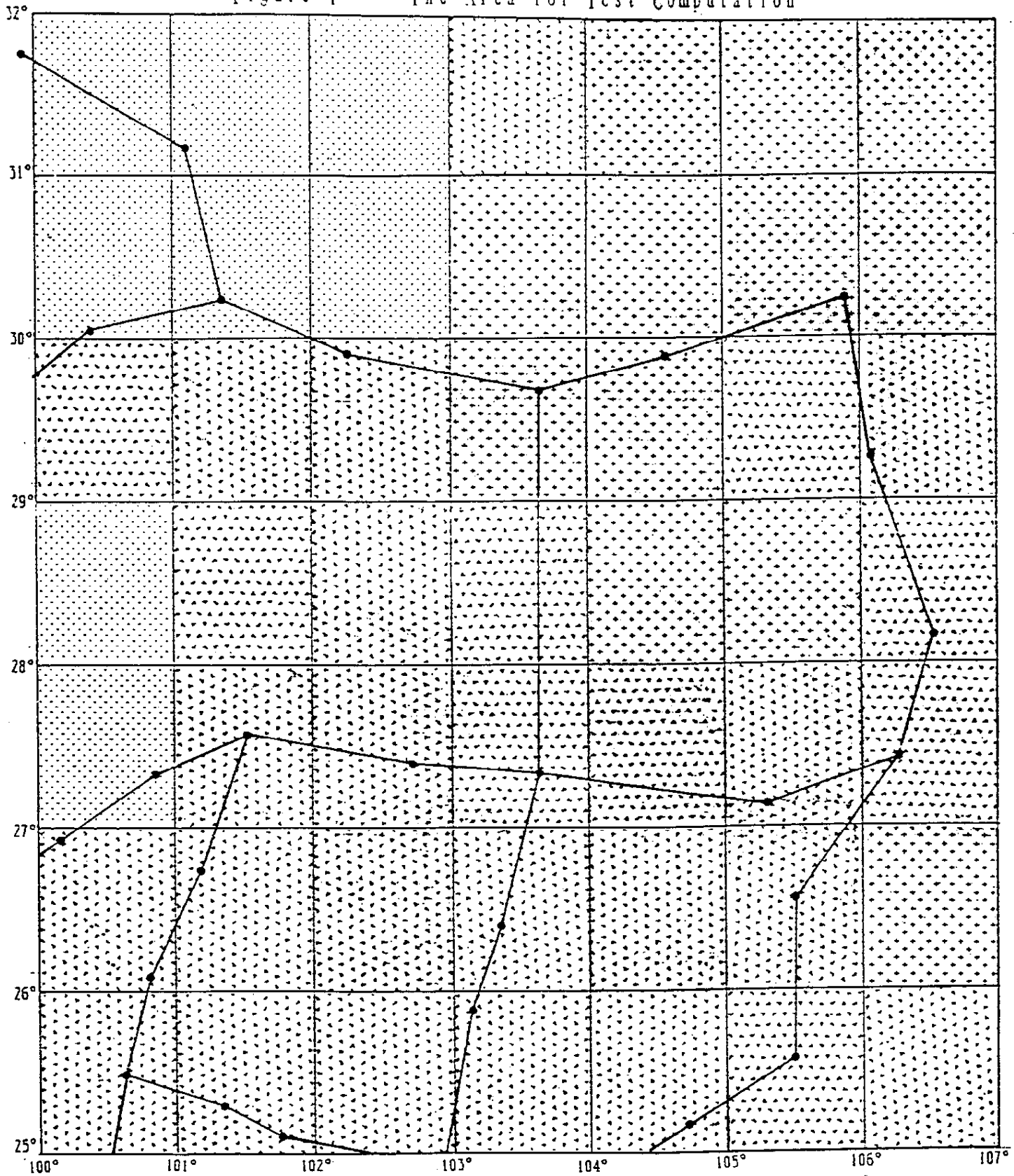

Legend

gravity data resolution

higher than 5′×5′

lower than 5′×5′

5′×5′

astro - gravimetric levelling line and point

LE GEOÏDE GRAVIMETRIQUE EN BELGIQUE

Premiers résultats

THE BELGIAN GRAVIMETRIC GEOID

First Results

C. Poitevin[1], Z. Jiang[2] & M. Everaerts[1]

[1] Centre de Géoph. Interne et de Géod. Spatiale, Observatoire Royal de Belgique, 3 Avenue Circulaire, B 1180 -Bruxelles
[2] LAREG, Institut Géographique National, 2 Avenue Pasteur, F 94160 - St-Mandé

Mots clés : Géoïde, gravimétrie, Belgique, nivellement, GPS.

Key Words : Geoid, gravimetry, Belgium, levelling, GPS.

Résumé : Le géoïde connaît un regain d'intérêt depuis l'avènement du positionnement précis par satellite, en particulier pour réaliser du nivellement par GPS. Après un bref rappel de notions élémentaires sur le géoïde, nous expliquons comment s'est constituée la banque de données gravimétriques belge et la façon dont ces données ont été exploitées pour aboutir au calcul d'un premier géoïde gravimétrique sur la Belgique. Ce géoïde a été adapté à 32 hauteurs géoïdales déduites d'observations GPS et de nivellement du nouveau réseau belge de référence BEREF. L'adéquation des résultats se situe au niveau de ± 5 cm en moyenne avec des écarts atteignant au maximum ± 12 cm dans les régions où la densité de mesures gravimétriques fait manifestement défaut. De nouvelles solutions seront bientôt proposées qui intégreront le maximum d'informations gravimétriques, topographiques et géodésiques disponibles en vue d'obtenir une précision sub-centrimétrique.

Abstract : The need of a precise geoid is growing with the increasing use of precise satellite positioning particularly for GPS levelling. After a brief recall of elementary notions about the geoid, we explain how the Belgian gravity data bank has been set up and how these data have been exploited for the computation of the first gravimetric geoid over Belgium. The geoid has been adapted to 32 geoidal heights deduced from GPS and levelling observations on the new Belgian reference network BEREF. The adequacy of the results is about ± 5 cm in the mean with variations reaching ± 12 cm maximum in areas where gravity data are clearly missing. New solutions will be proposed soon. These will include the maximum of gravimetric, topographic and geodetic informations in order to reach sub-centimeter accuracy.

1. Introduction

L'objet de notre propos est d'introduire ou de réhabiliter un concept qui faillit disparaître ou tout au moins être délaissé par beaucoup avec l'apparition de la géodésie tridimensionnelle : le géoïde. D'aucun s'imaginait qu'il était possible de s'affranchir du champ de la pesanteur et même de l'ellipsoïde de référence (Levallois, 1969, pg. 60).
L'avènement de la géodésie spatiale, plus particulièrement la disponibilité de récepteurs GPS (Global Positioning System) de plus en plus performants et les techniques de calcul de plus en plus élaborées, démontrent le contraire.

Les satellites ont permis de faire un bond prodigieux dans la connaissance précise des dimensions et de la forme de notre planète. D'un autre côté, nous disposons d'un patrimoine assez impressionnant de mesures effectuées à la surface de la Terre dont dépendent une grande partie de nos activités économiques et que nous devons continuer à exploiter. Ces mesures se réfèrent toutes à la verticale locale et donc implicitement au géoïde. Les combiner avec des mesures satellitaires, de caractère géométrique, se révèle souvent très délicat mais nécessaire car, hormis pour de petits réseaux locaux, les seules références pratiques demeurent les systèmes nationaux sur lesquels s'appuie la *carte de base*.

L'intervisibilité entre les stations de mesure n'est plus une contrainte avec les systèmes inertiels et GPS. Les distances s'accroissent et le topographe entre dans le domaine de la géodésie et plus particulièrement de la géodésie physique. Cette discipline très captivante l'est à un point tel qu'elle est souvent négligée par le praticien dont les impératifs, très compréhensibles, sont de produire un résultat dans un délai réduit, au risque d'une dégradation de la précision de ses observations.
C'est ce à quoi nous désirons remédier en apportant notre contribution par le calcul du géoïde gravimétrique, une tâche qui n'est concevable qu'à l'échelle du pays vu la quantité, la particularité des données à traiter et les techniques de calcul mises en oeuvre.

2. Le géoïde

Nous n'entrerons pas ici dans toutes les subtilités de la géodésie physique avec des notions telles que quasi-géoïde, co-géoïde ou telluroïde bien que nous les évoquerons. Le lecteur intéressé trouvera ces détails et leur explication dans 'Physical Geodesy' de Heiskanen & Moritz (1967), qui reste l'ouvrage de base en la matière et auquel on fera référence dans la suite par les initiales PG, ou dans Vanicek & Krakiwsky (1982) également très didactique. Pour une étude plus détaillée, on se reportera à (Moritz, 1980).

Une définition assez classique et intuitive du géoïde est qu'il correspond à *la surface de niveau coïncidant avec le niveau moyen des mers prolongée sous les continents par la condition d'y rester normale à toutes les lignes de force* (Levallois, 1969, pg. 21).

Malgré son apparente simplicité, cette définition suscite plusieurs interrogations comme, par exemple, le niveau moyen des mers, sa permanence, les références altimétriques... Des réponses nous viennent maintenant de l'espace avec les données d'altimétrie par satellite (Seasat, ERS1, Topex - Poséidon, etc.) mais le domaine d'exploration reste encore largement ouvert.

En fait, il est plus approprié de parler de hauteur géoïdale N. Celle-ci est la différence entre la hauteur ellipsoïdale h, purement géométrique, c'est-à-dire la distance entre le repère au sol et l'ellipsoïde de référence que l'on s'est choisi ou qui est imposé, et la hauteur orthométrique H telle qu'elle est obtenue par le nivellement et la gravimétrie au départ d'un datum que l'on s'est fixé. H représente une distance entre la surface topographique et 'une' surface équipotentielle correspondant normalement au géoïde. On écrit donc une équation très élémentaire dans sa forme, N = h - H (Fig. 1), mais dont la solution est difficile à obtenir car on ne remplit pas toujours les conditions sur les paramètres pour appliquer rigoureusement cette formule simple.

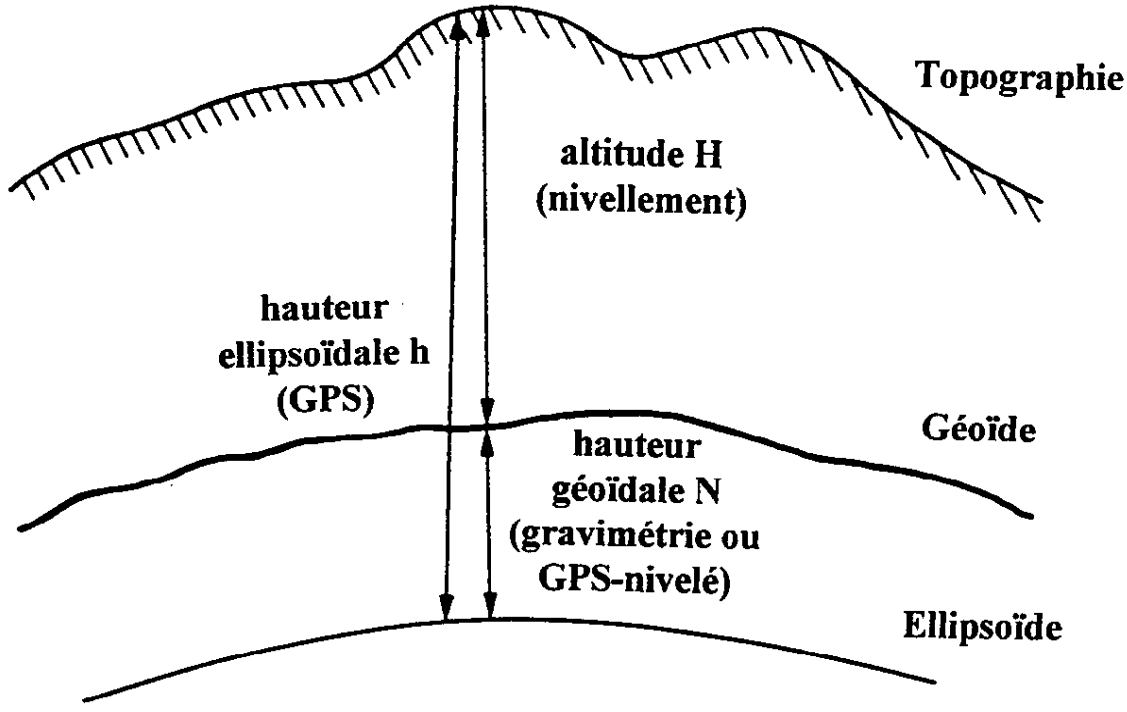

$$\mathbf{h = H + N}$$

Fig. 1 : Hauteur ellipsoïdale, altitude et hauteur géoïdale.

Il existe un moyen indépendant d'accéder à N via le potentiel gravitationnel perturbateur T, la différence entre le potentiel de la Terre réelle et le potentiel de la pesanteur sur l'ellipsoïde de référence, par la formule de Bruns (PG, éq. 2-144)

$$N = \frac{T}{\gamma}$$

où γ est la pesanteur normale, c'est-à-dire la valeur théorique de la pesanteur calculée sur un ellipsoïde de référence. La formule est donnée au § 5.1.2.

et l'équation fondamentale de la géodésie physique (PG, éq. 2-148)

$$\frac{\partial T}{\partial h} - \frac{1}{\gamma}\frac{\partial \gamma}{\partial h} T + \Delta g = 0$$

qui relie T à l'anomalie de pesanteur Δg définie plus précisément au § 4.3, une quantité calculable au départ des observations gravimétriques, g étant la pesanteur mesurée et h l'altitude. De longs développements mathématiques conduisent à la formule de Stokes (PG, éq. 2-163b)

$$N = \frac{R}{4\pi G} \iint_{\sigma} \Delta g \, S(\Psi) \, d\sigma$$

où R = rayon terrestre moyen (voir PG, pg. 87) ~ 6.371 km;
G = valeur moyenne de la pesanteur terrestre ~ 978.8 Gals;
ψ = distance sphérique utilisée comme rayon d'intégration;
$S(\psi)$ = fonction de Stokes (une fonction assez complexe dont une des expressions est donnée dans PG, éq. 2-164),

qui établit une relation directe entre N et Δg sous forme d'une intégration des anomalies de pesanteur étendue à l'ensemble de la surface terrestre. Or, nous ne disposons pas de mesures gravimétriques en tout point du globe.

En Belgique, nos prédécesseurs ont choisi comme ellipsoïde de référence l'Ellipsoïde International, appelé aussi Hayford 1924, qui n'est notamment pas une surface équipotentielle, les formules de la géodésie physique ne s'y appliquent donc théoriquement pas, les conditions requises sont énumérées dans (Levallois, 1970, pg. 147) et confirmées par (PG, pg. 64). Le datum altimétrique (repère IGNMK) n'a plus réellement de connexion avec le niveau moyen de la mer puisque choisi arbitrairement, pour des raisons entre autres de préservation, dans la cour de l'Observatoire Royal (IGM, 1949). Sa référence est située environ 2.32 m plus bas que les références des pays voisins. *Stricto senso,* nous n'utilisons pas de cotes orthométriques, ce qui n'a pas d'incidence vraiment préjudiciable compte tenu de la topographie du pays. Le système de représentation plane Lambert sécante utilisé en Belgique ne satisfait pas, à la précision requise, aux formules mathématiques de la théorie des projections cartographiques (Poitevin, 1988) et le Lambert belge 72, suite aux adaptations destinées à maintenir ses coordonnées proches du Lambert 50, nécessite une transformation (translation et rotation) additionnelle...
Brièvement, nous avons à résoudre chez nous ce à quoi sont également confrontés tous nos voisins : l'homogénéisation de nos systèmes de référence et la mise en concordance de nos observations dans un système standardisé pour pouvoir exploiter au mieux les données terrestres et satellitaires.

Ce qui est rassurant est qu'en prenant un certain nombre de précautions auxquelles il est fait allusion plus haut et en utilisant des données bien contrôlées et minutieusement validées, il est possible d'obtenir des résultats déjà très satisfaisants dans un certain nombre d'applications à condition de se tenir à des notions différentielles. Il faut entendre, dans ce cas-ci, que nous pouvons, localement ou même globalement, évaluer la forme du (quasi-)géoïde gravimétrique mais pas sa position absolue même si des mesures absolues de la pesanteur précises à 10^{-9} ont contribué à sa détermination. Pour leur part, les observations GPS de précision sont effectuées dans le mode différentiel et doivent subir certaines transformations avant de délivrer des hauteurs ellipsoïdales. De celles-ci on soustraira des altitudes rapportées au Deuxième Nivellement Général (DNG) pour obtenir des hauteurs géoïdales dites GPS-nivelées. Rien qu'en se rappelant l'arbitraire de la définition du datum du DNG, le repère IGNMK, on comprendra qu'un géoïde construit sur des points GPS-nivelés n'a pas non plus de position absolue bien établie. Par abus de langage, nous continuerons pourtant à appeler ces deux surfaces, gravimétrique et GPS-nivelée, géoïdes. Chacune d'elles possède des avantages et des inconvénients. Plutôt que d'opposer la méthode gravimétrique à la méthode géométrique, nous avons voulu voir dans quelle mesure les résultats qu'elles produisent se complétaient à l'avantage de l'utilisateur.

3. La banque de données gravimétriques belge

La banque de données gravimétriques belge est établie au Centre de Géophysique Interne et de Géodésie Spatiale attaché à l'Observatoire Royal de Belgique. Elle a été initiée en 1983 par une recherche systématique et un dépouillement méticuleux de toutes les archives encore accessibles et utilisables. D'abord limitée à la Belgique, nous l'avons progressivement, pour rencontrer les besoins de la géodésie et de la géophysique (Chacksfield & al., 1993), étendue aux régions limitrophes : Allemagne, Grand-Duché de Luxembourg (Poitevin & al.,1990), France et Sud-Est de l'Angleterre. Des données terrestres sur les Pays-Bas et des données marines sur la Manche et la Mer du Nord sont en cours d'intégration. Nous comptons, si possible, combiner ces dernières avec les données d'altimétrie par satellite (ERS1, Topex - Poséidon et Seasat) dont nous disposons déjà. En Belgique, de récentes campagnes gravimétriques ont été organisées par nos soins pour satisfaire les demandes des géologues, ce qui nous a permis d'établir 4.150 nouvelles stations de très haute précision sur 4.150 km² du territoire national.

La validation est une procédure extrêmement stricte qui garantit la *qualité* et l'*intégrité* de la banque de données gravimétriques belge. Elle est appliquée systématiquement, avant intégration dans la banque, à tout ensemble de données, qu'il provienne de sources extérieures ou de nos propres mesures effectuées sur le terrain. La validation est toujours accompagnée de *l'homogénéisation des réseaux dans les mêmes datums* plani-, alti- et gravimétrique, ce que l'on contrôle sur leurs intersections lorsqu'elles existent.

Actuellement, plus de 120.000 valeurs ont été incorporées définitivement dans la banque de données (Fig. 2). Le taux de rejet à la validation a été de 11,1 %, ce qui n'est pas trop élevé pour des données d'origines aussi diverses. On constatera, malheureusement, de graves lacunes dans la couverture gravimétrique du pays qu'il conviendrait de combler aussi bien pour satisfaire les besoins de la géodésie que ceux de la géophysique et de la géologie.

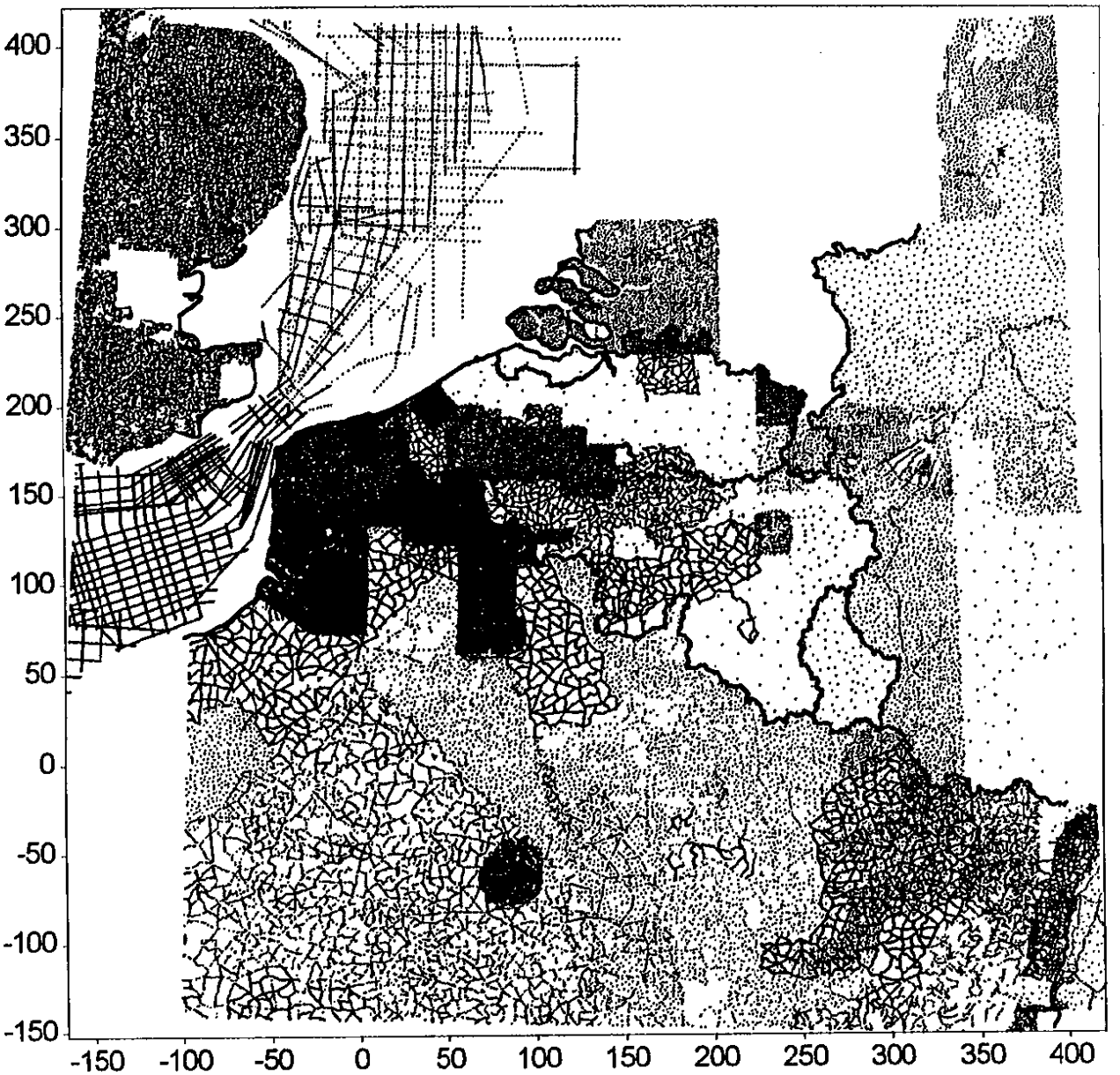

Fig 2: Localisation des mesures gravimétriques contenues dans la banque de données belge

4. Principe de calcul du géoïde gravimétrique

Comme dit précédemment (§ 2.), il faudrait théoriquement connaître la valeur de la pesanteur en chaque point du globe pour procéder à l'intégration des anomalies par la formule de Stokes. Ceci est bien sûr illusoire car il n'existe que très peu de mesures gravimétriques sur les océans et les mesures effectuées sur les continents sont beaucoup plus denses mais parfois aussi très éparses. De toute façon, les moyens de calcul ne le permettraient pas et le gain en précision ne le justifierait pas. Pour remédier à la situation, on pratique alors de la manière décrite ci-après qui se base sur la décomposition du contenu spectral du champ gravitationnel en trois gammes de longueurs d'onde.

4. 1 Les modèles géopotentiels

Grâce aux satellites artificiels, par l'étude des perturbations de leur orbite sous l'influence de l'attraction terrestre, on a pu établir des modèles géopotentiels représentatifs du potentiel gravitationnel de la Terre. Ces modèles se présentent sous la forme de développements en harmoniques sphériques, une classe particulière de polynômes qui permettent de modéliser au mieux la forme de notre planète. La circonférence terrestre divisée par le degré du développement donne approximativement la longueur d'onde de résolution d'un modèle géopotentiel, en bref, d'un potentiel. Il en existe en effet plusieurs, suivant l'usage auquel on les destine. C'est ainsi que, pour augmenter la résolution des potentiels utilisés en gravimétrie notamment, on combine, au cours de leur détermination, les données spatiales avec des anomalies gravimétriques moyennes et d'autres informations géophysiques. Le calcul d'un potentiel est une entreprise de grande envergure, tant sur le plan de la collecte des données que des moyens de calcul mis en oeuvre, mais il permet de condenser en deux ensembles de coefficients, C_{nm}, S_{nm}, un volume de données extrêmement important qu'on ne pourrait manier autrement. Les modèles géopotentiels, dans les limites de leur résolution et de leur précision propre, ont également l'avantage d'être globaux et de permettre de calculer, en n'importe quel point du globe, la valeur du potentiel gravitationnel et de ses quantités dérivées : hauteur géoïdale, anomalie de la pesanteur et déviations de la verticale. C'est ainsi qu'une première ébauche du géoïde sur la Belgique avec le potentiel GEM10C a été calculée (Poitevin, 1989, 1991). Ce potentiel étant complet jusqu'au degré et à l'ordre 180, sa résolution n'était que de 220 km mais suffisante pour donner une première idée de l'allure du géoïde sur le pays. Pour arriver à ce résultat, il a fallu, pour chaque point de calcul, synthétiser les 2 x 16.471 coefficients, C_{nm}, S_{nm}, dans le développement du potentiel en harmoniques sphériques. Actuellement, les potentiels gravimétriques atteignent en standard le degré 360, soit 2 x 65.338 coefficients et une longueur d'onde d'environ 110 km. C'est le cas du potentiel OSU91A (Rapp & al., 1991) que nous avons utilisé pour ce travail.

4.2 Les modèles numériques de terrain

La haute fréquence s'obtient à partir d'un Modèle Numérique de Terrain (MNT) dont la finesse du pas influencera la précision des calculs. En fonction de la disponibilité et des variations de la topographie, on choisira un pas de 5 à 1 km, voire mieux, et un débordement du MNT par rapport aux données gravimétriques d'au minimum une demi-longueur d'onde caractéristique du potentiel, soit ici 55 km. On calcule ensuite un MNT filtré en supprimant toutes les longueurs d'onde plus courtes que 55 km. Celui-ci représente la surface topographique de référence qui devrait correspondre au potentiel de degré 360. En

soustrayant le MNT filtré du MNT originel, on obtient le Modèle Résiduel de Terrain (MRT) qui sera utilisé pour calculer l'effet de la topographie. Numériquement, cette opération est réalisée en une étape.

4.3 Les anomalies gravimétriques

Le calcul des anomalies gravimétriques dites 'à l'air libre', Δg_{AL}, (PG, éq. 3-62 et 3-16, 3-17)

$$\Delta g_{AL} = g + F - \gamma$$

où $$F = -\frac{\partial g}{\partial h} h \approx -\frac{\partial \gamma}{\partial h} h \approx +0.3086\, h \ \ mGal$$

s'effectue en utilisant les valeurs de la pesanteur mesurées et, théoriquement, les altitudes normales (PG, éq. 4-44).

$$H^* = \frac{C}{\gamma}\left[1 + \left(1 + f + m - 2f\sin^2\Phi\right)\frac{C}{a\gamma} + \left(\frac{C}{a\gamma}\right)^2\right]$$

où $f = (a-b)/a$ est l'aplatissement géométrique;
a et b sont respectivement les grand et petit axes de l'ellipsoïde;
$m = \omega^2 a^2 b / kM$;

ω = vitesse angulaire de rotation de la Terre;
M = masse de la Terre;
k = constante gravitationnelle newtonienne;
Φ = latitude;

et C est le *nombre géopotentiel* $$C = W_0 - W = \int_0^H g\, dH$$ (PG, éq. 2-25)

où W_0 et W sont respectivement les potentiels au niveau zéro et considéré.

L'application de la formule de Stokes à ces anomalies a pour résultat une quantité ς appelée hauteur anomale (height anomaly) qui est la distance entre la surface topographique et le telluroïde, une surface non-équipotentielle proche de la surface topographique obtenue par reconstruction de la Terre réelle depuis le modèle ellipsoïdal (Molodenskii & al., 1962). Cette distance rapportée à l'ellipsoïde est dénommée hauteur du quasi-géoïde et a également pour symbole ς. Le quasi-géoïde n'est pas non plus une surface de niveau mais équivaut au géoïde sur les océans où ς = N et reste très proche de lui partout ailleurs sauf dans les régions montagneuses. La formule exprimant la différence N - ς est donnée par (PG, éq. 8-102).

$$N - \zeta = \frac{\bar{g} - \bar{\gamma}}{\bar{\gamma}} H = H^* - H \approx \frac{\Delta g_{Bouguer}}{\bar{\gamma}} H$$

En pratique, compte tenu de la topographie en Belgique, nous pouvons assimiler ς à N sans erreur appréciable pour la précision actuellement recherchée.

4.4 La procédure de retrait - restauration

La procédure de retrait (remove) consiste à retrancher des anomalies à l'air libre Δg_{AL} son contenu basse Δg_{POT} et haute Δg_{TOPO} fréquence pour obtenir des anomalies résiduelles $\Delta g_{Rés}$.

$$\Delta g_{Rés} = \Delta g_{AL} - \Delta g_{POT} - \Delta g_{TOPO}$$

Les anomalies résiduelles ainsi obtenues ont une variabilité (déviation standard) fortement atténuée qui permet d'appliquer la formule de Stokes avec un rayon d'intégration limité ψ_0 sans trop grande perte de précision. Le noyau d'intégration, $S(\psi)$ ou fonction de Stokes, peut subir diverses adaptations pour améliorer les performances du calcul ou se conformer à certaines hypothèses.

On restaure (restore) ensuite l'information géoïdale, après calcul ($\Delta g \rightarrow N$) en sommant les différentes composantes fréquentielles :

$$N = N_{POT} + N_{Stokes} + N_{TOPO}$$

Le résultat de cette opération de retrait-restauration fournit le 'meilleur' (quasi-) géoïde gravimétrique dans la zone où l'on dispose de mesures gravimétriques et d'un MNT.

4.5 Adaptation du géoïde gravimétrique aux points GPS - nivelés

Malgré tout, il est possible que le modèle géopotentiel utilisé ne soit pas des plus performants dans la région étudiée et introduise des perturbations à longue période, un décalage éventuellement assorti d'une inclinaison, dans le géoïde gravimétrique ainsi calculé. C'est pourquoi il est préférable, si l'on dispose de points GPS-nivelés, d'adapter le géoïde à ces hauteurs géoïdales géométriques. Pour ce faire, on utilise une transformation de similitude à quatre paramètres (Δx, Δy, Δz et un facteur d'échelle) ou toute autre technique adéquate, la valeur de ces paramètres n'ayant pas de signification particulière. Pour autant que les points GPS-nivelés soient de qualité, en nombre suffisant et bien répartis, le géoïde gravimétrique ainsi adapté peut être utilisé directement pour effectuer du nivellement par GPS. La précision de ce nivellement dépendra bien sûr de la précision du géoïde gravimétrique, que la méthode de Stokes ne permet pas d'évaluer. Par contre, les résidus de l'ajustement aux points GPS-nivelés fournissent une mesure de l'adéquation des méthodes géométrique et dynamique sans toutefois les départager. Ils peuvent cependant mettre en évidence des erreurs grossières auxquelles la méthode géométrique est plus vulnérable. La méthode dynamique est moins sensible à ce genre de problème car ses résultats proviennent de l'intégration d'un très grand nombre de données.

Il existe une autre technique de détermination du géoïde gravimétrique, appelée collocation, qui fournit une estimation de l'erreur ou plutôt de la cohérence interne des paramètres estimés. Elle soulève d'autres problèmes par la dimension des matrices utilisées lors des

calculs. Nous comptons l'appliquer dans un avenir proche et confronter ses résultats avec ceux de la méthode de Stokes.

5. Application au calcul du géoïde gravimétrique belge

Ce travail constitue un premier essai de calcul du géoïde gravimétrique sur la Belgique. Il n'a jamais été réalisé auparavant, d'une part parce que le besoin ne s'en faisait pas encore sentir et d'autre part parce que la densité des mesures gravimétriques n'était pas suffisante. La banque de données gravimétriques belge, grâce aux nombreuses valeurs accumulées et validées aussi bien sur le territoire national que dans les régions contiguës, offre maintenant cette possibilité avec la restriction du manque de données dans l'est du pays et de l'absence momentanée de données sur les Pays-Bas et la Mer du Nord. Dans ces deux dernières régions, la lacune sera bientôt comblée. Néanmoins, la tentative méritait d'être réalisée tout en sachant que les résultats ne seraient que provisoires.

5.1 Les données

Sauf mention explicite, les unités sont le mètre et le milliGal ou mGal. Le Gal, en hommage à Galileo Galilei, équivaut à une accélération de 1 cm sec^{-2}. Les axes des cartes reprises en figure sont gradués en km, la projection utilisée étant le système Lambert belge 72.

5.1.1 Le modèle géopotentiel

Le modèle géopotentiel utilisé est OSU91A (Rapp & al., 1991) complet jusqu'au degré et à l'ordre 360. Il est généralement admis comme potentiel de référence pour ce genre d'application. Les anomalies à l'air libre qui en sont déduites sont représentées à la figure 3. Le choix de la répartition des points est expliqué au paragraphe suivant.

5.1.2 Les anomalies gravimétriques

Afin d'économiser le temps de calcul pour ce premier essai, nous nous sommes volontairement limité à des données gravimétriques comprises entre 48°.8 et 51°.8 en latitude N et 2°.5 et 7°.0 en longitude E. De plus, nous avons effectué un échantillonnage avec un pas de 5 km sur les données contenues dans cette zone; il ne s'agit donc pas de valeurs moyennes. L'ensemble ainsi constitué comporte 3.722 points de mesure.
Une correction de -2.32 m a été appliquée aux altitudes des données belges pour les rapporter à la même référence altimétrique que les pays voisins (Fig. 4), soit au système du REUN (Réseau Européen Unifié de Nivellement). Cette correction a son importance ainsi que nous le verrons par la suite. Comme l'impose l'usage lorsqu'on établit des réseaux gravimétriques, les altitudes sont déterminées par rattachement aux réseaux nationaux. Il s'agit donc d'altitudes brutes et non pas de hauteurs normales, ce qui n'a en pratique pas réellement d'influence dans nos régions relativement peu escarpées.
Les coordonnées sont normalement établies sur l'Ellipsoïde International. Idéalement, on aurait dû effectuer la transformation pour se placer dans le World Geodetic System 1984 (WGS84) auquel se réfère le potentiel OSU91A, mais les paramètres proposés sont encore trop globaux, trop peu précis pour mériter d'être utilisés à ce genre de raffinement.
La réduction à l'air libre (PG, éq. 8-7)

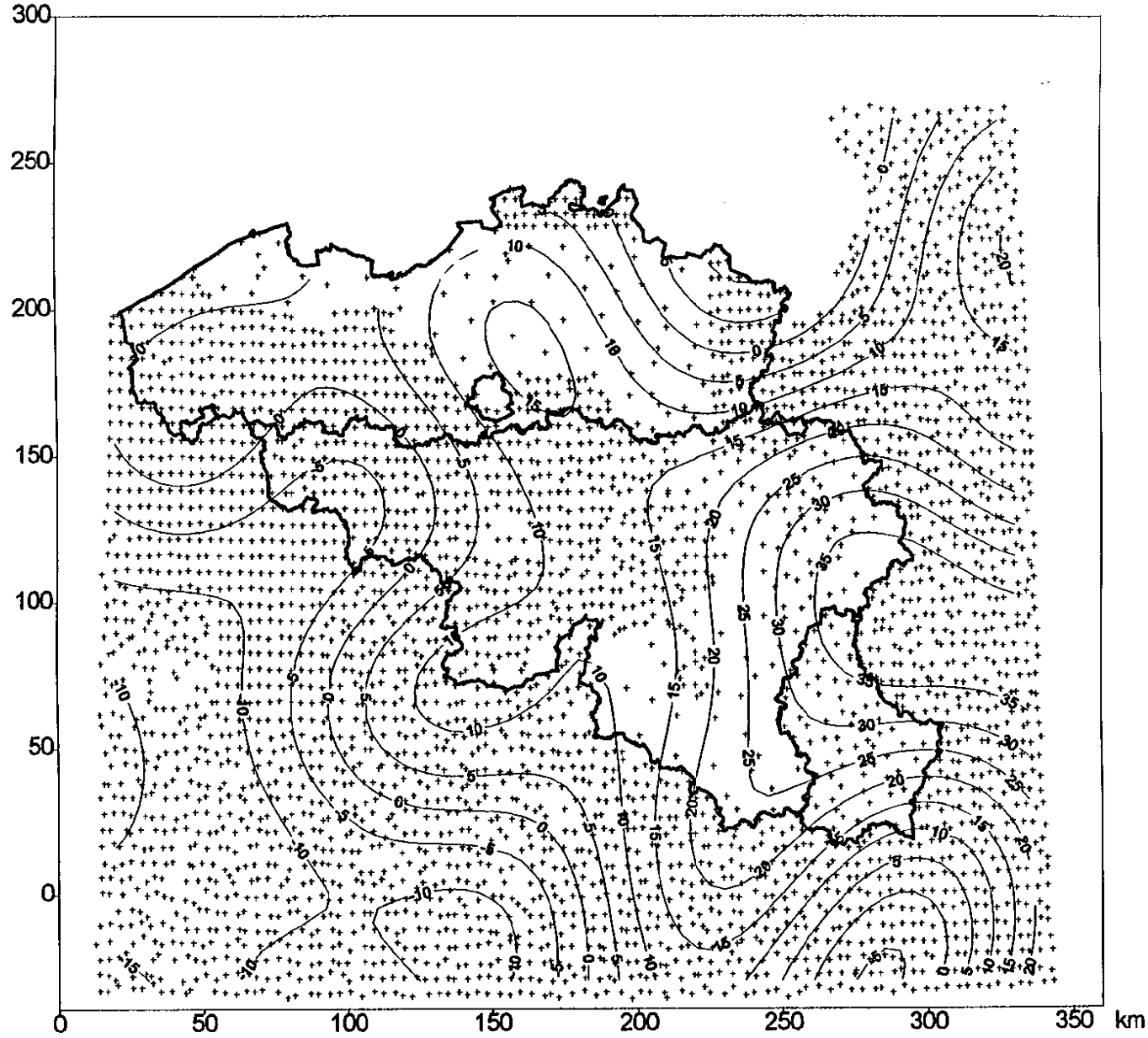

Fig 3: Anomalies à l'air libre calculées par OSU91A

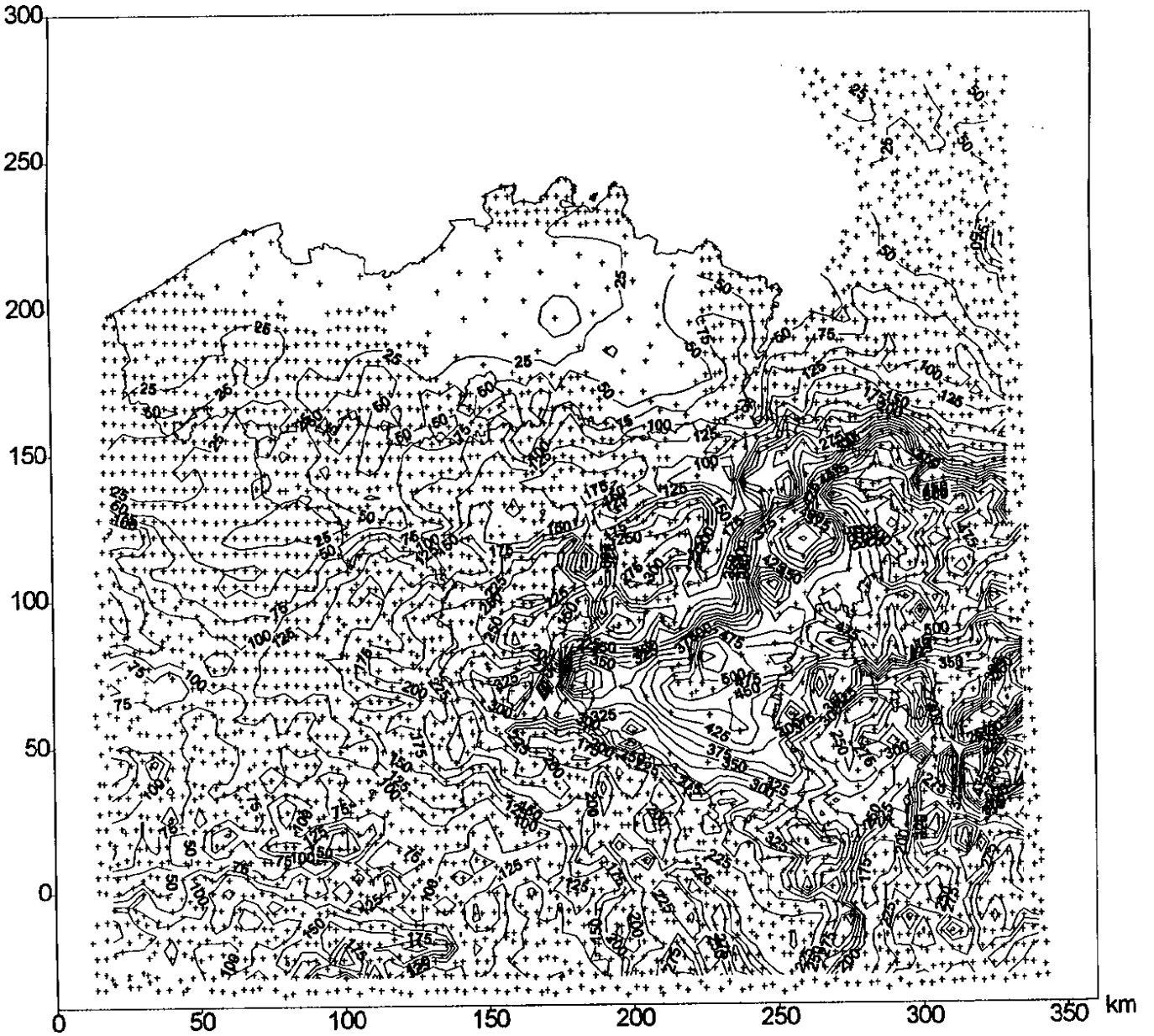

Fig 4: Altitudes

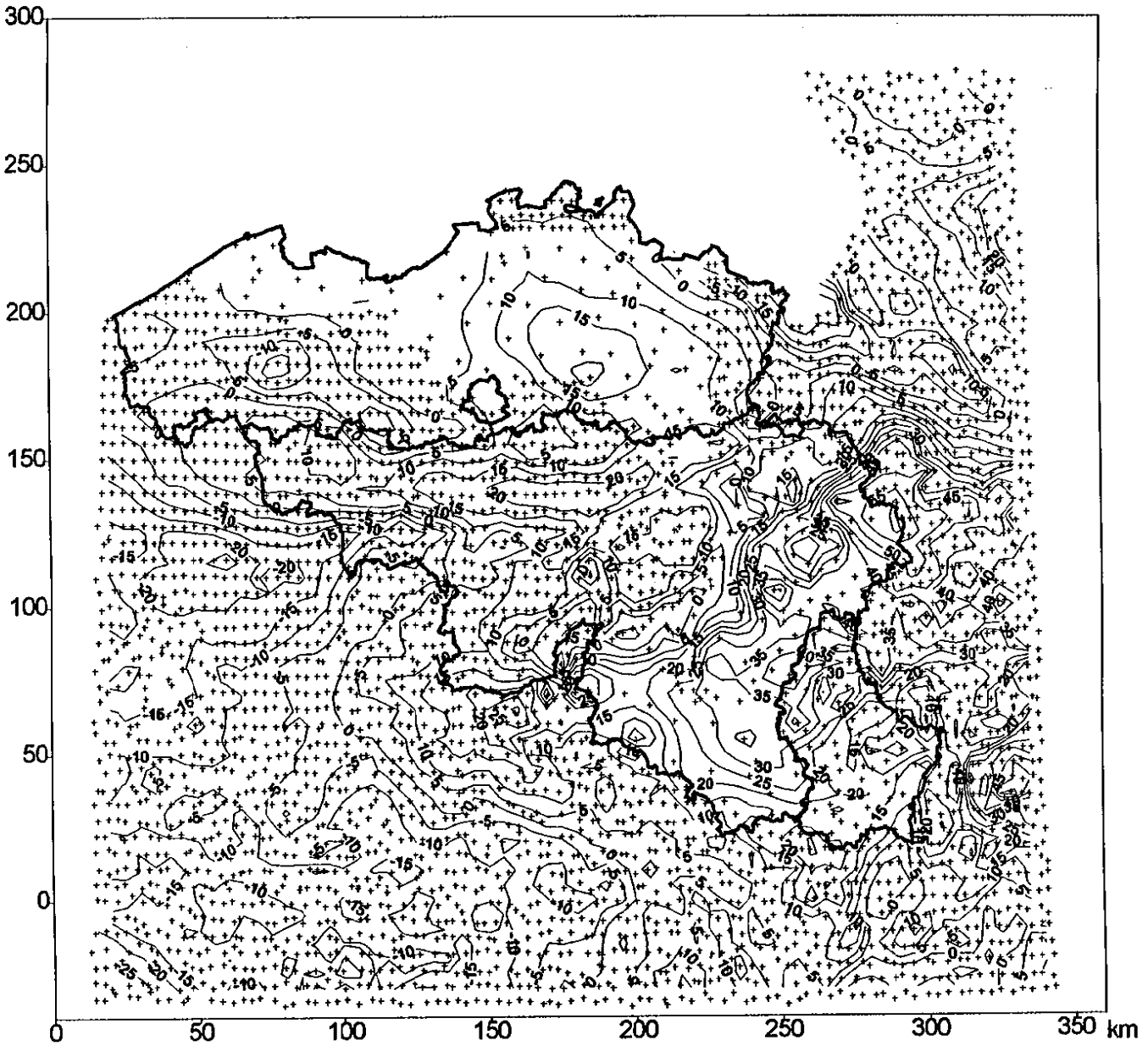

Fig 5: Anomalies à l'air libre calculées par la gravimétrie

$$\Delta g = g_P - \gamma_Q$$

est calculée en utilisant la pesanteur normale γ calculée par la formule finie de Somigliana (PG, éq. 2-78)

$$\gamma = \frac{a\gamma_a \cos^2 \Phi + b\gamma_b \sin^2 \Phi}{\sqrt{a^2 \cos^2 \Phi + b^2 \sin^2 \Phi}}$$

dans le Geodetic Reference System 1980 (GRS80). Cette formule a une expression plus appropriée au calcul dans (IAG, 1971). La pesanteur normale γ est la pesanteur théorique calculée sur un ellipsoïde de référence, dans ce cas-ci, celui correspondant au GRS80 en pratique identique à celui du WGS84. Ceci garantit la cohérence entre la réduction à l'air libre et OSU91A.

Enfin, on a appliqué une correction atmosphérique recommandée par l'Association Internationale de Géodésie (IAG, 1971) pour éliminer l'influence des masses atmosphériques; cette correction est presque constante pour ce qui nous concerne. Les anomalies à l'air libre calculées au départ des mesures gravimétriques sont représentées à la figure 5.

5.1.3 Le modèle numérique de terrain

Au moment des calculs, nous ne disposions pas de MNT sur la Belgique. On a donc généré un MNT au départ des informations altimétriques liées aux observations gravimétriques. Ceci signifie que ce MNT n'est pas plus homogène que la répartition des stations gravimétriques et comporte les mêmes lacunes. C'est bien évidemment un handicap pour une solution définitive du géoïde mais d'un autre côté cela permettra de souligner, en les accentuant, les manques dans la couverture gravimétrique du pays. La figure 6 représente l'effet du MRT sur les anomalies de pesanteur. Dans une étape ultérieure, nous espérons utiliser un MNT possédant un pas de 3 " x 3" (3" ~ 93 m) dans le sud et de 3" x 6" dans le nord de la Belgique.

5.2 Les calculs

Les calculs ont été effectués avec le logiciel GRAVSOFT (Tscherning & al., 1992) largement éprouvé et validé par l'IGeS (International Geoid Service, D.I.I.A.R. - Politecnico di Milano). Le travail a été réalisé à l'Observatoire Royal de Belgique en collaboration avec le Laboratoire de Recherche en Géodésie (LAREG), IGN - France, qui a mis au point une procédure permettant d'exécuter de façon très efficace et aisée la succession de programmes menant des données originelles au géoïde gravimétrique (Duquenne & al., 1994).

Après l'opération de retrait, on obtient des anomalies résiduelles (Fig. 7) beaucoup plus lisses que les anomalies gravimétriques. La déviation standard des données se réduit de 15.965 mGal à 6.812 mGal. On construit alors la grille des anomalies résiduelles en utilisant la technique de prédiction par collocation avec les paramètres standards : longueur de corrélation $\chi_{1/2}$ = 25 km et variance C_0 = 1 mGal. Ultérieurement, si le besoin s'en fait sentir, on déterminera plus précisément ces paramètres à l'aide de fonctions de covariance locale construites sur les observations elles-mêmes pour améliorer l'interpolation.

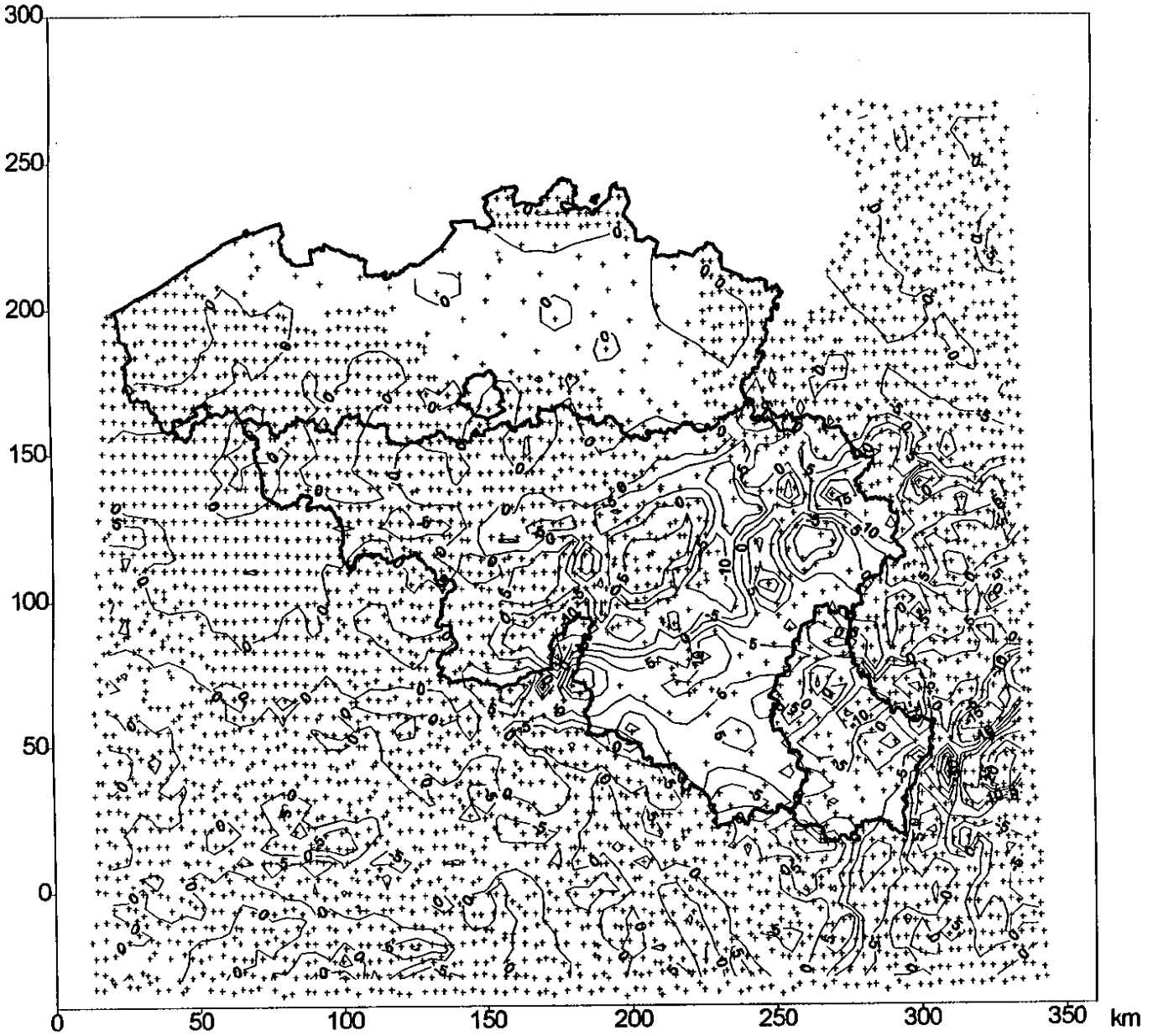

Fig 6: L'effet du MRT sur l'anomalie gravimétrique

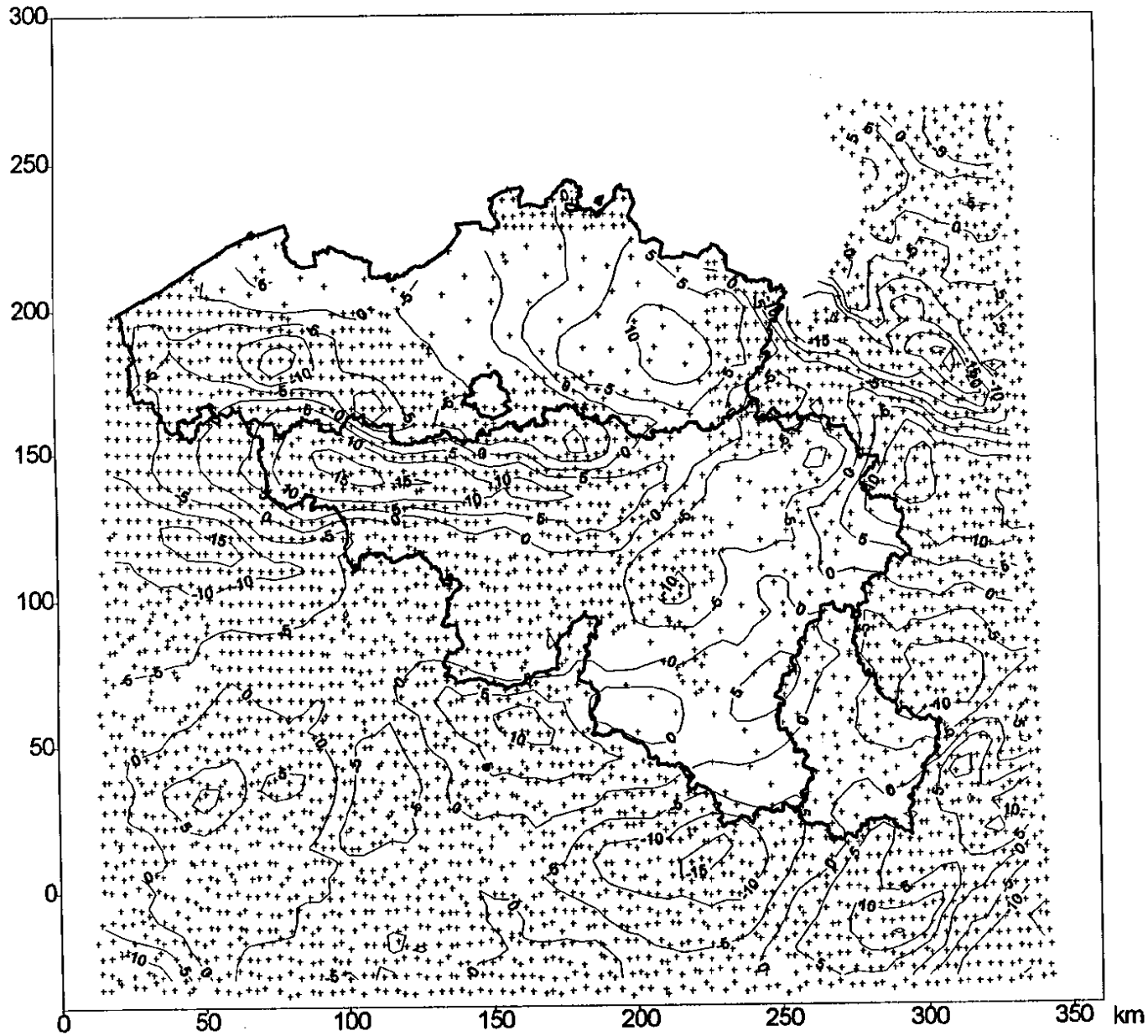

Fig 7: Anomalies résiduelles

La correction de terrain résiduelle a été limitée à un rayon de 55 km. Nous avons étendu le rayon d'intégration ψ_0 de la formule de Stokes, appliquée à la grille des anomalies résiduelles, à 55°.

Comme le MNT n'était pas encore disponible, nous avons limité la procédure de restauration à 1.068 points localisés sur le territoire belge ou à proximité, lorsque la densité de stations le justifiait.

La table suivante présente la contribution, en mètre, de chacune des gammes d'onde au géoïde totalement restauré :

information géoïdale	minimum	maximum	amplitude maximale	moyenne	déviation standard
N_{POT}	43.650	47.330	3.680	45.138	0.821
N_{Stokes}	-0.301	0.282	0.583	0.036	0.094
N_{MRT}	-0.079	0.135	0.214	-0.003	0.034
N_{TOTAL}	43.790	47.418	3.628	45.171	0.827

5.3 Les résultats

Les figures 8, 9 et 10 représentent successivement les grandes longueurs d'onde du géoïde gravimétrique calculées par le potentiel OSU91A, les moyennes longueurs d'onde obtenues par l'application de la formule de Stokes aux anomalies résiduelles provenant des observations gravimétriques et les courtes longueurs d'onde déduites du MRT. De la somme de ces trois gammes d'onde résulte le géoïde gravimétrique (Fig. 11) qui est normalement l'aboutissement de nos calculs.

6. Adaptation du géoïde aux points GPS-nivelés

Comme dit précédemment, le géoïde gravimétrique est susceptible d'être forcé par les longues périodes du potentiel OSU91A. Or, l'IGN-Belgique vient d'achever un réseau GPS d'ordre zéro, BEREF, comportant 32 stations en Belgique. Chacune des stations a été nivelée par rattachement au Deuxième Nivellement Général (DNG). Bien que les hauteurs géoïdales qui nous ont été communiquées ne soient pas encore définitives, on peut considérer que la précision relative sur les hauteurs ellipsoïdales est meilleure que 5 cm dans les Ardennes et que 3 cm dans le reste du pays, et celle sur les altitudes meilleures que 1 cm. Malgré le faible nombre de données, nous avons dessiné les courbes de niveau leur correspondant (Fig. 12). Cette carte est à mettre en relation avec la figure 8 qui représente le géoïde calculé par OSU91A. L'adaptation a été réalisée par moindres-carrés sur les 32 points GPS-nivelés en ajustant les paramètres de transformation sur les trois coordonnées et en tenant compte d'un facteur d'échelle. Les coefficients de cette transformation n'ont pas de signification précise, l'objectif étant seulement de mettre le mieux possible en correspondance les deux surfaces

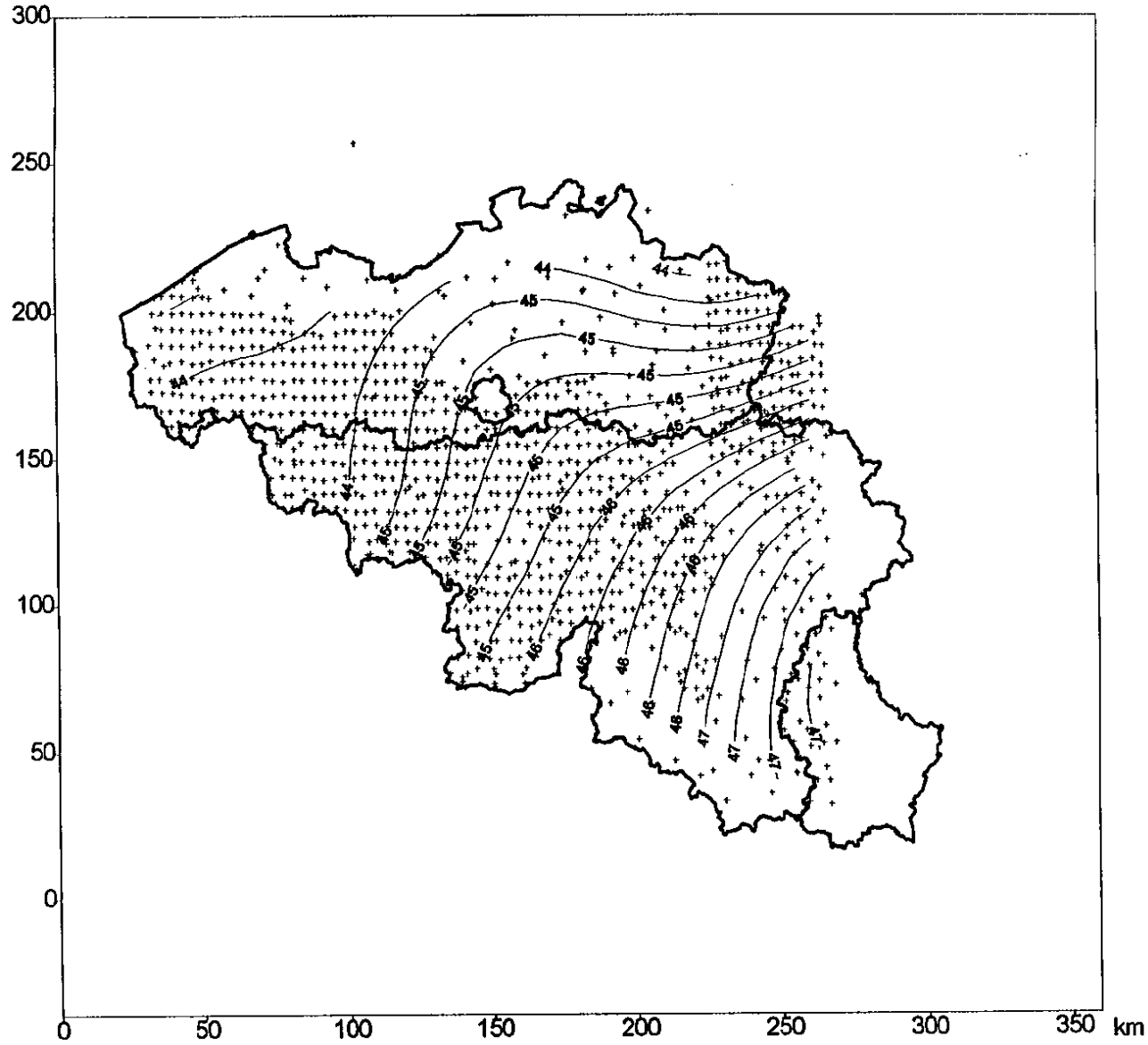

Fig 8: Hauteur du quasi-géoïde par OSU91A

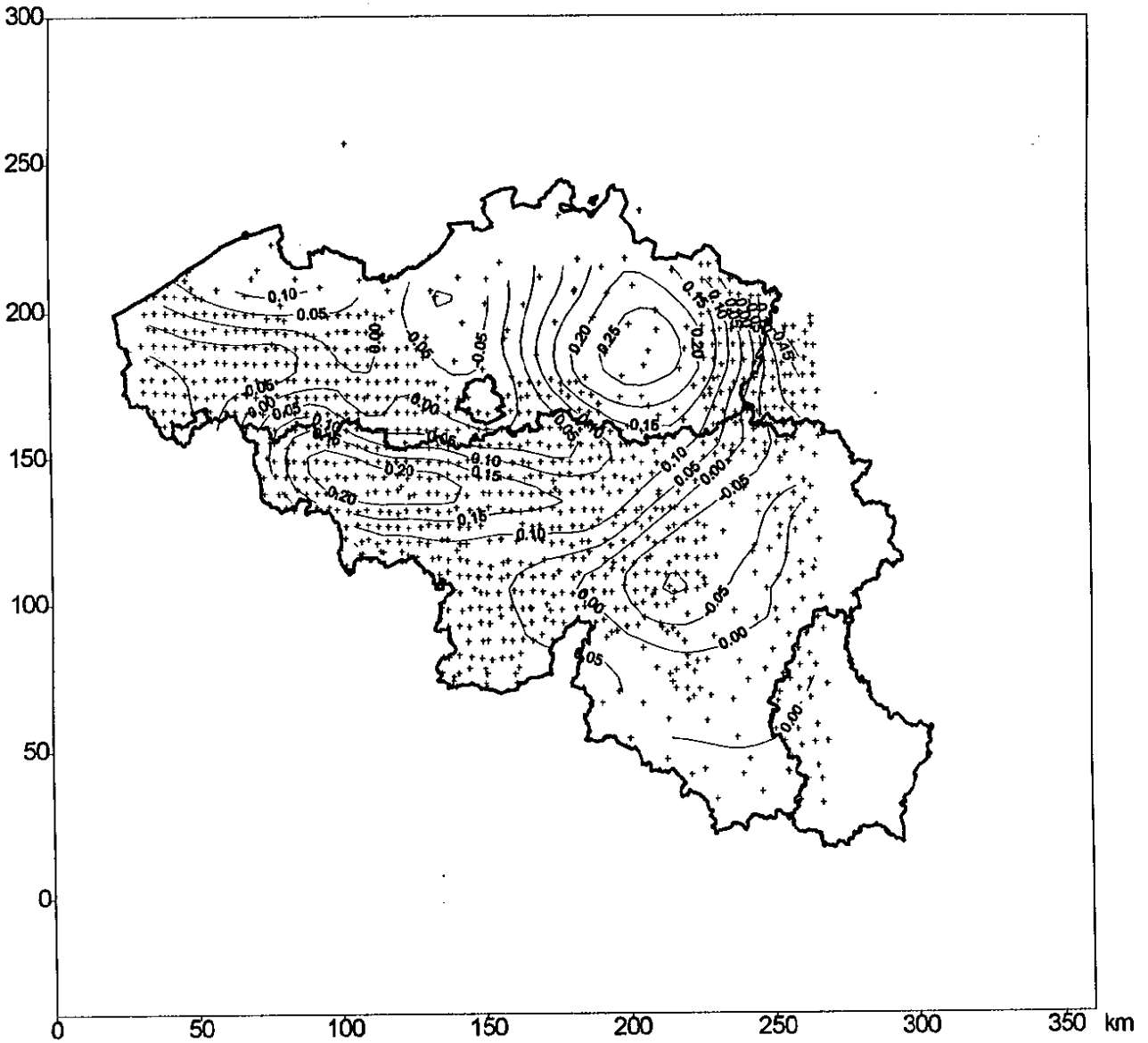

Fig 9: Quasi-géoïde résiduel (Intégrale de Stokes)

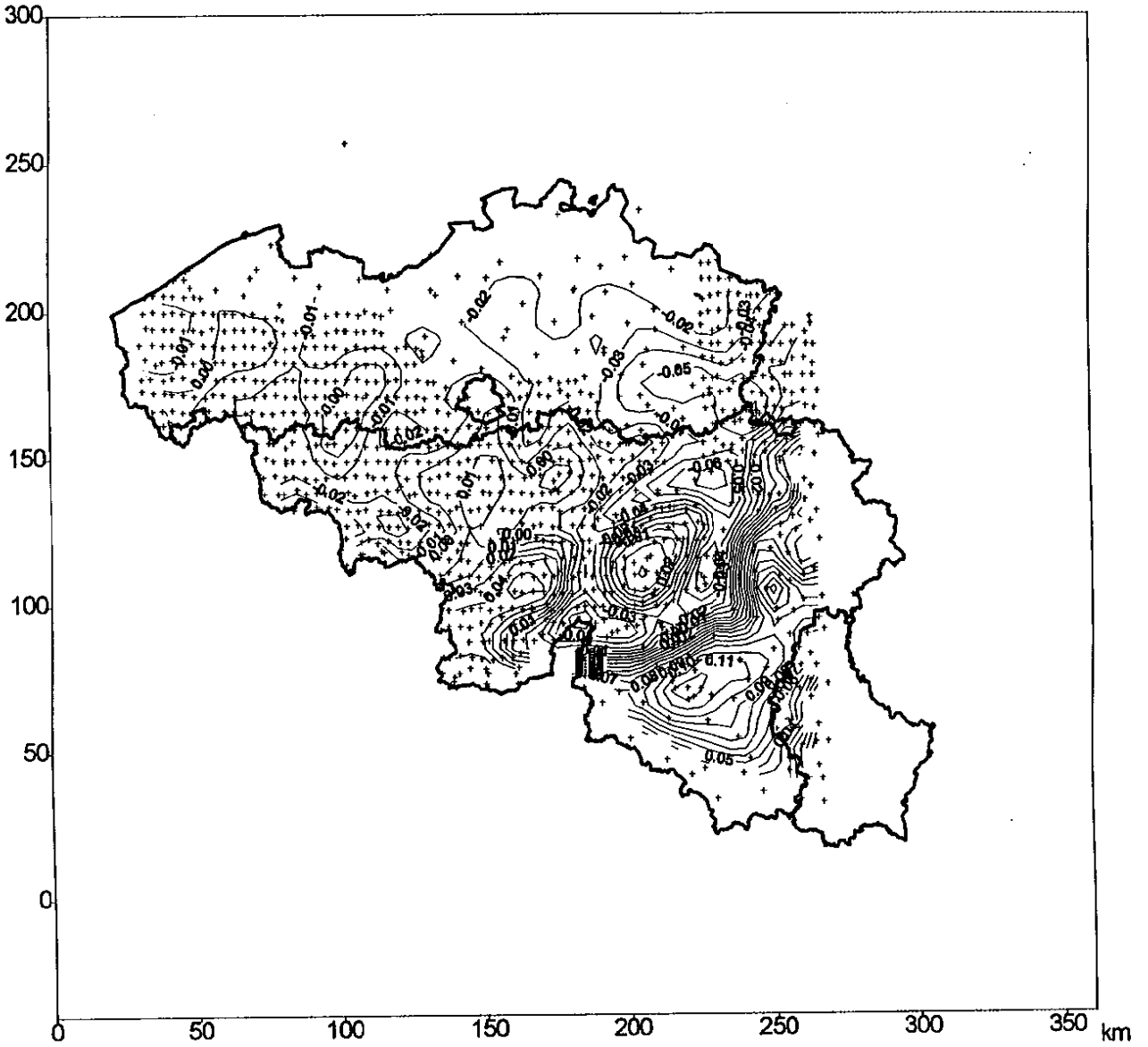

Fig 10: Effet du RTM sur le quasi-géoïde

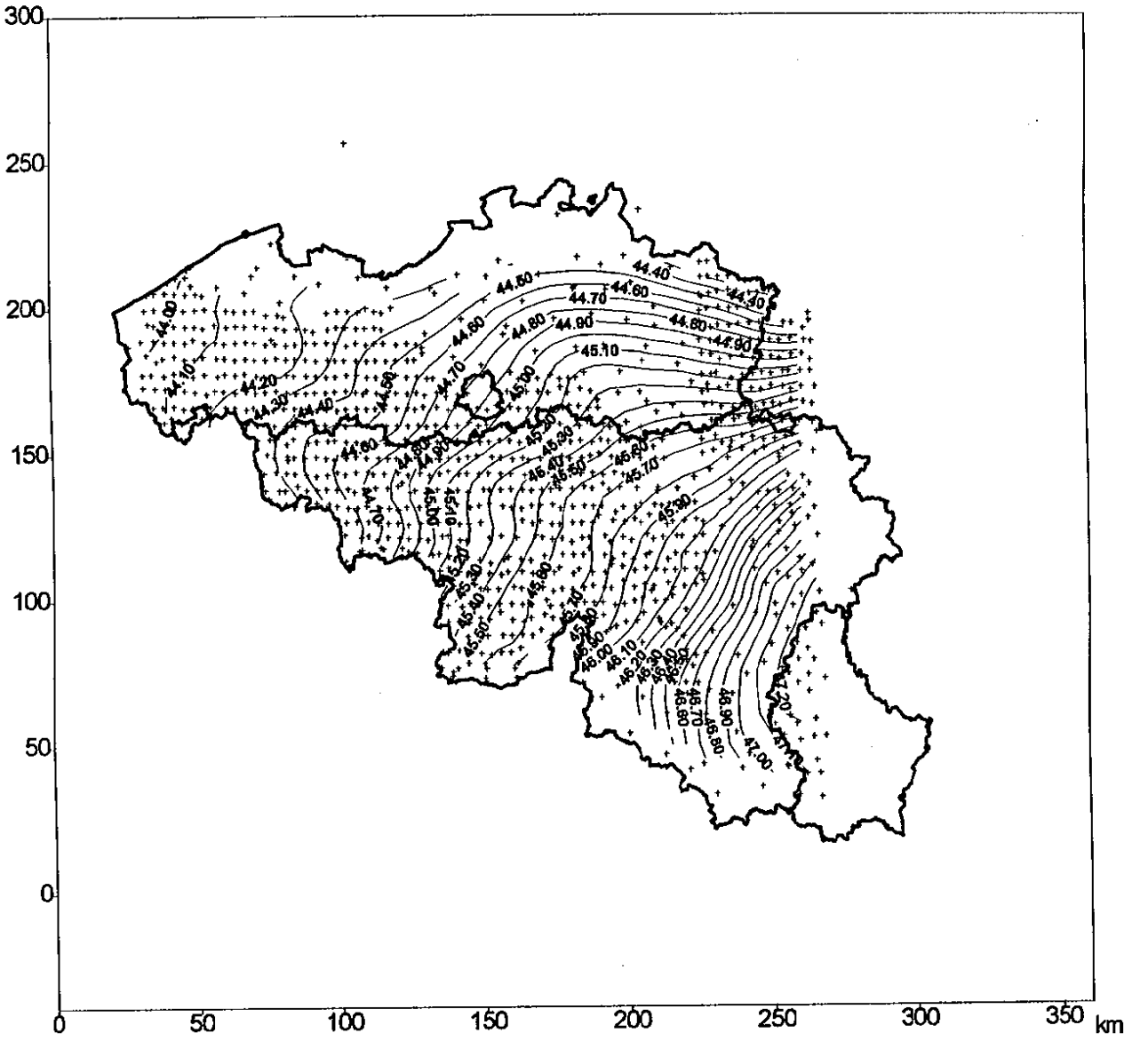

Fig 11: Hauteur du quasi-géoïde gravimétrique en Belgique

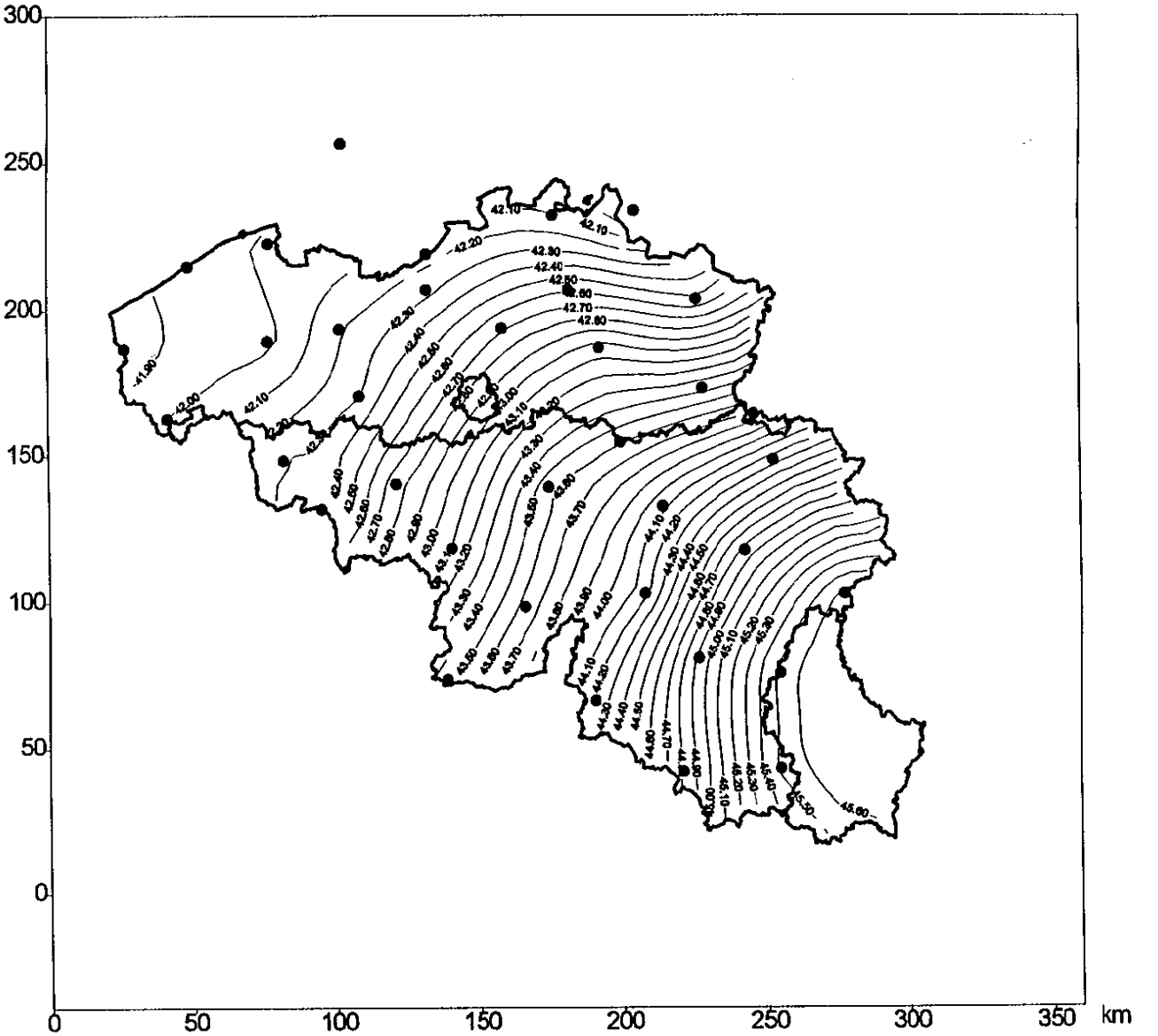

Fig 12: Points GPS nivelés dans le DNG, différences h-H

aux 32 points communs. Il est à signaler que les hauteurs du géoïde gravimétrique aux points GPS-nivelés sont le résultat d'une interpolation qui a pu altérer quelque peu leur précision.

Les points GPS-nivelés l'ont été dans la référence belge du DNG tandis que les données gravimétriques belges ont subi une correction d'altitude de -2.32 m, pour être rapportées à la référence altimétrique du REUN comme les altitudes des mesures gravimétriques des pays limitrophes. Ceci explique probablement, en grande partie, le décalage entre les deux surfaces présenté à la figure 13 mais il faut éventuellement tenir compte aussi d'une inclinaison relative introduite par le potentiel.

Finalement, on obtient le géoïde gravimétrique adapté aux points GPS-nivelés (Fig. 14). Celui-ci n'est pas nécessairement le 'meilleur' au sens de la géodésie physique mais certainement le plus approprié pour des usages pratiques, comme, par exemple, le nivellement par GPS.
La méthode de Stokes ne permet pas d'estimer la précision des calculs sinon l'erreur de troncature. De toute façon, cette erreur ne serait pas très significative suite aux manipulations de la technique du retrait-restauration et aux erreurs propres du modèle géopotentiel utilisé. On peut cependant estimer l'adéquation entre la méthode géométrique et la méthode gravimétrique en considérant les résidus de l'ajustement entre les deux surfaces (Fig. 15). La constatation s'impose que les résidus les plus élevés, dépassant 10 cm, sont tous les trois situés dans des régions où les mesures gravimétriques, et donc aussi, dans ce cas, l'information altimétrique, font défaut. Partout ailleurs, on peut considérer que l'adéquation est très bonne, si pas excellente, compte tenu de l'échantillonnage opéré sur les données (§ 5.1.2).

Le tableau suivant résume, en mètre, les principales informations concernant l'adaptation des deux surfaces :

données	**minimum**	**maximum**	**amplitude maximale**	**déviation standard**
N(GPS-nivelés)	41.834	45.646	3.812	1.151
N(gravimétrique)	41.832	45.755	3.923	1.147
ΔN	-0.117	0.112	0.229	0.051

7. Conclusions et prospectives

Malgré l'imperfection des données qui ont servi à ce premier calcul du géoïde gravimétrique sur la Belgique, les résultats sont concluants et on peut considérer que la précision centimétrique est atteinte sauf dans les régions où il existe un manque manifeste de données. Un de nos objectifs est de combler ces lacunes.

Nous envisageons d'utiliser la technique de collocation par moindres-carrés et de comparer les résultats ainsi obtenus avec ceux provenant de la méthode de Stokes. Cette technique présente des inconvénients, par exemple les dimensions des matrices de calcul, mais elle présente l'avantage de fournir une estimation de l'erreur interne des paramètres calculés.

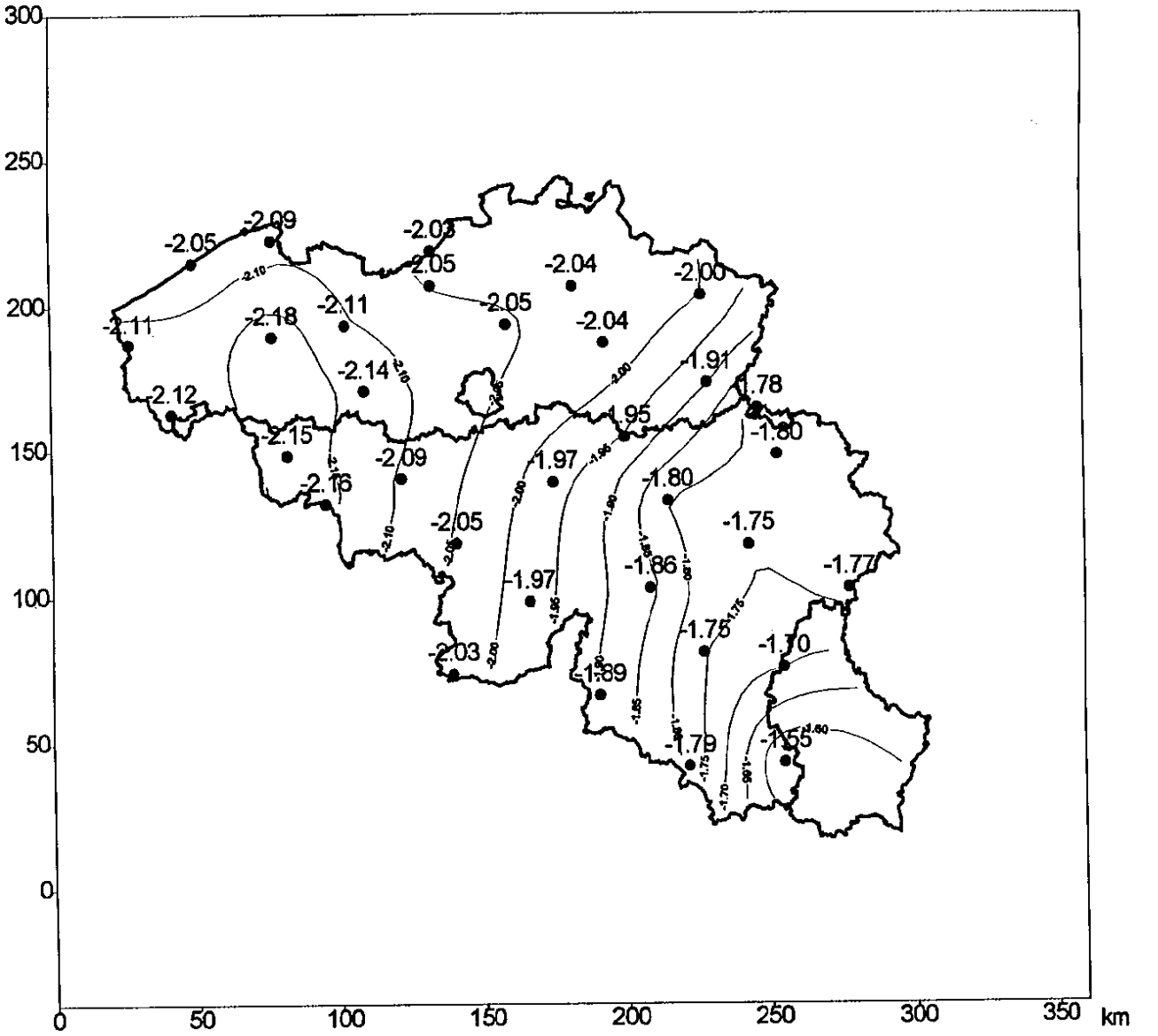

Fig 13: Décalage entre le quasi-géoïde gravimétrique et les points GPS-nivelés

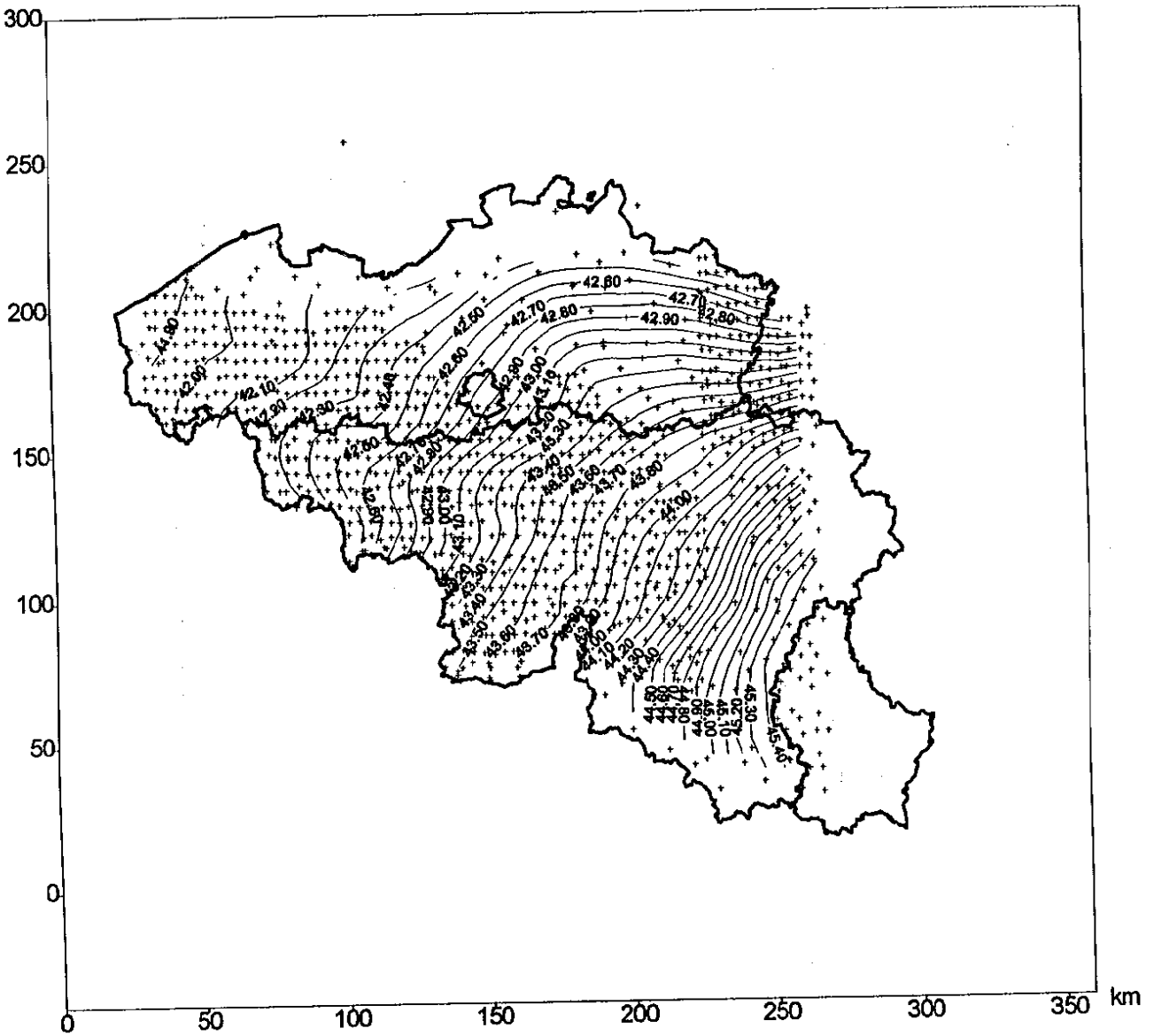

Fig 14: Hauteur du quasi-géoïde gravimétrique adapté aux points GPS-nivelés

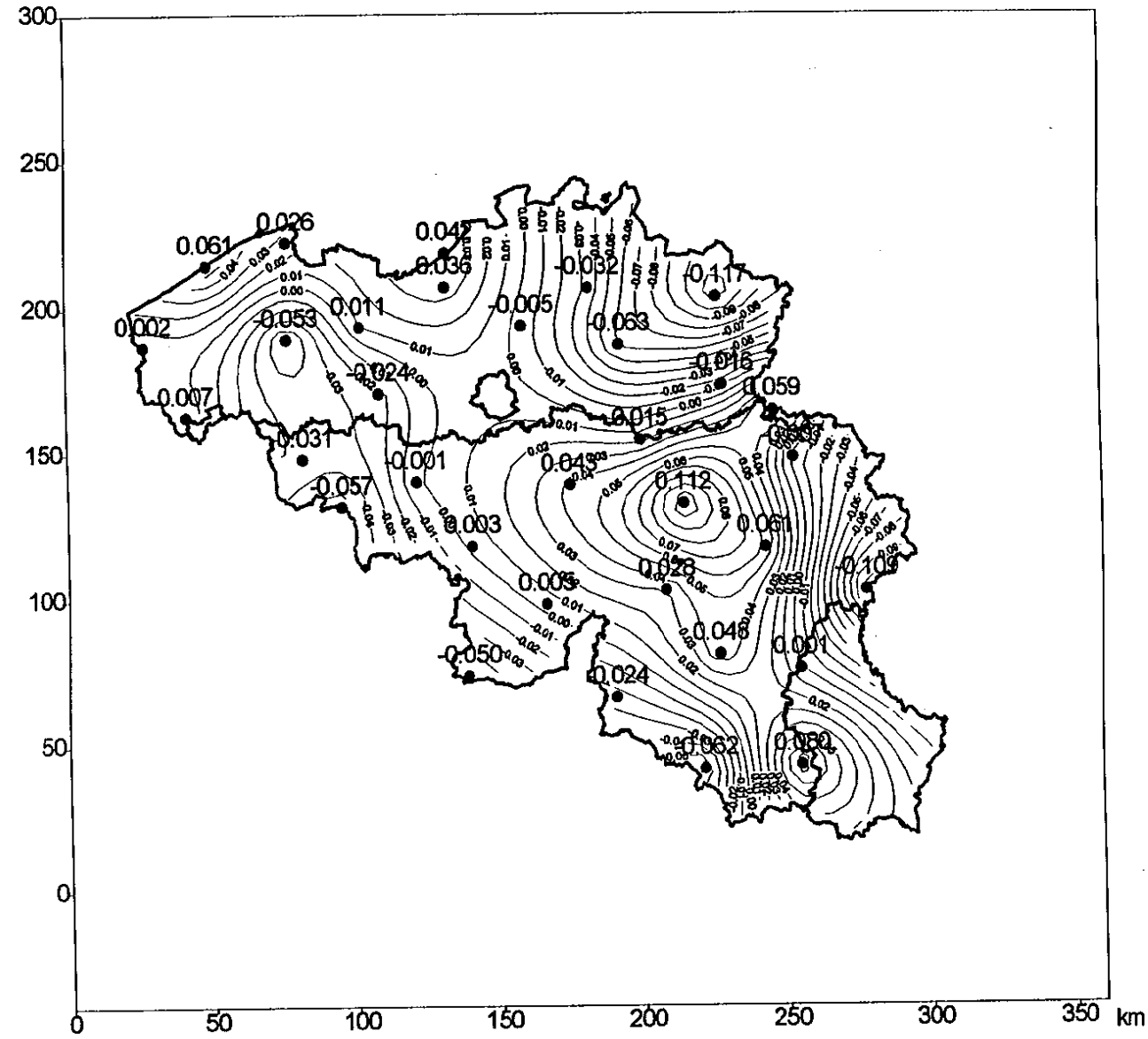

Fig 15: Résidus de l'ajustement du quasi-géoïde gravimétrique aux points GPS-nivelés

Dans une version ultérieure du géoïde gravimétrique, on utilisera un MNT détaillé et on tiendra compte des données gravimétriques sur les Pays-Bas et la Mer du Nord qui sont actuellement en voie d'intégration dans la banque de données gravimétriques belge. En densifiant, si faire se peut, la couverture gravimétrique de la Belgique et en utilisant les formules de transformation de coordonnées que nous espérons bientôt obtenir du réseau BEREF, il ne semble pas impensable d'atteindre une précision sub-centimétrique dans la détermination du géoïde gravimétrique. L'IGN-Belgique réalise pour le moment un réseau de points GPS-nivelés avec une densité d'un point par 8 km² (Voet, 1995). On peut imaginer, dans un but pratique, combiner ces données avec un futur géoïde gravimétrique en une banque de données qui serait utilisée comme référence altimétrique pour le pays. L'avantage de cette intégration serait d'augmenter la résolution de 8 km à 1 km ou mieux et de viser une précision globale de l'ordre du centimètre.

Remerciements

M. Z. Jiang a séjourné deux semaines à l'Observatoire Royal pour participer à ce projet. Nous remercions M. H. Duquenne du LAREG de l'IGN-France d'avoir obtenu les autorisations accordant ce séjour.
Les données GPS-nivelées ont été communiquées à titre scientifique par l'IGN-Belgique.
Les mesures gravimétriques françaises ont été mises à notre disposition par le Service Géologique National du BRGM et restent leur propriété.
Le Prof. R.H. Rapp nous a permis d'utiliser le potentiel OSU91A et le Prof. C.C. Tscherning nous a procuré le logiciel GRAVSOFT.
Il serait trop long d'énumérer les contacts multiples et fructueux que nous poursuivons avec le Bureau Gravimétrique International.
Qu'ils soient ici tous remerciés.

Références

Chacksfield B. C., De Vos W., D'Hooge L., Dusar M., Lee M. K., Poitevin C., Royles C. P., Verniers J. (1993) : *A new look at Belgian aeromagnetic and gravity data through image-based display thechniques.* Geological Magazine, Vol. 130(5), Cambridge Univ. Press, pp. 583-591, Sept. 1993.

Duquenne H., Jiang Z., Lemarie C. (1994) : *Geoid determination and levelling by GPS : Some experiments on a test network.* IGC-ICG joint meeting, Graz, Sept. 1994.

Heiskanen W., Moritz H. (1967) : *Physical Geodesy.* W. H. Freeman & Co., San Francisco, 364 pp., *Reprint* (1981), Inst. Phys. Geod., Tech. Univ. Graz, Austria.

IAG (1971) : *Geodetic Reference System 1967.* Publ. Spéc. n° 3 Bull. Geod., Paris.

IGM (1949) : *Deuxième Nivellement Général. Répertoire des définitions et des altitudes des repères. Fasc. 1.* IGM, Bruxelles.

Levallois J.-J. (1969) : *Géodésie générale. Tome 1. Méthodes générales et technique fondamentales.* Coll. Sc. IGN, Ed. Eyrolles, Paris

Levallois J.-J. (1970) : *Géodésie générale. Tome 3. Le champ de la pesanteur.* Coll. Sc. IGN, Ed. Eyrolles, Paris

Molodenskii M.S., Eremeev V.F., Yurkina M.I. (1962) : *Methods for the study of the external gravitationnal field and figure of the Earth.* Israel Prog. for Sc. Trans., Jerusalem.

Moritz H. (1980) : *Advanced Physical Geodesy.* H. Wichman, Karlsruhe and Abacus Press, Tunbridge Wells, Kent, 500 pp.

Poitevin C. (1988) : *Une définition plus précise des constantes belges de la représentation plane conforme de Lambert - Een nauwkeurige bepaling van de belgische constanten van de conforme vlakke voorstelling van Lambert.* Bull. Trim. Soc. Belg. Photogram. Télédétection et Cartogr., n° 171-172, pp. 41-43, blz. 44-46. Obs. Roy. Belg., Com. Sér. A, n° 93, Sér. Géoph. n° 164, 1989.

Poitevin C. (1989) : *Quel peut être l'apport de la gravimétrie à la tectonique récente et actuelle en Belgique ?* Ann. Soc. Géol. Belg., T. 112, fasc. 2, pp. 407-420.

Poitevin C., Flick J., Lambot P. (1990) : *Réactualisation du réseaus gravimétrique luxembourgeois par rattachement à la station absolue de l'Observatoire Royal de Belgique et IGSN71.* Bull. Soc. Natur. Luxemb., 90(1990), pp. 17-28

Poitevin C. (1991) : *Wat kan de gravimetrie bijdragen tot een beter begrijp van de recente en huidige tektoniek in België ?* Driemaand. Tijdschr. Belg. Veren. Fotogram. Teledetectie en Kartogr., Vol. nr. 183-184, blz. 55-80.

Rapp R. H., Wang Y. M., Pavils N. K. (1991) : *The Ohio State 1991 geopotential and Sea surface topography harmonic coefficient models.* OSU Rept. n° 410, Dpt. Geod. Sc. and Surv., The Ohio State Univ., Ohio, USA.

Tscherning C. C., Forsberg R., Knudsen P. (1992) : *The GRAVSOFT package for geoid determination.* First Continental Workshop on the Geoid in Europe, Prague, May 1992.

Vanicek P., Krakiwsky E. (1982) : *Geodesy : The Concepts.* North-Holland Publishing Co., 691 pp.

Voet P. (1995) : (preprint) *Het gebruik van GPS bij de uitbouw van het Belgisch planimetrich net.* Journées d'études : La technologie GPS pour les utilisateurs belges, ORB, IGN, ERM, Bruxelles 16-17 mai 1995, 20 pp.

GEOID COMPUTATIONS IN THE NORDIC AND BALTIC AREA

Rene Forsberg, Kort- og Matrikelstyrelsen, Rentemestervej 8,
DK-2400 Copenhagen NV, Denmark. E-mail: rf @ kms.min.dk

ABSTRACT

A joint Nordic geoid model, covering the Nordic and Baltic areas, with special solutions for Iceland and Greenland, are currently being computed in a cooperation project within the Nordic Geodetic Commission. In this paper a new preliminary high-resolution (2.5 km) geoid model is presented, computed using spherical FFT methods and terrain reductions. Compared to the previous joint solution (NKG-89), significant new data has entered the solution, especially for the areas around the Baltic. The results of the new geoid are compared to GPS-levelling along the Nordic N-S and E-W GPS profiles, as well as to local GPS/levelling surveys. In spite of significant improvements in data and methods, the new geoid models shows systematic errors much worse than in the NKG-89 model, which produced 10 cm-fits over GPS/levelling lines of 2000 km extent. The computation process and error screening is therefore ongoing. Examples of geoid-quasigeoid separations in Scandinavia conclude the paper.

INTRODUCTION

A continous geoid and gravity data base project have been carried out for a number of years within the Nordic Geodetic Commission (NKG), comprising the countries of Iceland, Norway, Sweden, Finland and Denmark. The currently adopted joint geoid model, termed NKG-89, was developed in 1989 using FFT methods on a 5 km UTM grid (Forsberg, 1990), and has successfully been used for many GPS comparisons (e.g., Kakkuri (ed.), 1994; Ollikainen, 1993; Poutanen, 1993, Forsberg and Madsen, 1990).

Fig. 1. Gravity data coverage (3' x 6' pixels) for southern part of Nordic and Baltic region

However, since the level of the NKG-89 geoid was defined in a geocentric system (implicitly determined by the OSU89B reference model), comparisons to GPS/levelling geoid heights produce a bias of typically 0.5-1 m. To avoid this bias it has been decided to compute a new geoid, in the end fitting the final geoid to the EUREF coordinate system, and the joint european UELN height datum. Another reason to compute a new geoid model was to obtain a higher resolution, and utilize improvements in methods (spherical FFT) and improved reference fields (OSU91A, soon the new DMA-GSFC enhanced WGS84 model), and the availability of much new gravity data, especially in eastern Europe.

This paper presents a preliminary new high-resolution geoid model of the Nordic and Baltic area, based on available gravity data, and most of the available digital terrain data.

The gravity data available for the new solution include data from all the Nordic geodetic agencies, new data from Germany, Poland (5' grid data), Lithuania, Latvia and Estonia, as well as most ocean adjoining areas. Fig. 1 and 2 shows the current gravity data coverage in the Nordic data base. Current main data voids are the southern Baltic Sea and parts of the North Sea, as well as in Russia. Compared to the earlier coverage underlying the NKG-89 geoid (see, e.g. Forsberg, 1993) the gravity situation has been much improved, especially in the Baltic region. It is planned to utilize ERS-1 and Topex/Poseidon satellite altimetry data to fill up the southern Baltic, unless some of the existing russian marine gravity data can be released.

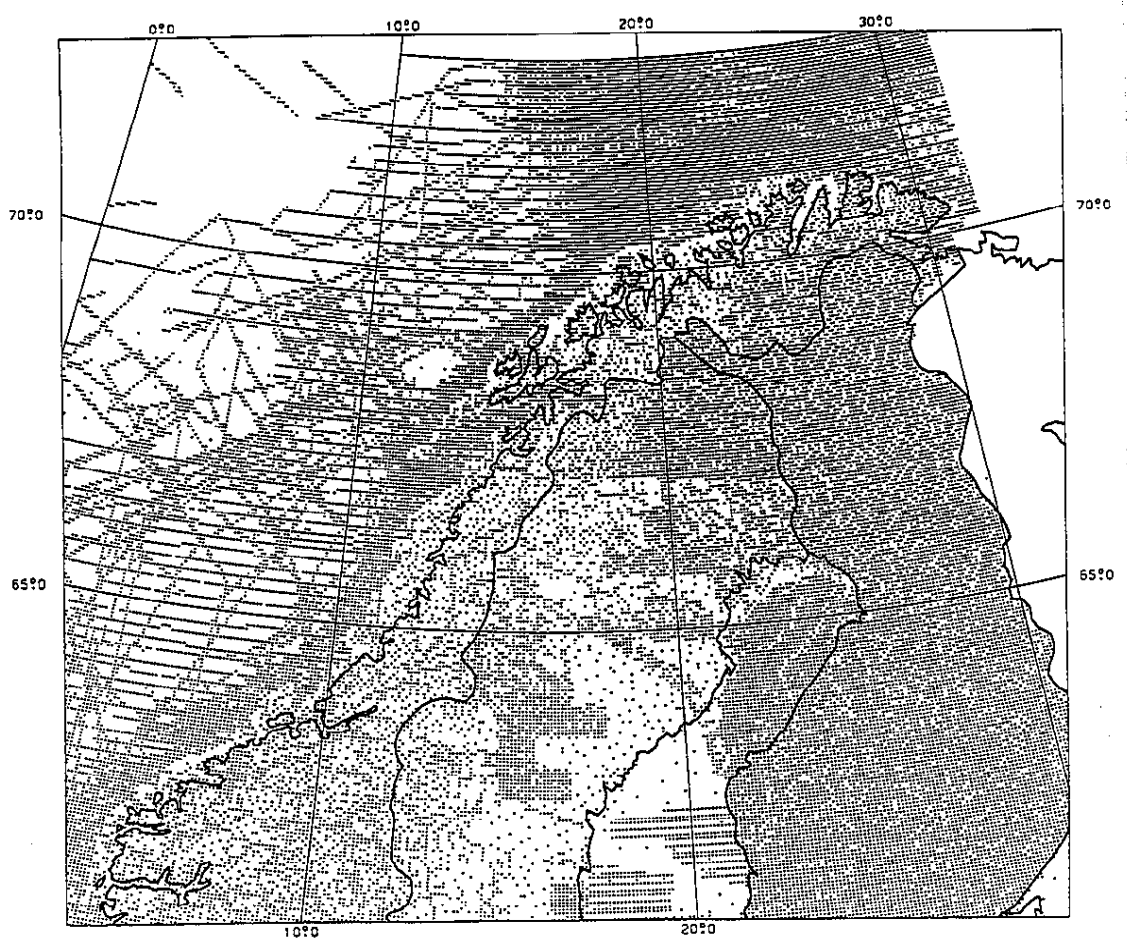

Fig. 2. Gravity data coverage, northern Nordic region

Detailed digital terrain data are a necessary part of the high-resolution geoid determination process. New dense DTM-data (100 m resolution) have been used in Norway for improved terrain correction computations according to agreed standard computation methods (D. Solheim, pers.comm.). In Sweden a complete set of 500 m-height data have been made available, and has been used for terrain correction computations in the mountainous regions (lowland regions have yet to be computed). Lithuania and Denmark also contributed new DTM data at 500 m or 1 km resolution, and for remaining regions more coarse models have been used, cf. Fig. 3.

A NEW HIGH-RESOLUTION FFT GEOID

The new geoid model is based on the Stokes' integration of gridded gravity data by the multi-band spherical FFT method (Forsberg and Sideris, 1993), using RTM terrain reductions for smoothing the data prior to FFT (cf. Forsberg, 1995). In the region of interest (53°-73° N, 0°-32° E) a "pixel-selected" subset of 139192 gravity points have been used.

The geoid solution is build up in the usual "remove-restore" fashion by three terms

$$\zeta = \zeta_1 + \zeta_2 + \zeta_3$$

where the first term is from a spherical harmonic reference field, the second term from terrain effects, and the third term from the residual gravity field. Because of the way RTM effects are used, the geoid computed will technically be a quasi-geoid, and hence height anomalies are obtained rather than geoid undulations. However, in the sequel the word "geoid" will be used rather loosely as a "generic" term for both quasi-geoid and the classical geoid. An example will be given on the typical magnitude of differences between geoid and quasi-geoid.

As reference field for the present computations a temporary combination reference field of JGM-2 and OSU91A have been used (provided by S. Kenyon, DMA). The reference field was computed in grids in order to facilitate rapid interpolation for the subsequent computations. The atmospheric correction on gravity (0.87 mgal at sea level) was included in the reference grids as well.

The RTM method reduces topographic data for topographic irregularities relative to a smooth mean height surface. This mean height surface was constructed by running averages over a basic 1.5' x 3' height grid, yielding a reference surface of resolution appr. 100 km. The computations of terrain corrections and subsequent RTM-reductions was done by prism integration, using classical terrain corrections as intermediate steps. Table 1 below shows the impact of the reference field and RTM terrain effects. The residuals after reduction are significantly smoother than the original data, with a bias value very close to zero.

Table 1. Statistics of data reductions

Unit: mgal	mean	std.dev.
Original data (144807 pts.)	-0.44	26.02
Δg - ref.field	-1.74	17.31
Δg - ref.field. - RTM	0.05	11.58

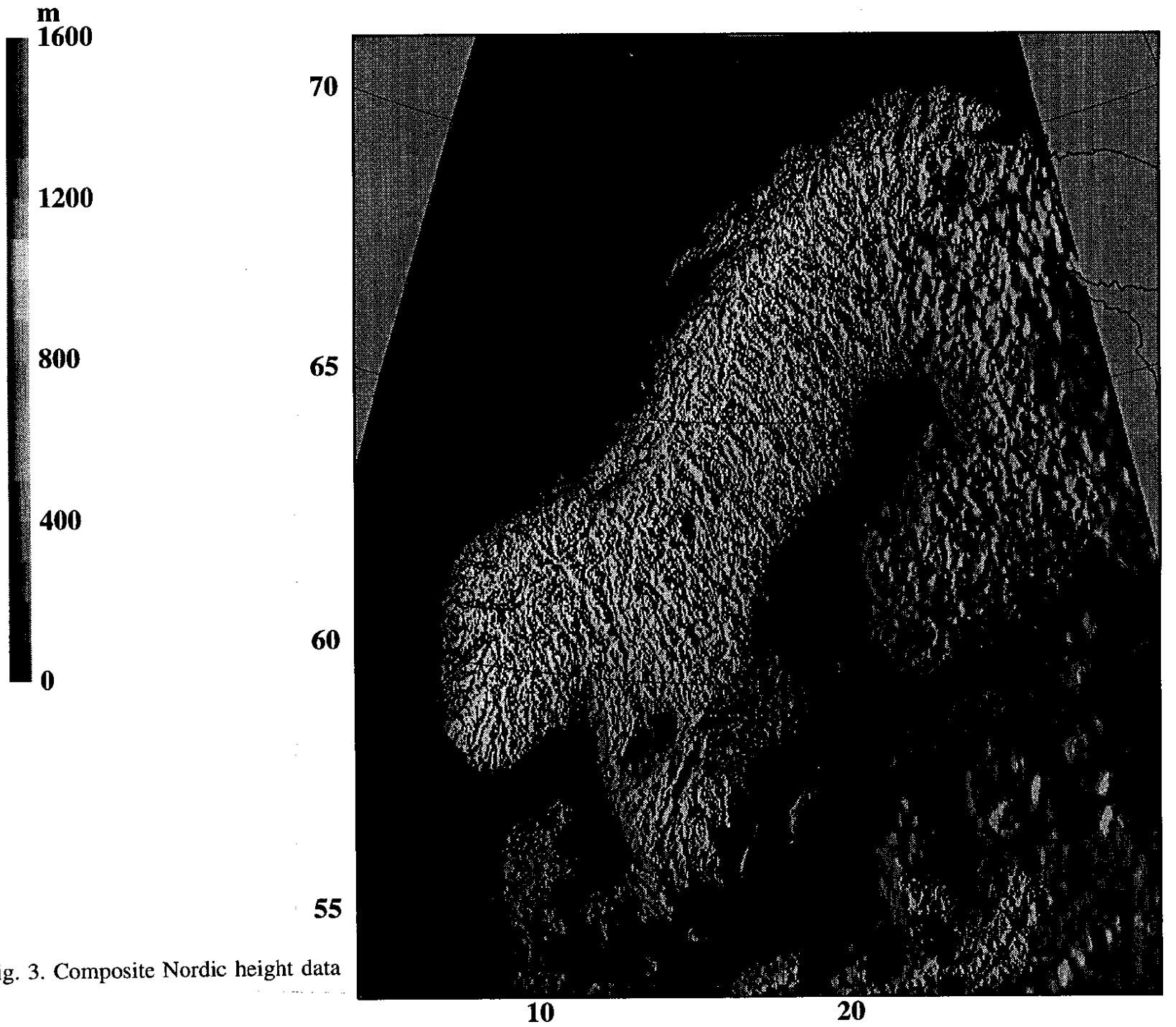

Fig. 3. Composite Nordic height data

The geoid solution has been carried out on a 1.5' x 3' grid, using least-squares collocation for data gridding, assuming a data correlation length $x_{1/2}$ of 25 km. The gridded, reduced gravity anomalies have subsequently been converted to geoid undulations by using 9-band spherical FFT methods. The FFT was carried out on a grid of 900 x 720 points, using a zero-padded border zone to limit the periodicity effects. The geoid contributions from gravity and topography are shown in Fig. 4 and 5, and the final geoid after restoring the reference field is shown in Fig. 6. The statistics of the contributions from FFT and the terrain is shown in Table 2.

The geoid model has been compared to GPS/levelling height anomalies along two traverses: A north-south line from the danish/german border to Tromsø ("IfE" line), and an W-E profile from Bergen in Norway to the russian/finnish border ("SWET" profile). Both of these lines are nearly 2000 km long, and done along 1st order levelling lines. The comparison of the NKG-89 geoid and the new geoid model is shown in Table 2 as well. The datum of the GPS traverses are ITRF91 (IfE data transformed onto SWET data using a common crossing point).

From Table 2 it is apparent that the new geoid model performs much worse than the older NKG-89 model. This is surprising, given that much improved data and methods have been used. The difference in the models is mainly a "bulge" over the mountainous regions, and could indicate systematic errors in the way the new RTM corrections were applied. However, bugs in the data can not be ruled out at the present preliminary stage. Additional computations are currently being carried out to try and isolate the error. Test computations repeating the computations of NKG-89 with the new data shows the same problems, and indicates data-related problems. Also differences between spherical and planar (UTM) FFT methods are insignificant and can not explain the problem.

Table 2. Geoid height statistics and comparisons on long GPS lines

Unit: meter	mean	std.dev.
Geoid effect from spherical FFT	0.01	0.54
Geoid contribution from RTM	0.00	0.15
Comparisons on GPS lines: *IfE:* NKG-89	0.12	0.10
IfE: New model	-0.42	0.18
SWET: NKG-89	0.34	0.12
SWET: New model	-0.24	0.33

That the new solution do perform reasonally good locally (a consequence of new and denser data) can be seen in Table 3. In this table is shown GPS- levelling geoid fits for three different regions:

1) *Southern Finland*, a region a low gravity variablity and dense gravity coverage - 12 points (part

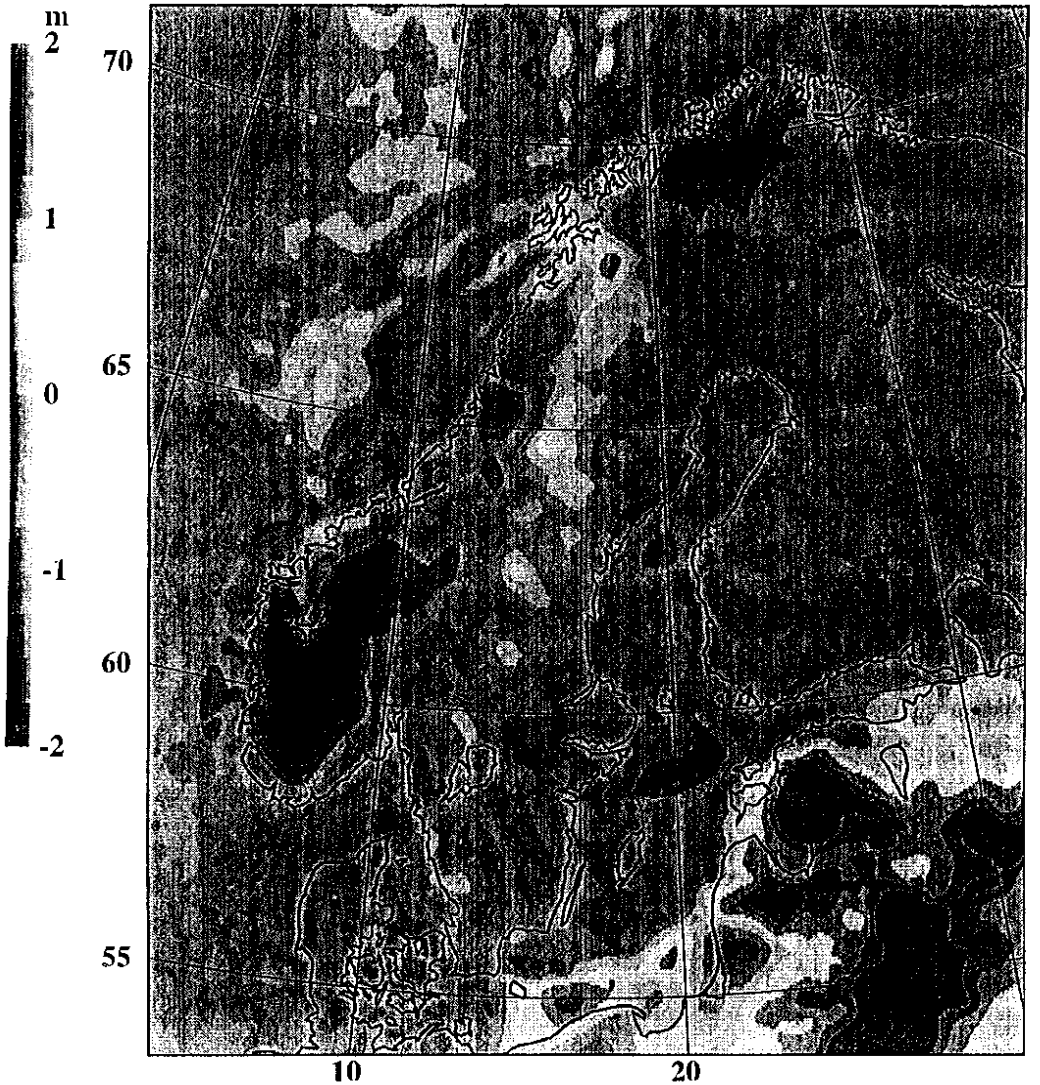

Fig. 4. Geoid contribution from residual gravity data (ζ_3, unit: m). Major systematic effects are apparent in the mountains of Norway, and in the Baltic area, where gravity data were earlier absent.

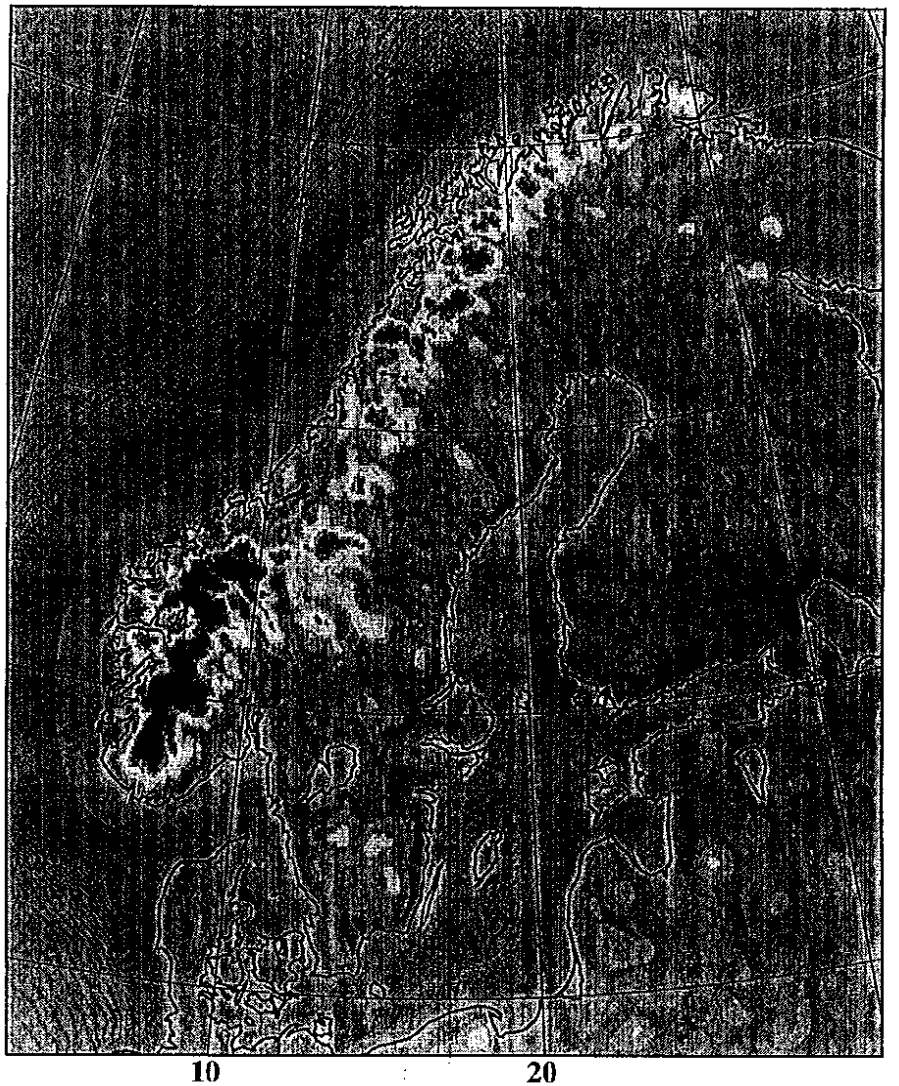

Fig. 5. RTM geoid contribution (ζ_2, unit: m). Same scale as in fig. 4.

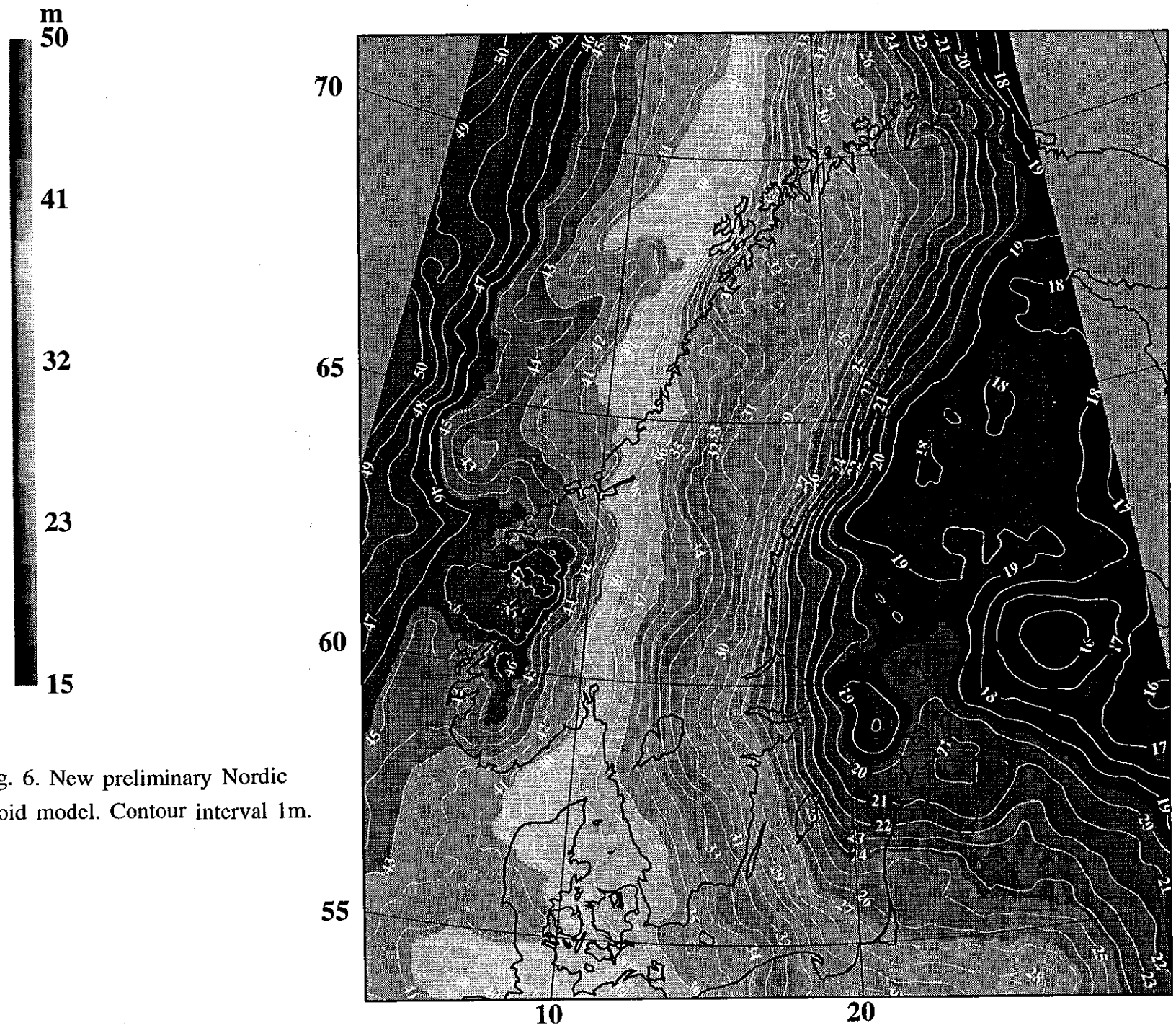

Fig. 6. New preliminary Nordic geoid model. Contour interval 1m.

of SWET traverse).
2) *Trondheim region*, Norway (moderately mountainous) - 20 points (provided by G. Simensen, NTH).
3) *Lithuania* - 38 points on first order levelling benchmarks (provided by E. Parseliunas, LTU).

Table 3 shows the mean and standard deviation of the computed geoid without any fit to GPS, and after a 4-parameter empirical datum fit of form

$$\Delta N = \cos\phi\cos\lambda\,\Delta X + \cos\phi\sin\lambda\,\Delta Y + \sin\phi\,\Delta Z + Rs$$

to the profile data (Forsberg, 1993). This datum parameter fit mainly absorbs errors in the geoid. From the table it can be seen that the NKG-89 and new geoid model perform comparably after the long wavelength errors are removed by the fitting process. In Lithuania, where the NKG-89 geoid model had no gravity data available, the new model performs relatively well.

Table 3. Local GPS-levelling geoid differences

Area and geoid model		Without local fit		After fit of 4-par. model	
		mean	std.dev.	mean	std.dev.
Finland	NKG-89	0.353	0.043	0.000	0.037
-	New	-.585	0.271	0.000	0.037
Trondheim	NKG-89	0.760	0.075	0.000	0.060
-	New	0.413	0.095	0.000	0.061
Lithuania	NKG-89	0.927	0.530	0.000	0.299
-	New	-1.332	0.402	0.000	0.103

Example of the geoid-quasigeoid separation

When producing large-scale national geoids it is of course important to discreminate between the geoid and the quasigeoid. The relations between the quantities involved are

$$h = H + N = H^* + \zeta$$

where h is the ellipsoidal height, H the (Helmert) orthometric height, H^* the normal height, N the geoid undulation, and ζ the height anomaly. The differences between N and ζ may to 1st order be expressed by (Heiskanen and Moritz, 1967)

$$\zeta - N = H_P - H_P^* \approx -\frac{\Delta g_B}{\gamma_o} H$$

This approximation may be viewed as exact when Helmert orthometric heights are used, as the Helmert approximation corresponds closely to the Bouguer plate approximations underlying the above formula. Fig. 7 shows the Bouguer anomalies of southern Norway, the most mountainous region in Scandinavia, and Fig. 8 the corresponding geoid-quasigeoid separations. The maximum value of the separation is 20 cm, and therefore highly significant. It is therefore important for users to be aware of the height systems in use, and perform the necessary geoid or height transformations as required. In the case of the Nordic geoid cooperation build both geoid and quasi-geoid may be built into the same interpolation package, and dependent on national height system (e.g. orthometric heights in Norway, normal heights in Sweden) the "correct" geoid answer is obtained.

Conclusions

In this paper a status for geoid computations in the Nordic countries have been given. A previous solution - NKG-89 - has yielded extremely good results - down to 10 cm r.m.s. over 1000 km - but newer solutions apparently suffer from systematic errors, the source of which are still under investigation. However, in the Baltic region, where gravity data were previously not available, the new model represents a significant improvement.

References

Forsberg, R.: Modelling the fine-structure of the geoid: Methods, data requirements and some results. Geophysical Journal International, 14, 403-418, 1993.

Forsberg, R: Terrain effects in geoid computations. Lecture notes, International School for the determination and use of the geoid, DIIAR, Politecnico Milano, Oct. 1994. International Geoid Service, 1994.

Forsberg, R. and M. G. Sideris: Geoid computations by the multi-band spherical FFT approach. Manuscripta Geodaetica, 18, 82-90, 1993.

Forsberg, R.: A New High-resolution Geoid of the Nordic Area. Proceedings, 1st International Geoid Commission Symposium, Milano May 1990.

Forsberg, R. and F. Madsen: High-precision Geoid Heights for GPS Levelling. Proc., GPS-90 symposium, Ottawa, pp. 1060-1074, Sept. 1990.

Heiskanen, W. and H. Moritz: Physical Geodesy. Freeman & Co., 1967.

Kakkuri, J. (Ed.): Final results of the Baltic sea level 1990 GPS campaign. Reports of the Finnish Geodetic Institute, 94:2, 1994.

Ollikainen, M.: The observations and first results of the Finnish GPS-network. IAG General Meeting, Beijing, Aug. 1993.

Poutanen, M., K. Gjerde, L. Jivall, F. Madsen: Establishment of a GPS network to control the Nordic geoid. IAG General Assembly, Beijing, August 1993.

Strang van Hees, G. (1990) Stokes formula using fast Fourier techniques. Manuscripta Geodaetica, 15: 235-239.

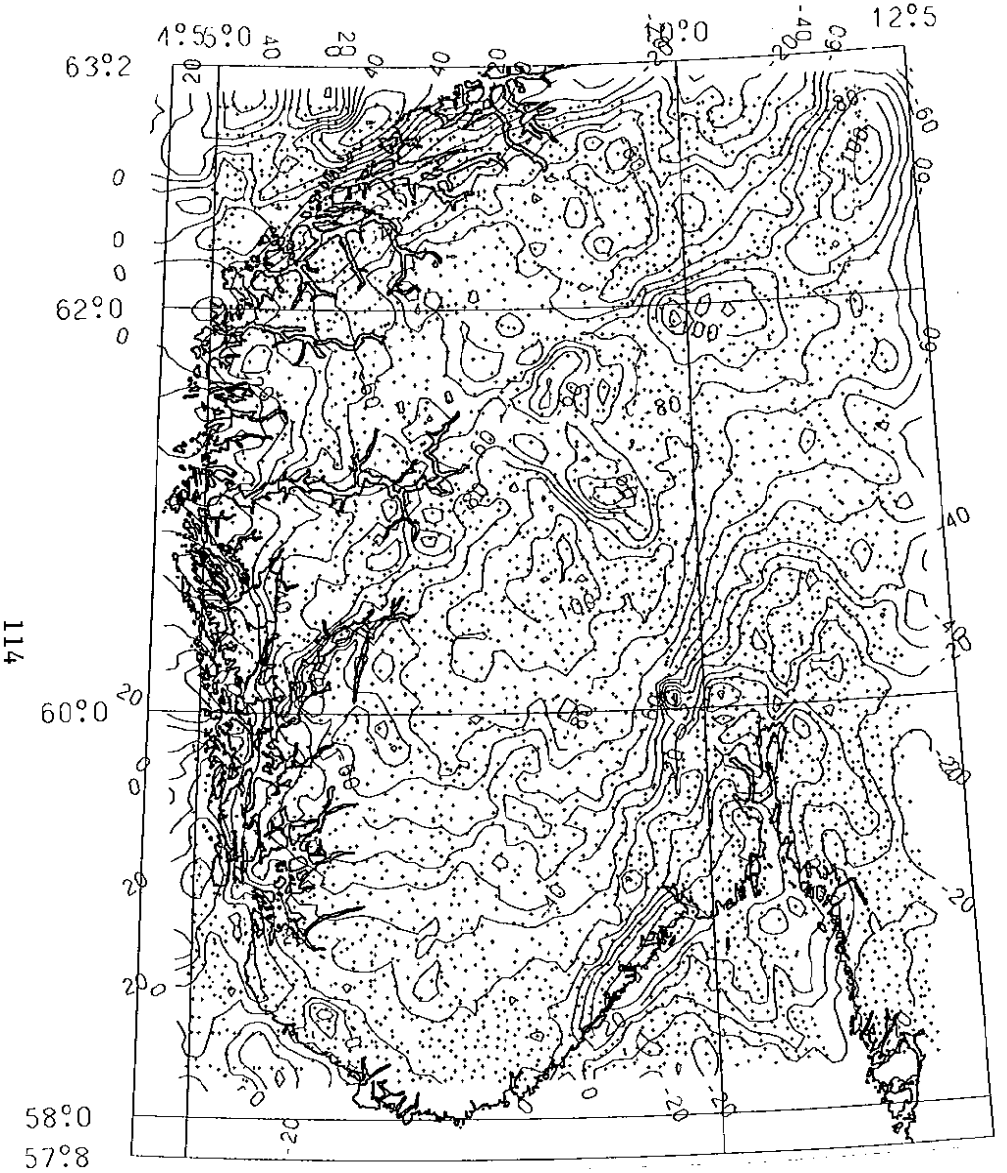

Fig. 7. Bouguer anomalies over southern Norway. C.i. 1 mgal.

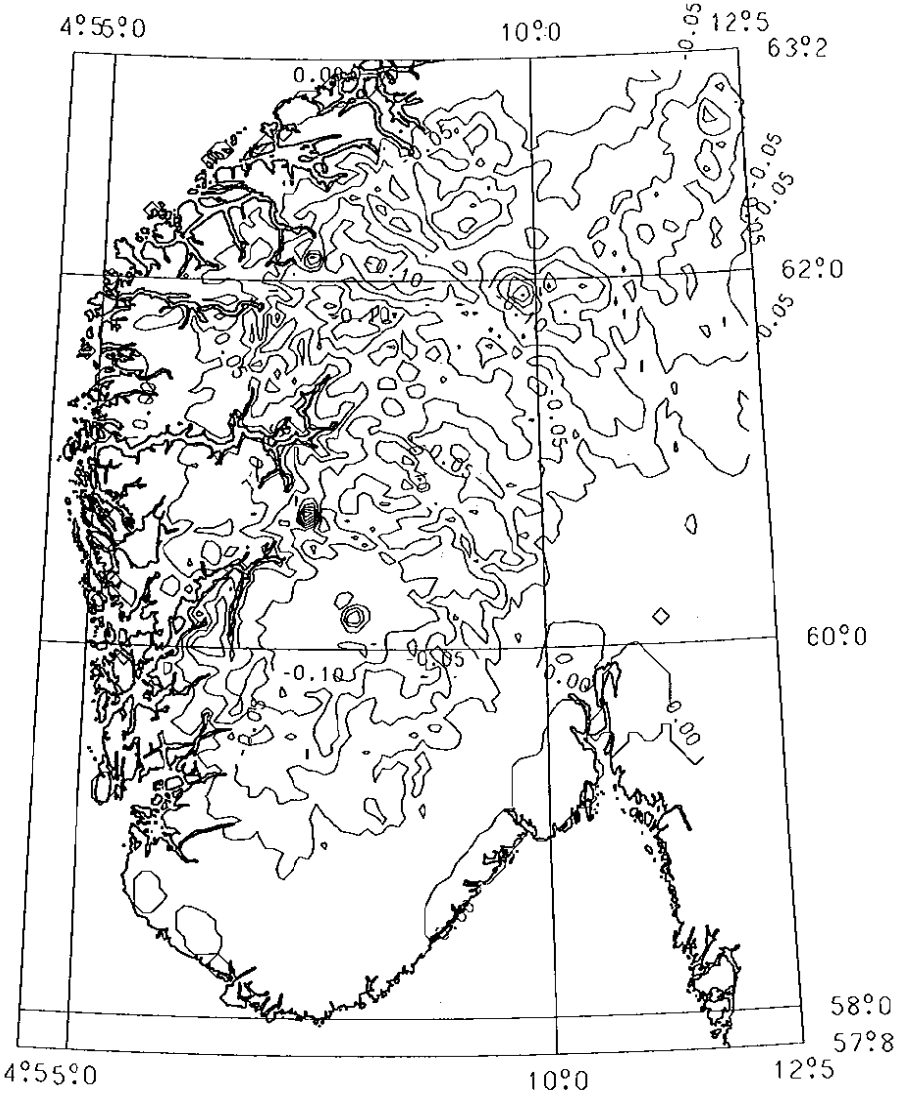

Fig. 8. Geoid-quasigeoid sepation, southern Norway, c.i. 2.5 cm.

THE GEOID IN THE SOUTHERN ALPS OF FRANCE

Henri DUQUENNE (1) (2), **Zhiheng JIANG** (1)

(1) Laboratoire de Recherche en Géodésie, Institut Géographique National, 94160 Saint-Mandé France.

(2) Ecole Supérieure des Géomètres et Topographes, 91000 Evry, France

ABSTRACT

In the scope of the determination of the French geoid, numerous developments and tests are undertaken, in order to delimit and solve the problems concerning the quality of data and methods. The paper presents an experimental determination of the geoid in a French region so called Alps, Provence and Côte d'Azur. A solution is obtained from gravity data, using Stokes integration and a remove-restore technique. It is compared with GPS and levelling derived height anomalies. Some conclusions are proposed, concerning the improvement in data processing and gravity measurement coverage. With the aim of suiting the gravimetric (quasi)-geoid to GPS levelling, an adjusment method is presented.

INTRODUCTION

The precise determination of the gravimetric geoid in the French Alps has been deemed until now as a difficult task. Owing to the roughness of the topography, it is necessary to use advanced methods, which were unavailable at the time of previous attempts, as one can see in (Levallois, 1971a), (Delomenie, 1987) and (Balmino, 1992). This problem is now overcome by remove-restore techniques implemented on modern computers. Secondly, the assessment of the quality of the results was more or less risky (Levallois 1971b). The development of GPS associated with the old spirit levelling technique provides now an efficient tool to compare gravimetric geoid undulations and point values on GPS station. The third obstacle in the way of the determination of the alpine geoid is still an haunting question, as it shall be shown later: the irregular distribution of the gravity data. Nevertheless, the determination of the geoid in this area is interesting on several account. By undertaking the task presented in this paper, the goals of the authors was multiple:

- To take part in the tests and comparisons of methods and software , in co-operation with the CNES/BGI, before the computation of a geoid covering whole France
- To compare gravimetric realisations of the geoid with a levelling and GPS network on an area where both methods may present some weaknesses
- To explore the performances of GPS levelling in mountainous area
- To estimate the possibility to check the vertical co-ordinates in GPS networks
- To examine the problems in merging foreign and French data, especially digital terrain model.

The location of the test area is shown in figure 1, and the regional topography in figure 2. The highest mountain in the area covered by the digital terrain model is the Mont Blanc (4807 m), and numerous mountain tops exceed 3000m in height (Monte Viso 3841 m, etc.).

GRAVIMETRIC GEOID COMPUTATION

Description of the data and their preparation

The data consisted of a geopotential model, digital terrain models and point gravity values.

The geopotential model was OSU91A, developed in spherical harmonics complete to degree and order 360 (Rapp, 1991).

The gravity data set was issued from the data base of the Bureau Gravimetrique International (BGI), which ensured the validation, (Toustou, 1991). A subset of 2769 values was extracted, setting a minimum distance of 4 km between points. The heights of the gravity station was checked by comparison with the digital terrain model described below. On Mediterranean Sea, only surface gravity measurements were taken into account. The gravity coverage and gravity free air anomalies are shown in figure 3. Table 1 give some statistics.

Table 1. Statistical description of gravity anomalies (free air, model OSU91A, residual) (unit: mgals).

	Min.	Max.	Mean	RMS	Std. dev
Δg_{FA}	-131.33	133.41	1.10	33.05	33.03
Δg_{Model}	-108.19	135.59	24.44	38.99	30.38
Δg_{RFA}	-86.3	106.87	6.04		18.93

In and around the area of interest, two digital terrain model were merged. The first one was a $7.5'' \times 10''$ grid covering the north-west part of Italy, and including bathymetry. The second one, covering France, was a little more accurate ($4.5'' \times 6''$), (see Duquenne, 1992), but did not contain any bathymetry. So it was decided to set the batymetry to 0 and not to apply terrain corrections at sea. During the merging process, the Italian DTM was shifted in latitude and longitude with respect to the French one, in order to minimise the discrepancies along the frontier. This was a tedious task as the frontier crosses a high mountainous region where all known interpolation techniques more or less failed. Appreciable improvement was however achieved: for latitudes between 45° and 46°, were the heights vary from 2000 to 4800 m, the RMS of the discrepancies falling down from 125 to 57 m. The merged grid was checked by comparison with existing maps at scale 1:25000, especially along the frontier. Its limits were 42° and 46° in latitude, 3° and 9° in longitude (11.5 millions values). Two others grid were derived: a coarse one ($1.5' \times 2'$) to accelerate integration processes and a filtered one for residual terrain model reduction. In the last case, a moving average window of $30' \times 40'$ was used. The map (figure 2) is issued from the coarse DTM and point out the roughness of the topography.

Remove restore and integration techniques

The applied remove-restore technique is derived from (Balmino, 1992), and can be summarised as follow:

- From gravity values g, compute free air gravity anomalies including atmospheric correction, using GRS80 formulae (Moritz, 1992) :

$$\delta g_{atm} = 0.874 - 9.9 \times 10^{-5} H \qquad \text{(mgal)}$$

$$\Delta g_{FA} = g + \delta g_{atm} + \frac{\partial g}{\partial H} H - \gamma_0$$

- From the detailed, coarse and filtered digital terrain models, compute the direct and indirect residual terrain effects on gravity:

$$\delta g_{RT} = \int_{\sigma} \frac{\rho(H - H_0)}{r^3} d\tau$$

$$\delta g_{IRT} \approx \frac{1}{\gamma_0} \frac{\partial \gamma}{\partial H} \delta W_{RT}$$

- From a geopotential model developed in spherical harmonics, compute the gravity anomaly of the model on the geoid:

$$\Delta g_{Model} \approx g_{Model} - \gamma_0 + N_{Model} \frac{\partial \gamma}{\partial h}$$

- Compute point residual free air anomalies and grid it:

$$\Delta g_{RFA} = \Delta g_{FA} - (\delta g_{RT} - \delta g_{IRT}) - \Delta g_{Model}$$

- Using Stokes' integration formula, compute residual undulations of the co-geoid on the wanted grid and on GPS points:

$$N_R = \frac{R}{4\pi\gamma} \int_{\sigma} \Delta g_{RFA} S(\psi) d\sigma$$

- Compute the indirect terrain effect on the geoid:

$$\delta N_R = \frac{1}{\gamma} \delta W_{RT}$$

- From the geopotential model and the above quantities, compute the geoid undulations

$$N = N_{Model} + N_R + \delta N_R$$

- Compute Bouguer anomalies and the correction to get the quasi-geoid:

$$\Delta g_B = \Delta g_{FA} - 2\pi G \rho H$$

$$\zeta = N - \frac{\Delta g_B}{\gamma} H$$

The figure 4 and the table 1 depict the residual anomalies, which are very smooth, with regard to the free air ones, except off the Hyères Islands, since no terrain corrections were applied at see. The integrations were performed by classical methods (no FFT), using "STOKES" and "TC" routines of the GRAVSOFT package (Tscherning et al., 1992). The finest DTM was used at distances less than 35 km, and the coarse DTM at a radius up to 55 km. This may be considered as insufficient, keeping in mind the roughness of the topography, but was limited by the available amount of mass storage memory of the computer (a PC with 100 MHz-processor). The figures 5 shows the obtained solution.

COMPARISON OF THE GRAVIMETRIC QUASI-GEOID AND HEIGHT ANOMALIES DERIVED BY GPS AND SPIRIT LEVELLING.

The French Institut Géographique National is completing a new geodetic network (RGF) in order to replace the old so called "New French Triangulation" (NTF). The new network will comprise a reference network of 23 points, which is already completed (Willis, 1994), and a first order network (RBF) of about 1000 GPS points, that is to say 1 point every 20-25 km. Provisional co-ordinates are available for half of the points, just for the southern part of France. The normal heights of all the points have been measured, so that height anomalies may be derived, the local precision of which may be estimated at 0.02 m in flat areas, and two or three times more in the mountains. So it was possible to compare 66 anomalies with the

gravimetric quasi-geoid. Figure 6 render the differences $\zeta_{RBF} - \zeta_{Gravi}$ between the RBF derived height anomalies and the gravimetric quasi-geoid. Discrepancies appear, due to a lot of causes (see (Forsberg and Masden, 1990), (Duquenne et al., 1995)):

- difference between the reference system of the network (close to EUREF, but at present not well fixed as final adjustment is not completed) and the reference of the gravimetric quasi-geoid
- difference between the quasi-geoid and the reference of the French height system (IGN69)
- errors in the coefficients of the geopotential model, especially long wavelength errors
- errors in residual geoid undulation N_R
- errors in GPS and levelling network.

In order to remove the long wave length effects and to point out the two last kind of errors, a trend was subtracted of the discrepancies $\zeta_{RBF} - \zeta_{Gravi}$, using a 3-parameters regression. A first computation permitted to fully confirm the existence of two suspected blunders (magnitude: 0.20~0.40 m) in the (provisional !) GPS network. After one correction and one rejection, the results are as follows:

constant bias: −1.087 m

mean slope toward east: 16.2 mm/100 km, 0.03″

mean slope toward north: 47.0 mm / 100 km, 0.10″

standard deviation of the residuals: 0.116 m

maximum residual: 0.296 m

The residuals are mapped in figure 7. They seem to be greater than the errors expected from the RBF and levelling network, and the errors in the gravimetric quasi-geoid might account for the major part of them. In the figure 8, where the gravity points have been plotted, the largest residuals (0.10 ~ 0.25 m) appear to be located in the high mountainous area and near the Mediterranean Sea, where the gravity data are lacking. On the contrary, residuals are smaller (0 ~ 0.12 m) in the north-eastern part of the test area, where the topography is smooth and the gravity data are numerous and well distributed. There is no doubt that the residuals could be reduced down to 0.05 m in this favourable conditions, by a local adjustment. These remarks allow to conclude that, in view of a gravimetric geoid with homogenous precision, it needs to increase the gravity coverage in the French Alps. Slight improvement may be expected from introducing other existing data (satellite altimetry on Mediterranean), or by refining the strategy to sample the gravity data in the Alps, or by using better terrain reduction. It is also well known that GPS and levelling measurements are especially affected by systematic errors in mountainous area. But the lack of gravity data remains the main problem.

COMBINED ADJUSTMENT OF GRAVITY AND GPS LEVELLING SOLUTION.

In view of the use of GPS for levelling, an adjustment method is proposed in this section. This method is implemented as a part of the software PILI, which the second author of this paper is developing. The goal is clearly to adapt the gravimetric (quasi-)geoid to a set of levelled GPS reference points. Two kinds of errors may be considered: . 1) The accidental ones, introduced by some random causes are nothing special but the ordinary surveying errors which often obey the normal deviate and can be eliminated in least square sense. 2) The systematic ones in our case are caused by the differences in reference systems, the long wave-length errors of the

geopotential model used, the biases existing in the gravity data and in the digital terrain model (DTM) etc. The later biases can be furthermore divided into two parts: a) Global tendency, which happens due to reference systems and to the discrepancy between the geopotential model and the gravity and DTM data. This depends on the method applied, especially when the r.r. technique is applied; b) Local deformation, which is caused by the systematic surveying errors, local reference systems (in border areas of a country for example) and the use of different data sources etc. The systematic errors are usually represented and then determined by using the linearised approximation models.

Combined adjustment model.

The principles for the combined adjustment are:

1) For the gravity geoid data: taking the *difference of the geoidal height* as the observation to establish the *relative observation equation* in order to eliminate the local deformation and short-wavelength errors. The unknown parameters will be locally determined. For this purpose, the whole gravity geoid (usually in grid form) should be divided into several smaller pieces according to certain specifications: geographical location, relief of topography, different data sources etc. A reasonable division is a very important factor to reach the best adjustment result.

2) For the GPS and levelling data: taking the *geoidal height* itself as the observation to establish the *absolute observation equation* in order to absorb the long-wavelength errors. The unknown parameters for the reference system transformation will be globally determined.

3) Establish the constraint condition to combine the various divided pieces (sub-zones) of gravity geoid and to determine the local and global parameters

4) Perform the combined adjustment as a whole or in groups to determine the final geoid and its adjusted precision, both usually in grid form. For this purpose, the problems concerning the weight, the sparse linear system and the adjustment in groups etc. have to be studied.

Observation equations

Some notations for this section: ζ^{GPS} = height anomaly corresponding to the quasi-geoid determined by GPS and levelling combination; ζ^{g} = height anomaly corresponding to the quasi-geoid determined by gravity method; $\overline{\zeta}$ = adjusted height anomaly; $\Delta\zeta_{ij}^{g}$ = difference of height anomaly; P_{ij}, P_{ij}^{g} = weight of relative observation equation; P_k, P_k^{GPS} = weight of absolute observation equation; V_{ij}, V_k = residual of adjustment; $T(F)$, $\Delta T(F)$ = global transformation model an its differential with F as the set of parameters; $t(f)$ = local deformation model with f as the set of parameters.

Denoting i, j, k the points on the quasi-geoid and introducing the systematic error models: the global transformation function $T(F)$ and local deformation function $t(f)$, the *generalised relative and absolute observation equations* is:

$$P_{ij}^{g}:\ V_{ij} = \overline{\zeta}_j - \overline{\zeta}_i - \Delta\zeta_{ij}^{\ g} + \Delta T(F) + t(f)$$

$$P_k^{GPS}:\ V_k = \zeta_k^{g} - \zeta_k^{\ GPS} + T(F)$$

In the following paragraphs, the practical formulas of the weight P, the systematic models $T(F)$ and $t(f)$ as well as the constraint conditions for the common points in the adjacent pieces are given.

Global transformation model T(f)

The various wavelength errors in the gravity solution may be approximated by different kinds of functions in order to fit the (quasi-)geoid to a set of GPS levelling points.

Periodic model represented by a trigonometric function:

Supposing the periodical errors dependent on latitude and longitude, the following trigonometric function may be used to approximate them:

$$\Delta\zeta^{T} = \sum_{n=1}^{P_n}\left[x_{n,\varphi}\cos(\omega_n\varphi) + y_{n,\varphi}\sin(\omega_n\varphi) + x_{n,\lambda}\cos(\omega_n\lambda) + y_{n,\lambda}\sin(\omega_n\lambda)\right]$$

where P_n is the total number of the introduced periodic terms, n is the sequential number of the periodic terms. More complicated function may be chosen to take into account the correlation of periodic errors in longitude and latitude. As already said, one of the advantages of this method is to make possible to benefit of the "relative" precision of a gravity geoid. The corresponding relative form of the above formula is:

$$\Delta\zeta_{ij}^{T} = \sum_{n=1}^{P_n}\{\ x_{n,\varphi}\left[\cos(\omega_n\varphi_j) - \cos(\omega_n\varphi_i)\right] + y_{n,\varphi}\left[\sin(\omega_n\varphi_j) - \sin(\omega_n\varphi_i)\right]$$
$$+ x_{n,\lambda}\left[\cos(\omega_n\lambda_j) - \cos(\omega_n\lambda_i)\right] + y_{n,\lambda}\left[\sin(\omega_n\lambda_j) - \sin(\omega_n\lambda_i)\right]\ \}$$

Similitude transformation model:

For the very errors due to reference system difference, the well known 7 parameter similitude datum shift transformation model in Cartesian co-ordinates can be used. Considering that the resulting error in geoid is not so sensible to the rotations, it can be simplified as 4 parameters $(\Delta X, \Delta Y, \Delta Z, k)$ where $\Delta X, \Delta Y, \Delta Z$ are the three translations and k the scale term, for only the vertical direction to the geoid:

$$\Delta\zeta^{S} = \cos\varphi\cos\lambda\Delta X + \cos\varphi\sin\lambda\Delta Y + \sin\varphi\Delta Z + k\times r$$

where r is the earth radius. The relative form of this formula (k is cancelled) is:

$$\Delta\zeta_{ij}^{S} = (\cos\varphi_j\cos\lambda_j - \cos\varphi_i\cos\lambda_i)\Delta X + (\cos\varphi_j\sin\lambda_j - \cos\varphi_i\sin\lambda_i)\Delta Y +$$
$$(\sin\varphi_j - \sin\varphi_i)\Delta Z$$

Polynomial model:

This model may be adequate to absorb non-periodic large scale systematic errors, such as systematic levelling errors:

$$\Delta\zeta^{P} = \zeta_0^{P} + \sum_{p,q} Q_{p,q}(\varphi-\varphi_o)^p(\lambda-\lambda_o)^q\cos^q\varphi, \qquad p,q = 0,1,2,...$$

where φ,λ are the latitude and longitude, φ_0,λ_0 is the mean value of λ,φ. The $Q_{p,q}$ are the polynomial coefficients. The relative form of this formula can be easily written out (note: $\zeta_0^{P},\varphi_o,\lambda_o$ will be cancelled or can be ignored):

$$\Delta\zeta_{ij}^{P} = Q_{1,0}(\varphi_j'-\varphi_i') + Q_{0,1}(\lambda_j'-\lambda_i')\cos\varphi_i +$$
$$Q_{2,0}(\varphi_j'^2-\varphi_i'^2) + Q_{0,2}(\lambda_j'^2-\lambda_i'^2)\cos^2\varphi_i + Q_{1,1}(\varphi_j'\lambda_j' - \varphi_i'\lambda_i')\cos\varphi_i$$

$$\varphi' = \varphi - \varphi_0, \quad \lambda' = \lambda - \lambda_0$$

Local deformation model

Speaking in view of differential, when the divided pieces of the gravity geoid are small enough, the local deformation can be approximated by a linear function:

$$\Delta\zeta^R = \Delta\zeta_0^R + a(\varphi - \varphi_0) + b'\cos\varphi_0(\lambda - \lambda_0) = \Delta\zeta_0^R + a(\varphi - \varphi_0) + b(\lambda - \lambda_0),\ b = b'\cos\varphi_0$$

where the constant and coefficients can be determined with some conditions.

Constraint condition

Some constraint conditions are needed to combine the gravity geoid pieces in the sense of least square solution. They should satisfy: (1) a geoid piece should be optimally fitted to the levelled GPS points which are contained in the gravity geoid piece itself; (2) the common points belonging to the different adjacent pieces will have the same adjusted values; (3) "repeated observations" are allowable, for example, when there exist several gravity geoid solutions on the same surface (that is, for a point there are several gravity geoid solutions) calculated from the different sources of gravity data. This constraint condition has the same form with that of the local deformation model *t(f)* with the unknown coefficients to be determined. Suppose the wanted function can be approximated and represented by a differential plan in 3D space, one can write:

Constraint equation for common *point observation k at the intersection of the geoid pieces number l, m, n, ...*

$$d\zeta_0^l + a^l(\varphi_k - \varphi_0^l) + b^l(\lambda_k - \lambda_0^l) = d\zeta_0^m + a^m(\varphi_k - \varphi_0^m) + b^m(\lambda_k - \lambda_0^m) =$$
$$d\zeta_0^n + a^n(\varphi_k - \varphi_0^n) + b^n(\lambda_k - \lambda_0^n) = \ldots$$

Constraint equation for a *relative observation (i,j) in border of the geoid pieces number l, m*:

$$d\zeta_{ij}^{l,m} = d\zeta_0^l - d\zeta_0^m + a^l(\varphi_j - \varphi_0^l) + b^l(\lambda_j - \lambda_0^l) - a^m(\varphi_i - \varphi_0^m) - b^m(\lambda_i - \lambda_0^m)$$

This equation will be solved in practical computation by ordering: $d\zeta_0^l = d\zeta_0^m$.

Weights

Denoting M_{GPS}, M_g the mean square errors of the observations for GPS/levelling and gravity solution, μ_0 the unit mean square error, weights are defined as follows:

relative observation equation: $P^g = \dfrac{\mu_0^2}{M_g^2}$;

absolute observation equation: $P^{GPS} = \dfrac{\mu_0^2}{M_{GPS}^2}$;

In order to *fix* or to *free* an observation: $P \to \infty$ or $P \to 0$.

Results

An adjustment has been attempted with the gravimetric quasi-geoid and the levelled GPS network described above. Only one local set of parameters was introduced as unknowns. The weights P^{GPS} and P^G were fixed to 2 and 1 respectively. (It would be better to use the variance-covariance matrix of the GPS and levelling networks adjustments, but this was not available). After rejection of one point (as above), the precision of the adjustment was estimated by the following indicators:

standard deviation of unit weight: 0.0196 m

standard deviation of the residuals on levelled GPS points: 0.043 m

maximum residual on levelled GPS points: 0.106 m

The figure 8 shows the residuals, to be compared with those of the 3-parameters regression (fig. 7).

The method seems very useful for blunder detection: if the weight of a suspicious GPS point is decreased down to a small value (i.e. 1/100), its residual take a value close to the true error, which appears more clearly than in the case of a simple 3 or 4-parameters adjustment.

SUMMARY AND CONCLUSION

In the scope of the research on evaluation of methods for gravimetric geoid determination, partial results have been obtained. In a mountainous area, remove restore technique gave a precision of about 0.12 m, proved by comparison with a levelling GPS network. Nevertheless, the precision is reliant to the quality of the data, and a fine DTM is not sufficient to replace lacking gravity data. A combined adjustment of a gravimetric quasi-geoid and height anomalies derived from a GPS and levelling network has been presented, which seems to be efficient for blunder detection and GPS levelling applications.

ACKNOWLEDGEMENTS

The authors wish to thank all Organisations and Persons who provided so kindly the many data and software that contributed to this work:

Prof. R. Forsberg, C.C. Tscherning and P. Knudsen for the GRAVSOFT software

The Bureau Gravimetrique International, for the gravity data set

The Ohio State University and Prof. R.H. Rapp, for the global geopotential model

The AGIP Society, the National Research Council and the National Geological Survey of Italy for the Italian DTM; the data exchange between Italy and France was made easier with the help of Prof. Sansò

The Service des Cartes Dérivées et Thématiques et the Service de Géodésie et Nivellement (Institut Géographique National) for the French DTM and the geodetic data.

Prof. G. Balmino, for his advice and friendly encouragements.

REFERENCES

Balmino, G., Balma, G., Sarrailh, M. and Toustou, D. (1992). Géoïde gravimétrique français, état d'avancement et programme de travail au GRGS/BGI. Toulouse, France.

Delomenie, M. (1987). Calcul d'un géoïde gravimétrique sur la France. Rapport de stage, IGN & BGI.

Duquenne, H. (1992). The new digital terrain model of France. Presented at the First Continental Workshop on the geoid in Europe. Prague, Czech Republic.

Duquenne H., Jiang Z., Lemarié C. (1995). Geoid determination and levelling by GPS: some experiment on a test network. In: Gravity and Geoid. IAG symposium n° 113, Graz, Austria, Sept. 1994.

Forsberg, R., Masden, F. (1990). High-precision geoid heights for GPS levelling. In: Proceedings of the Second International Symposium on Precise Positioning with the Global Positioning System. Ottawa, Canada.

Heiskanen, W. A. and Moritz, H. (1967). Physical Geodesy. Reprint Institute of Physical Geodesy, Technical University, Graz, Austria, reprint 1981.

Levallois, J.J. (1971a). Calcul du géoïde gravimétrique sur le territoire de la France. Présenté à la XV^{e} Assemblée Générale de l'AIG, Moscou.

Levallois, J.J. (1971b). Comparaison d'un géoïde astro-géodésiqie et gravimétrique sur le territoire français. Présenté à la XV^{e} Assemblée Générale de l'AIG, Moscou.

Moritz, H. (1992). Geodetic Reference System 1980. in Bulletin Géodésique, The Geodesist Handbook 1992.

Rapp, R.H., Wang, Y.M., Pavlis, N.K. (1991). The Ohio State University 1991 Geopotential and Sea Surface Topography Harmonic Coefficient Models, O.S.U. Report num. 410.

Sideris, M. G. and Forsberg, R. (1990). Review of Geoid Prediction Methods in Mountaneous Regions. In Determination of the Geoid, Present and Future, IAG Symp. n° 106, Milan, Italy.

Toustou, D. (1991). Chaîne de validation interactive des données gravimétriques: DIVA. Note technique n° 10, Bureau Gravimétrique International, Toulouse, France.

Tscherning, C.C., Forsberg, R. and Knudsen, P. (1992). The GRAVSOFT Package for Geoid Determination. Presented at the First Continental Workshop on the geoid in Europe. Prague, Czech Republic.

Willis, P., Boucher, C., Botton, S., Fagard, H. (1994): The RRF Network: A densification of the ITRF for France, *IERS/IGS Workshop*, Paris, March 1994, IGN CC/G n 603

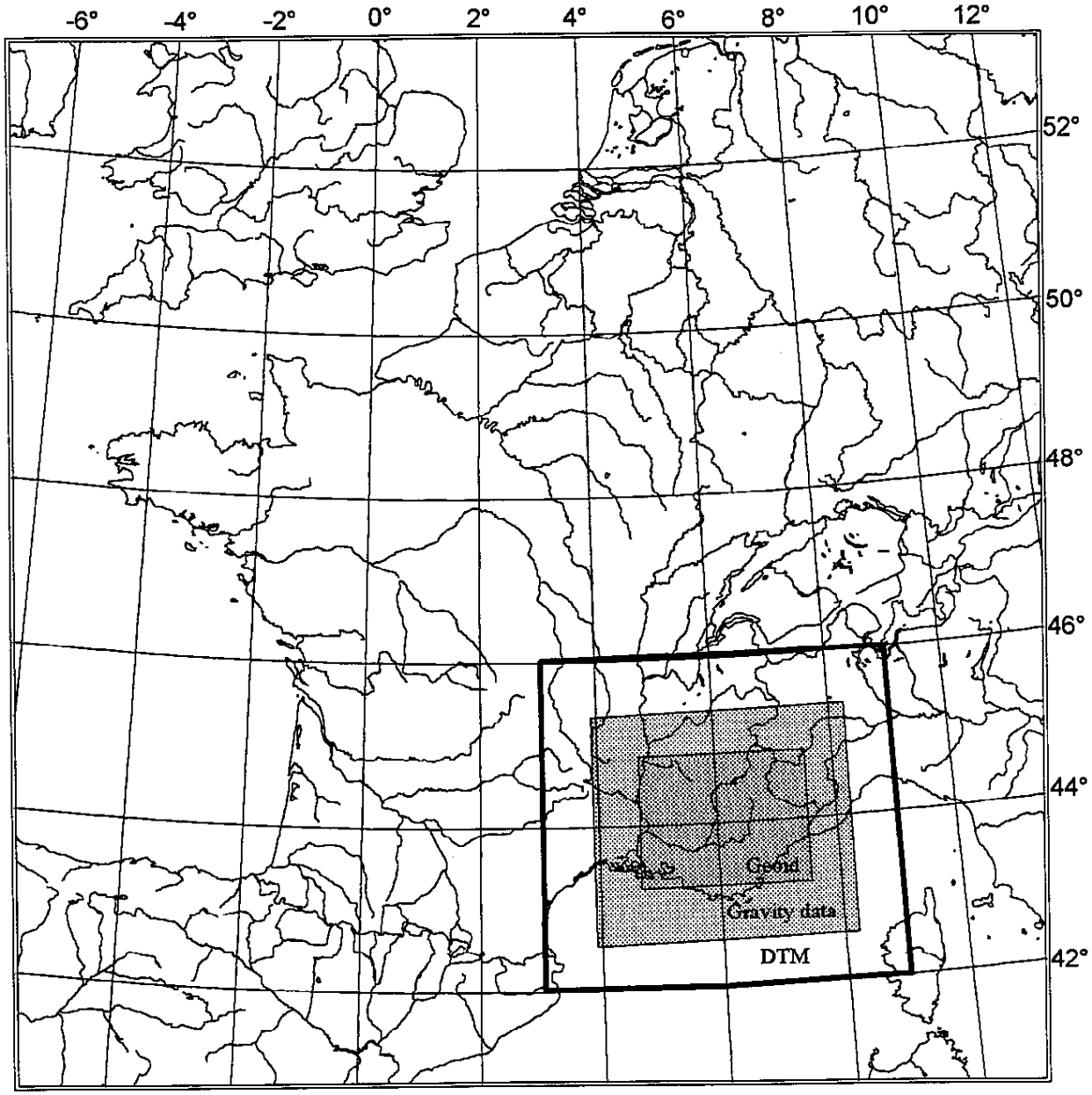

Fig. 1. Location of the test area: limits of the DTM, the gravity data set and the geoid.

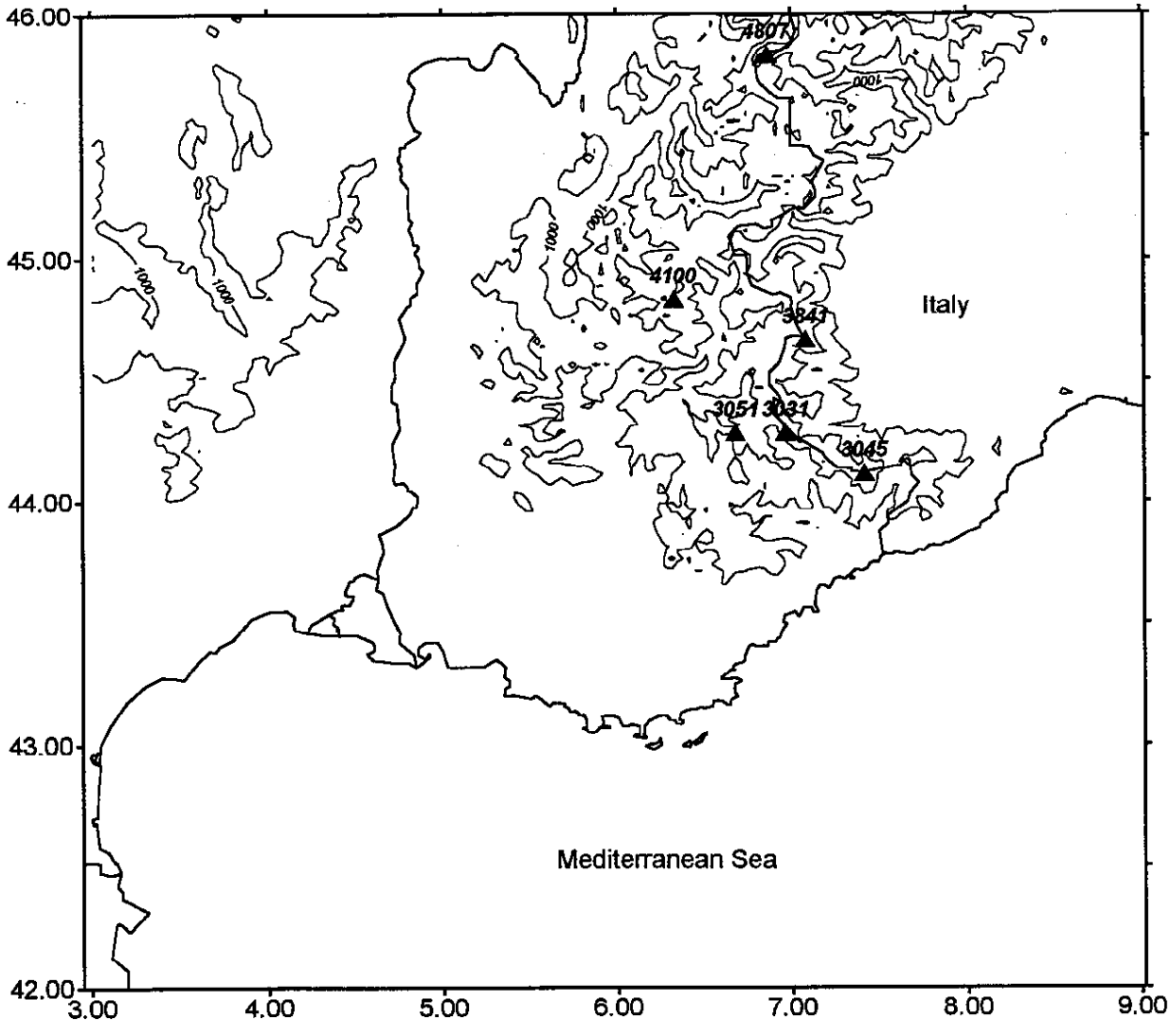

Fig. 2. Regional topography. Contour interval 1000 m. Some of the highest summits are plotted.

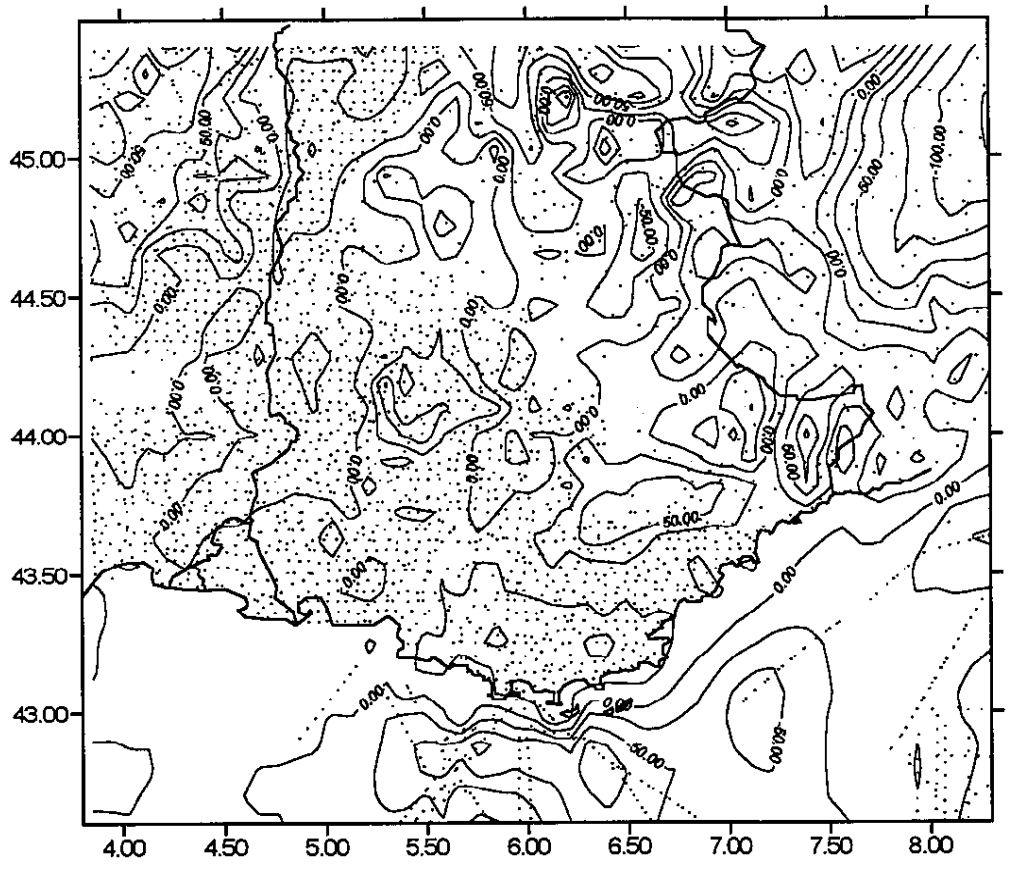

Fig. 3. Sampled gravity points and free air anomalies (mgal). Contour interval 25 mgal.

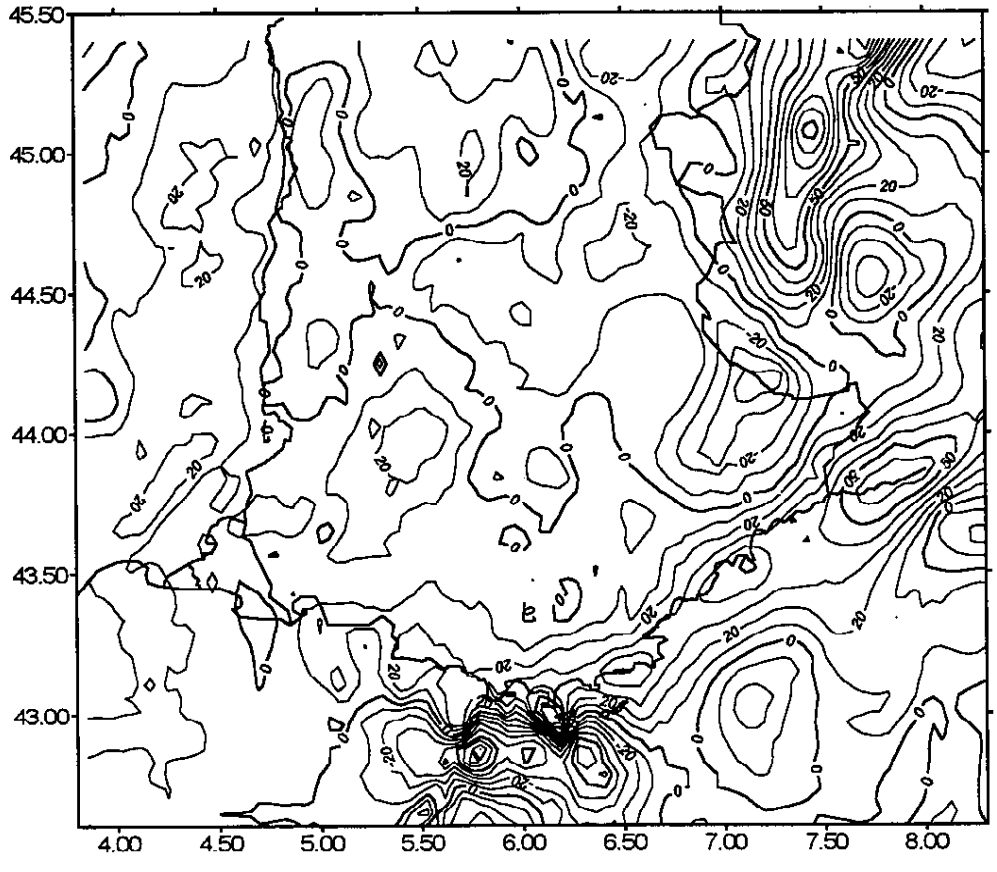

Fig. 4. Residual anomalies. Contour interval 10 mgal.

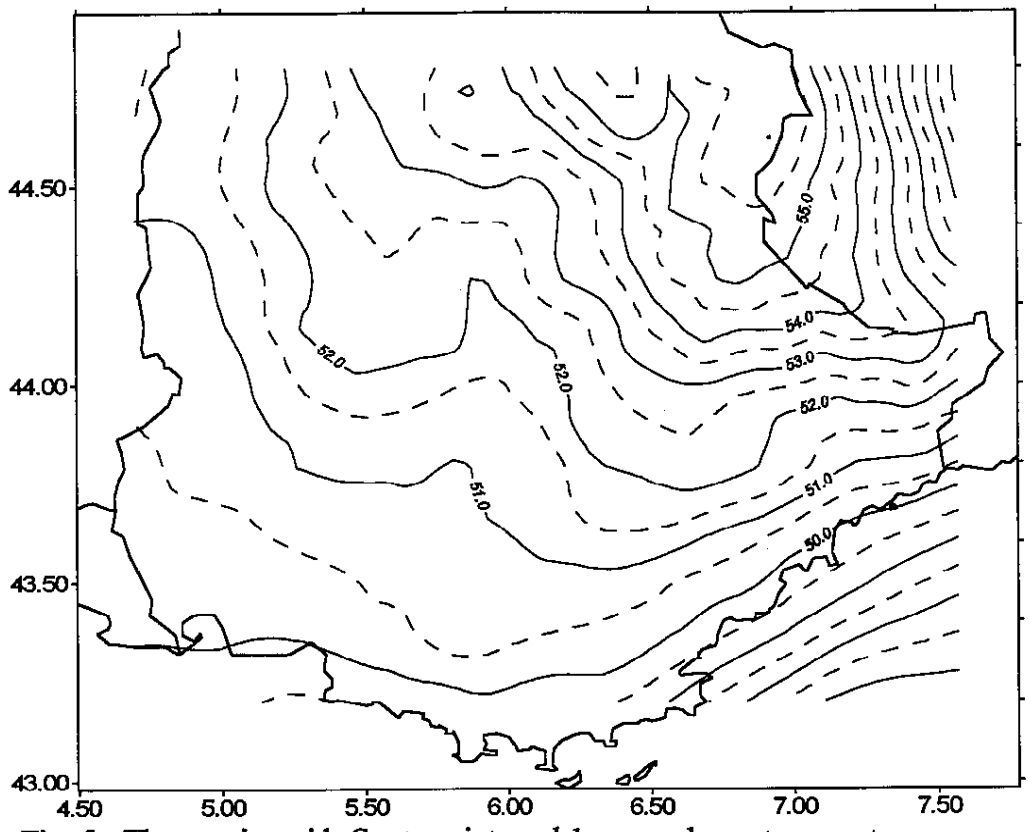

Fig. 5. The quasi-geoid. Contour interval 1m, supplementary contours every 0.5 m (dashed lines)

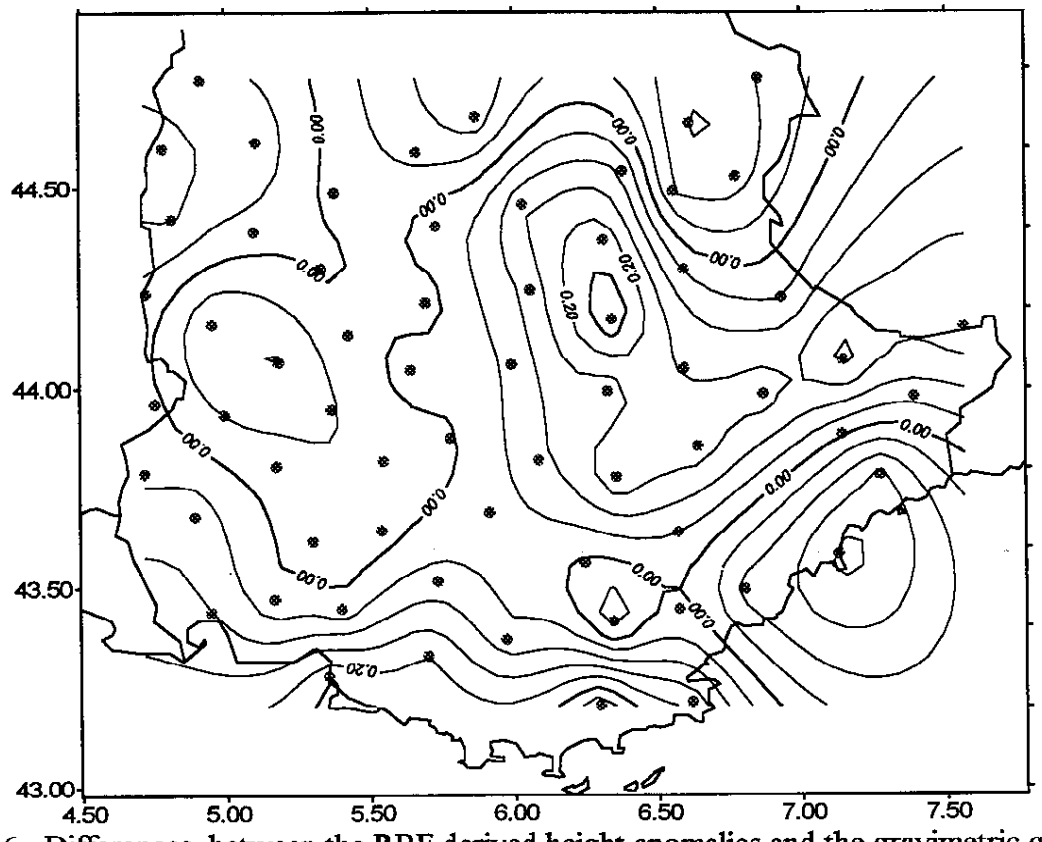

Fig. 6. Differences between the RBF derived height anomalies and the gravimetric quasi-geoid. Constant bias removed. Contour interval 0.05 m. Grey circles represent the RBF GPS levelled points.

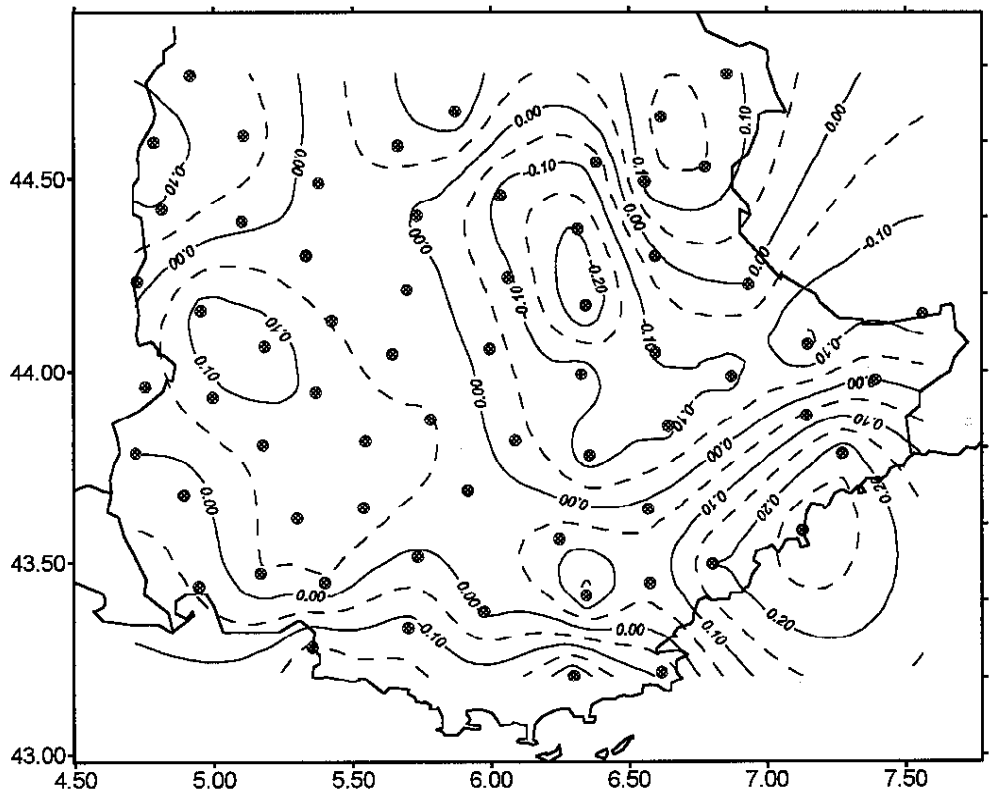

Fig. 7. RBF GPS points and residual differences between the RBF derived height anomalies and the gravimetric quasi-geoid, after a 3-parameters regression. Contour interval 0.10 m, supplementary contours every 0.05 m (dashed lines).

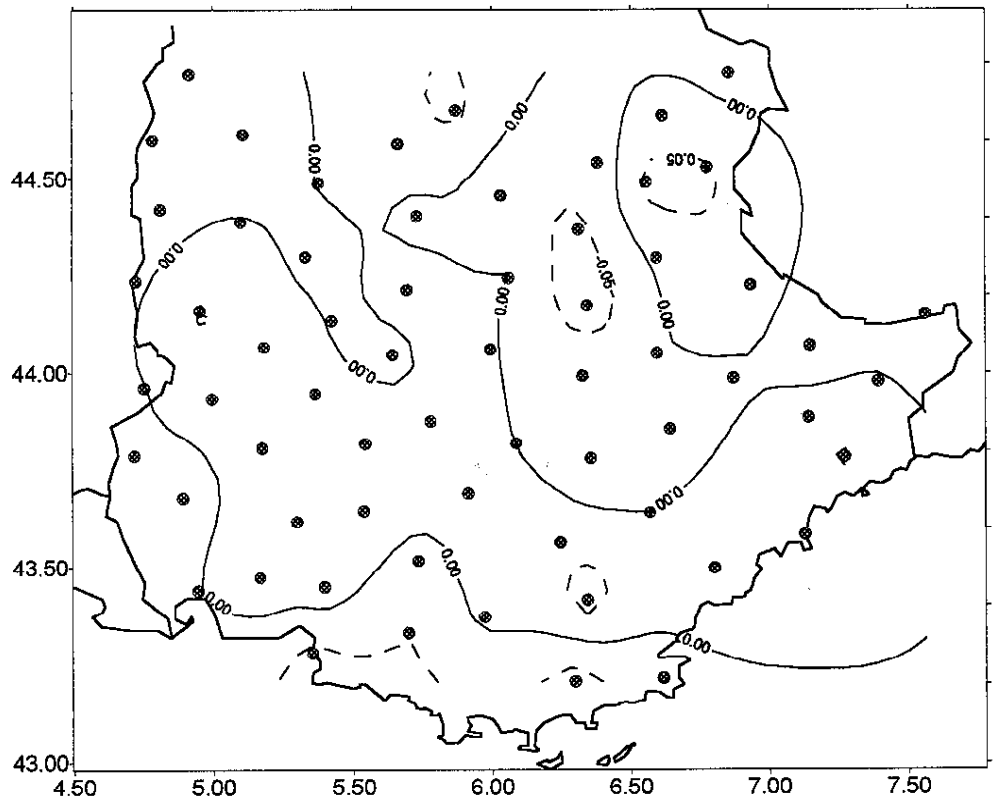

Fig. 8 Residual differences between the RBF derived height anomalies and the gravimetric quasi-geoid, after a combined adjustment with PILI software. Contour interval as in fig. 7

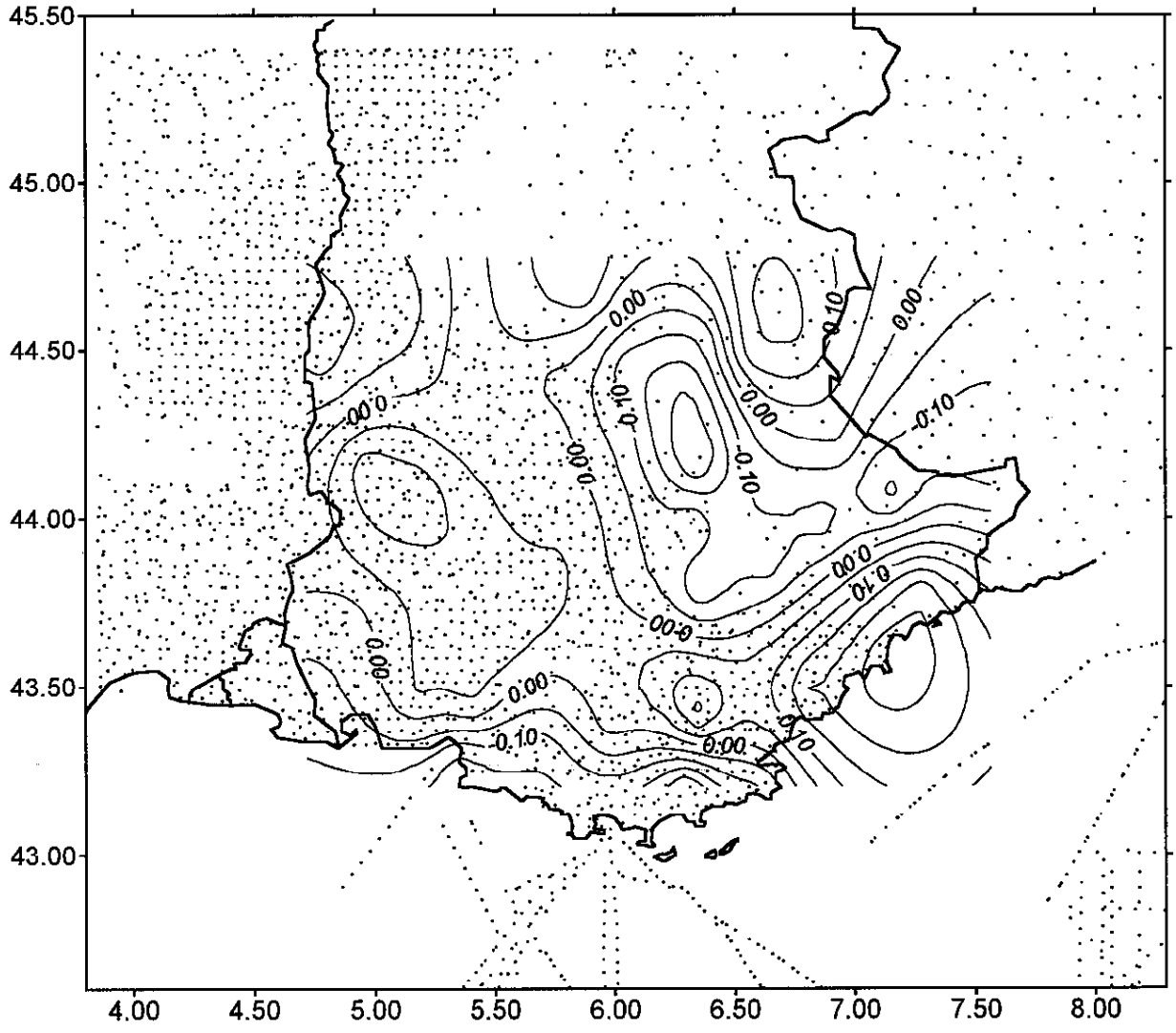

Fig. 9 Residuals of the regression of $\zeta_{RBF} - \zeta_{Gravi}$ and the gravity coverage: the correlation between large residuals and lack of gravity data seems to be evident.

Geoid models for Great Britain and the North Sea

R G Hipkin

Department of Geology & Geophysics
University of Edinburgh
West Mains Road
Edinburgh EH9 3JZ

Abstract

This paper describes the new model geoid for Great Britain called EDIN91, as well as its recent predecessors, EDIN89 and EDIN891, also noting the objectives for the next geoid EDIN95, now in preparation. EDIN91 appears to identify a north-south trend of 0.28 mm km^{-1} in the global gravity model OSU91A over an 800 km baseline in Britain. Accepting this trend and allowing for the 697.7 mm difference in ellipsoidal radius to adjust OSU91A to ITRF90 gives an absolute correction of 3.3 ± 10.3 mm for the Newlyn Datum, based on six GPS/MSL tide gauge geoid heights given by Dodson et al (1995). This result may yet prove spurious because there are known small adjustment errors in the gravity data set. A definitive assessment of the quality of the new geoid awaits the outcome of a re-evaluation of the gravity and topographic data now taking place in preparation for EDIN95 and the availability of better distributed GPS control in northern Britain.

1 The British geoid models EDIN89, EDIN891, EDIN91 and EDIN95

The geoid model EDIN89 (Stewart & Hipkin, 1990) covered a region of Great Britain and the North Sea 1000 by 900 km in size. It was computed using a conventional fast Fourier transform algorithm from land and marine Bouguer gravity anomalies on a 2 km grid, a 2 km digital model of mean topographic heights and the global potential model OSU86E. A detailed review of the methodology and the practical error budget of the computation are described in Hipkin (1995).

This paper reports a recomputation using essentially the same local gravity and topographic information but using the model OSU91A for the global field. A provisional version was initially computed using a semi-empirical correction for the change from OSU86E to OSU91A; this was called EDIN891. The full recomputation is called EDIN91.

The geoid model EDIN891 attempted to provide some of the improvements of the new global potential model, without a complete recomputation of the geoid. The semi-empirical correction was based on the proposition that components of the global model with wavelengths shorter than 300 km would be completely corrected by the local gravity and topographic data but that changes in the global model with longer wavelengths would modify the computed geoid. The geoid height difference between the two global potential models was calculated and then filtered with a low pass filter whose response diminished with a cosine taper from 1 at 1000 km wavelength to zero at 300 km wavelength. All wavelengths shorter than 300 km were suppressed completely. Adding this low-pass filtered version of the geoid height difference OSU91A - OSU86E to EDIN89 gave the provisional geoid model EDIN891.

EDIN891 has now been superseded by the model EDIN91 described here. EDIN91 still uses the same gravity and topographic model as EDIN89 but differs both in the global gravity model used and in the implementation of the transformation. A new geoid model EDIN95 is in preparation using an extended and readjusted gravity data set to reduce the effect of long wavelength errors in the global model.

With the greater computing power now available, the Fourier transform of some 225000 values could be carried out for EDIN91 in a single operation. EDIN89 had been computed in four separate transformations, each covering a 700 km square; the final model was obtained by merging the four areas, adjusting their relative datum levels by minimising the misfit along the centre of the 400 km overlap.

2 Transformation algorithms

For all the Edinburgh models, the transformation from gravity anomaly to geoid height was carried out using a two-dimensional fast Fourier transform. For this, the gravity and topographic data were gridded at 2 km intervals of the Transverse Mercator Projection of the Ordnance Survey of Great Britain. By using map projection coordinates, the 'flat Earth' approximation inherent in the conventional use of the Fourier transform only introduces errors of the order of the wavelength divided by the circumference of the Earth. Because the Fourier technique can in any case only transform components with wavelengths less than about one third of the length of data, the maximum error due to the 'flat Earth' approximation is of the order of the data length divided by 120 000 km (Hipkin, 1995). This makes the approximation good to better than 1% for a data set 1000 km across. The transform is only applied to gravity ***residuals*** with respect to the global potential model. The resulting residual geoid has an amplitude of less than 1 m so the transformation error will be less than a centimetre for components with wavelengths of 300 km or less. The use of map projection coordinates also eliminates the need for ellipsoidal corrections: the map projection already transforms an ***ellipsoidal*** surface onto the plane.

Although recent work by Strang van Hees (1989) and Haagmans et al (1994) has shown that Stokes' integral (a ***rigourous*** transformation for ***regularised*** gravity anomalies available on the ***whole*** of a ***spherical*** surface) can be evaluated efficiently using Fourier methods, the real problems do not lie with the transformation algorithm: the conceptually simpler 'flat Earth' approximation is entirely adequate and indeed has some advantages. The real problems with geoid computation lie first with the inadequacy of the gravity and topographic data and secondly with the need to localise the transformation.

Hipkin (1995) examined in detail the accuracy available when well distributed and accurate gravity and topographic data were available, finding RMS corrections of only about 3 mm for the relative geoid at sites in a test network near Matlock in the English Peak District. There, the gravity and topographic data could be legitimately interpolated onto 500 m and 100 m grids respectively. The accuracy specification for the original gravity observations had been set at 0.04 mgal. This study did not address the consequences of less accurate or well distributed data, nor the effect of long wavelengths remaining in residual gravity because of errors of omission or commission in the global potential model. It sought only to demonstrate that the practical algorithm was intrinsically capable of sub-centimetric accuracy.

3 Long wavelengths in the residual anomalies.

The quality obtained with a Fourier technique (whether conventional or the Strang van Hees application to Stokes integral) depends upon having a band limited operand: there must be no significant power either at wavelengths longer than about one third of the data length or at wavelengths shorter than twice the sampling interval. How to deal with short wavelengths

was described in the Matlock study but the absence of long wavelengths depends on the quality of the global potential model and is investigated here.

Free air anomalies were computed from the OSU91A model at 0.1° and 0.2° intervals of latitude and longitude and then interpolated onto the same 2 km grid as the local gravity and topographic data. The spectrum of the residual anomalies rises monotonicly over the whole range from shortest to longest wavelengths and gives no indication of being long wavelength limited. In the space domain, the residuals over the 1000 by 900 km region were neither trend-free nor zero-mean: local free air gravity minus OSU91A had a mean value of 0.9158 mgal with a least squares linear trend of 0.0026 mgal km^{-1} eastwards and - 0.0024 mgal km^{-1} northwards. Geoid solutions with and without removing this trend were computed but not removing it will certainly bias the Fourier transformation and EDIN91 was derived from trend-free residual anomalies. As a consequence, it will be subject to an error with a linear trend but with an indeterminate amplitude. It is hoped that the two-stage algorithm devised for EDIN95 will reduce this problem.

4 Conclusions and comparisons with GPS/MSL

The accuracy of a geoid model can be assessed in two ways: first, an internal error budget can be evaluated by looking at the inherent accuracy of the gravity and topographic data and at the imperfections in the algorithm by which they are transformed to geoid height; secondly, there can be an external comparison with a completely independent method of geoid determination. The second approach is philosophically more satisfactory but is probably not to be available for small local networks where a ***relative*** gravimetric geoid appears to be more accurate than any other technique. At longer wavelengths, the position of mean sea level with millimetric accuracy is directly available at a tide gauge bench mark. Ellipsoidal heights obtained with modern GPS receivers and software should be good to a centimetre but unmodelled errors with long range levelling means that the GPS site needs to be within a few tens of kilometres from the coast.

EDIN891 was compared with tide gauge data and GPS observation undertaken by the University of Nottingham (Dodson et al, 1995). There was good agreement for the southerly 500 km of the area - simply a datum shift of 483 ± 49 mm, but EDIN891 was very anomalously higher than GPS/MSL at Aberdeen by 974 mm. (See Table 1) The discrepant behaviour in the north was seen both in the raw OSU91A geoid heights and in EDIN891 but not in a Stokes integral geoid computed by Featherstone and Olliver (1994), which was not based on OSU91A and which used a more recent adjustment of British gravity data. This suggested one possible source of the discrepancy: there may have been a small error in Northern Britain in either OSU91A or the local gravity data set used here, which was not being corrected by the empirical transfer. The rigourous recomputation to give EDIN91 was directed towards identifying the source of this discrepancy.

The EDIN91 computation suggests three interesting conclusions but is not definitive because of known deficiencies in the adjustment of North Sea gravity data and the scarcity of GPS control in northern Britain. The first conclusion is that the long-wavelength trend in the residual anomalies has been translated into a small north-south slope in the model over Britain; the second is that the 'error' in the Edinburgh geoids at Aberdeen is now just part of this slope and is very consistent with it; the third is that the internal consistency of EDIN91 is much better than EDIN891 so that the absolute vertical datum for Britain may have been determined with an unprecidentedly high precision.

Table 1 shows the effect of taking the trend (0.69288 + 0.0002797 N) m from the difference EDIN91 - GPS/MSL. (N is the grid northing in kilometres. There is no detectable east-west trend.) After removing this trend, the residuals at six tide gauge sites, which span some 800 km north-south range, have a standard deviation of only 10.2 mm. It is understood that the difference in the radius of the reference ellipsoids used for the GPS and for the OSU91A

gravity model causes a displacement of 697.7 mm over the whole of Britain, so that the ***absolute*** vertical datum correction for Newlyn appears to be very well determined indeed as 3.3 ± 10.2 mm.

Site	Easting (km)	Northing (km)	EDIN89	EDIN891	EDIN91 raw	EDIN91 trend	EDIN91 residual
Newlyn	146.37	29.00	540	557	704.9	701.0	3.9
Portsmouth	462.91	101.27	974	435	709.4	721.2	-11.8
Dover	631.90	140.80	1240	530	745.6	732.3	13.3
Sheerness	591.10	174.47	1204	464	730.2	741.7	-11.5
Lowerstoft	654.38	292.50	1385	465	782.1	774.7	7.4
Aberdeen	395.59	806.75	1099	974	917.2	918.5	-1.3

Table 1: Geoid height difference EDIN - GPS/MSL (mm)

The trend removed from EDIN91 is [692.88 + 0.2797 Northing (km)] mm. The Nottingham University GPS/MSL estimate of geoid height was supplied in a letter from A H Dodson (1995).

While the magnitude of the north-south slope can be modified by changes in the data preprocessing (eg not removing the trend in the residual free air anomalies, varying the marginal taper, padding out the data), all give qualitatively similar results. The simple detrend with no padding or tapering adopted for EDIN91 gives (as expected) the most consistent result.

Conclusion derived from these results must remain provisional: the task of computing the new geoid EDIN95 has begun and significant long wavelength errors in the earlier gravity data adjustment of North Sea data has been detected. It is anticipated that this may mofify the EDIN91 geoid at longwavelength, possibly even removing the bias and trend with respect to free air anomalies computed from OSU91A. However, the central point is likely to remain: a local and relative gravimetric geoid can now be readily computed with verified centimetric accuracy, and the prospect of determining the absolute datum with a similar accuracy now appears in sight.

Acknowledgements

Long standing collaboration with Vidal Ashkanazi and Alan Dodson and their coworkers at the University of Nottingham is gratefully acknowledged, together with the work of unravelling tide gauge bench mark heights by Trevor Baker of the Proudman Oceanographic Laboratory, Bidston.

References

DODSON, A H; BINGLEY, R M & STEWART, M P (1995) Using high precision GPS to aid absolute geoid datum definition, pp 511-518 in *Gravity and Geoid, International Association of Geodesy Symposium 113 (eds Sünkel, H & Marson, I)* Springer-Verlag, New York.

HAAGMANS, R H N; DE MIN, E & VAN GELDEREN, M (1993) Fast evaluation of convolution integrals on the sphere using 1D FFT, and a comparison with existing methods for Stokes' intergal. *Manuscripta Geodetica,* **18**, 227-241.

HIPKIN, R G (1995) How close are we to a centimetric geoid? pp 529-538 in *Gravity and Geoid, International Association of Geodesy Symposium 113 (eds Sünkel, H & Marson, I)* Springer-Verlag, New York.

STEWART, M P & HIPKIN, R G (1990) A high resolution, high precision geoid for the British Isles, pp 39-46 in *Sea Surface Topography and the Geoid, International Association of Geodesy Symposia 104* (eds Sünkel, H & Baker, T) Springer-Verlag, New York.

STRANG VAN HEES, G (1990) Stokes formula using fast Fourier techniques. *Manuscripta Geodetica,* 15, 235-239.

RAPP, R H; WANG, Y H & PAVLIS, N K (1991) The Ohio State 1991 geopotenital and sea surface topography harmonic coefficient models. *Report 410 Department of Geodetic Science and Surveying, Ohio State University, Columbus,* 94pp.

The new Italian quasigeoid: ITALGEO95.

R. Barzaghi, M.A. Brovelli, G. Sona,

DIIAR - Sez. Rilevamento, Politecnico di Milano. P.zza L. da Vinci, 32 - 20133 Milano, Italia

A. Manzino

Dip. Georisorse e Territorio, Politecnico di Torino. C.so Duca degli Abruzzi, 24 - 10129 Torino, Italia

D. Sguerso

Dip. Ing. Civile e Ambientale, Università di Trento. Mesiano di Povo 77 - 38050 Trento, Italia

Abstract

The last estimate of the Italian quasigeoid, ITALGEO95, has been accomplished during the first half of 1995.
This new computation has been based on a revised data set of gravity covering the area $36° \le \varphi \le 47°$, $6° \le \lambda \le 19°$ and an implemented DTM, having a grid mesh of nearly 250 m. The method used to get the estimate is the remove-restore technique (with some minor modifications) plus Fast Collocation which allows to obtain the solution over the entire area in one step only.
The final product is the estimate of ζ over a regular grid of 3'x3'in the zone $36° \le \varphi \le 47°$, $6° \le \lambda \le 19°$.
This quasigeoid has been tested with GPS/leveling measurements which showed a good agreement with it; strong improvements have been reached both with respect to the pure geopotential model (OSU91A) and the previous Italian geoid (ITALGEO90).

1. Introduction

A new detailed estimate of the quasigeoid has been computed over an area covering Italy and surrounding seas. The aim of this computation is to provide an updated and reliable reference surface to be used in connection with GPS measurements, altimetric observations and for geophysical investigation in the central Mediterranean area. This quasigeoid, named ITALGEO95, has been based on a new validated gravity data set covering the area $36° \le \varphi \le 47°$, $6° \le \lambda \le 19°$ and on a DTM which is, on each side, two degrees larger than the area containing gravity. The estimation technique is the usual remove-restore method, while the computation of ζ_r from Δg_r is based on Fast Collocation (Bottoni and Barzaghi, 1993) which allowed the estimate of ζ_r in one step only. The result is a quasigeoid grid in $36° \le \varphi \le 47°$, $6° \le \lambda \le 19°$ with a grid mesh of 3'x3'. The ITALGEO95 estimate follows a previous geoid computation on the same area

which was carried out in 1989, the ITALGEO90 (Benciolini et al., 1991). Several improvements have been introduced with respect to it. Gravity and DTM data bases used in ITALGEO90 were mainly based on Italian data and practically no integration with other data sources was performed. This led to an estimate which was reliable on land areas, where data were present. Another step forward has been done from the methodological point of view. ITALGEO90 was derived via remove-restore technique and collocation. Due to collocation computational limits, the N_r estimate was obtained in eleven different blocks which partially overlapped. These local solutions were then merged together to get a global regular grid of 7.5'x7.5' in the area $35.9583 \leq \varphi \leq 47.3333$, $6.4523 \leq \lambda \leq 518.9525$; the global geopotential model IFE88 was used to fill in gaps in the areas were no $\hat{N}_r$ was provided (i.e. on the seas surrounding Italy and on Corse, since the eleven zones cover the peninsular part of Italy and its two main islands, Sicily and Sardinia).
Both merging procedure and lack of data on sea led to discontinuities in the final estimate which reflected in a quite poor agreement with GPS/leveling data, especially in the south. The procedure adopted in ITALGEO95, based on Fast Collocation together with the new implemeted data base of gradity and DTM, tried to overcame exactly this fragmentation problems in order to get a homogeneous, and reliable estimate both on land and on marine areas.
Finally, another relevant difference with respect to ITALGEO90 is the global geopotential model used in the remove-restore procedure. In ITALGEO95 the more recent OSU91A model was assumed as a reference field in order to remove and restove the long wavelength components of gravity and geoid.
The comparisons of ITALGEO95 with the available GPS/leveling data, distributed quite homogeneously over the entire estimation area, gave good results, which sharply improve the ITALGEO90 performances, especially where poor results were present, i.e. in the southern part of Italy.

2. Data acquisition and preparation

Gravity data

In the area

$$36° \leq \varphi \leq 47° \quad 6° \leq \lambda \leq 19°$$

all the available free air gravity anomalies were considered and merged together to ensure a proper coverage, suitable for the 3'x3' geoid computation grid. Data were collected from:

- the Italian gravity data base, the same used in ITALGEO90 (Carrozzo et al., 1982; Benciolini et al., 1991). These are mainly land data and cover quite densely the peninsular part of Italy, Sicily and Sardinia. This data base consists of 240489 gravity stations;

- Morelli's gravity maps over the Adriatic and Tyrrhenian Seas (Morelli, 1970; Morelli et al., 1975a; Morelli et al., 1975b). These are mean gravity anomaly values on a 5'x5' grid coming from a digitalization performed by prof. D. Arabelos. These data showed a gap in the central Tyrrhenian part which has been filled in at DIIAR digitizing the Morelli's map on this area. The total number of data coming from this file is 20344;
- BGI point gravity anomaly data mainly on land areas on the nothern border of Italy plus data covering the Corsica Island. From this source 35411 gravity stations were collected.

Since gravity anomalies listed above refer originally to different normal gravity field, the first step was to reduce all this data the same normal field, i.e. to the GRS80 normal gravity. Further more, data were also reduced by selecting those closer to the center of a 1'x1' grid over to the computation area. In this way, from the original 296244 gravity observations, a smaller data base of 105695 Δg values was extracted. This has been done mainly to homogenize the distribution of gravity data which in some areas is uselessly dense. Further more a gravity data base which is nearly 1'x1' is for sure suitable for producing a 3'x3' geoid grid. It must also be remarked that on some part of the sea we have data with a 5'x5' spacing, (i.e. those coming from Morelli's map digitalization). This however is not so troublesome because gravity on sea is much more regular than on land, so that the interpolation procedure from 5'x5' to a 3'x3' grid (the one used in Fast Collocation) can be accomplished quite reliably.
The coverage of the reduced data set is shown in Fig. 1. It can be immediately seen that a large data gap is present over the ex Yugoslavia region. This deficiency could have coused problems in the north-east corner of the prediction grid and on the Adriatic sea too. However, since the correlation length of residual gravity is of the order of 15' (see Fig. 2), no relevant effects are to be expected on the remaing part of the estimation grid.

DTM

In order to obtain a smoothed gravity field to be input in the collocation procedure, gravity data must be reduced both for the geopotential model and terrain effect. To compute properly the terrain effect, a detailed DTM model has been prepared over the area

$$34° \leq \varphi \leq 49° \qquad 4° \leq \lambda \leq 21°$$

As mentioned before, the area considered for DTM is two degree larger than the area containing Δg. This has to do with the terrain effect computation which must be carried out taking into account large window of DTM data for each gravity station point. Many different DTMs were merged together to form a unique homogeneous height data base (where homogeneity refers to data spacing, not to precision). The different data sources are listed below, with their main characteristcs.

- Italian DTM, covering mainly land areas. Data are on a regular geographical grid with 7.5"x10" spacing (Carrozzo et al., 1982).

- Morelli bathymetry on sea; these are grided data 5'x7.5' (Morelli et al., 1975b).
- Austrian DTM covering whole Austria with resolution 11.25"x18.75".
- French DTM in the Alps area ($42.75° \leq \varphi \leq 48$, $5° \leq \lambda \leq 8°$) and over Corsica with resolution 9"x6".
- Swiss DTM (RIMINI) with grid spacing of 250 m on a regular (x,y) grid in the national Swiss map projection system.
- German DTM in the strip $47° \leq \varphi \leq 48°$, $7° \leq \lambda \leq 13°$ having resolution 30"x50".
- ETOPO5U in the remaining parts of the considered area. This global data base has grid mesh of 5' both in latitude and in longitude.

Since these DTM models have different spacings the merging procedure was designed to reduce all them to a common grid mesh, namely the one of the Italian DTM. This has been done by simple bilinear interpolation without taking into account the different accurancy of the various DTM. The bilinear interpolation was applied to the various height data bases but not to the Italian DTM which maintained the original values. The information stored in the final global DTM are the heights in meters coupled with a code which relates to the DTM sources used to compute those values.
This data base is stored in binary form and contains 7202 x 6122 heights (and codes) on a regular geographical grid of 7.5"x10".

3. Quasigeoid computation method and results

The remove-restore procedure and Fast Collocation (Barzaghi et al., 1992) were used to get the quasigeoid estimate. The basic scheme of this method has been applied following these steps:

(a) removal of the long wavelength component of the gravity data using the global geopotential model OSU91A in the measuring points $(\varphi_i, \lambda_i, h_i)$

$$\Delta g_0(\varphi_i, \lambda_i, h_i) - \Delta g_M(\varphi_i, \lambda_i, h_i);$$

(b) Residual Terrain Effect (RTE) computation and subtraction of such an effect to produce residual gravity values

$$\Delta g_r(\varphi_i, \lambda_i, h_i) = \Delta g_0(\varphi_i, \lambda_i, h_i) - \Delta g_M(\varphi_i, \lambda_i, h_i) - g_{rtc}(\varphi_i, \lambda_i, h_i);$$

(c) Outliers rejection on $\Delta g_r(\varphi_i, \lambda_i, h_i)$;

(d) gridding of $\Delta g_r(\varphi,\lambda,h)$ to produce a 3'x3' regular grid of $\Delta g_r\left(\varphi_j^G,\lambda_j^G\right)$ over the area $36°\le\varphi\le47°, 6°\le\lambda\le19°$ ($\left(\varphi_j^G,\lambda_j^G\right)$ longitude and latitude of grid knots);

(e) Fast Collocation computation of $\Delta\hat{g}_r\left(\varphi_j^G,\lambda_j^G,0\right), \Delta\hat{g}_r\left(\varphi_j^G,\lambda_j^G,1000m\right)$ from $\Delta g_r^G\left(\varphi_j^G,\lambda_j^G\right)$ to evaluate $\frac{\partial\Delta\hat{g}_r}{\partial h}\left(\varphi_j^G,\lambda_j^G\right)$;

(f) computation of $\Delta g_r(\varphi_i,\lambda_i,0)$ from $\Delta g_r(\varphi_i,\lambda_i,h_i)$ and $\frac{\partial\Delta\hat{g}_r}{\partial h}\left(\varphi_j^G,\lambda_j^G\right)$;

(g) gridding of $\Delta g_r(\varphi_i,\lambda_i,0)$ to produce $\Delta g_r\left(\varphi_j^G,\lambda_j^G,0\right)$ on the 3'x3' grid;

(h) estimation, via Fast Collocation, of $\hat{T}_r\left(\varphi_j^G,\lambda_j^G,0\right)$ and $\hat{\Delta}g_r\left(\varphi_j^G,\lambda_j^G,0\right)$ on the 3'x3' grid;

(i) evaluation of $\frac{\partial T_r}{\partial h}\left(\varphi_j^G,\lambda_j^G\right)$ via fundamental equation of geodesy

$$\frac{\partial\hat{T}_r}{\partial h}\left(\varphi_j^G,\lambda_j^G\right) = -\Delta\hat{g}_r\left(\varphi_j^G,\lambda_j^G,0\right) - 2\frac{\hat{T}_r\left(\varphi_j^G,\lambda_l^G,0\right)}{R}$$

R = mean Earth radius;

(l) computation of $\hat{T}_r\left(\varphi_j^G,\lambda_j^G,h_j^G\right)$ using $\hat{T}_r\left(\varphi_j^G,\lambda_j^G,0\right)$ and $\frac{\partial\hat{T}_r}{\partial h}\left(\varphi_j^G,\lambda_j^G\right)$;

(m) restore of the model and of the residual terrain effect on the $\left(\varphi_j^G,\lambda_j^G,h_j^G\right)$ 3'x3' prediction grid, to get

$$\zeta\left(\varphi_j^G,\lambda_j^G,h_j^G\right) = \zeta_r\left(\varphi_j^G,\lambda_j^G,h_j^G\right) + \zeta_{rtc}\left(\varphi_j^G,\lambda_j^G,h_j^G\right) + \zeta_M\left(\varphi_j^G,\lambda_j^G,h_j^G\right).$$

Some comments are in order to clarify the described procedure.
The global geopotential model OSU91A gives a good description of the geopotential field in this area, apart from the Corsica Island where it appears to be completely flat, both in Δg and in ζ. This causes a mismodelling which reflects into the residual values derived at step (a). To overcome this model deficiency, we decided to remove and then restore the total effect of the reference Corsican topography (the same reference heights used for RTE computation described here after) in all the points contained in the window $40° \le \varphi \le 44°$, $7° \le \lambda \le 11°$ centered on Corsica Island. In such a way the low frequency component of geopotential field of Corsica, which is not present in the OSU91A model, is assumed to be connected to the reference DTM used for RTE.
The Residual Terrain Effect was computed with respect to a reference DTM which has been related statistically to the global geopotential model previously removed.
In order to do that, we considered a subset of 8577 points, homogeneously distributed, of the gravity data base derived at step (a). Then, we reduced the data of the Residual Terrain Effect computing it with various reference height fields. These different reference DTMs were obtained via moving average from the detailed DTM; the best coupling between model and residual terrain computation was reached with the smoothed DTM derived from a moving average of 20' window size, sampled at 5'x5'. This means that using the OSU91A geopotential model and such a reference height data base, we obtained the minimum mean and the minimum variance of the residual gravity values Δg_r.
Step (d) through step (f) were applied to verify the interaction between gridding procedure with height information in $\Delta g_r(\varphi_i, \lambda_i, h_i)$.

The statistical analysis $\Delta g_r(\varphi_i, \lambda_i, h_i)$ (step (b)) and $\Delta g_r(\varphi_i, \lambda_i, 0)$ (step (f)) showed that no significant correlation with the height is present in $\Delta g_r(\varphi_i, \lambda_i, h_i)$. In gridding the gravity data to determine $\Delta g_r\left(\varphi_j^G, \lambda_j^G, 0\right)$ on a regular grid, we had to face the problem due to the lack of data over ex Yugoslavia. As it is quite natural, we set $\Delta g_r\left(\varphi_j^G, \lambda_j^G, 0\right) = 0$ in that region, since no information are provided there. In principle, using Fast Collocation, step (h), (i) and (l) could be condensed in one step only, i.e. compute $\hat{T}_r$ on sparse (φ, λ, h) points from gridded data (g). However, this is so CPU time consuming that the computation we did should have lasted one month: steps (h) to (l) are much more efficient from the computational point of view even though this is an approximate procedure (differences between the rigorous and the approximate approach on some test points amount to a maximum of few centimetres).
The computer program used for RTE (this effect has been computed using a window of 120 km around each point) and gridding computations are TC and GEOGRID of the GRAVSOFT package (Forsberg, 1994; Tscherning, 1994) while global geopotential model functionals Δg_M and ζ_M have been evaluated using F388 program by prof. Rapp (1994).

We finally remark that the h_j^G of the grid in (l) was obtained via bilinear interpolation from the four neighbouring points of the detailed DTM. The numerical results of the estimation procedure detailed above are summarized in Table 1.

	Δg_0 (mgal)	$\Delta g_0 - \Delta g_M$ mgal)	$\Delta g_r \div (c)$ (mgal)	$\Delta g_r \div (g)$ (mgal)	$\hat{\zeta}_r$ (m)	$\hat{\zeta}$ (m)
n	105695	105695	105308	52188	57681	57681
E	11.87	-7.57	-3.66	0.24	0.07	44.24
σ	62.86	33.47	17.91	14.57	0.59	5.02
Max	348.82	309.67	117.36	111.07	2.33	54.96
min	-578.43	-631.00	-197.34	-118.28	-1.94	25.37

Table 1: Remove-restore statistics.

The empirical and model covariance functions used in each Fast Collocation estimation are plotted in Fig. 2; the final resulting quasigeod is shown in Fig. 3.

4. Comparisons with GPS/leveling data

Many reliable GPS campaigns have been carried out in the last years in Italy. Two geotraverses have been measured: one moving from the Brennero Pass along the Adriatic coasts to Noto in Sicily (this is the Italian part of the European geotraverse); the second starts in Rome (Monte Mario) and reaches Reggio Calabria in front of Sicily (Tyrrhenic geotraverse) (Birardi, 1993).
During the last two years, the Istituto Geografico Militare Italiano (IGMI) started a GPS measurement campaign which is planned to cover densely the Italian territory (Surace, 1993). Furthermore, in the framework of the TYRGEONET project (Achilli et al., 1991), GPS measurements have been made in several part of Italy.
Finally, we took into account data over Sardinia (Asili et al., 1995), so that the estimated quasigeoid has been tested over the entire Italian territory.
All these GPS stations have been connected to the Italian national height system through spirit leveling so that an estimation of N in these points is possible.
The statistics of the differences between N_{GPS} and ζ (ITALGEO95), N_{GPS} and N(ITALGEO90), N_{GPS} and N (OSU91A) are presented in Table 2, while the distribution of GPS stations is described in Fig. 4.

		E (m)	σ (m)	Max (m)	min (m)
Adriatic geotraverse n=56	$N_{GPS}-\zeta(95)$	0.76	0.54	1.81	-0.41
	$N_{GPS}-N(90)$	0.06	0.75	0.96	-1.93
	$N_{GPS}-N(OSU91A)$	0.45	0.63	2.43	-0.76
Tyrrhenic geotraverse n=28	$N_{GPS}-\zeta(95)$	0.16	0.11	0.51	0.01
	$N_{GPS}-N(90)$	-0.48	0.38	0.25	-1.57
	$N_{GPS}-N(OSU91A)$	0.03	0.37	0.90	-0.54
IGMI (South) n=29	$N_{GPS}-\zeta(95)$	-0.90	0.18	-0.54	-1.19
	$N_{GPS}-N(90)$	-1.56	0.73	-0.46	-2.99
	$N_{GPS}-N(OSU91A)$	-0.66	0.47	0.78	-1.65
IGMI (North) n=13	$N_{GPS}-\zeta(95)$	-0.29	0.08	-0.15	-0.41
	$N_{GPS}-N(90)$	-0.83	0.15	-0.54	-1.14
	$N_{GPS}-N(OSU91A)$	-0.79	0.43	-0.30	-1.63
Tyrgeonet (South) n=12	$N_{GPS}-\zeta(95)$	-0.91	0.12	-0.68	-1.06
	$N_{GPS}-N(90)$	-1.19	0.44	-0.18	-1.78
	$N_{GPS}-N(OSU91A)$	-0.94	0.36	-0.42	-1.46
Tyrgeonet (North) n=20	$N_{GPS}-\zeta(95)$	-0.36	0.20	0.08	-0.75
	$N_{GPS}-N(90)$	-0.93	0.28	-0.30	-1.28
	$N_{GPS}-N(OSU91A)$	-0.63	0.45	0.09	-1.48
Sardinia n=29	$N_{GPS}-\zeta(95)$	-1.13	0.18	-0.61	-1.55
	$N_{GPS}-N(90)$	-1.25	0.37	-0.10	-1.76
	$N_{GPS}-N(OSU91A)$	-0.74	0.30	-0.25	-1.40

Table 2: N_{GPS} versus geopotential models.

The statistics show that a good fit between ITALGEO95 and GPS/leveling has been reached. The standard deviations of the differences are quite homogeneous all over Italy and improve in each case both with respect to OSU91A geoid (as expected) and ITALGEO90.
However, the result of the comparison with the Adriatic geotraverse is quite poor and this reveals the existence of some unsolved problems.

Firstly, it must be taken into account that we compared a quasigeoid and GPS/leveling data which are geoid heights. This can induce distortions especially in areas where a relevant topography is present. Then, it must be mentioned that this is the oldest GPS campaign in Italy and that those data are not so reliable as the remaining GPS measurements. In addition to the previous comments, it is to stress that probably also the geopotential estimation procedure can give problems in areas where a rough geopotential field is present. Infact, a closer inspection of the plot of the differences along the geotraverse (see Fig. 5.) allows to identify two main "domains" which are homogeneous. If we consider separately the sets of differences from point (A) to point (B) and from point (C) to the end, we have statistics which are close to the ones in Tab. 2; in fact from (A) to (B) we have σ=22 cm and from (C) to the end σ=20 cm. We think that this behaviour can be explained taking into account the particular feature of the geopotential field along this geotraverse.
From the northernmost point to point (A) we have a strong geoid variation, which amounts to 13 m in 250 km; then the geotraverse proceeds to south nearly along an isoline of the quasigeoid to point (B). From point (B) to point (C) we again have a strong field variation, 4 m in 100 km.
Finally, in the last part of the geotraverse, we are still along a contour line of the quasigeoid and consequently we have a good fit between ITALGEO95 and GPS/leveling data.
So, the critical points along the geotraverse are connected to strong geoid variations; this probably has to do with global geopotential model distortions occuring in such areas which the remove-restore method cannot compensate properly.

5. Conclusions

The new Italian quasigeoid, computed via remove - restore technique and Fast Collocation, provided a reliable geopotential field estimation over the area $36° \leq \varphi \leq 47°$, $6° \leq \lambda \leq 19°$. This estimate has been tested via comparisons with GPS/leveling measurements which cover Italy quite homogeneously.
The mean value of the standard deviations is of 15 cm if the Adriatic geotraverse is excluded. This data set seems to indicate that mismodellings are still present; further researches are needed to clarify the reasons of such a high discrepancy (σ=54 cm) between the quasigeoid and these GPS/leveling measurements. Furthermore, in the near future, comparisons will be carried out with altimetry to test the effectiveness of the quasigeoid in the seas surrounding Italy.

Acknowledgments

The authors wish to thank all the Italian research groups and institutions which supplied the GPS/leveling data sets that have been used in the comparisons.

References

V. Achilli, M. Anzidei, P. Baldi, M. Bacchetti A. Banni, V. Barrile, C. Bonini, P. Briole, F. Campolo, G. Capone, A. Capra, G. Casula, M. Crespi, R. De Marco, S. Di Filippo, D. Dominici, A. Fotiou, C. Gasparini, L. Giovani, I. Guerra, F. Jacop, M.C. Jannuzzi, E. Livieratos, A. Maramai, C. Marchesini, M. Marchetti, P. Marsan, M. Marsella, S. Pondrelli, G. Puglisi, F. Quareni, F. Radicioni, F. Riguzzi, C. Rondoni, G. Salemi, A. Stoppini, A. Souriau, L. Surace, M. Vecchi, F. Vespe, A. Vettore, F. Vodopivec, 1991. *"Tyrgeonet: campagna GPS 1991"*. Proceedings of 10th annual Meeting of GNGTS, CNR, Rome, November 6th-8th, 1991.

S. Asili, A. Banni, E. Falchi, F. Resta, G. Sanna, 1995. *"Determinazione dello scostamento tra geoide ed ellissoide WGS84 in Sardegna"*. Presented at the 14th Annual Meeting of GNGTS, CNR, Rome, October 23rd-25th, 1995.

R. Barzaghi, M. Brovelli, F. Sansò, C. C. Tscherning, 1992. *"Geoid computation in the Mediterranean Area"*. Mare Nostrum, Geomed Report n. 1. DIIAR - Politecnico di Milano.

B. Benciolini, A. Manzino, D. Sguerso, 1991. *"ITALGEO90: risultati globali, validazioni e confronti"*.

G. Birardi, 1993. *"The Italian North-South GPS traverse and a proposal for a "first order" Italian geoidal net"*. Bulletin Geodesique, vol. 67, n. 4.

G. Bottoni, R. Barzaghi, 1993. *"Fast Collocation"*. Bulletin Geodesique, vol. 67., n. 2.

M.T. Carrozzo, A. Chiarenti, M. Giada, D. Luzzo, C. Margiotta, D. Maglietta, M. Pedone, T. Quartu, F. Zuanni, 1982. *"Data bases of mean height values and gravity values"*. Proceedings of the 2nd International Symposium on the Geoid in Europe and Mediterranean Area.

R. Forsberg, 1994. *"Terrain effects in geoid computations"*. Lecture Notes of the International School for the Determination and Use of the Geoid. IGeS, DIIAR - Politecnico di Milano.

C. Morelli, 1970. *"Physiography, Gravity and Magnetism of the Tyrrhenian Sea"*. Bollettino di Geofisica teorica e applicata, XIII, pp. 275-309.

C. Morelli, M. Pisani, C. Gantar, 1975a. *"Geophysical Anomalies and Tectonics in the Western Mediterranean"*. Bollettino di Geofisica teorica e applicata, XVII, p. 67.

C. Morelli, C. Gantar, M. Pisani, 1975b. *"Bathymetry, gravity and magnetism in the Strait of Sicily and the Jonian Sea"*. Bollettino di Geofisica teorica e applicata, XVII, pp. 39-58.

R.H. Rapp, 1994. *"The use of geopotential coefficients models in computing geoid undulations"*. Lecture Notes of the International School for the Determination and Use of the Geoid. IGeS, DIIAR - Politecnico di Milano.

L. Surace, 1993. *"Il progetto IGM95"*. Bollettino di Geodesia e Scienze Affini, n. 3.

C.C. Tscherning, 1994. *"Geoid determination by least-squares collocation using GRAVSOFT"*. Lecture Notes of the International School for the Determination and Use of the Geoid. IGeS, DIIAR - Politecnico di Milano.

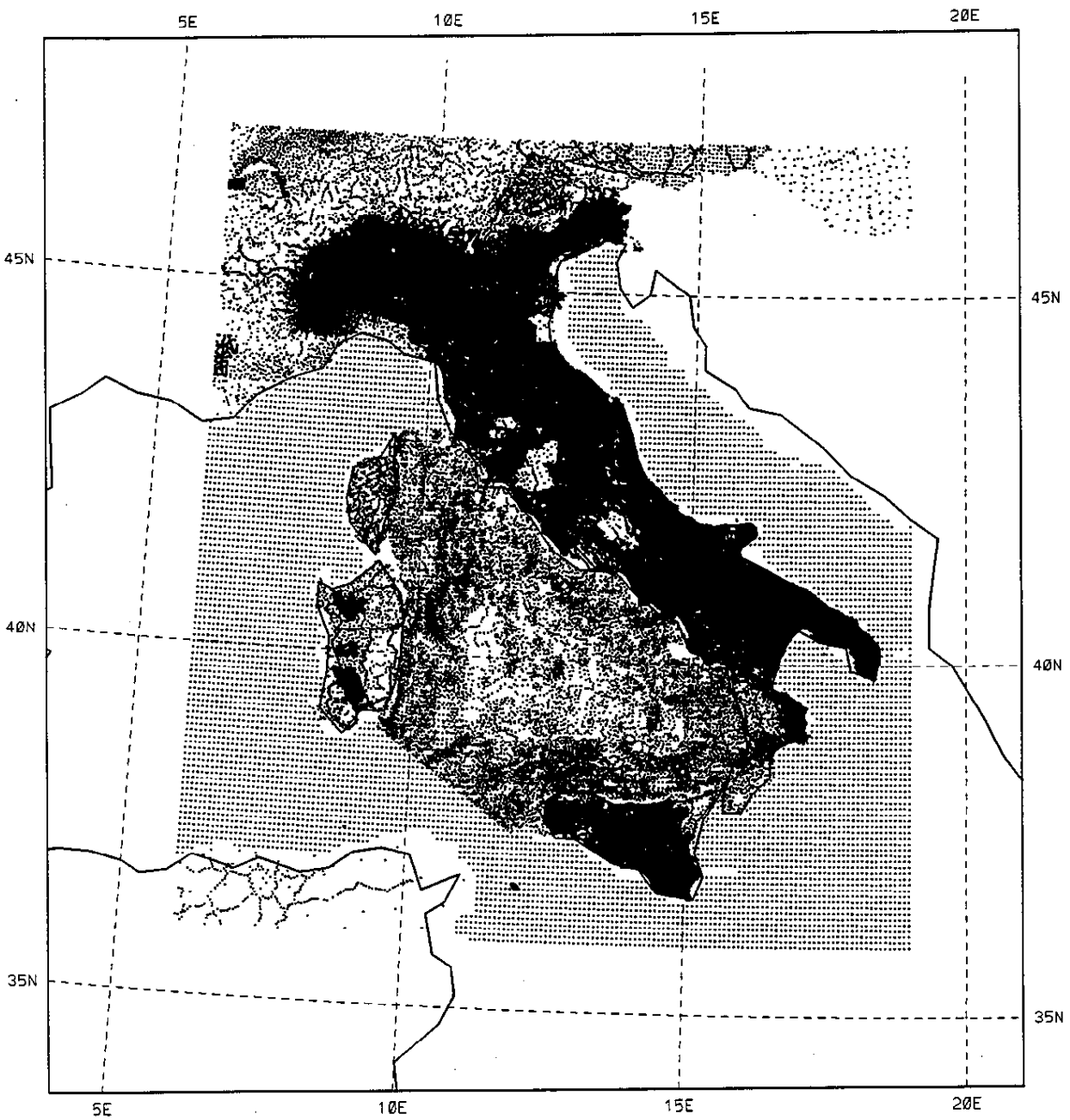

Fig. 1: The gravity data base

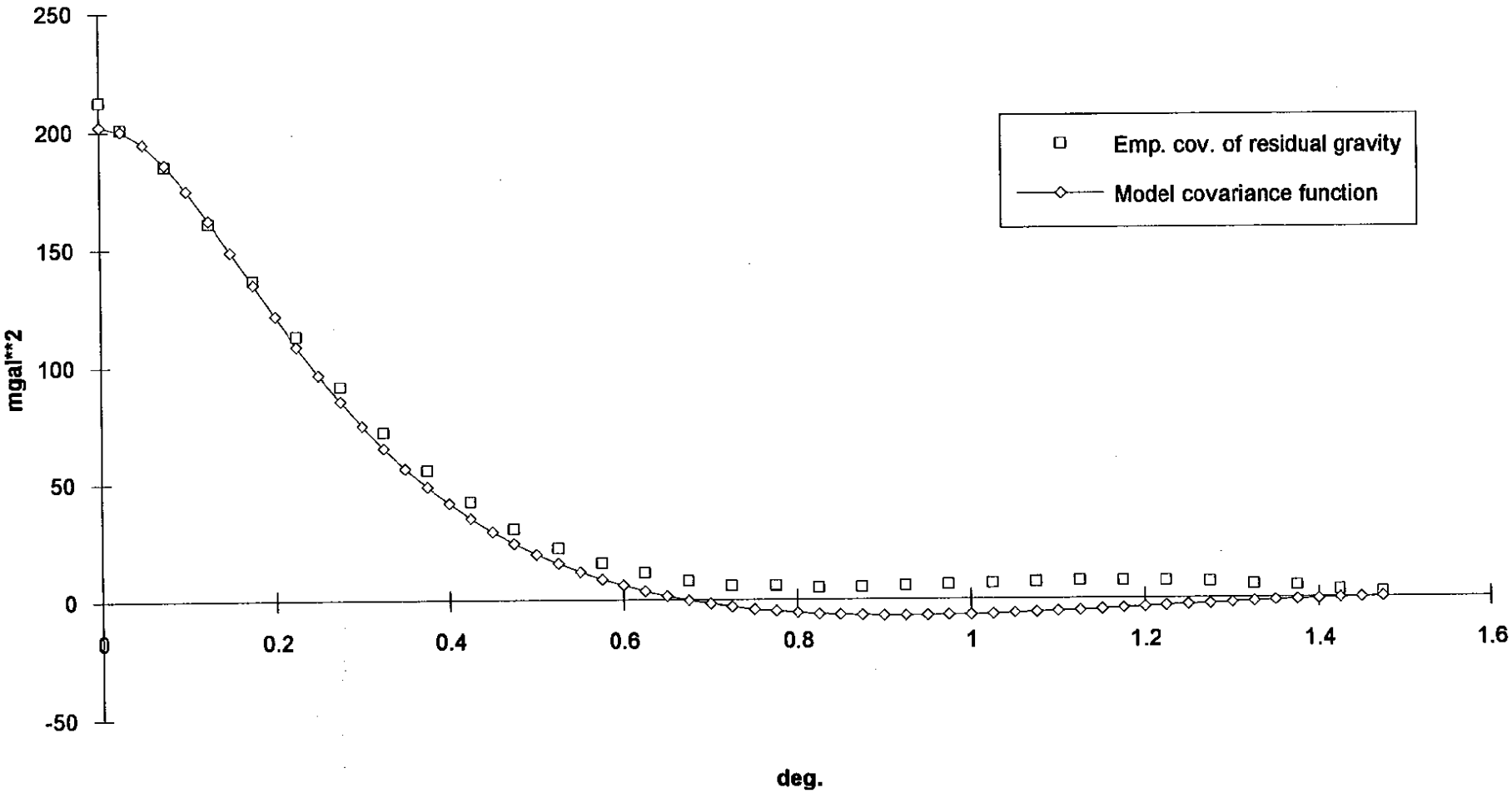

Fig. 2: The empirical and the model covariance functions of residual gravity

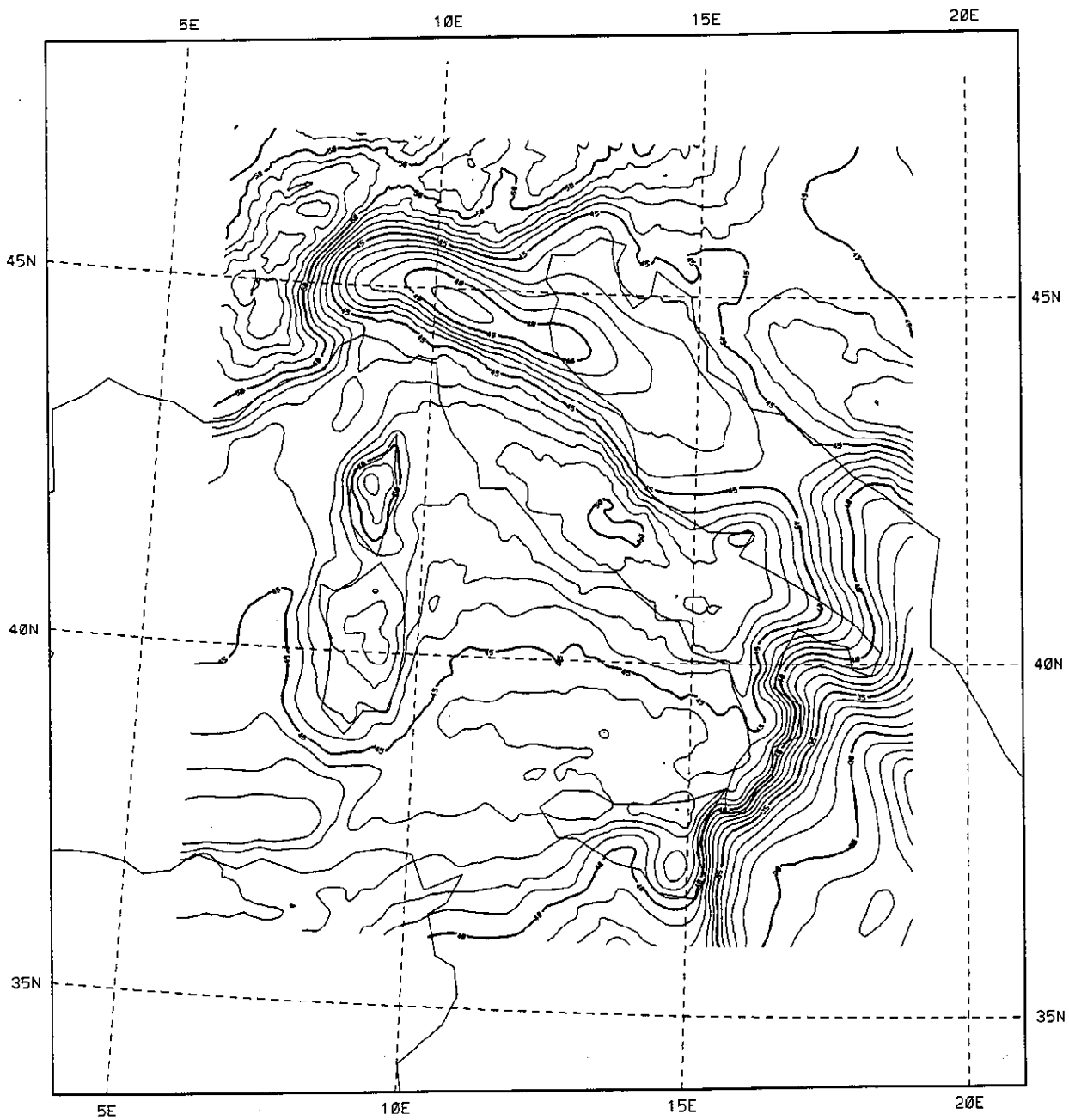

Fig. 3: The Italian quasigeoid ITALGE095

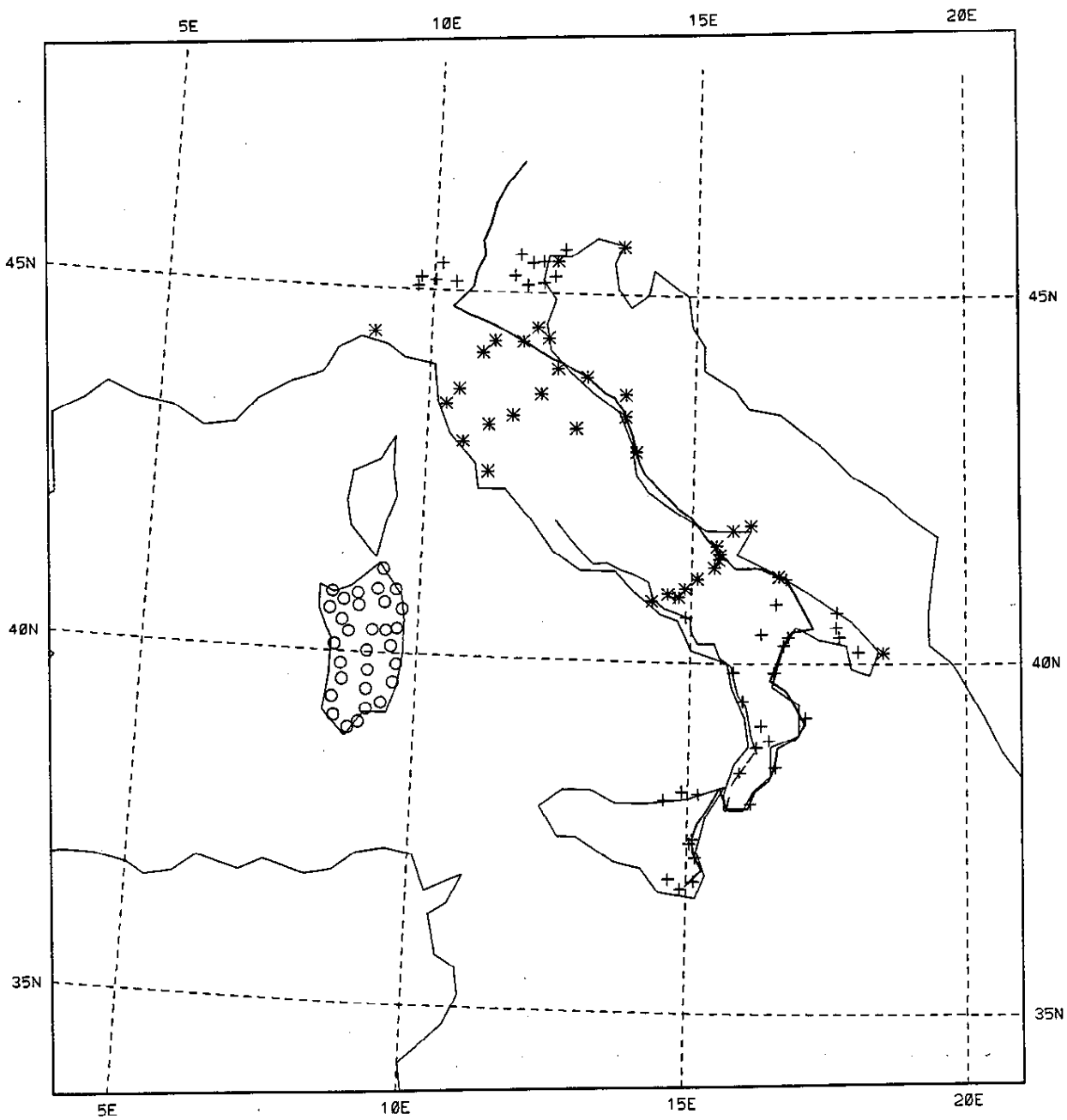

Fig. 4: GPS data
- geotraverse
* TYRGEONET
+ IGMI
° University of Cagliari

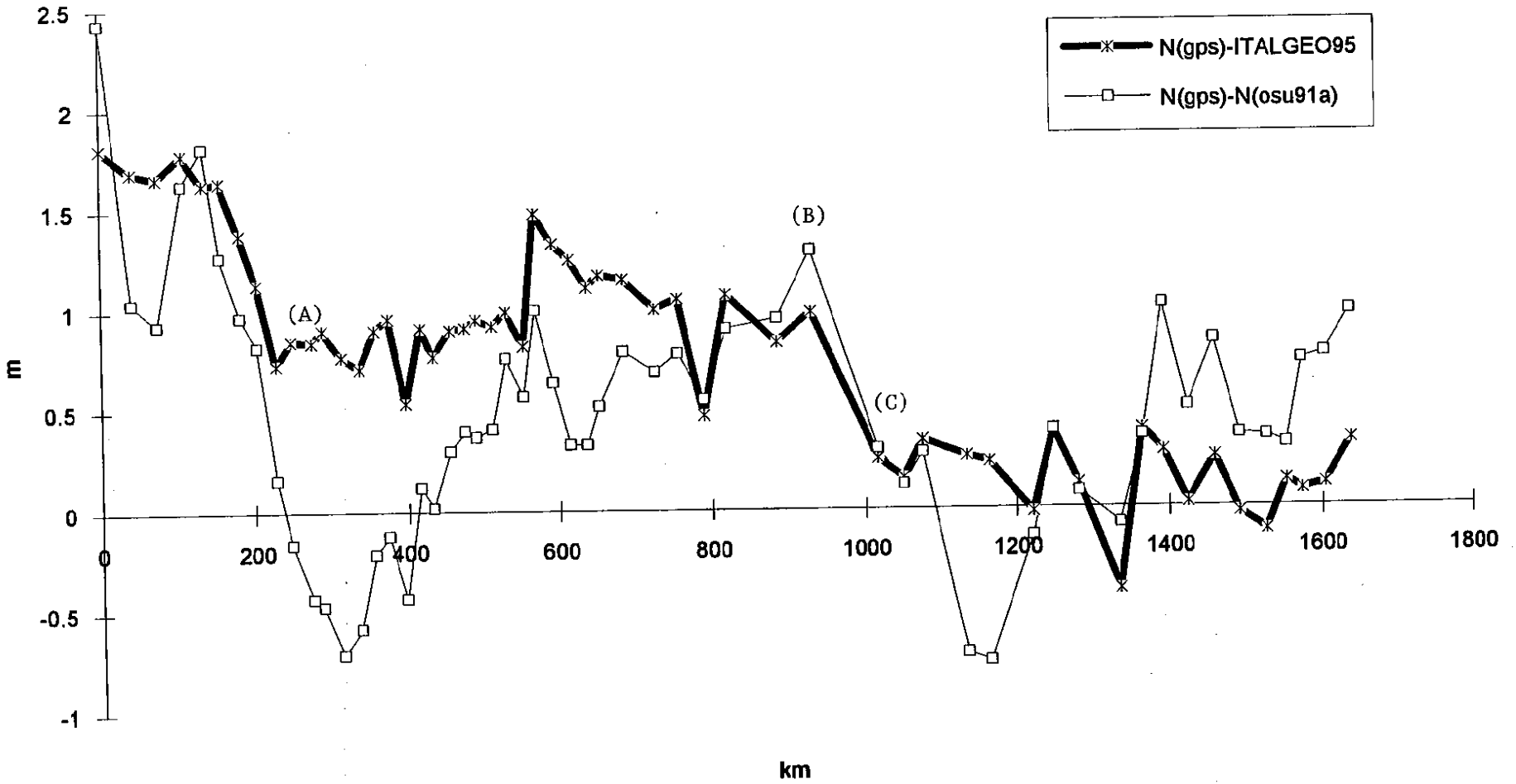

Fig. 5: Residual along the Adriatic geotraverse

Gravimetric Geoid for Poland Area Using Spherical FFT

Adam Łyszkowicz
Department of Planetary Geodesy, Space Research Centre
Bartycka 18A, 00-716 Warsaw, Poland

Rene Forsberg
Geodetic Division, National Survey and Cadastre
Rentemestervej 8, DK-2400 Copenhagen NV, Denmark

1. Introduction

In 1961 an astro-gravimetric determination of the geoid for the area of Poland was performed by Bokun at the Institute of Geodesy and Cartography in Warsaw (Bokun,1961). The densification of Polish horizontal network enabled preparation second (in 1970) and third (in 1978) version of the astro-gravimetric geoid. The resolution of this astro-gravimetric solution is about 20 km and the relative accuracy was estimated to ± 65 cm.

At present demands on gravity field determination have increased, mainly through the advent of the Global Positioning System, providing three-dimensional relative positioning with cm accuracy, even over longer distances. In order to transform the purely geometrically defined ellipsoidal heights from GPS into heights related to the earth's gravity field, that are needed by most users, it is necessary to know the corresponding height reference surface (geoid resp. quasigeoid) with an accuracy comparable to that of GPS and levelling, which is in order of a few cm/100 km resp. dm/1000 km.

In order to achieve the geoid at this level of accuracy, high resolution point or mean gravity field data with an average spacing resp. block size « 10 km is needed, as e.g. gravity data and topographic information. The first gravimetric geoid for the territory of Poland computed by the collocation-integral method (Łyszkowicz,1993) comprised about 6000 mean free-air gravity anomalies. In second gravimetric solution (Łyszkowicz and Denker,1994) new gravity data (about 8000 mean anomalies) and topographic information from Poland territory were included. In this paper a new attempt is made towards a detail geoid and quasigeoid determinations for the Poland territory. For this purpose, high resolution mean gravity data with the spacing 2 km x 2 km have been made available for the whole area of Poland. The computations were carried out using integral formulas evaluated by spherical Fast Fourier Transforms (FFT). Although gravity field variation can be modelled with the desire accuracy from sufficiently dense and accurate gravity and topography data, the solution presented in the following is suffering from lacking gravity data in some parts of neighbouring counties (Byelorussia) and the Baltic Sea.

The final results geoid and quasigeoid are presented in form of a contour line map, and also in computer applicable form by FORTRAN subroutine in connection with an input grid file. The grid files contain geoid/quasigeoid heights for a grid with mesh size 1.5' x 3.0'.

2. Computational method

The computation of the new gravimetric geoid for Poland (geoid94) combining a geopotential model (GM), mean free-air gravity anomalies Δg_F, and heights H in a digital terrain model, was based on the following formulas:

$$N = N_{GM} + N_{\Delta g} + N_H \tag{1}$$

$$\Delta g = \Delta g_F - \Delta g_{GM} - \Delta g_H \tag{2}$$

The GM part of Δg and N was obtained by the spherical harmonic representation of the anomalous gravity field.

The medium and high frequencies were obtained by Stokes' integral equation with terrain corrected mean gravity anomalies on a 1.5' x 3' grid:

$$N_{\Delta g} = \frac{R}{4\pi G}\iint_E \Delta g \; S(\psi) d\sigma \tag{3}$$

where $S(\psi)$ is Stokes' function and E is the area of integration. The two dimensional multi-band Fast Fourier Transform (FFT) technique (Forsberg and Sideris, 1993) was used. which allows the evaluation of the spherical Stokes integral without approximations, relating to flat-earth postulate. Proper zero padding (100%) was applied to the gridded data to eliminate the effects of circular convolution.

Since Stokes' formula is valid for Δg on the geoid, all masses above it must be mathematically shifted inside the geoid via terrain reduction. The computation of Δg_H accounts, for this shift through a Helmert reduction, i.e. condensation of the topographic masses on the geoid. The term N_H in equation (1) is called the indirect effect on the geoid and accounts for the change of equipotential surfaces after a terrain reduction is applied to Δg. In flat areas these effects might be negligible, but in the Polish mountains they may reach 15 cm. Helmert's condensation to first order was used, and the geoid term was computed from heights on a 1.5' x 3.0' digital terrain model using the following equations:

$$\Delta g_H = c \tag{4}$$

$$N_H = -\frac{\pi G \varrho H^2}{\gamma} \tag{5}$$

where c is the classical terrain correction, G is Newton's gravitational constant; ϱ is the density of the topographic masses, assumed constant.

In practice the free-air anomalies Δg_F were obtained by gridding terrain - corrected Bouguer anomalies, and applying the linear height term for restoring mean free-air anomalies i.e. producing mean Faye anomalies.

In Poland the national height system is based on normal heights and therefore a national "geoid" should be a quasi-geoid rather than geoid. The classical dilemma in determining the "physical" geoid height N is that a knowledge of the density of the topographic masses above the geoid is required. The same problem occurs in the definition of the orthometric height. The basic observable in geodetic levelling is the geopotential number C at a surface, with practical formulas for orthometric and normal heights

$$H_{Helmert} = \frac{C}{\bar{g}} \approx \frac{C}{g + 0.0424\, H} \tag{6}$$

$$H^* = \frac{C}{\bar{\gamma}} = \frac{C}{\gamma_o - 0.1543\, H^*} \tag{7}$$

where $H_{Helmert}$ are the classical orthometric heights build on an assumption of a constant density 2.67 g/cm^3, using Bouguer plates to estimate the mean gravity value inside the earth, and H^* is the normal height. It is simple at the above approximation level to convert between geoid and quasigeoid. For a point P at the surface of topography equations (6) and (7) results in the simple formula

$$\zeta - N = H_{Helmert} - H^* = \frac{g - \gamma_o + 0.1967\, H}{\gamma_o} H = \frac{\Delta g_B}{\gamma_o} H \tag{8}$$

where Δg_B is the Bouguer anomaly.

3. Used data

3.3. Geopotential model

One of the most important kinds of information for gravity field approximation today is a good reference field supplied by a geopotential model. By subtracting the reference field information from the observations, the prediction based on the residual observation is of improved accuracy. This is particularly true for the fast Fourier transform method. From the numerical computation point of view, it may reduce the leakage error caused by the existence of long wavelength parts which cannot be resolved using only gravity data of limited extent.

For the determination of the long wavelength part of the earth's gravity field various models are now available. From the existing OSU higher degree geopotential solution, we chose to use the OSU91A model (Rapp and Pavlis,1990).

3.2. Topographic data

For the computation of terrain reductions, 0.5' x 0.5' mean elevations elaborated in Department of Planetary Geodesy (Łyszkowicz, 1994) are available for the area of Poland. Additionally 5' x 7.5' mean elevations are available for the territory of Czech Republic, Slovak Republic, Hungary, Romania and Western Ukraine The mean 5' x 5' heights from ETOPO5 model were used for the areas without any elevations. All elevations data have been carefully checked for gross errors by visual check of plotted test contour line maps. From the existing data set a new 1.5' x 3.0' mean elevation grid was created by bilinear interpolation for the territory $45^o < \varphi < 75^o$ and $0^o < \lambda < 35^o$.

Table 1. Description of gravity anomalies sources

Gravity data set	Description	Number	Normal gravity	Gravity reference system	Vertical reference system	Horizontal reference system
1	mean 5' x 7.5' from Czech and Slovak	1402	GRS80	IGSN71	Baltic	S-JTSK
2	Polish terrestrial mean 2 x 2 km	78 401	Helmert	Potsdam	Baltic	Borowa Góra
3	mean 5'x 7.5' from Romania	2770	Cassini	IGSN71	Baltic	?
4	mean and point gravity data from the southern Scandinavia	27993	GRS80	IGSN71	DNN	ED50
5	mean 5' x 5' from Germany and Austria	2763	GRS80	IGSN71	DHHN	ED50
6	mean 5'x 7.5' from Western Ukraine	768	GRS80	Potsdam	Baltic	?
7	mean 5'x 7.5' from Hungary	1147	Cassini	Potsdam	EOMA	HD-72
8	mean 1'x 1' for southern part of Baltic Sea	14 981	Helmert	Potsdam	Baltic	Borowa Góra

3.3. Gravity data

For the determination of gravimetric geoid or quasigeoid and gravimetric vertical deflections in the Poland area, high resolution point free-air and mean gravity anomalies have been collected in Department of Planetary Geodesy until October 1994 in the region $47^o < \varphi < 57^o$ and $11^o < \lambda < 26^o$ from the following institutions:

1) Research Institute of Geodesy, Topography and Cartography, Prague
2) Institute of Geodesy and Cartography, Warsaw
3) Institute of Geodesy and Geophysics, Bucharest
4) National Survey and Cadastre, Geodetic Division, Copenhagen
5) Institute für Erdmessung, Hannover
6) Lviv Technical University, Faculty of Geodesy, Lviv
7) Institute of Geodesy, Cartography and Remote Sensing, Budapest
8) Department of Planetary Geodesy, Space Research Centre, Warsaw.

Gravity data anomalies given in table 1 are not uniform and several corrections were introduced. In our study we introduced to the gravity anomalies the correction for the gravity formula differences, the gravity system differences and the atmospheric corrections. Subtracting the reference anomalies computed from the geopotential model OSU91A the residual anomalies were calculated by

$$\Delta g_{res} = \Delta g_F + \Delta g_A + tc - \Delta g_{ref} + \Delta g_{formula} \qquad (9)$$

where Δg_{res} is the reduced free-air anomaly, Δg_A is the correction for the atmospheric effect, tc is terrain correction, Δg_{ref} is reference anomaly and $\Delta g_{formula}$ is correction for the gravity formula differences.

4. Practical results

For the FFT computations the gravity data had to be gridded. This was done using a fast collocation prediction procedure (KMS GEOGRID program) with an internal search algorithm utilizing only 4 closest points in each quadrant around the prediction point. The reduced gravity data (Fig. 1) were gridded in 1.5' x 3.0' grid for the area $47^o < \varphi < 57^o$ and $11^o < \lambda < 26^o$, using point data and mean values. Table 2 gives the statistics about the source, residual and gridded residual anomalies in the considered area. The gravimetric geoid computation was performed in one step for the entire area yielding a 300 x 400 grid for FFT excluding zero-padding.

Table 2. Statistics of the source, residual and gridded (1.5' x 3.0') residual anomalies (in mGal)

anomalies	number	mean	stand. dev.	min.	max.
source	130226	1.07	19.27	-72.67	159.15
residual	130226	-0.20	9.82	-86.67	102.82
gridded res.	120000	-0.07	12.55	-85.48	95.17

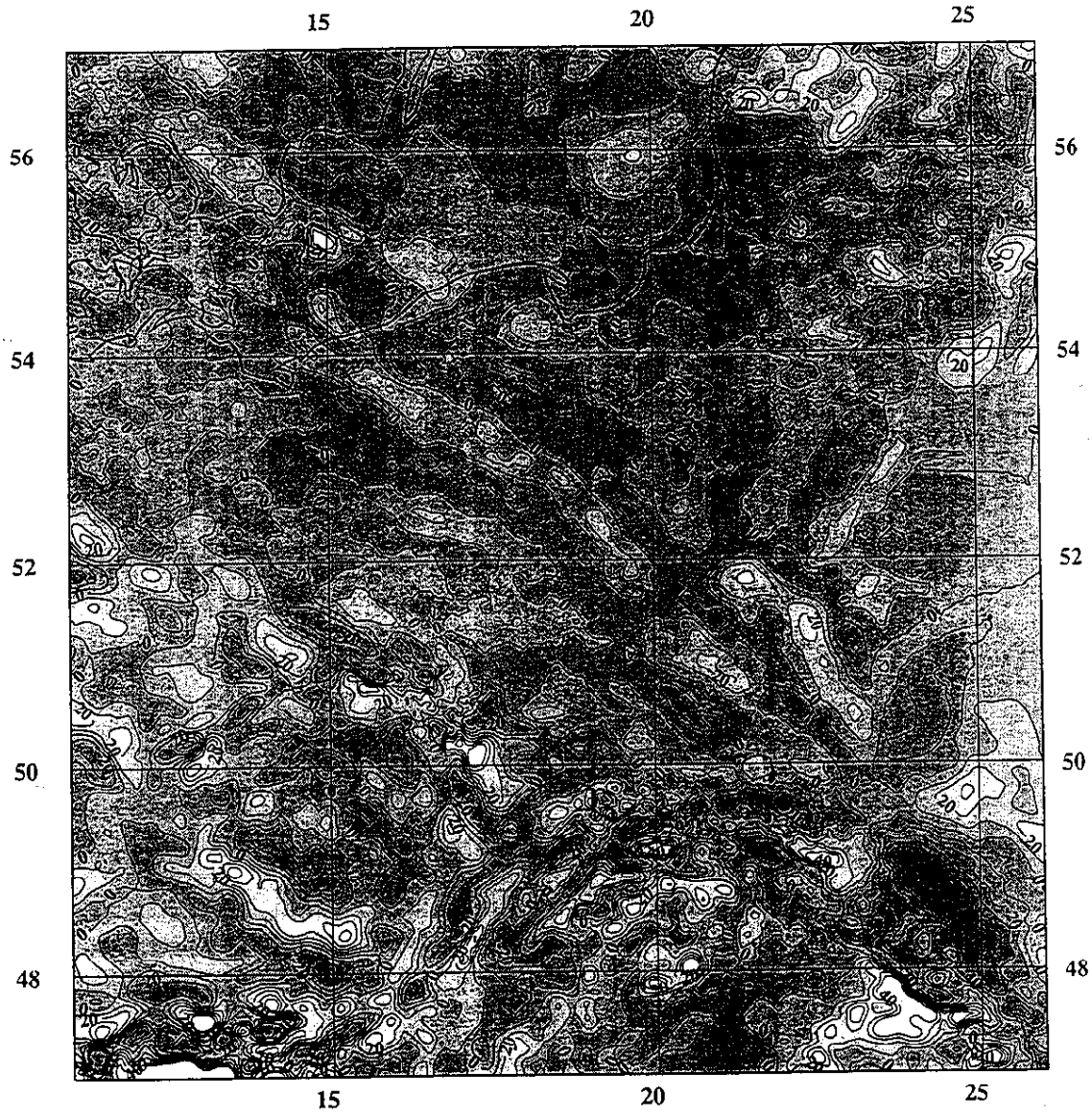

Figure 1. Reduced free-air gravity anomalies (contour interval 10 mGal)

The geoid indirect effect was computed using equation (5) with the grid mesh 1.5' x 3.0'. The indirect geoid effect is significant only in a few mountainous areas where it reaches values from one to a few decimeters. On the remaining territory it is on the level of a few millimetres. Final geoid undulations (solution #1) were computed by adding the contributions from the geopotential model OSU91A from the gravity data and from the topography. Then computed geoid was converted to quasigeoid (solution #2), using the Bouguer anomaly approximation. The geoid - quasigeoid corrections are significant only in few mountainous areas where they attain values from one to few decimeters. Table 3 gives the statistics of the reference, residual and final geoid/quasigeoid solutions.

The final result is presented in a form of contour map (Fig. 2) and also in digital form by the computed geoid/quasigeoid heights for a regular grid with a mesh size 1.5' x 3.0'. Totally, 120 000 geoid/quasigeoid heights are stored in grid files, from which geoid/quasigeoid heights and deflections of the vertical can be computed for stations with given latitude and longitude using subroutine GEOIP.

Table 3. Statistics of the reference, residual (computed by FFT), and final geoid undulations (in meters)

geoid	mean	stand. dev.	min.	max.
reference	35.98	7.14	21.04	51.08
residual	-0.05	0.45	-3.40	1.21
final #1	35.93	7.21	21.24	51.54
final #2	35.91	7.19	21.24	50.77

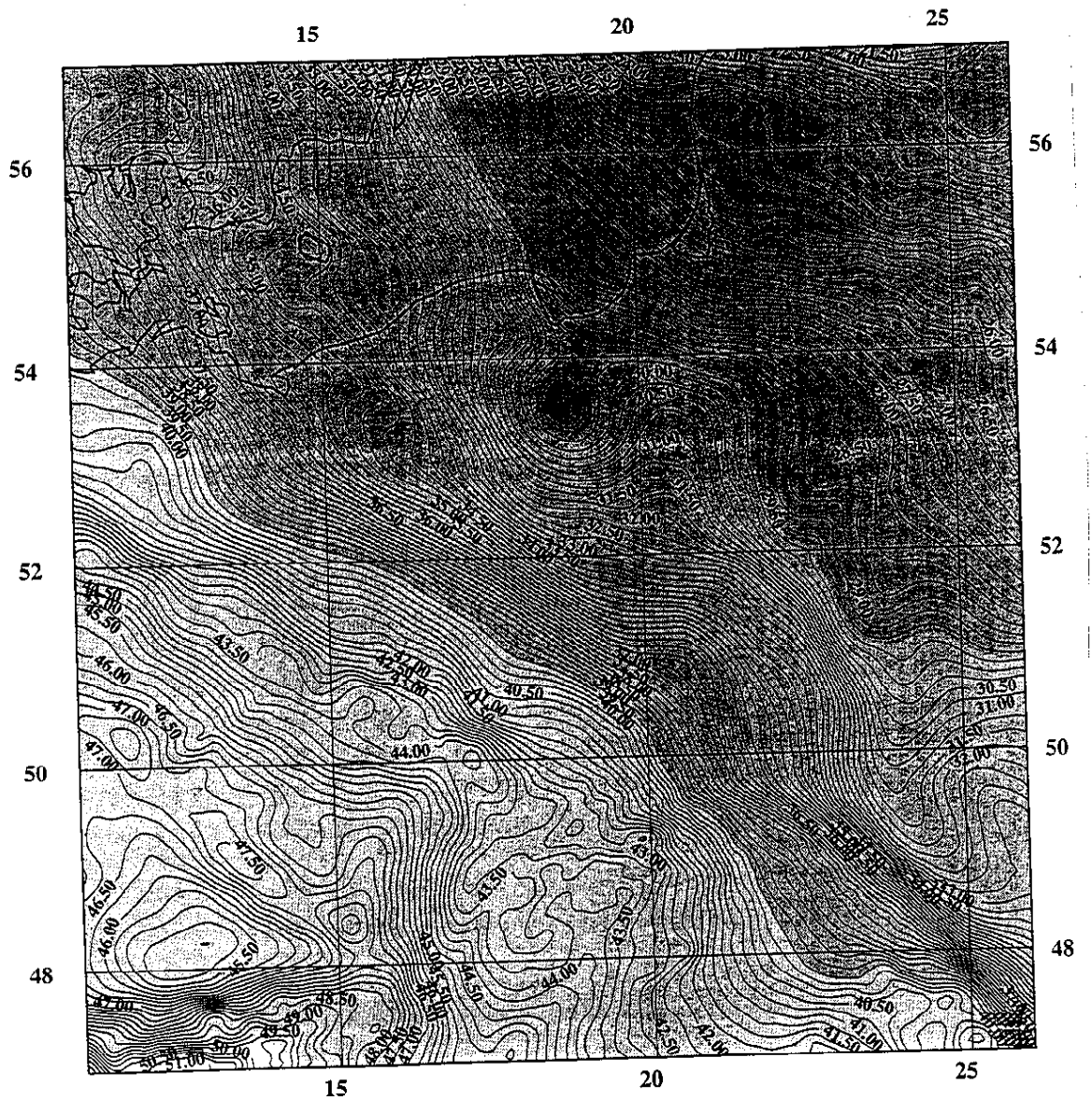

Figure 2. Final spherical FFT geoid solution, reference system GRS80

Table 4. Comparison of GPS/levelling results to gravimetric quasigeoidal heights (in meters).

	pts	mean	stand. dev.	min.	max.
before fit	13	-0.31	0.15	-0.49	0.01
after 4-par fit	13	0.00	0.06	-0.11	0.11

To evaluate the absolute accuracy of the quasigeoid , data from EUREF-POL (Zieliński et al., 1994) and Baltic Sea Level Project (Zdunek,1994) GPS networks together with levelling data were used to derive the geoidal undulations for comparison with the gravimetric quasigeoidal heights. The computed ellipsoidal heigths were referred to WGS84 ellipsoid and their standard deviations do not exceed ± 3 cm.

All GPS stations have been connected to the national levelling network, which consists of normal heigths. The connection of the GPS stations to the levelling network has been carried out by spirit levelling to a nearby benchmark. The accuracy of the levelling heigths may be estimated to about 2...6 cm depending on the type of connection measurements. So we can expect an accuracy of the GPS derived quasigeoid heigths of the order of ± 6 cm.

To minimize the long wavelength errors, the systematic datum differences between the gravimetric geoid and the GPS/levelling data were removed by the following four parameter transformation equation:

$$N' = N + b_o + b_1 \cos\varphi \cos\lambda + b_2 \cos\varphi \sin\lambda + b_3 \sin\varphi \qquad (10)$$

where b_o is the shift parameter between the vertical datum implied by the GPS/levelling data and the gravimetric datum, and b_1, b_2 and b_3 are the three translation parameters in x, y, z axes between the coordinate system implied by the GPS data and the one implied by the gravimetric data.

The statistics of the absolute differences between the two types of quasigeoidal heights are summarized in table 4. The comparison of the gravimetric solution with GPS/levelling derived quasigeoid heights shows bias -31 cm and standard deviation of ± 15 cm. The use of the four parameter datum shift fit eliminates the possible tilt of the gravimetric geoid as well, yielding geoid fit at only ± 6 cm which is consistent with the accuracy of GPS/levelling derived heights.

Acknowledgements

The work was sponsored by the research contract of Komitet Badań Naukowych, grant S60501404.

References

Bokun J., 1961, Astro-gravimetric Geoid Determination Referred to Krasovsky's ellipsoid in the Area of Poland (in Polish), Proceedings of the Institute of Geodesy and Cartography, vol. VIII, z.1

Forsberg R., Sideris M.G., 1993, Geoid computations by the multi-band spherical FFT approach, Manuscripta Geodaetica, 18, pp. 82-90

Łyszkowicz A., 1993, The Geoid for the Area of Poland, Artificial Satellites, Planetary Geodesy No 19, vol. 28 No 2

Łyszkowicz A. Denker H., 1994, Computation of a Gravimetric Geoid for Poland Using FFT, Artificial Satellites, Planetary Geodesy No 21, vol. 29 No 1

Łyszkowicz A., 1994, Opis algorytmu badania geoidy na obszarze Polski, dane grawimetryczne i wysokościowe, grawimetryczna baza danych GRAVBASE ver. 1.0, Report No 11, Polish Academy of Sciences, Space Research Centre, Warsaw

Rapp R.H. , Pavlis N.K., 1990, The Development and Analysis of Geopotential Coefficients Models to Spherical Harmonic Degree 360, Journal of Geophysical Research, vol. 95, no B13, pp. 21885-21911

Zdunek R., 1994, Baltic Sea Level Project - National Report, Baltic Sea Level Workshop, Dresden, 9 - 10 Sept.

Zieliński J.B. ,Jaworski L. ,Zdunek R., Seeger H. ,Engelhardt G. ,Töppe F. ,Luthardt J. ,1994, Final Report about EUREF-POL 1992 GPS Campaign, Symposium of the IAG Subcommission for the EUREF, Warsaw, Poland

A NEW GRAVIMETRIC GEOID IN THE IBERIAN PENINSULA

M.J. Sevilla

Instituto de Astronomía y Geodesia (UCM-CSIC).
Facultad de Ciencias Matemáticas.
Universidad Complutense. 28040 MADRID. SPAIN

ABSTRACT

A new high precision gravimetric determination of the geoid of the Iberian Peninsula has been made, using the following data types: a) a global geopotential model, namely the OSU91A spherical harmonic coefficients set, b) a set of 186813 point free air gravity anomalies covering the Iberian Peninsula and surrounding regions, including recent new data, and c) a 1000x1000 meters digital terrain model for Spain and the ETOPO5U for the rest of the area.

The method used for the computations was the Stokes' integral in convolution form. The input data were gridded gravity anomalies. To evaluate the integral, the Fast Fourier Transform and Fast Hartley Transform techniques were applied. Discrete spectra of the kernel function is used. 100 % zero padding was appended around the signal matrix to avoid circular convolution effects. The terrain correction was applied to the data and the corresponding indirect effect was taken into account.

The geoid computed has been compared to geoid undulations obtained by GPS/Levelling, and a precision of 1.0 ppm has been obtained. The results, corresponding to the 1D-FFT solution, in the GRS80 system, are presented in form of contour maps.

1. INTRODUCTION

Geoid determination is a major problem of Physical Geodesy. Today the whole international geodetic and geophysical community is interested in this task and a great number of international workshops and symposiums on this topic are held. Recently into the International Association of Geodesy, the International Geoid Service has been created. The use of geoid related data, in particular its undulation, is widespread in all branches of the Geodesy and it is natural to find it in other Earth Sciences as in Geophysics, Oceanography etc., as well as in Civil Engineering.

The computation of the geoid over large areas is possible in the framework of international collaboration. In the Iberian Peninsula the collaboration between the "Instituto de Astronomía y Geodesia (UCM-CSIC)" at Madrid, the Spanish "Instituto Geográfico Nacional" and the "Instituto Portugues de Cartografia e Cadastro", in the frame of the IBERGEO Project, has made possible the accomplishment of the Iberian geoid. This collaboration has provided the most recent and precise gravimetric data and a modern digital terrain model.

The first determination of a preliminary geoid in a small zone in the center of Spain was made in 1991, using the least squares collocation (LSC) method (Sevilla et al., 1991a), and the first gravimetric geoid of Portugal, also with LSC, was computed in 1992 (Sevilla and Rodríguez-Velasco, 1993). The geoid of the center of Spain was refined in 1993 taking into account terrain effects (Gil et al., 1993). The first determination of a gravimetric geoid in the whole Iberian Peninsula was made last year (Sevilla, 1994).

Now, a new and detailed geoid has been computed in the Iberian Peninsula and surrounding regions, between the limits $35<\varphi<45$ for latitudes and $-10.5<\lambda<5.5$ for longitudes, in a grid with mesh sides of 2.17 and 2.67 kilometres in latitudes and longitudes direction, respectively. The geoid solution was computed based on the following data types: A) the geopotential model OSU91A spherical harmonic

coefficients set (Rapp et al., 1991), complete to degree and order 360, B) a set of 186813 point free-air gravity anomalies covering the Iberian Peninsula and the surrounding regions, the gravity data being corrected for atmospheric and terrain effects, and C) a 1000x1000 meters digital terrain model for Spain and the ETOPO5U revised for the rest of the area.

All data has been tested and validated. The LSC method has been applied systematically to predict free air gravity anomalies with validation purposes, using the spherical harmonic coefficient set OSU91A to reduce anomalies. Gross errors have been detected in 2% of the marine data and in 1% of the land data. The terrain effects have been taken into account by means of the remove-restore technique, and the Helmert's second condensation reduction has been used to reduce gravity anomalies. The indirect effect on the geoid has been considered in consequence.

The method used in the computations of the contribution of the local gravity data to the geoid was Stokes' integral in convolution form. The input data were fully reduced gridded gravity anomalies. To evaluate the Stokes' formula, three techniques were used: the first is the planar Fast Hartley Transform (FHT) (Tziavos, 1993a,b); the second is the spherical miltiband Fast Fourier Transform technique with 2D discrete FFT (Forsberg and Sideris, 1993) and the third is the spherical 1D-FFT technique (Haagmans et al., 1993), which allows the evaluation of the discrete spherical Stokes' integral without any approximation, parallel by parallel. In all computations discrete spectra of the kernel function is used. 100 % zero-padding was appended around the signal matrix in order to avoid circular convolution effects.

The final geoid was obtained by adding the contribution of the model and the contribution of the reduced gravity anomalies as well as the indirect effect. The various results have been analysed and compared. The definitive results, referred to the GRS80 system, are presented in a map covering the region contoured at 50 cm intervals. This map is constructed from the 262144 predicted geoid undulations. The geoidal height mean square error obtained by comparison with GPS undulations is almost everywhere less than 1 ppm.

2. GRAVITY ANOMALIES DATA BANK

A number of 186813 point free-air gravity anomalies (118423 marine and 68390 land data) in the area ($35<\varphi<45$, $-10.5<\lambda<5.5$) were used in the geoid computation. This data came from the sources shown in Table 1. The accuracy of these data ranges from 0.1 to 10 miligals due to the different sources used in the collection of initial data.

As the different files referred to different datums, in a first step datum transformations were performed to standardize all the data. The standardized data are referred to the Geodetic Reference System 1980 (Moritz, 1984) for theoretic gravity and to the International Gravity Standardization Net for the measured gravity. For details about the formulae used, see (Sevilla et al.,1991b).

Table 1. Source data bank

File Name	Points	Source
Iberired.dat	136	IGN First order gravity network
Spainiag.dat	27589	IAG-IGN Gravity survey of Spain
Spainign.dat	904	IGN Recent gravity data of Spain
Spainest.dat	2949	IGN Data of Gibraltar Strait
Portugal.dat	4327	IPCC Data from Portugal
Spaingmg.dat	4933	GEOMED Marine gravity anomalies
Iberdmam.dat	31494	DMA Marine data from DMA
Iberdmat.dat	32859	DMA Land data from DMA

File Name	Points	Source
Ibernoaa.dat	81996	NOAA Marine data from NOAA
Iberia.dat	186813	The whole set of gravity data

IGN: Instituto Geográfico Nacional (Spain), IAG: Instituto de Astronomía y Geodesia (Madrid), IPCC: Instituto Portugues de Cartografia e Cadastro (Portugal), GEOMED: International GEOMED Group (Milan), DMA: Defense Mapping Agency (USA), NOAA: National Oceanic and Atmospheric Administration (USA)

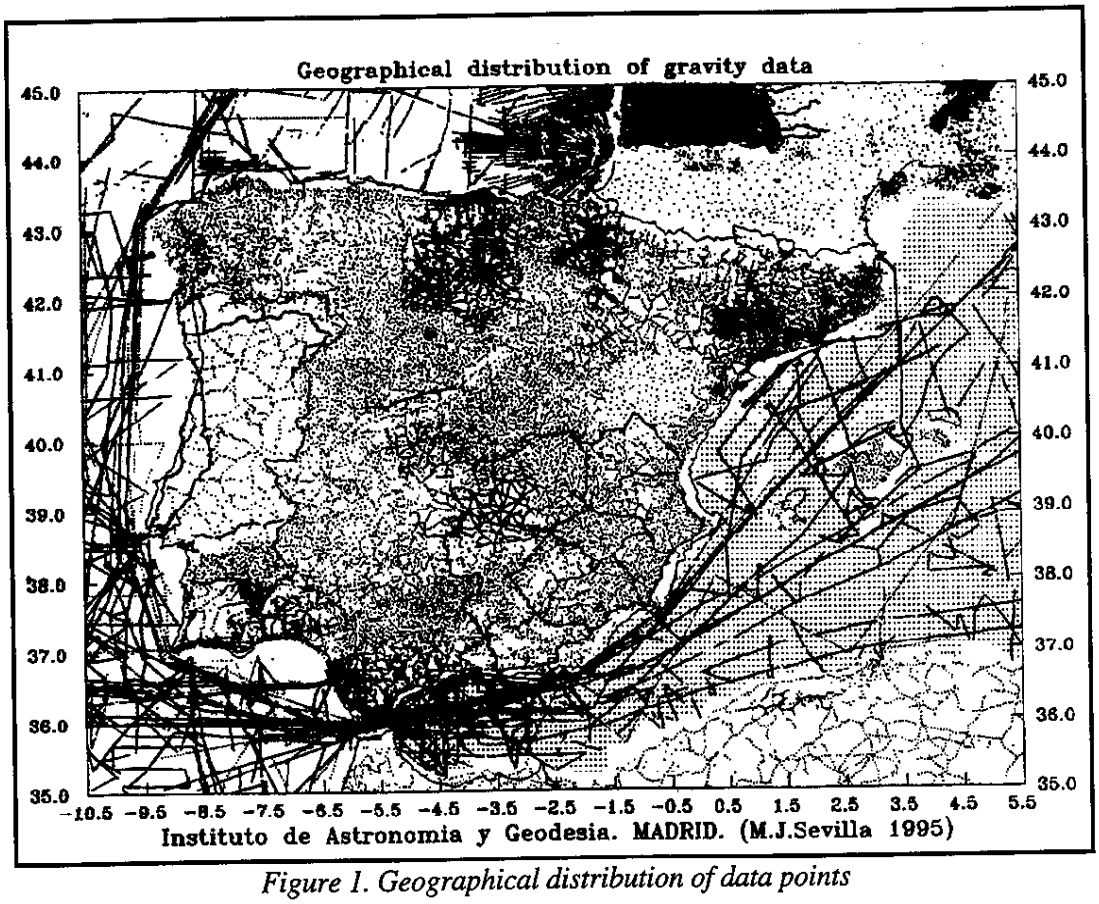

Figure 1. Geographical distribution of data points

To remove the atmospheric effect from the gravity anomalies a correction has been added to the free air gravity anomalies. This correction is given by the polynomial (Pavlis, 1991)

$$\delta g_A = 0.8658 - 9.727x10^{-5} H + 3.482x10^{-9} H^2 \quad \text{(mgal)}$$

where H is the orthometric height of the gravity station in meters. This function represents the tabulated values of IAG, 1971 (Moritz, 1984). The minimum and maximum values of the *atmospheric correction* are 0.61 and 0.87 mgals respectively.

All data sets have been checked carefully to remove repeated points, and validated for gross errors by applying different procedures (section 4). Figure 1 shows the geographical distribution of the available gravity data and Figure 2 shows a map of free air gravity anomalies contoured at 50 mgal interval.

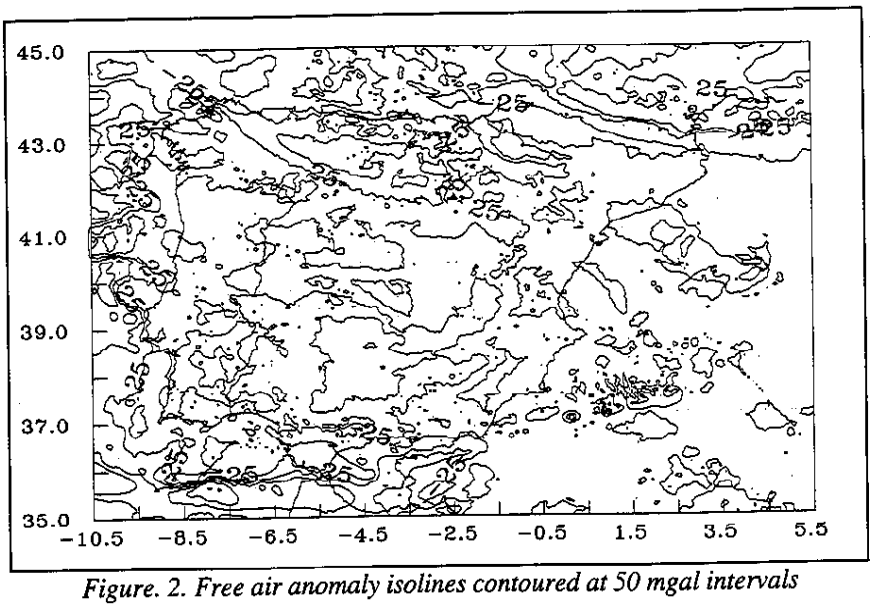

Figure. 2. Free air anomaly isolines contoured at 50 mgal intervals

3. GEOPOTENTIAL MODEL

The spherical harmonic representation of the Earth's gravity field W is (Heiskanen and Moritz 1967)

$$W(r,\vartheta,\lambda)=\frac{GM}{r}\{1+\sum_{n=1}^{\infty}(\frac{a}{r})^n\sum_{m=0}^{n}(C_{nm}\cos m\lambda+S_{nm}\sin m\lambda)P_{nm}(\cos\vartheta)\}+\Phi$$

where: r, θ, λ are the polar coordinates (geocentric radius, colatitude and longitude, respectively) of the point where W is to be determined, GM is the geocentric gravitational constant, a is the semi major axis of the reference ellipsoid, $P_{nm}(\cos\theta)$ are the fully normalized associated Legendre functions of the first kind, C_{nm}, S_{nm} are the fully normalized spherical harmonics coefficients of the Earth's gravitational field and Φ is the potential of the centrifugal force, $\Phi = (1/2)\,\omega^2 r^2 \sin\varphi$, ω being the angular velocity of the Earth's rotation.

The potential of a rotational reference ellipsoid is represented by the expansion

$$U(r,\vartheta)=\frac{GM'}{r}\{1+\sum_{n=1}^{\infty}(\frac{a}{r})^{2n}P_{2n}(\cos\vartheta)\}+\Phi$$

where M' is the mass of the reference ellipsoid. The standard representation of the disturbing potential is given by

$$T(r,\vartheta,\lambda)=W-U=\frac{GM}{r}\sum_{n=2}^{\infty}(\frac{a}{r})^n\sum_{m=0}^{n}(\Delta C_{nm}\cos m\lambda+\Delta S_{nm}\sin m\lambda)P_{nm}(\cos\vartheta)$$

where ΔC_{nm} and ΔS_{nm} are the differences between the coefficients of the geopotential and ellipsoid potentials (the difference M-M' is assumed to be small) and M' can be replaced by M.

Taking into account the boundary condition of the physical geodesy we get the following expansions: for *gravity anomalies*

$$\Delta g(r,\vartheta,\lambda)=\frac{GM}{r^2}\sum_{n=2}^{\infty}(n-1)(\frac{a}{r})^n\sum_{m=0}^{n}(\Delta C_{nm}\cos m\lambda+\Delta S_{nm}\sin m\lambda)P_{nm}(\cos\vartheta) \qquad (1)$$

and, with the Bruns equation, for *geoid undulation*

$$N(r,\vartheta,\lambda) = \frac{GM}{r\gamma}\sum_{n=2}^{\infty}\left(\frac{a}{r}\right)^n \sum_{m=0}^{n}(\Delta C_{nm}\cos m\lambda + \Delta S_{nms} sinm\lambda) P_{nm}(\cos\vartheta) \quad (2)$$

where γ is the normal gravity value at $P(r,\theta,\lambda)$. In practical works the index n runs up to the maximum degree of the model. These formulae can be evaluated by various techniques (Tscherning et al.,1983).

The *reduced anomalies* Δg_{red} are obtained by substracting the model gravity anomalies Δg_{mod}, computed by, (1) from the observed gravity anomalies Δg_{obs}

$$\Delta g_{red} = \Delta g_{obs} - \Delta g_{mod} \quad (3)$$

These anomalies reflect the local characteristics of the area because the long wavelengths have been eliminated.

The geopotential model OSU91A (Rapp et al, 1991) complete to degree and order 360 has been used to obtain the reduced free-air gravity anomalies (3) and the geoid model (2). This model fits well the anomalous gravity field of the area (Sevilla, 1994) (see Table 2). Figure 3 shows a map of free air minus model gravity anomalies contoured at 30 mgal interval. The residual anomalies and the geoid model have been computed using the GEOCOL10 program (Tscherning, 1995).

Table 2. Statistics of gravity data in the Iberian Peninsula area

	Mean	St. Dev	Minimum	Maximum	Range
Latitude	39.63	2.94	35.000	45.000	10.000
Longitude	-2.58	4.69	-10.500	5.500	16.000
Height	-167.11	917.82	-4984.0	2950.1	8020.1
Free-air	-1.32	40.93	-180.10	192.90	373.00
OSU91A	3.31	30.42	-114.72	89.67	204.39
Free air-OSU91A	-4.63	22.48	-116.32	173.66	289.98

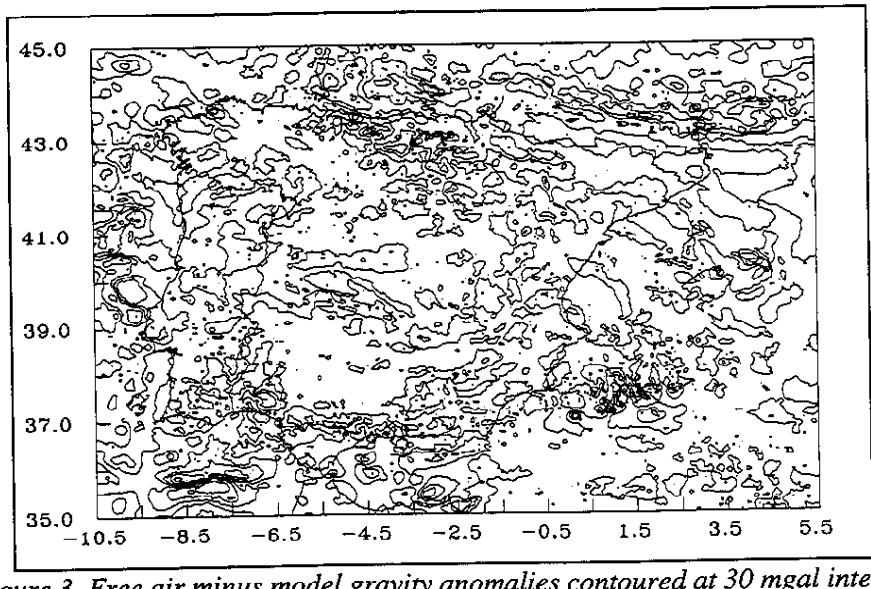

Figure 3. Free air minus model gravity anomalies contoured at 30 mgal interval

4. GRAVITY DATA VALIDATION

The validation procedure, i.e. the way of rejecting data which lack a minimum level of guarantee and reliability, is one of the main tasks when working with gravity anomalies. It is necessary to compare the observed value to the predicted one, estimated by a powerful method.

A validation procedure has been applied using least squares collocation. The application of LSC method requires a homogeneous and isotropic gravity field. The early studies in the Iberian Peninsula area show that gravity field is not homogeneous (Sevilla 1994, Sevilla et al., 1992). The same conclusion may be drawn from the mean and standard deviation values. For this reason it was decided to subdivide the whole area in small blocks. The total area is divided in 2° x2° overlapping zones. In all zones residual anomalies have been computed by removing the OSU91A. The data of each zone are divided in two sets A and B which have no common observations but the same distribution. From these residual anomalies two empirical covariance functions have been computed separately for all zones. These empirical functions have been used to estimate the values of the parameters of a model covariance function.

The choice of covariance functions for validation purposes is easy because collocation is used to predict the same quantity of the gravity field which is held as data. The quality of the predicted anomalies does not depend so much on the covariance function if the observed and predicted quantities are of the same kind (Tscherning, 1983).

Let Δg_{pred} be the predicted anomaly by using LSC from a set of values Δg_{red} in a 2°x2° area. This value is given by (Moritz, 1980)

$$\Delta g_{pred} = C_{\Delta g} C^{-1} \Delta g_{red}$$

where $C_{\Delta g}$ is the covariance vector between observations Δg_{red} and predictions Δg_{pred} and C is the sum of the covariance matrix of the Δg_{red} quantities, and the variance-covariance matrix of the associated noise. We consider homogeneous and isotropic covariance functions. In the local areas with the reduced anomalies empirical covariance functions have been computed. Then the parameters in a Tscherning-Rapp model (Tscherning and Rapp, 1974) were estimated using the least squares iterative inversion technique (Knudsen, 1987). Then we can compute the difference

$$\Delta g_{red} - \Delta g_{pred}$$

The estimation of the mean square error for the difference Δg_{red} -Δg_{pred} is obtained by

$$\sigma^2(\Delta g_{red} - \Delta g_{pred}) = C_0 - C_{\Delta g} C^{-1} C_{\Delta g}^T$$

C_0 being the variance of the gravity values.

A gross error is then detected if (Tscherning 1991)

$$|\Delta g_{red} - \Delta g_{pred}| > k\left[\sigma^2(\Delta g_{red} - \Delta g_{pred}) + \sigma^2_{\Delta g}\right]^{1/2}$$

where k is a constant generally having the value 3 and $\sigma^2_{\Delta g}$ is the estimated variance of the observations.

Predictions have been done in the whole set B by using data of set A and reciprocally, for all areas. By inspecting the results of a first calculation we applied iteratively the following criterion (Sevilla et al.,1991a,b). In normal zones, if $|\Delta g_{red} - \Delta g_{pred}| > 20$ mgal the Δg_{red} is rejected and a flag 1 is associated. This criterion works in an iterative way, repetition of the occurrence being the reason for the final decision about rejection.

As pointed by Tscherning (1983), it is difficult to establish whether a large discrepancy between predicted and observed values is due to an error in the prediction (owing to a lack of data or strong local

changes in the gravity field) or to an observation error. In our case, we used statistical results to study this problem, but the suspicious points with differences larger than twice the tolerance (20 mgal) were eliminated (flag 1). This procedure has been applied by using the GRAVSOFT package (EMPCOV, COVFIT and GEOCOL10 programs) (Tscherning et al., 1994). Gross errors have been detected in 2% of the marine data and 1% of the land data.

The collocation method allows the data to be treated in any spatial distribution. It is not necessary for the data to be gridded or for their distribution to be continuous (gaps are tolerated) unlike the Stokes method. Against these advantages also there are several disadvantages, the first one being the great amount of computational time that the collocation method takes due to the need to solve a system of linear equations with the same number of unknowns as the number of observation data. The method of Least Squares Collocation is described in several books and papers (e.g. Krarup, 1969, Moritz 1980, Sansò, 1980, Tscherning 1985).

5. TOPOGRAPHIC MODEL. TERRAIN EFFECTS

A digital terrain model (MDT200) is available for Spain with spacing 200x200 m. This model was provided by the *Instituto Geográfico Nacional* (García et al. 1992). This model was generated by digitization of level isolines and quoted points of cartographic series 1:200000; all data were corrected geometrically and altimetrically and checked by geomorphologic and external control. It was complemented by the ETOPO5U (a global topographic model) in the areas outside the Spanish territory. From these two models a new model covering the whole area with 1000x1000 meters spacing has been produced. Thus it was possible to make the terrain reduction without finding faults in the data (Sevilla and Rodríguez-Velasco, 1994a). Figure 4 shows the topography of the area.

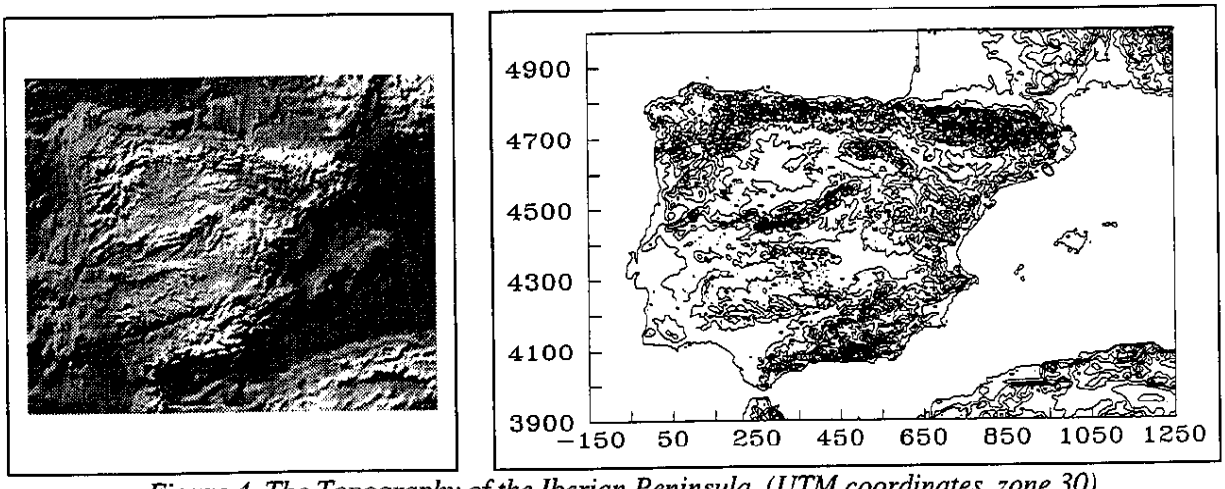

Figure 4. The Topography of the Iberian Peninsula. (UTM coordinates, zone 30)

The topography has been taken into account in geoid computation by means of the Helmert's second condensation reduction. This means that we need to compute the terrain correction and the indirect effect on the geoid (Heiskanen and Moritz, 1967).

5.1. Terrain Correction

The classical terrain correction in planar coordinates and for constant density ρ is given by (Forsberg, 1984, 1994)

$$c_P = G\rho \int_{-\infty}^{\infty}\int_{-\infty}^{\infty}\int_{z=h_P}^{h} \frac{z-h_P}{\left[(x-x_P)^2+(y-y_P)^2+(z-h_P)^2\right]^{3/2}}\,dxdydz \qquad (4)$$

where ρ is the constant density of the topographic masses, (x_P,y_P,h_P) are the coordinates of the computation point and (x,y,z) are the coordinates of the integration points. The integral is extended over the irregularities of the topographic mass body relative to a Bouguer plate passing through the computation point.

This terrain correction is added to the reduced anomalies (3) in order to get *fully reduced anomalies* according to Helmert's second condensation reduction. These anomalies are obtained by

$$\Delta g = \Delta g_{obs} - \Delta g_{\mathrm{mod}} + \delta\Delta g + c \tag{5}$$

where Δg_{obs} is the free-air gravity anomaly corrected for atmospheric attraction, Δg_{mod} is the model anomaly computed by (1), $\delta\Delta g$ is the indirect effect on gravity which, being very small, is neglected and c is the classical terrain correction computed through (4).

The computation of the terrain correction has been done in all the individual data points by applying the prism integration procedure implemented in the program TC of the GRAVSOTF package (Tscherning et al., 1994). We have not used any program based on the FFT for computing the terrain corrections, because FFT needs gridded data. Preliminary results of our data show that there are some differences between the direct and the gridded corrections and we think the direct prism integration is more accurate. The statistic of the terrain correction is shown in Table 3.

5.2. Indirect effect

The indirect effect of Helmert's second condensation reduction on the geoid, considering the first two terms in planar approximation, is (Sideris, 1990)

$$N_{ind} = -\frac{\pi G\rho}{\gamma} h^2(x_P,y_P) - \frac{G\rho}{6\gamma}\iint_E \frac{h^3(x,y)-h^3(x_P,y_P)}{s^3}dxdy$$

where s is the planar distance between the computation point (x_P,y_P) and data point (x,y).

Given a MxN digital height grid on the plane, the corresponding discrete integral is

$$N_{ind} = -\frac{\pi G\rho}{\gamma} h^2(x_P,y_P) + \frac{G\rho\Delta x\Delta y}{6\gamma} h^3(x_P,y_P)\sum_{x=x_1}^{x_M}\sum_{y=y_1}^{y_N}\frac{1}{s^3} - \frac{k\rho\Delta x\Delta y}{6\gamma}\sum_{x=x_1}^{x_M}\sum_{y=y_1}^{y_N}\frac{1}{s^3}h^3(x,y) \tag{6}$$

The second term and the third term on the right-hand side of (6) are 2D discrete convolutions. Since the summations in both the x and y directions are 1D convolutions, (6) can be evaluated by the 1D FFT either row by row or column by column, yielding the indirect effects for all grid points. The 1D FFT formula for evaluating (6) column by column along x is (Sideris and She, 1995)

$$N_{ind} = -\frac{\pi G\rho}{\gamma} h^2(x_P,y_P) + \frac{G\rho\Delta x\Delta y}{6\gamma} h^3(x_P,y_P) F_I^{-1}\left\{\sum_{x=x_1}^{x_M} F_I\left\{\frac{1}{s^3}\right\} F_I\{1\}\right\} -$$
$$-\frac{G\rho\Delta x\Delta y}{6\gamma} F_I^{-1}\left\{\sum_{x=x_1}^{x_M} F_I\left\{\frac{1}{s^3}\right\} F_I\{h^3\}\right\} \tag{7}$$

where F_I and F_I^{-1} are the 1D Fourier transform operator and its inverse. The formula for the direction y is similar.

For the computation of the indirect effect in the Iberian Peninsula, we have taken a 1601x1301 digital height grid from the DTM 200, then we have computed the indirect effect for the geoid grid by bilinear interpolation. To evaluate the formula (7) we have used the INDI program (Sideris, 1994). The statistic of the indirect effect is shown in Table 3.

Table 3. Statistics of terrain effects in the Iberian Peninsula area

	Mean	St. Dev	Minimum	Maximum	Range
Terrain Correction	0.48	1.63	0	78.61	78.61
Indirect Effect	-0.02	0.03	-0.41	-0.41	0.41

6. GEOID COMPUTATION METHODS

Geoid undulations have been determined for the Iberian Peninsula using the classical remove-restore technique. The predicted undulations are obtained by the formula

$$N = N_{mod} + N_{ind} + N_{gra}$$

where N_{mod} is the contribution of the spherical harmonic model OSU91A (2), N_{ind} is the contribution of a terrain reduction (7) and N_{gra} is the contribution of the terrestrial gravity field observations: free-air anomalies after the removal the effect of the global geopotential model and the topography.

The method used in the computations of the contribution of the local gravity data to the geoid was the Stokes' integral. For the sphere it is (Heiskanen and Moritz, 1987)

$$N_{gra} = \frac{R}{4\pi\gamma}\iint_{\sigma}\Delta g(\varphi,\lambda)S(\psi)d\sigma \qquad (8)$$

where R is the mean Earth radius, γ is the normal gravity, σ is the sphere of integration, Δg is the gravity anomalies reduced to the geoid and $S(\psi)$ is the Stokes function given by

$$S(\psi) = \frac{1}{t} - 4 - 6t + 10t^2 - (3 - 6t^2)\ln(t + t^2), \qquad t = sin\frac{\psi}{2}$$

The input data were fully reduced gridded gravity anomalies (5). To evaluate the Stokes' formula, three techniques were used: The first one is the planar Fast Hartley Transform (FHT) (Bracewell, 1986; Li and Sideris 1992; Tziavos, 1993a,b); the second one is the spherical multiband Fast Fourier Transform technique with 2D discrete FFT (Forsberg and Sideris, 1993) and the third one is the spherical 1D-FFT technique (Haagmans et al., 1993, Sideris and She, 1995), which allows the evaluation of the discrete spherical Stokes' integral without any approximation, parallel by parallel.

In order to reduce the spectral leakage due to the periodicity of the discrete transformation and the effect of the circular convolution on our computations we extended the size of each gravity matrix by 256x256. This was done by appending zeros around the gravity anomalies, i.e., a 100% zero padding was used distributed in both parts. Also, we have used discrete spectra of the kernel function that is more efficient than the analytical one in geoid calculations.

6.1. 1st Method: Planar FHT approximation

In planar approximation the Stokes formula (8) can be written as follows

$$N_{gra}(x_P, y_P) = \frac{1}{2\pi\gamma}\iint_{E}\Delta g(x,y)\left[(x - x_P)^2 + (y - y_P)^2\right]^{-1/2}dxdy$$

where (x_P,y_P) are the planar coordinates of the computation point, (x,y) are the actual point, γ is the mean value of the normal gravity and Δg are point gravity anomalies. This integral can be transformed in the frequency domain (Tziavos, 1993a). Thus, Stokes' integral formula may be written as a 2D convolution in the form

$$N_{gra}(x,y) = \frac{1}{2\pi\gamma}\Delta g(x,y) * l_N(x,y)$$

where * is the convolution operator, $\Delta g(x,y)$ are the fully reduced anomalies (5). The kernel function $l_N(x,y)$ is given by.

$$l_N = (x^2 + y^2)^{-1/2}$$

Then the FFT technique can be applied for the computation of the geoid undulation. In the computations the discrete form of Stokes formula is used. Thus we have

$$N_{gra}(x_P,y_P) = \frac{\Delta x \Delta y}{2\pi\gamma}\sum_{x=x_1}^{x_M}\sum_{y=y_1}^{y_N}\frac{1}{s}\Delta g(x,y)$$

were Δx, Δy are the grid spacings in x and y directions and s is the planar distance between the computation point (x_P,y_P) and the data point (x,y). This equation is a two-dimensional convolution and can be evaluated be the 2D-DFT (Schwarz et al., 1990) as follows

$$N_{gra}(x_P,y_P) = \frac{\Delta x \Delta y}{2\pi\gamma}\boldsymbol{F}^{-1}\left\{\boldsymbol{F}\left\{\frac{1}{s}\right\}\boldsymbol{F}\{\Delta g\}\right\}$$

The singularity in the origin $(x=0,y=0)$ can be avoided evaluating separately the effect at the computation point as

$$\delta N(x_P,y_P) \approx \frac{\sqrt{\Delta x \Delta y}}{\gamma\sqrt{\pi}}\Delta g(x_P,y_P) \qquad (9)$$

To evaluate the convolution, instead the FFT, we have used the Fast Hartley Transform (FHT). This is a real transform and its spectrum is real, so with the FHT we can save half of the computer memory and also we spend less computer execution time (Tziavos, 1993a,b). The use of the FHT is made in just the same way as the FFT if the data length is an integer power of 2 (Li and Sideris, 1992). This is the alternative used in our 1st computation of the Iberian geoid (Sevilla 1994). Tziavos has shown that the results obtained by using FHT are identical to those obtained by the FFT. To evaluate the planar FHT we have used the GUNDFHT program (Tziavos 1993a). In the FHT case we have

$$N_{gra}(x,y) = \frac{1}{2\pi\gamma}\boldsymbol{H}^{-1}[\Delta G(u,v)\, L_N(u,v)]$$

Here $\boldsymbol{H}^{-1}$ denotes the inverse Hartley Transform, (u,v) are the frequencies and $\Delta G(u,v)$ and $L_N(u,v)$ are the Hartley Transforms of $\Delta g(x,y)$ and $l_N(x,y)$ respectively.

6.2. 2nd Method: Multi-band Spherical FFT

The multiband spherical FFT approach is a generalization of the Strang van Hees (1990) spherical FFT geoid prediction method, allowing virtually error-free spherical FFT solution through utilization of continuously merged "stripes" of transforms.

It is possible to modify the classical spherical Stokes formula so that it may rather well be represented by a two-dimensional convolution formula, which may be efficiently evaluated by FFT. Stokes formula my be put in convolution form in (φ,λ) by using the formula

$$sin^2\frac{\psi}{2} = sin^2\frac{\Delta\varphi}{2} + sin^2\frac{\Delta\lambda}{2}\cos\varphi_P\cos\varphi$$

where $\Delta\varphi = \varphi - \varphi_p$, $\Delta\lambda = \lambda - \lambda_p$, (φ_p,λ_p) are the coordinates of the computation point, and approximating the cosines product by

$$\cos\varphi_P\cos\varphi \approx \cos^2\varphi_m - sin^2\frac{\Delta\varphi}{2}$$

where φ_m is a mean latitude for the area.

With these transformations the Stokes formula becomes a formal convolution integral in φ and λ with kernel $S(\psi)$ and modified data $\Delta g\cos\varphi$, and we can write

$$N_{gra} = (\Delta g\cos\varphi) * S = \boldsymbol{F}^{-1}\{\boldsymbol{F}(\Delta g\cos\varphi)\boldsymbol{F}(S)\} \qquad (10)$$

Forsberg and Sideris (1993) proposed to subdivide the area in narrow bands along the longitude direction. To improve the approximation they use the following expression

$$\cos\varphi_P\cos\varphi = \cos\varphi_P\cos(\varphi_P - \Delta\varphi) - \cos^2\varphi_P\cos\Delta\varphi + \cos\varphi_P sin\varphi_P sin\Delta\varphi$$

and thus equation (10) yields an FFT convolution solution for gridded geoid undulations which is an exact solution of the Stokes' integral for points along the latitude parallel $\varphi=\varphi_p$.

The discrete form of (8) is

$$N_{gra}(\varphi_P,\lambda_P) = \frac{R\Delta\varphi\Delta\lambda}{4\pi\gamma}\sum_{i=1}^{M}\sum_{j=1}^{N}S(\psi)\Delta g(\varphi_i,\lambda_j)\cos\varphi_i$$

where φ_i,λ_j denote the coordinates of the data point, $\Delta\varphi$, $\Delta\lambda$ are the grid spacing in latitude and longitude, M and N are the number of parallels and meridians in the grid. The contribution to N of the singular point $\Delta g(\varphi_p,\lambda_p)$, is evaluated separately by (9).

If N_i is the FFT geoid solution obtained from (10) using the latitude $\varphi_p=\varphi_i$ in setting up the kernel S, the result at a latitude φ between two reference latitudes φ_i and φ_{i+1} may be obtained through linear interpolation between the solutions n the neighbouring bands

$$N(\varphi) = \frac{\varphi - \varphi_{i-1}}{\varphi_i - \varphi_{i+1}}N_i + \frac{\varphi_i - \varphi}{\varphi_i - \varphi_{i+1}}N_{i+1}$$

To evaluate the multiband spherical FFT we have used the SPFOUR program belonging to the GRAVSOFT package (Tscherning et al., 1994).

6.3. 3rd Method: 1D-FFT

This method is an exact approach to evaluate the Stokes' integral on the sphere using 1D-FFT techniques. Haagmans et al. (1993) note that the Stokes' function values, for a certain longitude difference between computation and integration points are the same for all computation points on one parallel, but different for computation points on different parallels. Therefore, only one east-west convolution is carried out by means of FFT. The north-south integration can be performed by a pointwise integration. This allows to use a correct kernel function everywhere in the integration area.

The Stokes' formula is written as

$$N_{\varphi_P\varphi}(\lambda_P) = \frac{R\Delta\varphi\Delta\lambda}{4\pi\gamma} \sum_{\varphi=\varphi_1}^{\varphi_M} \left[\sum_{\lambda=\lambda_1}^{\lambda_M} S_{\varphi_P\varphi}(\delta\lambda)\Delta g_\varphi(\lambda)\cos\varphi \right] \qquad (11)$$

were $N_{\varphi P\varphi}(\lambda_P)$ denotes the geoid undulation at all points on the parallel φ_P. The brackets in (11) contain 1D discrete convolution with respect to λ and can be evaluated by the 1D-FFT. By the addition theorem of DFT the evaluation formula can be written in the form

$$N_{\varphi_P\varphi}(\lambda_P) = \frac{R\Delta\varphi X\lambda}{4\pi\gamma} \boldsymbol{F}_1^{-1}\left\{ \sum_{\varphi=\varphi_1}^{\varphi_M} \boldsymbol{F}_1\left\{S_{\varphi_P\varphi}\right\}\boldsymbol{F}_1\left\{\Delta g_\varphi \cos\varphi\right\}\right\}, \qquad \varphi_P = \varphi_1,\varphi_2,\ldots,\varphi_M$$

where $\boldsymbol{F}_1$ and $\boldsymbol{F}_1^{-1}$ are the 1D Fourier transform operator and its inverse. Through this expression we get the geoid undulation for all points on one parallel. The results obtained by this method are exactly the same as those obtained by direct numerical integration. We only need to deal with one 1D complex array each time resulting in a considerable saving in computer memory as compared to the 2D-FFT technique (Sideris and She 1995). To evaluate the 1D spherical FFT we have used the FFTGEOID program (Sideris, 1994).

7. IBERIAN GEOID 1995

In a first experiment (Sevilla 1994), the gravimetric solution by FHT was performed in two overlapping areas in the west and east parts of the region. The geoid undulation differences obtained in this common block are between -2.5 m and 1.5 m. The distribution of the points with differences greater than 1 meter mainly correspond to the borders of the overlapping area. These differences are kept under 1 meter in an inner zone limited by the meridians of longitudes -3.7196 and -1.23253 degrees. The good agreement between the solutions in the central part confirms that many of the differences can be due to the edge effects. They can also be a result of the poor quality of the topographic model outside the Spanish territory.

In a second experiment (Sevilla and Rodríguez-Velasco 1994b,) the effect of the extension of the computation areas on the results obtained by the FHT has been studied, and the conclusion was the need of an improved DTM and spherical approximations.

In the final computations, object of this paper, new precise gravity data and a refined DTM are included in the data used. The geographic limits of geoid calculation in the Iberian Peninsular are $35<\varphi<45$ for latitudes and $-10.5<\lambda<5.5$ for longitudes. For geoid calculation 185097 validated free air anomalies (marine and land data) have been used. For the computations, data were gridded in a 1.19'x1.88' grid for the region, using weighted means with a power equal 3. The result is a grid with 262144 predicted geoid undulations.

The three solutions (a planar and two spherical) are compared and the 1D-FFT solution was accepted as the IBERIAN GEOID 1995 (Figure 5). Table 4 shows the statistic of the three solutions and their differences. The maximum and minimum differences between planar and spherical solutions are in the borders of the area (see also Figures 6 and 7).

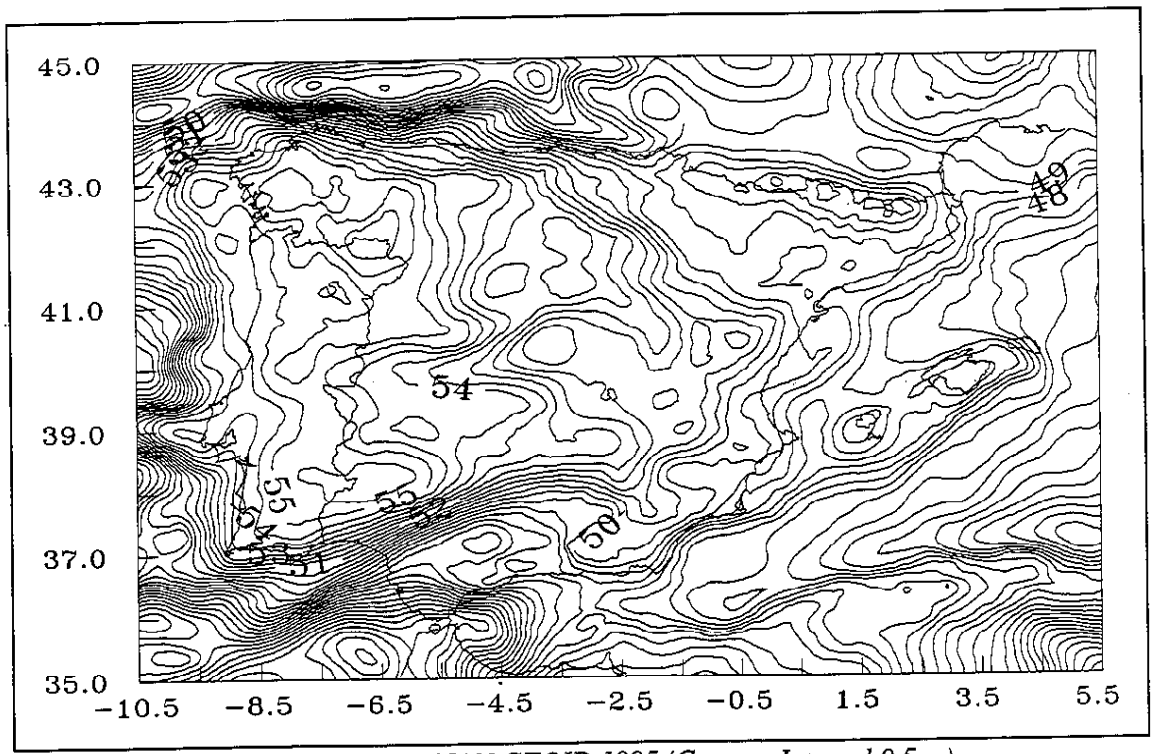

Figure 5. The IBERIAN GEOID 1995 (Contour Interval 0.5 m)

Table 4. Statistics of the IBERIAN GEOID 1995 (m)

	Points	Mean	S.D.	Minimum	Maximum	Range
OSU91A model	262144	49.94	3.72	36.87	57.48	20.61
FHT GEOID	262144	49.93	3.71	36.88	57.67	20.79
2DFFT GEOID	262144	49.79	3.76	36.83	57.21	20.38
1DFFT GEOID	262144	49.79	3.75	36.74	57.16	20.42
FHT-2DFFT	262144	0.14	0.47	-2.21	3.37	5.58
FHT-1DFFT	262144	0.14	0.45	-2.27	3.19	5.46
2DFFT-1DFFT	262144	0.00	0.07	-0.96	0.72	1.68

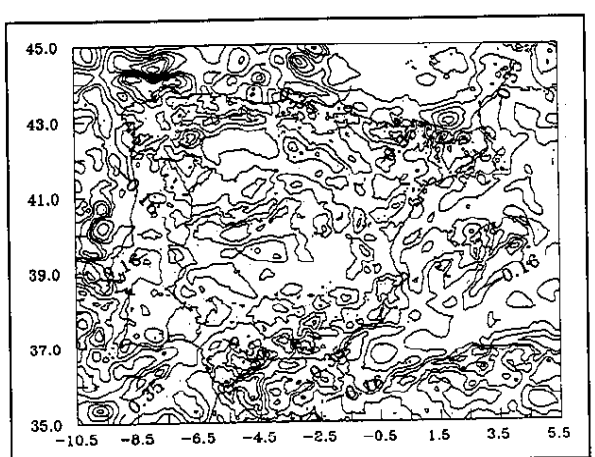

Figure 6. FHT-1DFFT Difference

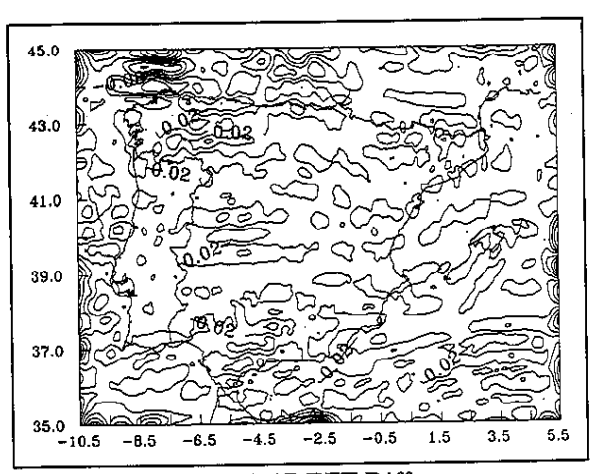

Figure 7. 2DFFT-1DFFT Difference

8. GPS/LEVELLING.

Unfortunately no accurate GPS/levelling data are available in the Iberian Peninsula, necessary for making an independent check of the geoid accuracy. A rough check of the geoid is possible in areas with GPS stations with locally determined sea level heights. One such comparison of a GPS survey is the EUREF stations (Figure 8) (Gubler and Poder 1992).

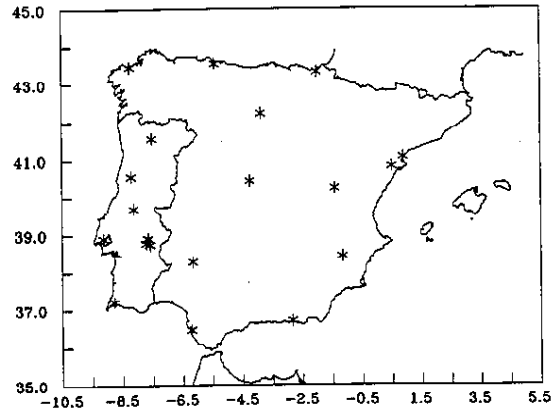

Figure 8. GPS points in the Iberian Peninsula (RETRIG/92)

The 1D-FFT geoid solution achieves a better agreement with the GPS/levelling data available in the region compared to the FHT and the 2D-FFT geoids, as shown in Table 5.

Table 5. Statistics of the differences between the FFT geoids and the GPS/levelling (in ppm.)

	Baselines	Mean	S.D.	Minimum	Maximum	Range
GPS-FHT	157	0.492	1.009	0.003	4.713	4.710
GPS-2DFFT	157	0.417	0.951	0.004	3.849	3.845
GPS-1DFFT	157	0.441	0.950	0.002	4.256	4.254

Considering the rough topography and the uncertain orthometric heights of GPS stations the fitting can be considered as satisfactory. The large bias is mainly due to a GPS datum discrepancy.

9. CONCLUSIONS

A gravimetric geoid has been computed from 186813 free air gravity anomalies, a DTM and geopotential model OSU91A. The area covered is the whole Iberian Peninsula.

Fast Fourier Transform method has been adequate to compute a geoid obtaining 262144 predicted geoid undulations in a 1.2'x1.8' grid and in the GRS80 reference system.

Different FFT solutions have been compared and the 1D-FFT solution has appeared to be the most efficient one for geoid undulations computations using discrete spectra for the kernel function and 100 % zero-padding to reduce the effect of circular convolution. Comparisons between 2D-FFT and 1D-FFT solutions give small differences and between FHT and 1D-FFT results show large differences at the borders. Comparisons to other previous partial geoids in this area show a good agreement.

The geoidal height mean squares errors estimated from comparison with GPS are almost everywhere lower than 30 centimeters, and the relative agreement of gravimetric geoid with respect to the GPS/levelling data results are better than 1 ppm. Further investigation is needed in order to improve the topographic model outside Spain and to control the results with external sources as new precise GPS networks.

This IBERIAN GEOID 1995 set is the complete high-resolution and high-precision gravimetric geoid in the Iberian Peninsula which is available on request from the Spanish "Centro Nacional de Información Geográfica". A collection of 20, 2 x4 geoid plots is also available.

ACKNOWLEDGEMENTS

This work is a contribution to the GEOMED Project sponsored by the European Union contract no. sc1*-ct92-0808 and by the project CE93-0001 of the Spanish DGICYT. I gratefully acknowledge the support of Institutions who have provided the data. I also gratefully acknowledge the support of Prof. C.C. Tscherning, Prof. I.N. Tziavos and Prof. M.G. Sideris who has provided the main software package.

REFERENCES

Bracewell, R.N. (1986): The Hartley transform. Oxford Univ. Press.
Forsberg, R. (1984): A study of terrain reductions, density anomalies and geophysical inversion methods in gravity field modelling. *Rep. No.355 of the Dept. of Geodetic Science and Surveying*. The Ohio State Univ. Columbus.
Forsberg R. and M.G. Sideris (1993): Geoid computations by the multi-band spherical FFT approach. *Manuscripta Geodaetica* Vol. 18, pp. 82-90.
Forsberg, R. (1994): Terrain Effects in Geoid Computations. Lecture Notes. International School for the determination and use of the Geoid. International Geoid Service. DIIAR. Milan.
García Asensio, L.,J.J. Lumbreras, G. Martín y C. Heras (1992): La altimetría en el SIG del IGN: Modelos digitales del terreno. *Nota Técnica de Geodesia NTG 5*. IGN Madrid.
Gil, A.J., M.J. Sevilla and G. Rodriguez-Caderot (1993): Geoid determination in central Spain from gravity and height data. *Bulletin Géodésique* Vol. 67, pp. 41-50. Springer-International.
Gubler, E. and K. Poder (Eds) (1992): Reports of the IAG Subcommission for the European Reference Frame (EUREF). Veröffentlichungen der Bayerischen Kommission für die Internationale Erdmessung, Hefl Nr 52. München.
Haagmans R.H.N., E. de Min and M. van Gelderen (1993): Fast evaluation of convolution integrals on the sphere using 1D-FFT, and a comparison with existing methods for Stokes' integral. *Manuscripta Geodaetica* Vol. 18, pp. 227-241.
Heiskanen W.A. and H. Moritz (1967): Physical Geodesy. W.H. Freeman, San Francisco.
Knudsen, P (1987): Estimation and modelling of the local empirical covariance function using gravity and satellite altimeter data. *Bulletin Géodésique* Vol. 61, pp 145-160.
Krarup, T (1969): A contribution to the mathematical foundation of physical geodesy. The Danish Geodetic Institute, Medd. No 44.
Li, Y.C. and M.G. Sideris (1992): The fast Hartley transform and its application in Physical Geodesy. *Manuscripta Geodaetica* Vol. 17, pp 381-387.
Moritz, H.(1980): Advanced Physical Geodesy. Herbert Wichmann Verlag, Karlsruhe.
Moritz, H.(1984): Geodetic Reference System 1980. *Bulletin Géodésique Vol. 58*, pp. 388-398.
Pavlis, N.K. (1991): "Estimation of geopotential differences over Intercontinental Locations Using Satellite and terrestrial Measurements. *Rep. No.409 of the Dept. of Geodetic Science and Surveying*. The Ohio State University. Columbus.
Rapp, R.H.,Y.M. Wang and N.K. Pavlis (1991): "The Ohio State 1991 Geopotential and Sea Surface Topography Harmonic Coefficient Models. *Rep. No. 410 of the Dept. of Geodetic Science and Surveying*. The Ohio State University. Columbus.
Sansó, F (1980): The minimum mean square estimation error principle in physical geodesy. (Stochastic and nonstochastic interpretation). *Boll. Geod. Sci. Aff.*, No. 2, pp. 111-129.
Schwarz, K.P., M.G. Sideris and R. Forsberg (1990): The use of FFT techniques in physical geodesy. *Geophys. J. Int.* Vol. 100, pp. 485-514.

Sevilla, M.J.,A.J. Gil, and F. Sansó (1991a): The gravimetric geoid in Spain: first results. In *Determination of the geoid. Present and future.* Ed. by R.H.Rapp and F.Sansó. IAG Symp. 106, pp 276-285. Springer Verlag.
Sevilla, M.J., G. Rodríguez-Caderot, J. Otero, A.J. Gil, P. Zamorano and P. Romero (1991b): GEOMED. Gravity data validation: status report. In *Determination of the geoid. Present and future.* Ed. by R.H.Rapp and F.Sanso. IAG Symp. 106, pp 468-475. Springer Verlag.
Sevilla, M.J., G. Rodríguez-Velasco y M. Lisboa (1992): Análisis y validación de la gravimetría de Portugal. *Revista del Instituto Geografico e Cadastral,* Vol. 11, pp. 5-20. IPCC, Lisboa.
Sevilla, M.J., and G. Rodríguez-Velasco (1993): Preliminary determination of a gravimetric geoid in Portugal. *Mare Nostrum 3,* pp. 139-150. DIIAR, Milan, Italy.
Sevilla, M.J. (1994): Regional quasigeoid determination in the Iberian Peninsula. *Mare Nostrum 4,* (Ed. by D. Arabelos and I.N. Tziavos) pp 65-75. Univ. of. Thessaloniki.
Sevilla, M.J., and G. Rodríguez-Velasco (1994a): Digital terrain model for Spain. *Mare Nostrum 4,* (Ed. by D. Arabelos and I.N. Tziavos) pp 19-31. Univ. of Thessaloniki.
Sevilla, M.J., and G. Rodríguez-Velasco (1994b): The Fast Hartley Transform applied to the Iberian Geoid determination. *III Hotine-Marusi Symp. on Mathematical Geodesy.* L'Aquila.
Sideris, M.G. (1990): Rigorous gravimetric terrain modelling using Molodensky's operator. *Manuscripta Geodaetica* Vol. 15, pp. 97-106.
Sideris, M.G. (1994): Geoid determination by FFT Techniques. Lecture Notes. International School for the determination and use of the Geoid. International Geoid Service. DIIAR. Milan.
Sideris, M.G. and B.B. She (1995): A new, high-resolution geoid for Canada and part of the U.S. by the 1D-FFT method. *Bulletin Géodésique* Vol. 69, pp. 92-108.
Strang van Hees, G. (1990): Stokes formula using fast Fourier techniques. *Manuscripta Geodaetica* Vol. 15, pp. 235-239.
Tscherning, C.C. and R.H. Rapp (1974): Closed covariance expressions for gravity anomalies, geoid undulations and deflections of the vertical implied by anomaly degree variance models. *Rep. No.208 of the Dept. of Geodetic Science and Surveying.* The Ohio State University, Columbus.
Tscherning, C.C. (1983): Determination of a (quasi) geoid for the Nordic Countries from heterogeneous data using collocation. *Proc. 2nd. Int. Symp. on Geoid in Europe and Mediterranean Area.* Rome. Istituto Geograf. Milit. Firenze, pp. 388-411
Tscherning, C.C., R.H. Rapp and C. Goad (1983): A comparison of methods for computing gravimetric quantities from high degree spherical harmonic expansions. *Manuscripta Geodaetica* Vol. 9, pp 249-272.
Tscherning, C.C. (1985) Local approximation of the gravity potential by least squares collocation. In *Local gravity Field Approximation.* Ed by K.P.Schwarz. Univ. of Calgary. pp 277-362.
Tscherning, C.C. (1991): A strategy for gross-error detection in satellite altimeter data applied in the Baltic-sea area for enhanced geoid and gravity determination. In *Determination of the geoid. Present and future* Ed. by R.H. Rapp and F.Sanso. IAG Symp. 106, pp 95-107. Springer Verlag,
Tscherning, C.C., P. Knudsen and R. Forsberg (1994): Description of the GRAVSOFT package. Geophysical Institute, University of Copenhagen. Technical Report, 4. ed.
Tscherning, C.C. (1995): GEOCOL10 Program. Unix version 1995.03.06.
Tziavos, I.N. (1993a): Numerical Considerations of FFT Methods in Gravity Field Modelling. *Wissenschaftliche Arbeiten der F.V. n.188.* Univ. Hannover. Hannover
Tziavos, I.N. (1993b): Gravity Field modelling using the Fast Hartley Transform. Proc. *Session G3 EGS XVIII General Assembly,* Wiesbaden, pp 46-53.

IBERIAN DEM.

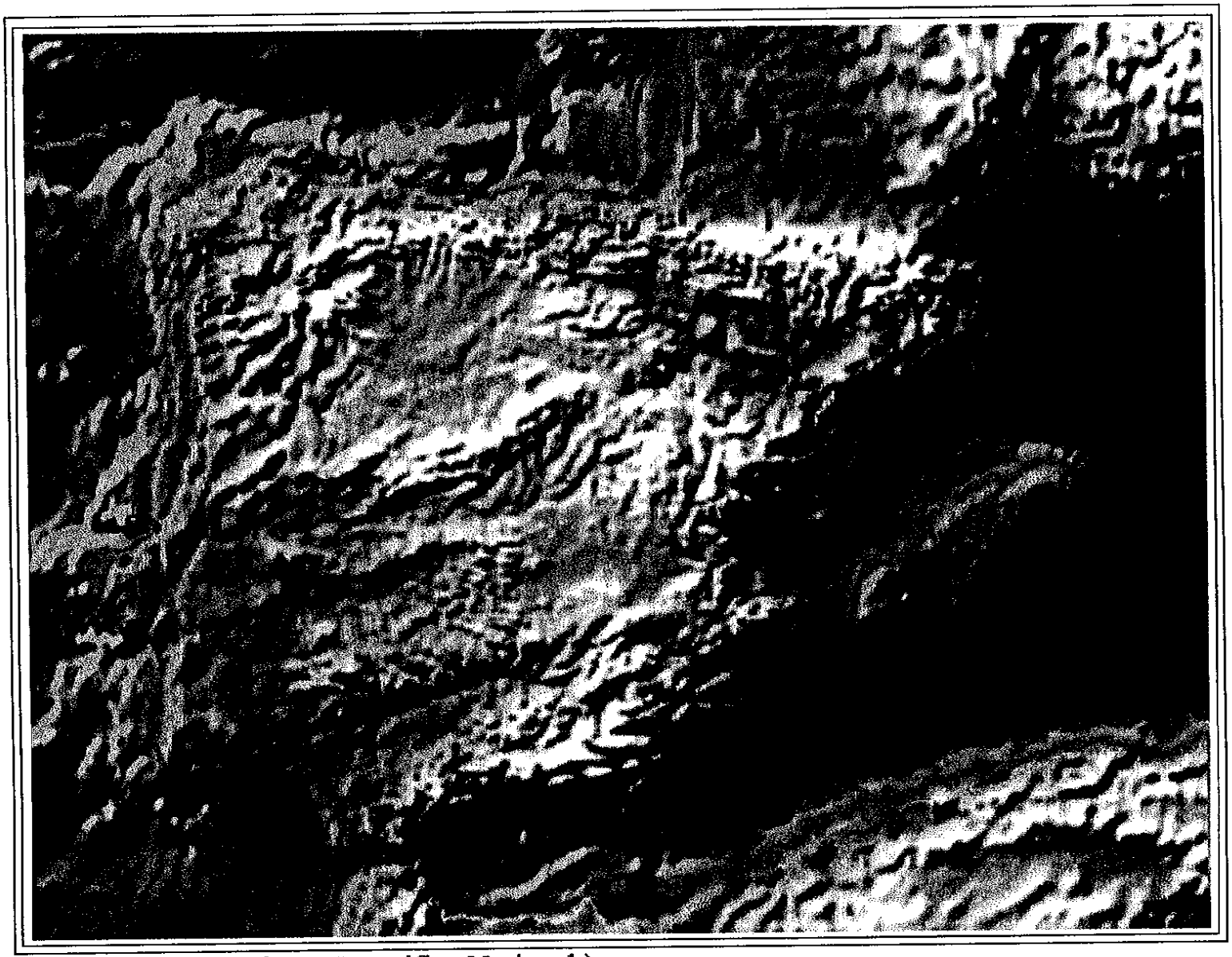

(DEM source: Instituto Geográfico Nacional.)

Instituto de Astronomía y Geodesia. MADRID.(M. J. Sevilla - F. Sánchez)

IBERIAN GEOID 1995.

(Contour Interval 0.5 m)

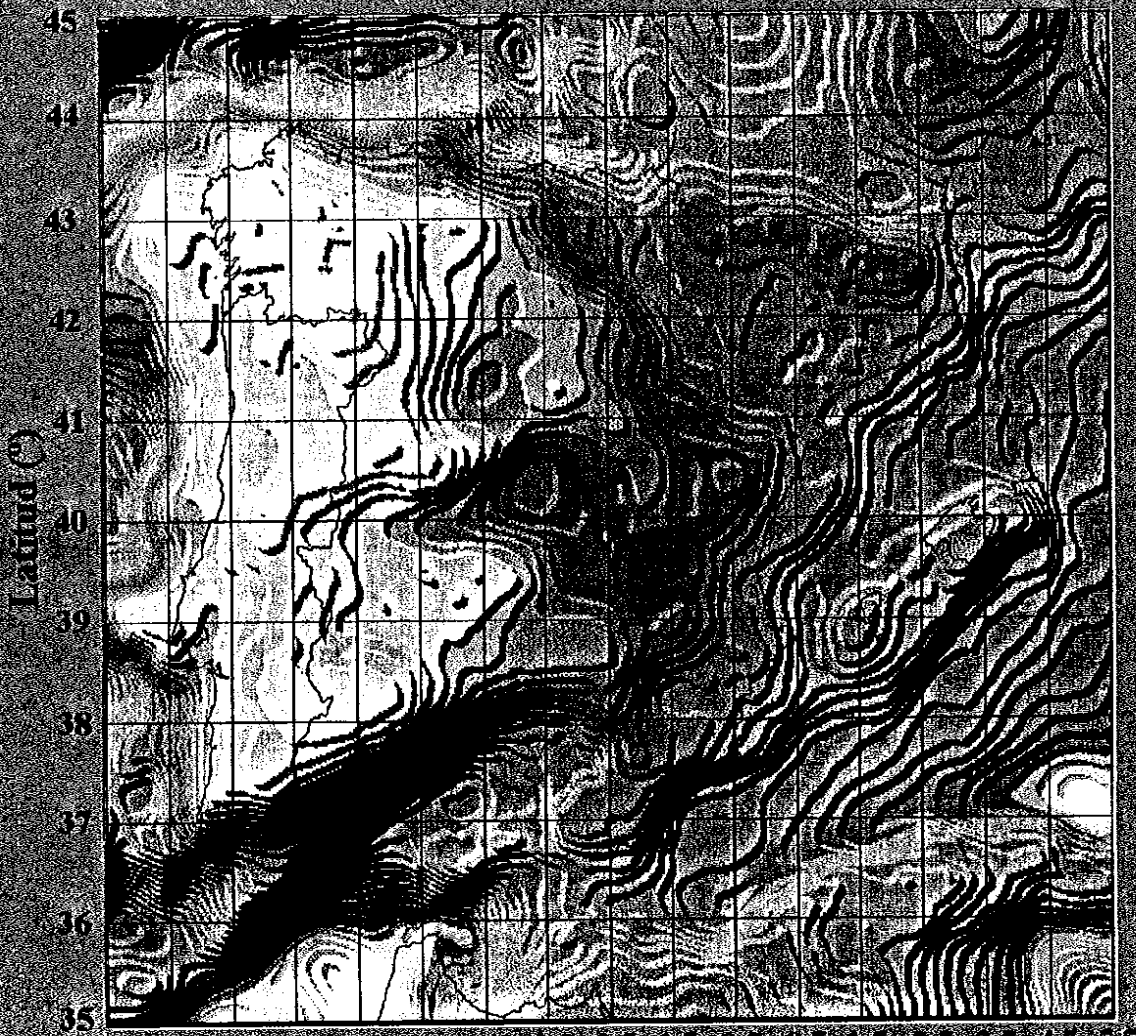

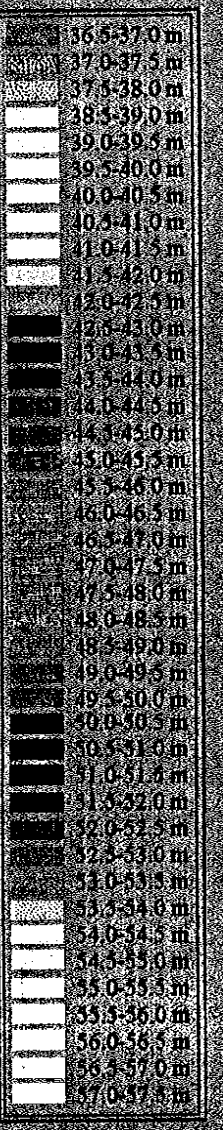

Instituto de Astronomía y Geodesia. MADRID.(M. J. Sevilla 1995)

National Geoid Investigations in Switzerland

U. Marti: Swiss Federal Office of Topography, Wabern
B. Bürki, H.-G. Kahle: Geodesy and Geodynamics Laboratory,
Swiss Federal Institute of Technology, Zurich

Abstract

The task of the new geoid and quasigeoid computation in Switzerland is realised in a joint project of the Swiss Federal Institute of Technology (ETH) Zurich, the Federal Office of Topography (L+T), Wabern and the Astronomical Institute of the University of Berne (AIUB). The main objective is to calculate a geoid and a quasigeoid with an accuracy of better than a few centimetres over the whole country (200 km x 300 km), which is not only useful for combining levelling data with GPS-derived ellipsoidal heights but also for many other purposes such as positioning and height determination using GPS techniques.

This is realised by a combined evaluation of all available data of the gravity field such as deflections of the vertical, gravity values and GPS levelling. In the mountainous region of Switzerland much attention has to be given to the reduction of the observed values by means of a high resolution digital terrain model. After the subtraction of further mass models such as the Moho-depth and the Ivrea-body the residuals are interpolated by means of multivariate collocation methods.

1. Observations

Since 1990 about 100 astrogeodetic stations have been observed with the transportable zenith camera system of the ETH Zurich for the geoid determination. All these observations and the older observations back to 1980 had been re-evaluated using the PPM star catalogue which is consistent with the ICRS Reference system at the level of the needed accuracy. There are now about 300 stations with 600 components of the deflection of the vertical in a homogeneous system available. Some additional 300 stations are available in other reference systems. Comparisons revealed that with a few exceptions there are no significant differences of the astronomical coordinates of these stations. Therefore the complete data set consists of 600 astrogeodetic observations which can be used for the geoid computation. Their distribution and the observed deflections of the vertical can be seen in fig. 1.

The observation of the GPS base-network (LV95) of Switzerland had been completed in 1993. This 3D reference network consists of 104 control points, including 5 EUREF stations. 80 of these stations are connected to the first order levelling network of Switzerland and therefore can be used for the geoid determination. A preliminary evaluation shows that the observed ellipsoidal heights have an accuracy of about 5 cm. This is not adequate for a geoid determination at the 1 cm level. Therefore these observations at the moment are only used to control long wavelength drifts. An other problem in using GPS is the fact that the first order levelling network of Switzerland had never been adjusted rigorously and so in many regions only approximate orthometric heights are available. This fact will be corrected in a special project LN95. But its results will not be available before 1999.

The third data set used for the determination of the geoid are about 2500 gravity stations. Not included in this number are the measurements which had been performed along the first order levelling lines and the many data with access restrictions. The gravity values are mainly used in regions with only few astrogeodetic observations and along the borders. They are of special interest for the definition of the new national height system LN95.

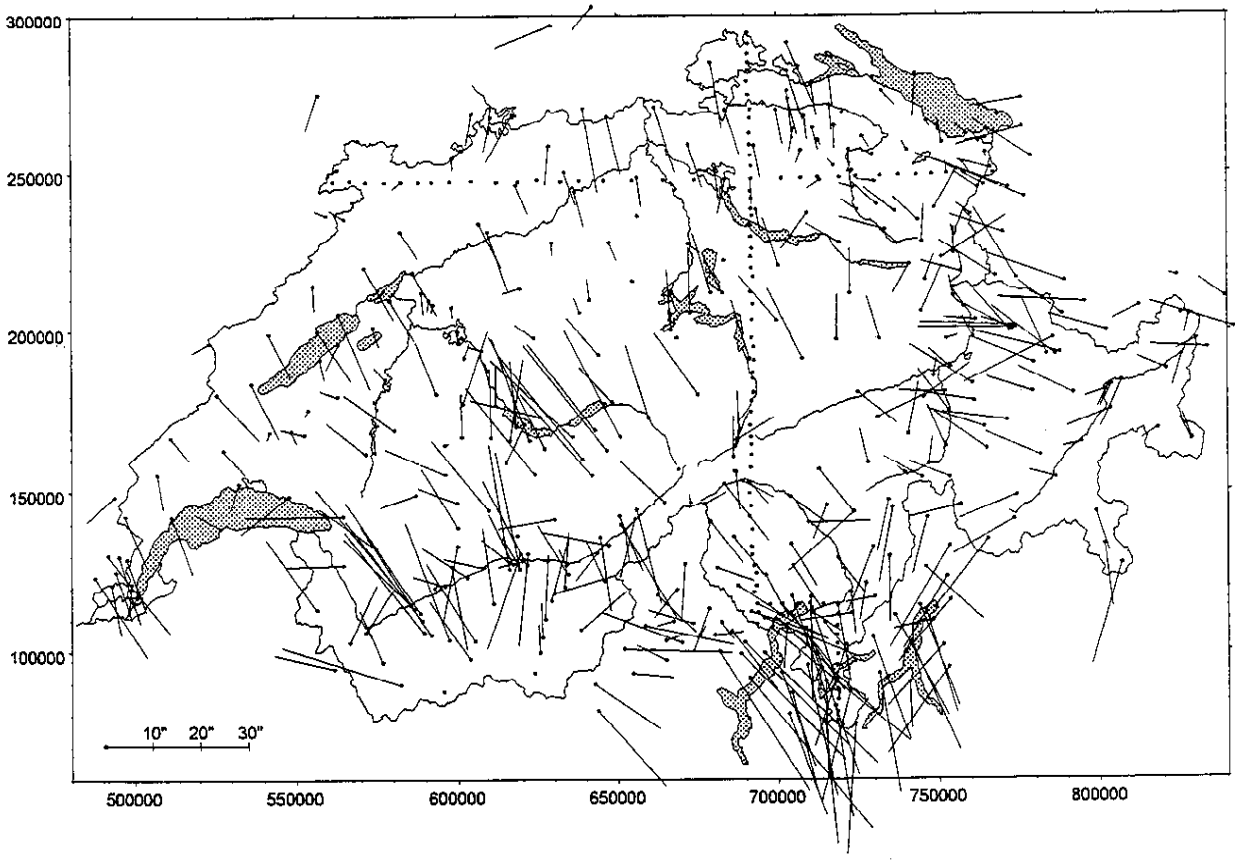

Fig. 1: Astrogeodetic stations of Switzerland with observed deflections of the vertical

2. Mass Models and Reduction of the Observations

The main purpose of introducing mass models is to smoothen the gravity field information for interpolation and if we want to determine the geoid (not quasigeoid) also to continue the gravity vectors from the earth's surface down to sea level.

The most important model is certainly the topography. It is most responsible for short wavelength changes of the gravity field. Until now a digital height model (DHM) with a resolution of 250 meters (RIMINI) had been used for the reduction of gravity field information. Since 1990 the Swiss Federal Office of Topography (L+T) is digitising its 1:25000 maps and generates a DHM with a resolution of 25 meters (DHM25). This work will be completed in early 1996. For the calculations presented in this paper about 85% of DHM25 was available. Data are still missing in the south-eastern part of Switzerland. The comparison of calculating the topographic effect once with RIMINI and once with DHM25 revealed differences of up to 9 mgal for the gravity or up to 2" for the deflections of the vertical, respectively. This shows the importance of a high resolution DHM.

DHM25 does not include any information about density anomalies. They have to be introduced in separate models where necessary. Our 2 dimensional approach to model surface densities is, to form closed polygons and to calculate the topographic effect in the enclosed areas with another than the standard density. Figure 2 shows the 3 different kinds of polygons we introduced in our software: Type 1 is used for modelling the effects of the water masses of the lakes. It is formed by the lake's contours and must be characterised by its elevation. A prerequisite to use these models is, that the lake's ground and not the surface is included in the DHM. At the moment this is not the case for DHM25 but it will be available in 1996. The 2nd kind of polygons which is characterised by a density and a constant thickness of the geological structure is used to model glaciers and some sedimental basins where no better information is

available. The 3rd kind is used for the near surface parts of larger structures like the sediments of the Po-plain or the Ivrea zone. Their deeper parts are treated in separate models.

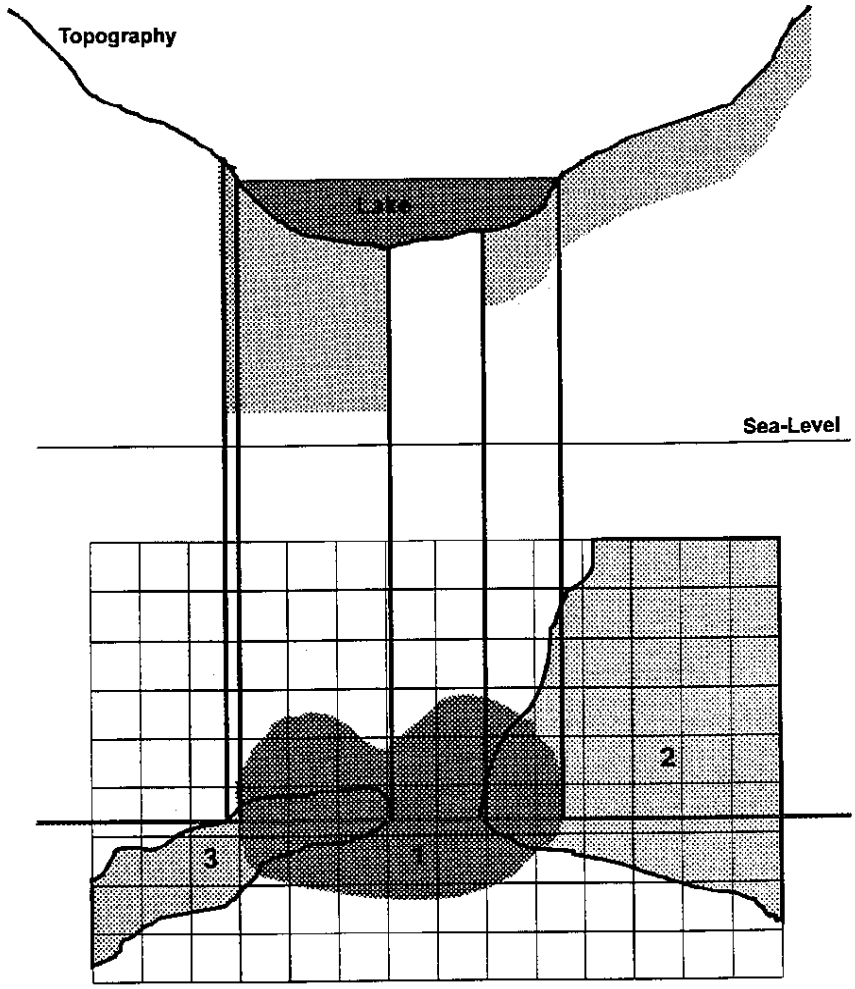

Fig. 2: Treating of near surface density anomalies in the calculation of the topographic effect

The effects of deeper geological structures are calculated separately. These models are either formed by a grid of vertical prisms (for instance depth of the Moho) or by irregularly shaped polyeders (for instance Ivrea zone).

The effect of reducing the gravity field measurements by the influence of the models described above (Topography, Moho, Po-plain) can be seen in figure 3 with the example of the deflections of the vertical. The remaining residuals are smooth and can mainly be interpreted as a general trend which we modelled with a polynomial of degree 3. This trend has not been investigated intensively but it seems to be most likely an effect of windowing the models of the topography and of the Moho-discontinuity. Therefore we neglect completely the effects of the masses beyond the boundaries of our models. A hint for this assumption can be found in [Geiger et al., 1992] where 'far masses' generate even stronger trend effects. After removing the trend we obtain the residuals of figure 4. Besides of measuring noise, they show systematic signals which can be interpolated by means of multivariate collocation methods.

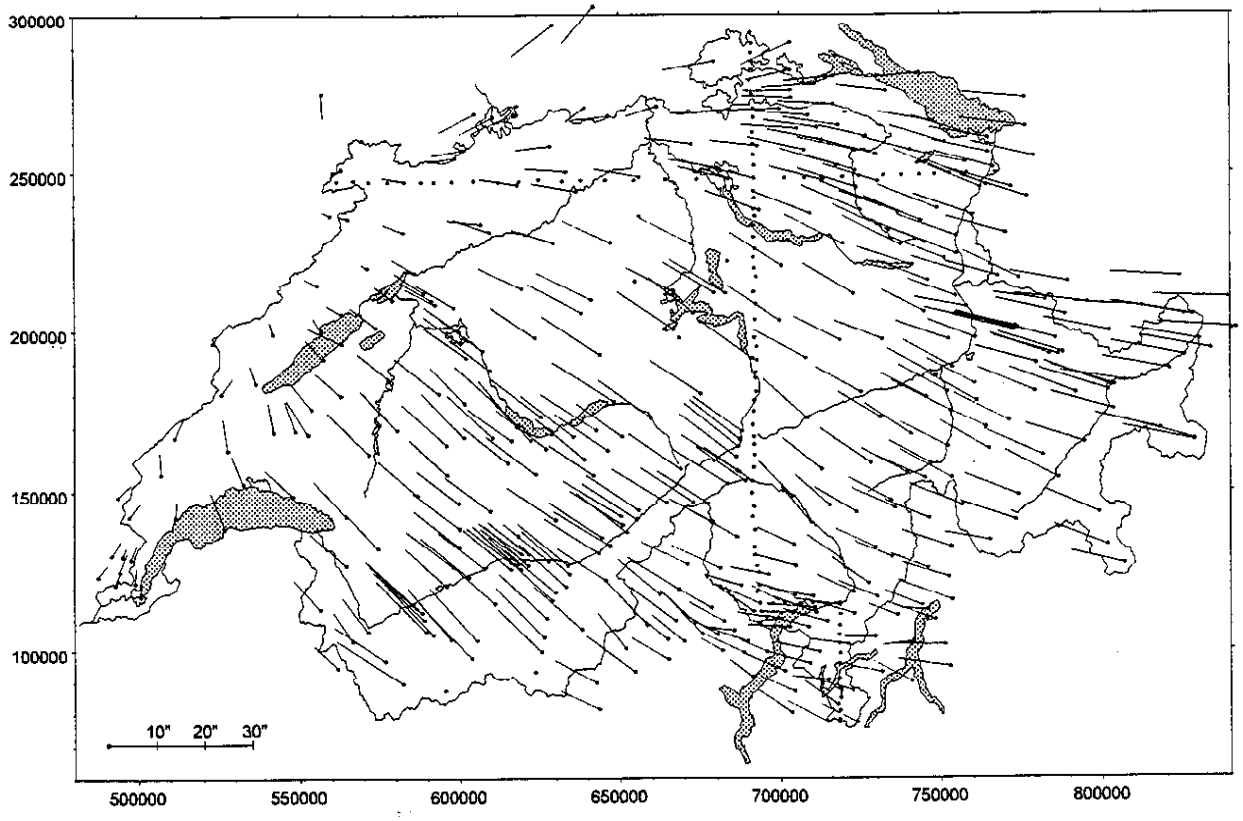

Fig. 3: Residuals of the deflections of the vertical after removing the influences of topography, Moho discontinuity, Ivrea zone and sediments of the Po-plain.

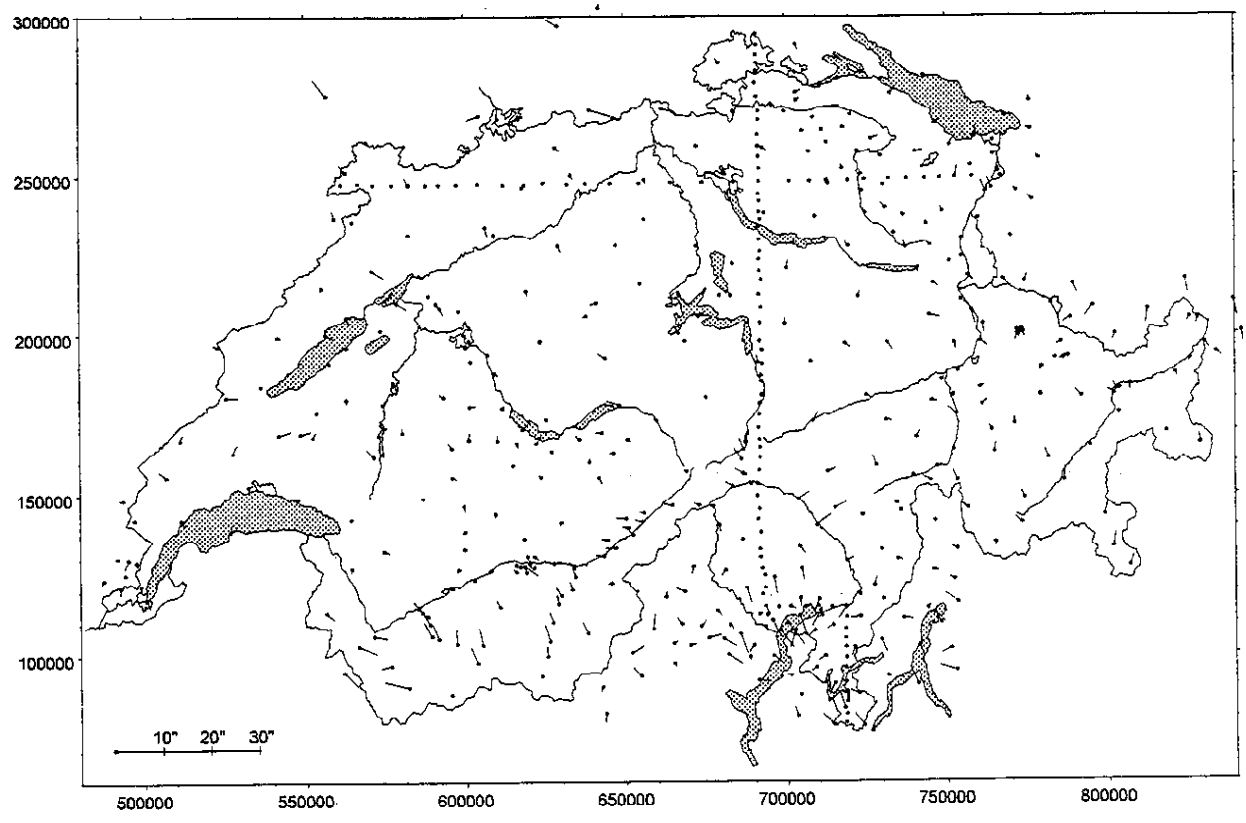

Fig. 4: Residuals of the deflections of the vertical after removing the influences of mass models and a trend of degree 3.

3. Tests of the variance-covariance functions

The result of an interpolation by means of collocation is dependent on the used variance-covariance functions between the measurements. In our tests, 2 different variance-covariance models have been compared 2-dimensionally as well as 3-dimensionally:

1. An inverse distance model ($^1/_r$), as it was used in local geoid determinations in Switzerland [Wirth, 1990].
2. The 2-dimensional 3rd Order Markov-Model as proposed by Jordan, 1972 and applied in the last national geoid determination [Gurtner, 1978].

The graphs of the tested correlation-functions (Fig. 5) show that the $^1/_r$-model is very similar to the 3rd Order Markov model. Its advantage is its much faster computation because of the simplicity of the formulas. The basic function is the auto-covariance function between the geoid undulations N, which for the 3rd order Markov model has the form

$$\Phi_{NN}(r) = \sigma_N^2 (1 + \frac{r}{d} + \frac{r^2}{3d^2}) e^{-r/d}$$

and for the $^1/_r$-model

$$\Phi_{NN}(r) = \sigma_N^2 (\frac{1}{\sqrt{\frac{r^2}{d^2} + 1}})$$

In case of the 2-dimensional approach r is the horizontal distance between the stations, whereas for the 3-dimensional approach it is a function of the horizontal distance and the height difference between the stations. Both functions contain 2 parameters σ^2 and d, which are determined empirically. The characteristical distance d depends on the density of the observations and on the degree of smoothness of the residuals. As it can be seen in Figure 5, where a value of 1 on the horizontal axis corresponds to d, the characteristical distance of the $^1/_r$-model will be about double the value of the characteristical distance of the 3rd order Markov-model. The parameter σ^2, which in collocation is the variance of the signal, has no effect on the geoid calculation itself, but behaves like a scale factor for the calculated a priori errors. It corresponds in general to the mean remaining residuals after removing a trend function and after centring the residuals to a value of 0.

For the 3-dimensional approach there is in principle a third parameter which increases artificially the distance r between two stations which do not have the same altitude.

All other auto-covariance and cross-covariance functions are then given by the well-known relations between geoid undulations, deflections of the vertical and gravity values (Stokes, Vening-Meinesz, differential relations)

Soon it was realised that the 3-dimensional approach is difficult to handle correctly because the distribution of the gravity field measurements is more or less 2-dimensional. Even in local investigations of areas where we have gravity measurements on mountains as well as in tunnels underneath it was not possible to generate a collocation model that results in a realistic downward continuation [Marti, 1995]. How much airborne gravity data can help to solve this problem has to be tested yet. Therefore we compared only the solutions of the 2-dimensional approaches.

As seen in figure 6 the differences are in general less than 2 cm. Only in the south-west we obtain significantly larger differences of up to 6 cm because of a poor distribution of the gravity field information. So we can conclude that the two models are equivalent and give more or less the same results.

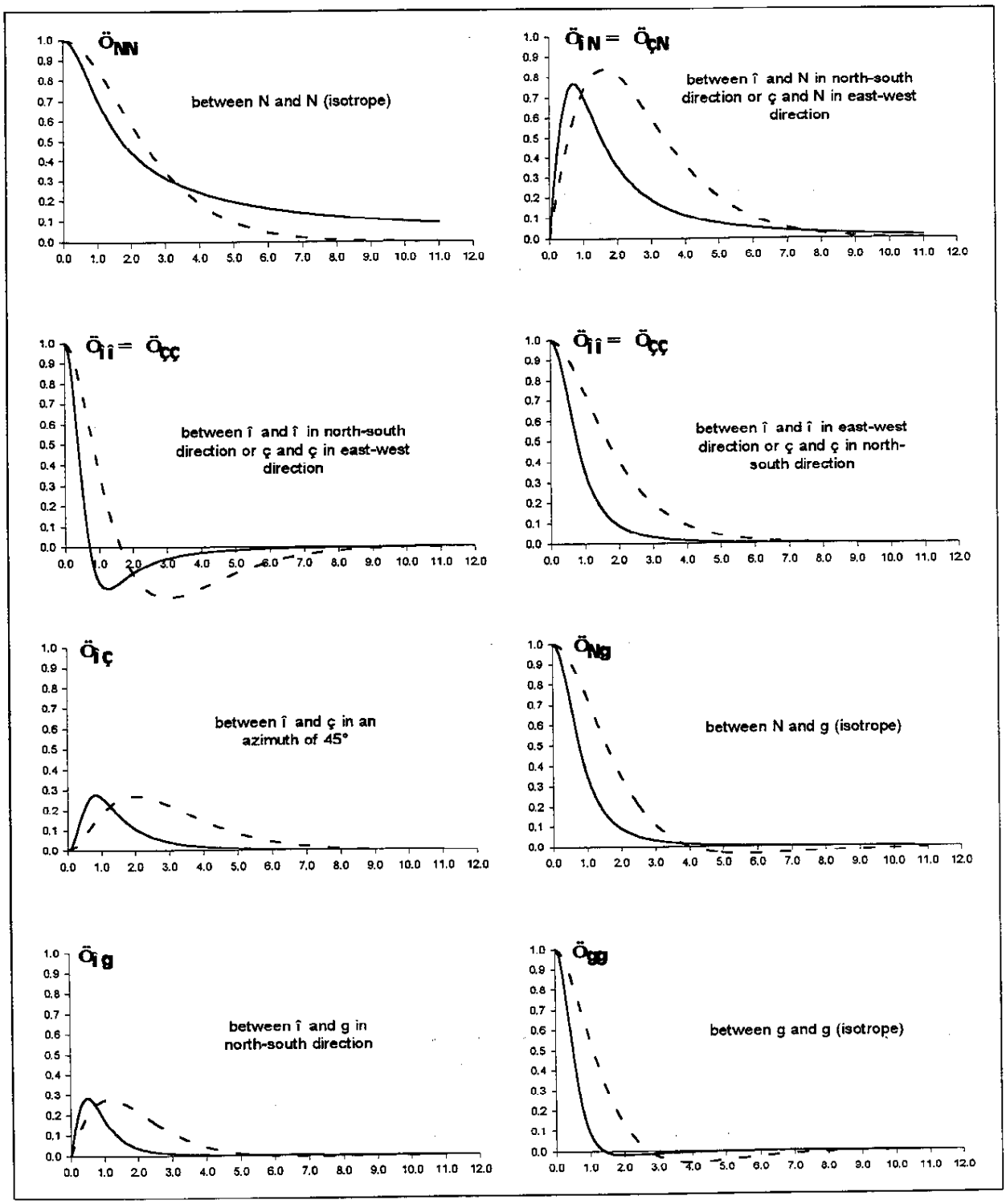

Fig. 5: Comparison of the correlation-functions of the 3rd order Markov model and the 1/r-Model with the Parameters $d = \sigma = 1.0$

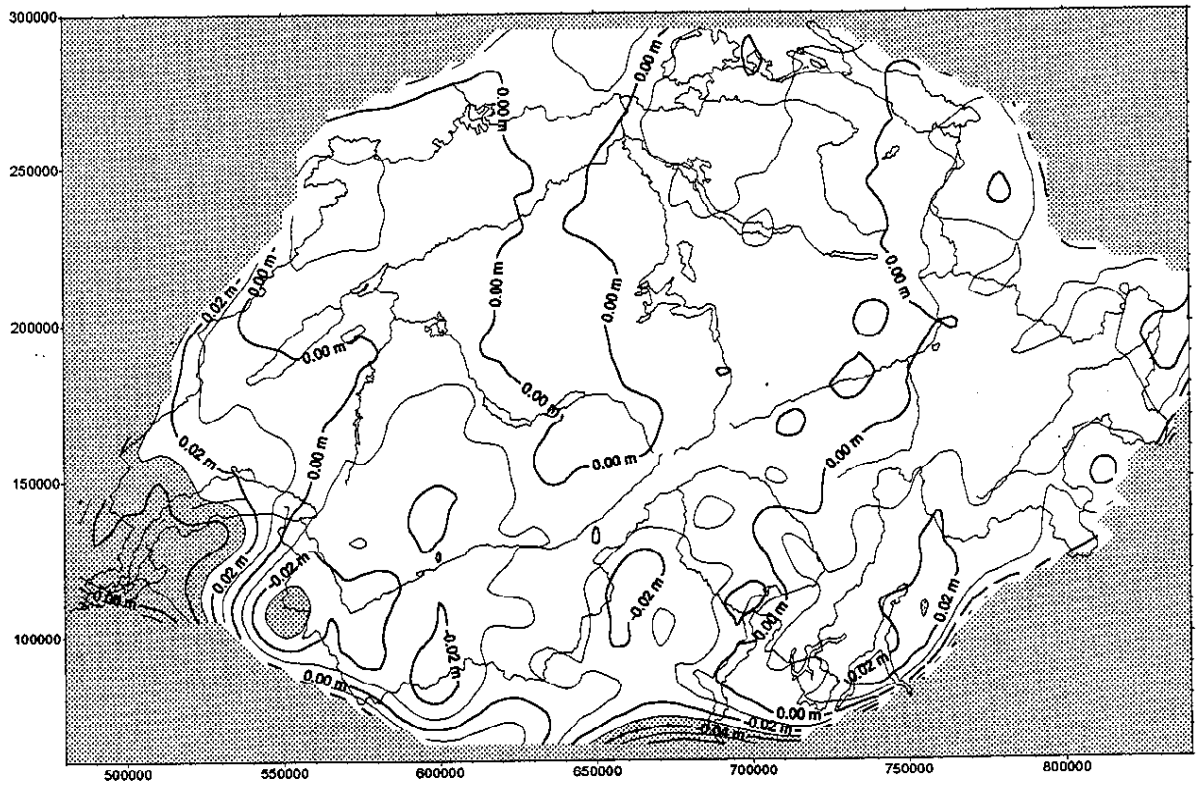

Fig. 6: Differences of a geoid computation with the 3rd order Markov model and the 1/r model

4. A priori Calculations and Comparison of different solutions

Regarding the a priori errors the 2 compared variance-covariance functions are equivalent. Therefore in this chapter we do not have to distinguish between the two models. The a priori calculations for the accuracy of the astrogeodetic geoid determination relative to the SLR-station in Zimmerwald is displayed in fig. 7. The results showed that in most parts of Switzerland an accuracy of better than 4 cm relative to the SLR-station in Zimmerwald can be reached by using only the astrogeodetic information. The greatest a priori errors of about 6 cm occur in the vicinity of Geneva and in some valleys of the south-east.

In a first test we eliminated about 50% of the astrogeodetic observations and calculated a new solution for the geoid and the formal errors. The a priori errors increased now to a value of 6 cm in most parts of Switzerland and to maximal values of 9 cm in the region of Geneva. The effect on the geoid undulations (after applying a shift), shown in figure 8, is in general less than 4 cm. This indicates that only with astrogeodetic observations it is possible to determine the geoid on a level of a few centimetres.

We also calculated the formal errors of a pure gravimetric geoid solution (Figure 9). Also here we can see that in most parts they are better than 4 cm. But if we compare the 1 cm isolines of figure 7 and 9 we see that gravity values help considerably in increasing locally the accuracy of the solution.

A good method to control long wavelength errors of the geoid is to introduce GPS levelling into the calculations. Only 7 additional GPS levelling stations (with a mean error of 2 cm) increase the relative accuracy of the geoid to a level of better than 3 cm everywhere in Switzerland. But at the moment there are still problems including these data in the evaluation process which are mentioned earlier in this paper.

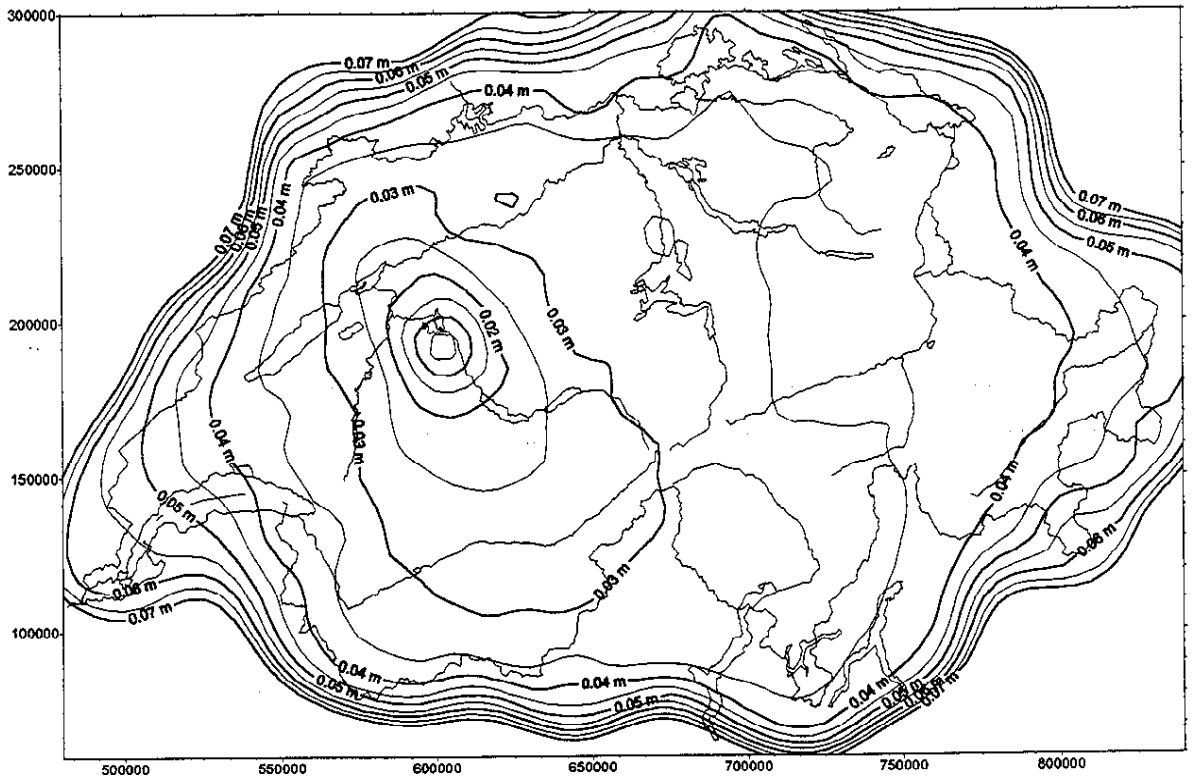

Fig. 7: Formal error of the astrogeodetic geoid referred to Zimmerwald (600000 / 190000). The greatest error (>5 cm) occurs near Geneva at the SW-edge of Switzerland.

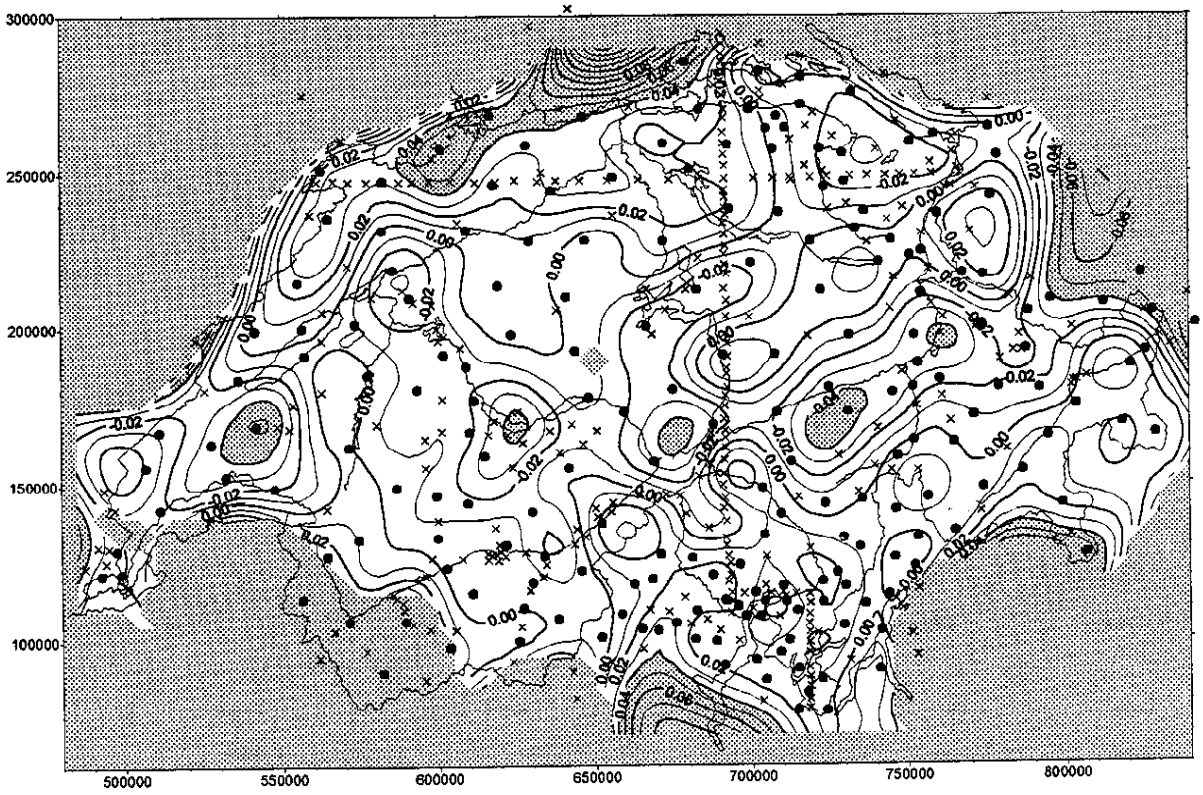

Fig. 8: Differences of the astrogeodetic geoid by using the complete data set or only a selection (crosses = eliminated points, dots = included in both calculations)

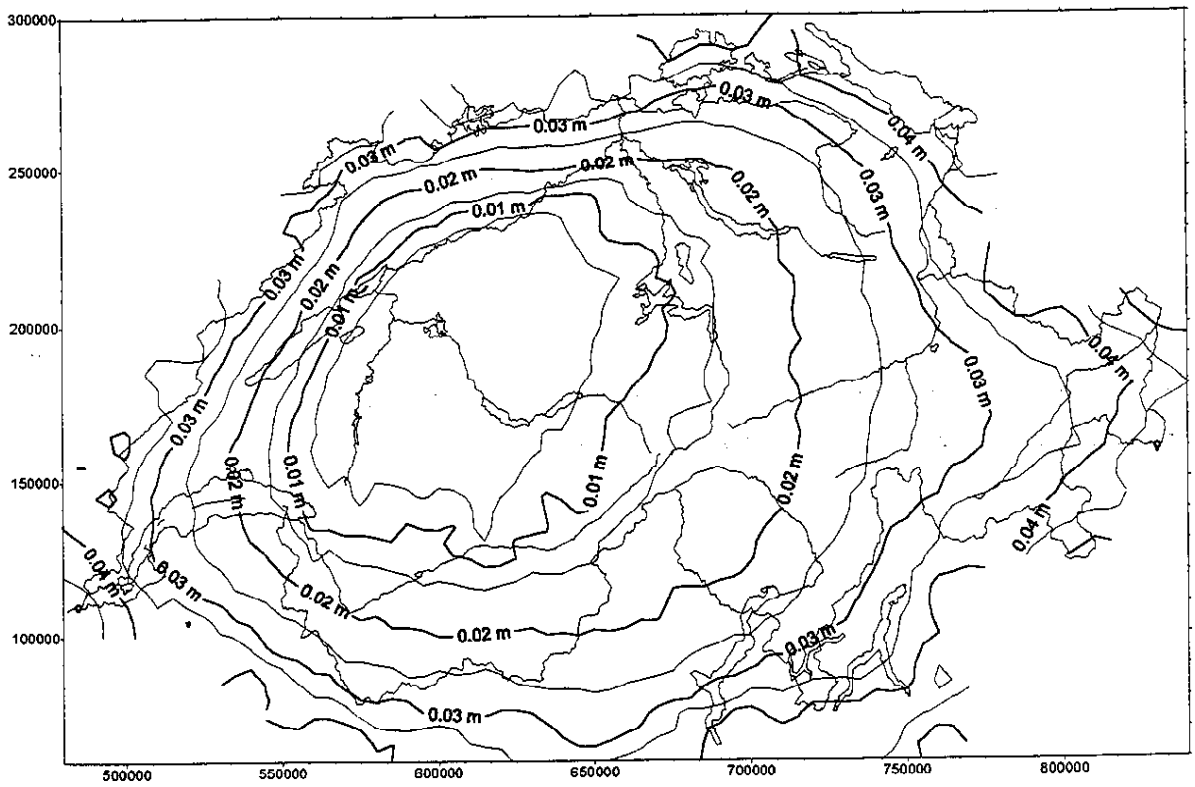

Fig. 9: Formal error of the gravimetric geoid

5. Calculation of the Geoid and Quasigeoid

The geoid is obtained by adding the effects of the reduced mass models (Bruns theorem) on sea level to the cogeoid obtained by collocation. In this case the assumptions we made on the distribution of the densities in the interior of the earth is important. We can avoid this problem by calculating a quasigeoid where these assumptions are of no importance. The resulting differences between the geoid and the quasigeoid (and therefore also between orthometric heights and normal heights) can reach up to 60 cm in the region of the highest mountains in southern Switzerland.

The geoid which is displayed in fig. 10 was calculated with only the astrogeodetic data in the Swiss geodetic datum CH1903 and the inverse distance collocation model. The assumption was, that CH1903 is parallel to the ITRS system. This is not strictly fulfilled. Therefore it is possible that the presented solution has a long wavelength trend which could be determined by introducing GPS levelling data or to fit our solution to a global geoid model.

The presented solution has been calculated with a resolution of 5 km. Detailed structures, especially the main valleys are clearly visible. The effect of the Ivrea zone which causes geoid undulations of up to 10 meters is masked by the large effect of the Po plain and therefore it can not be seen easily on the plot.

It is possible to transform this solution to the new Swiss reference system CH1903+ and the European datum ETRS89. With our software it is also possible to interpolate deflections of the vertical with an accuracy of better than 1" and gravity values with an accuracy in the order of 1 mgal.

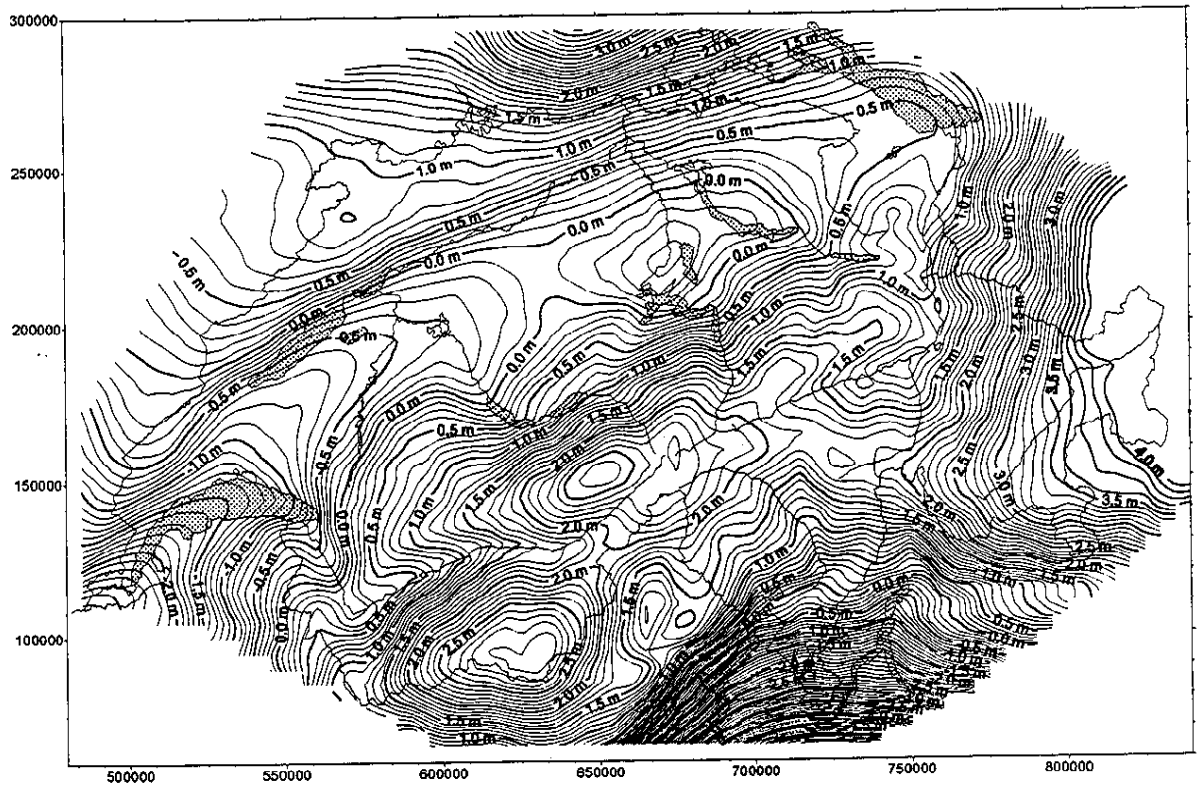

Fig. 10: Astrogeodetic geoid in Swiss datum CH1903

References

Bürki, B. (1988): Integrale Schwerefeldbestimmung in der Ivrea-Zone und deren geophysikalische Interpretation. Geodätisch-geophysikalische Arbeiten in der Schweiz. Vol. 40.

Geiger A. (1989): Gravimetrisches Geoid der Schweiz: Potentialtheoretische Untersuchungen zum Schwerefeld im Alpenraum. Geodätisch-geophysikalische Arbeiten in der Schweiz. Vol. 43.

Geiger A., U. Marti, B. Wirth (1992): The role of Terrain in Local Gravity Field Modelling. First Continental Workshop on the Geoid in Europe. Prague 1992.

Gurtner, W. (1978). Das Geoid in der Schweiz. Mitteilungen des Instituts für Geodäsie und Photogrammetrie Nr. 20.

Jordan S. (1972): Self-Consistent Statistical Models for the Gravity Anomaly, Vertical Deflections and Undulations of the Geoid. Journal of Geophysical Research, Vol. 77, No. 20

Marti U. et al. (1992): Local and National Geoid Investigations in Switzerland. First Continental Workshop on the Geoid in Europe. Prague 1992.

Marti, U. (1995): Test of Collocation Models for the Swiss Geoid Computation. IAG Symposia 113. Gravity and Geoid.

Wiget A., B. Vogel, D. Schneider (1994): Die neue Landesvermessung LV95 der Schweiz. Zeitschrift für Satellitengestützte Positionierung, Navigation und Kommunikation 1/94

Wirth, B. (1990): Höhensysteme, Schwerepotentiale und Niveauflächen. Geodätisch-geophysikalische Arbeiten in der Schweiz. Vol. 42.